REF. 20

FINAL REPORT

OF

EDISON ELECTRIC INSTITUTE

MECHANISM OF LIGHTNING FLASHOVER

RESEARCH PROJECT

(EEI Project RP50)

Prepared by
Edwin R. Whitehead

Submitted by
IIT RESEARCH INSTITUTE
Chicago, Illinois

to
EDISON ELECTRIC INSTITUTE

Available from
EDISON ELECTRIC INSTITUTE
90 Park Avenue
New York, N.Y. 10016

EEI Publication No. 72-900
Price $3.50

FOREWORD

In December 1962, the Edison Electric Institute Board of Directors on the recommendation of the Transmission & Distribution Committee authorized a research project on the Mechanism of Lightning Flashover (EEI research project RP50). The project, which was carried out at the IIT Research Institute in Chicago, Illinois, under the direction of Dr. E. R. Whitehead, was completed in 1971. While major financial support was provided by EEI, the Bonneville Power Administration under the operation of the Electric Research Council has also contributed.

The report which follows is a summary of the program. The work was carried out under the general supervision of a steering committee which, at the conclusion of the project, consisted of D. W. Gilman (Chairman), San Diego Gas & Electric Company; G. S. Haralampu, New England Electric System and B. D. Miller, The Detroit Edison Company.

ABSTRACT

The results of a three-phase experimental, statistical, and analytical study of the mechanisms of lightning strokes to, and insulation flashover on, HV and EHV lines are presented. A device called the Pathfinder, developed during the initial phase of the study, is described together with its signal code and associated interpretation table of "backflash" and "shielding failure" events. Experimental studies using approximately 4600 Pathfinder instruments on 400 miles of line yielded 138 operations on 89 separate strokes of which 48 caused shielding failures and 39 caused backflash events. Statistical studies covered over 100,000 kilometer-years experience on lines from 69 to 500 kV voltage rating.

It is found that insulator flashovers occur both as a result of direct strokes to the phase conductor, the "shielding failure mechanism", and as a result of strokes to the shielding ground wire, the "backflash mechanism". The shielding failure mechanism predominates when large shielding angles are associated with high towers and low footing resistances to ground. The backflash mechanism predominates when high tower footing impedances are associated with low tower heights and low insulation levels.

Analytical models based on modern knowledge of lightning stroke processes are found useful in correlating experimental data on shielding failures, predicting performance of ineffectively shielded lines, and in providing guidelines for the design of effective shielding. The theoretical foundations of the backflash mechanism are adequate to explain the field results of this study, though refinements are needed in several important areas. It is concluded that, with properly shielded lines, EHV and UHV lines can, in general, be designed for specific tripout rates approaching 0.3 per one hundred kilometer-years and, under favorable conditions, specific tripout rates well below this figure appear achievable.

TABLE OF CONTENTS

LIST OF FIGURES

LIST OF FIGURES

LIST OF SYMBOLS

Symbol	Definition
S	Shield wire or ground wire
W	Phase conductor
a	Horizontal offset between S and W
$\bar{b}$	Mean vertical separation between S and W
$\bar{C}$	Mean spacing between S and W
b_t	Vertical separation between S and W at the tower
H_t	Height of shield wire S at the tower
$\bar{H}$	Mean height of shield wire S
Y_t	Height of phase conductor W at the tower
$\bar{Y}$	Mean height of phase conductor W
$\bar{Y}'$	Effective mean height of W including ground angle
$\bar{r}_{ss}$	Mean striking distance between stroke leader and shield wire S
$\bar{r}_{sw}$	Mean striking distance between stroke leader and phase conductor W
$\bar{r}_{sg}$	Mean striking distance between stroke leader and ground
$\bar{r}_{ss,c}$, $\bar{r}_{sw,c}$, $\bar{r}_{sg,c}$	Critical striking distances corresponding to the critical prospective stroke current to ground

LIST OF SYMBOLS (cont.)

Symbol	Definition
$\bar{r}_s$	Striking distance when $\bar{r}_{ss} = \bar{r}_{sw} = \bar{r}_{sg}$
$\bar{r}_{sc}$	Critical striking distance $\bar{r}_s$ for critical prospective current to ground
K_{sg}	$K_{sg} = \bar{r}_{sg}/\bar{r}_{ss}$ when $\bar{r}_{sg} \neq \bar{r}_{ss}$
K_{sw}	$K_{sw} = \bar{r}_{sw}/\bar{r}_{ss}$ when $\bar{r}_{sw} \neq \bar{r}_{ss}$
K	A deviation constant for use with Fig. 9 to provide a shielding angle margin
θ_t	Shielding angle at the tower
$\bar{\theta}_s$	Mean shielding angle. Positive for S inboard of W. Negative for S outboard of W.
$\bar{\beta}$	Arc sin $\bar{C}/2\bar{r}_s$
$\bar{\theta}_1$	$\bar{\theta}_1 = \bar{\theta}_s + \bar{\beta}$ = Arc sin $(K_{sg} - K\bar{Y}/\bar{r}_s)$
$\bar{\theta}_2$ and $\bar{\theta}_3$	Angles defining exposure arcs of Fig. 7.
E	Basic insulation level or critical impulse sparkover voltage of insulation in kV for negative polarity 1.2/50 microsecond waves
Z	Surge impedance of phase conductor W in the presence of ground wires
I_c	$I_c = 2\ E/Z$ critical stroke current to conductor in kA.
I_{oc}	$I_{oc} = 1.1\ I_c$ critical prospective stroke current to earth in kA.
I_o	Prospective stroke current to earth in kA.

LIST OF SYMBOLS (cont.)

Symbol	Definition
$\bar{r}_s$	$\bar{r}_s = 6.7\ I_o^{0.8}$ meters
$\bar{r}_{sc}$	$\bar{r}_{sc} = 6.7\ I_{oc}^{0.8}$ critical striking distance from leader to shield wire S
T.D.	Thunderstorm days per year
T.H.	Thunderstorm hours per year
G.F.D.	Ground flash density
T.M.B.	Top middle and bottom phase conductors
$\bar{Y}$	$\bar{Y}$ for irregular terrain = $\frac{1}{n} \sum_{m=1}^{m=n} Y_m$

FINAL REPORT
ON
EDISON ELECTRIC INSTITUTE
RESEARCH PROJECT RP50

"Mechanism of Lightning Strokes to Transmission Lines"
(IITRI Project E8004)

January 1971

1.0 Introduction and objectives

In 1950 the AIEE (IEEE) Lightning and Insulator Subcommittee published a working-group report entitled "A Method of Estimating Lightning Performance of Transmission Lines." As a considered composite of the views of United States specialists, the report was widely accepted in this country as providing a useful basis of comparing proposed line designs for lightning performance. Comparison of estimated performance with that of existing lines revealed both good and poor agreement, with differences generally ascribed to the statistical variability of lightning incidence and uncertainties in data (1).

Application of the "AIEE Method" to the design of early EHV (345 kV) lines led to simplifications in structure resulting from the use of 25° - 35° shielding angles in accordance with the recommended minimum of 30°. One ground wire was widely used, though two were used on some lines.

Initial operating experience revealed lightning tripout rates roughly 10 to 15 times those estimated, and led to extensive field and theoretical studies to account for such a

(1) For all numbered references, see List of References. References listed are illustrative, not comprehensive.

serious discrepancy. The three basic mechanisms leading to lightning sparkover of transmission lines, Figure 1, are:

1.11 Stroke to tower or shield (ground) wire with resultant transfer impedance voltage across the insulator string. For simplicity in reference, this is commonly called the "backflash mechanism."

1.12 Stroke directly to a phase conductor with resultant surge impedance voltage across the insulator string. For simplicity in reference, this is commonly called the "shielding failure" mechanism.

1.13 Stroke to earth near the line with resultant electromagnetically - induced voltage across the insulator string. This is commonly called the "induced voltage" mechanism.

It is generally accepted that the induced voltage mechanism as defined in 1.13 is not a significant factor in lightning performance of EHV lines. Accordingly, investigations of the so-called "anomalous" lightning flashovers were largely directed toward more rigorous studies of the backflash mechanism (1.11) assuming perfect shielding. Other investigators questioned the shielding efficiency of ground wires and attributed the excessive tripout rates to poor shielding design. (2,3,4,5,6)

The uncertainty generated by the poor performance of early 345 kV lines and the lack of agreement on the cause among recognized specialists led the Overhead Systems Subcommittee of the EEI Transmission and Distribution Committee to establish a Task Force to study and make recommendations for an EEI Research Project on "The Mechanism of Lightning Strokes to Transmission Lines." EEI estimates of a multi-billion dollar expenditure for several years for EHV lines clearly provided the economic justification for research to discriminate clearly between the

"backflash" and "shielding failure" mechanisms and furnish guidelines for design improvements leading to superior lightning performance of EHV and UHV lines.

Following a preliminary survey, and recommendation of the research, the Task Force was converted to a Steering Committee to supervise a three-phase program consisting of:

Phase 1	Instrumentation feasibility and preliminary program planning.
Phase 2	Instrument prototype development, pilot manufacture and installation, EEI member company solicitation and selection of participating companies. Previous reports summarized the results of these activities.
Phase 3	Full scale installation and subsequent five-year minimum data-gathering and analysis period.

The fundamental reason for this research is the need to understand the principal mechanisms by which lightning results in impulse sparkover, and subsequent power follow flashover, of the insulation of EHV and UHV lines. The result of such understanding is the proper allocation of resources to appropriate protective measures. Accordingly, the objectives of this research were the determination of the relative roles of the flashover mechanisms on existing lines, the engineering extrapolation of these roles to proposed lines, and the development of guidelines for line design for superior lightning performance.

2.0 Plan of Research

The plan of research adopted for Phase 3 was divided into three distinct, though related tasks:

2.1 The analysis of an expected total of approximately 100 Pathfinder instrument operations to discriminate between insulation sparkovers for strokes to the phase conductor or strokes to the tower or ground wire for specific conductor configurations, ground profile, and tower footing resistances. There are 4600 Pathfinder instruments, on 433 miles of line, from 110 kV to 345 kV line voltage, owned by 12 EEI member companies located from Florida to Vermont, Michigan to Missouri, Texas to Colorado. The emphasis of this phase is on detailed knowledge of individual events.

2.2 A large-scale statistical study of the lightning performance of existing HV and EHV lines as affected by conductor configurations, line profile and grounding conditions. The emphasis of this phase is on statistical data appropriately grouped for analysis.

2.3 The development of the simplest analytical models which exhibit the important features found in phases 2.1 and 2.2 and which thereby serve to extrapolate the known performance of existing lines to that of proposed designs. The emphasis of this phase is on design guidelines, though secondary benefit lies in improved estimates of lightning stroke characteristics.

3.0 Summary, Conclusions and Recommendations

The results of this research have been annually reported to the Edison Electric Institute, on a cumulative basis, in order that they could be brought to bear on the design of new lines as rapidly as possible. Upon request, specific designs have been reviewed for participating companies. For those who have had a close and continuing interest, this report should serve to consolidate their information. For those who, though generally interested, have not followed the periodic reports in detail, it is hoped that the following summaries, discussions and appendices will comprise a concise but complete outline of the essential results of the research.

3.1 Pathfinder Operation Summary

Figure 2 shows the paths of negative lightning current for a stroke to the tower and for a stroke to the phase conductor and the corresponding signals displayed by the Pathfinder instrument. Also shown is the signal displayed when system-frequency fault current passes thru the device. Table 1 shows the resulting event interpretation code for a double circuit line based on shielding failures for low-current negative-polarity strokes and backflash events for high-current strokes of negative or positive polarity. Table 2 shows a summary of Pathfinder instrument operations and the interpretations in accordance with Table 1. An important caution should be stressed here. The data of lines 5 and 12 of Table 2 cannot be taken as the general division of lightning sparkovers between shielding failures and backflash events. The factors affecting this division are discussed later in this report.

Figure 3 shows the Pathfinder circuit and Figures 4 and 5 show the instrument mounted on transmission towers, Fig. 6 shows the transmission line configuration codes.

3.2 Summary of Statistical Studies

The lines summarized in Tables 3 and 4 were selected for their superior lightning performance. The objective of this selection was to determine the physical and electrical parameters which set these lines apart from those with known lightning characteristics as revealed in the Pathfinder data.

TABLE 1

PATHFINDER SIGNAL CODE WITH PROBABLE INTERPRETATIONS

Signal	Red Disc		Green Cross		Black Triangle		Probable Interpretations		
							Stroke to	Polarity	Type of Fault
Circuit	1	2	1	2	1	2			
	X						Conductor	-	None
	X				X		Conductor	-	Line to ground
			X				Ground Wire	-	None
			X		X		Ground Wire	-	Line to ground
			X	X			Ground Wire	-	Note 1
			X	X	X	X	Ground Wire	-	Double Circuit
					X		Ground Wire	-	Note 2
	X			X			Conductor	-	Note 3
	X			X	X	X	Conductor	-	Note 4
	X	X					Ground Wire	+	Note 1
	X	X			X	X	Ground Wire	+	Double Circuit
									Note 5

Notes:

1. Double circuit sparkover without power follow.
2. Stroke to ground wire. Current-time curve below activation level.
3. Stroke to circuit (1), backflash on circuit (2) without power follow.
4. Stroke to circuit (1), backflash on circuit (2) with power follow.
5. Multiple-conductor faults frequently involve conductors which do not have instruments connected.

TABLE 2

SUMMARY OF PATHFINDER OPERATIONS

As of

January 1, 1971

Line Number	Data Description		Numerical Data
1	Pathfinder instrument operations		138
2	Number of separate lightning strokes		89
3	Number of strokes causing tripouts		81
4	Percent strokes causing tripouts		91
5	Number of strokes causing shielding failures		48
6	Type of fault from shielding failures		
7	Top single-conductor tripouts	37	
8	Middle single-conductor tripouts	2	
9	Multiconductor	3	
10	Double circuit tripouts	1	
11	No tripout	5	
12	Number of strokes causing backflash events		39
13	Type of fault from backflash events		
14	Top single-conductor tripouts	18	
15	Multiple-conductor tripouts	3	
16	Double-circuit tripouts*	16	
17	No tripout	2	
18	Indicated number of negative strokes		83
19	Indicated percent of negative strokes		93
20	Instrument malfunction or current reversal		2

* Double-circuit tripouts may also be multiconductor on one or both circuits.

TABLE 3

Data for 50 transmission lines, 115 kV to 230 kV, in regions having 35-50 thunderstorm days per year. References (7) and (8) 84,000 km-years, 52,000 mi.-year. Tripouts adjusted to 40 T.D. per year.

Characteristics	Minimum One Line	Average All Lines	Maximum One Line
Tripouts per 100 miles per year	0.00	0.175	0.50
Tripouts per 100 kilometers per year	0.00	0.109	0.31
Mile years	210	1040	6500
Kilometer years	338	1675	10460
Basic insulation level-BIL	950	1300	1625
Mean shield wire height-feet	42	69	110
Mean shield wire height-meters	13	21	34
Mean shielding angle-degrees	-6	18	39
Mean ground resistance-ohms (35 lines)	2	23	94

TABLE 4

Lightning tripouts for 500 kV lines in the U.S.S.R. from reference (9) adjusted to 30 thunderstorm days per year. 37780 kilometer years or 23400 mile years

Specific tripouts per 100 kilometers	miles	BIL kV	Ground resistance ohms	Ground wire height meters	Shield angle degrees
0.15	0.24	1800	under 5	under 30	20*

* In exceptional cases this angle might be as high as 30 deg.

Table 4 has been taken from reference (9) for 500 kV lines in the U. S. S. R. in regions having 20-25 thunderstorm days per year. In order to avoid excessive adjustment, the data presented here have been adjusted to 30 thunderstorm days.

3.3 The Reference Analytical Model

The term reference analytical model describes the simplest analytical model of the shielding failure mechanism which has been found capable of utilizing conductor and ground wire heights, basic insulation levels, profile and terrain factors, and shielding angles to account for the variations in lightning performance among the lines of the Pathfinder field study and those of the statistical sample. The reference model may be made successively more complicated to accommodate deviations from reference conditions or even in some basic assumptions, without affecting its primary function. The effects of the principal deviations will be discussed later in an appendix. Some of these deviations are evident and can be readily incorporated in design decisions. Others are theoretical in character and their objective evaluation is doubtful at this time. When the economic penalty is negligible, suitable design margins for these unknown factors can easily be applied. Figure 7 shows the reference model as applied to the mean conductor configuration (using average conductor locations with respect to earth) to illustrate ineffective shielding and Figure 8 shows this model as applied to illustrate effective shielding. Other equivalent models have been employed to facilitate computer programs to estimate tripouts resulting from ineffective shielding.(10,11)

Analytical models based on a combination of geometrical and electrical quantities have been called "electro-geometrical" models. The most important quantity in such models is the "striking distance" $\bar{r}_s$, a term first used by Benjamin Franklin (12). Although striking distances are determined by the stroke leader voltage with respect to earth, no direct measurements of this voltage are available. It is possible, however, to relate this voltage, and thus the striking distance, to the prospective stroke current I_o to earth. The details of this development are left for Appendix 2. The relations used in the present study are:

$$\bar{r}_s = 6.7\ I_o^{0.8} \text{ meters} = 22\ I_o^{0.8} \text{ feet} \qquad (1)$$

$$I_{oc} = 1.1\ I_c \text{ kiloamperes} \qquad (2)$$

$$I_c = 2\ E/Z \text{ kiloamperes} \qquad (3)$$

E = Basic insulation level or critical impulse sparkover voltage for negative polarity 1.2/50 microsecond waves.

Z = surge impedance of phase conductor

In equation (1), I_o is any prospective current to a zero resistance ground and $\bar{r}_s$ is general and applicable to the situation depicted in Figure 7, while I_{oc} in equation (2) is a critical value as determined from (3) applicable to the critical condition for effective shielding as shown in Figure 8, and $\bar{r}_{sc}$ is a critical value as shown.

3.4 Design of Shielding Configuration

The curves of Figure 9 reduce the complexity of shielding design to a few basic steps. Their derivation is left to Appendix 7.2.These steps are:

3.41 Determination of the mean conductor configuration from the proposed profile assuming flat transverse earth plane.

3.42 Determination of the critical mean striking distance $\bar{r}_{sc}$ from equations (1) (2) and (3).

3.43 Determination of the critical mean shielding angle $\bar{\theta}_{sc}$ from Figure 9.

These steps determine a critical mean configuration which will provide "reference" (usually good)shielding. Numerous deviations from mean conditions,however,do exist. Some of these can readily be identified and their influence incorporated directly. Others are intangible and their statistical distribution unknown. The final steps are, therefore,

3.44 Determine the degree to which such factors as transverse ground angle, deviation of conductor height from the average, and exceptional spans such as river and valley crossings are to affect the mean shielding angle for the entire line. Normally provisions for these deviations will largely accommodate the intangibles. Deviations effects are discussed in Appendix 3. Assign a deviation factor K and read the adjusted mean shielding angle $\bar{\theta}_s$ from Figure 9. If the line profile is sufficiently uniform so that specific deviations need not be considered a deviation factor of K=1.2 should be used.

3.45 Extreme mountainous terrain or long, high river crossings may require special consideration and even the installation of a third ground wire.

An illustrative shielding design procedure is carried out in Appendix 7.1 for conditions requiring consideration of substantial deviations from the reference model as a base case and unusual conditions requiring special treatment beyond the normal capability of the deviation factor K.

3.5 The Backflash Mechanism

The theory of the backflash mechanism has been developed along increasingly sophisticated lines for over 40 years, and the modern literature is replete with analytical, experimental, and statistical investigations of the lightning performance of lines based on this mechanism. As stressed earlier, the Pathfinder field study was designed to give detailed data on a limited number of lightning sparkover events, and it was recognized that the partial instrumentation of conductors and other limitations of the field sample would not, taken alone, yield results of broad statistical significance. It was, however, of great importance that the Pathfinder device be able to respond to both shielding and backflash mechanisms to establish maximum confidence in the results. Table 2 shows that all the kinds of operations anticipated by the interpretation code of Table 1 have been observed. The backflash operations confirm the various kinds of events predicted by backflash theory and operation and maintenance records. Table 3 furnishes information of significance with respect to both backflash and shielding failure mechanisms. Since these lines have such a low specific tripout rate, it is clear that they are extremely well shielded. A rough estimate of the average specific tripout rate for these lines, based on a coupling factor of 0.3 and an earth ionization resistance reduction factor of 0.5, yields a specific rate of 0.3 tripouts per 100 miles per year. This value falls well within the range indicated in the table. It should be noted, however, that

Table 3 reflects a very large statistical sample in terms of mile-years so that individual extreme events are obscured.

Table 5 summarizes the grounding conditions and types of faults for the individual backflash events giving Pathfinder instrument operations. Unfortunately, it has not been feasible to obtain resistance measurements on every individual tower supplying backflash events, though many useful values are available. Nevertheless, this table reveals the full range of backflash events predicted by theory, except midspan flashovers which are now believed to be very rare if they occur at all. Of interest is the prominence of double-circuit faults on sample lines having high tower footing resistance or continuous counterpoise implying such footing resistances. In these circumstances it is the high transient surge impedance to remote reference ground which is responsible for insulation sparkover, and the double-circuit faults are expected even for strokes of moderate current magnitude. On the other hand, it is found that double-circuit faults can also occur on towers having very low footing resistance. Under these circumstances it is the stroke which must be extreme in either current magnitude, rate of rise with time, or both, calling into play induction mechanisms causing the required insulator sparkover voltage. The backflash mechanism will be discussed in more detail later with reference to analytical studies at distributed grounding systems (counterpoises).

3.6 Estimation of Lightning Performance

While the development of an estimating method was not an assigned objective of the present research it was recognized that the results of this investigation might well have a substantial influence on the directions to be taken and on

the confidence levels to be attached to proposed methods. Accordingly, it has been the policy of the Steering Committee to make the results of the field and analytical studies available to all interested groups on the same cumulative basis as reported to the Edison Electric Institute. Although formal EEI, IEEE, and CIGRE publication of results has occurred periodically, the normal printing delays limit the effectiveness with which other related work can be influenced. In particular, the cognizant committees of IEEE and CIGRE have been kept informed on a continuing basis and the resulting interaction has been most fruitful. Reference (11) is one example of this interaction in the application of the Monte Carlo computer technique to the estimation problem. Cooperative efforts are currently under way with a task group of the IEEE Lightning and Insulator Sub-committee to develop a modern version of Reference (1). (11,14-19)

3.7 Conclusions

3.71 The Pathfinder instrument signals, taken together with the line geometry at the location of the lightning sparkover, the type of fault and lightning stroke characteristics have effectively discriminated between shielding failure and backflash events for 89 separate strokes yielding 138 instrument operations

3.72 Depending on conditions of tower geometry line profile, terrain, tower footing impedance and insulation level, both the shielding failure and backflash mechanisms can contribute significantly to the lightning tripout rate.

3.73 Shielding failures dominate the lightning tripout rate when large shielding angles are associated with low tower footing impedances to ground.

3.74 Backflash events dominate the lightning tripout rate when high tower footing impedances are associated with low insulation levels and low conductor heights.

3.75 Shielding failures can be reduced to rare events when the shielding angles of the overhead ground wires are properly coordinated with the mean heights and spacings of the conductors and ground wires. Because the coordination is statistical in nature, due regard to geometrical and electrical deviations must be taken.

3.76 Backflash lightning tripouts can be reduced to rare events through well-known protection techniques developed over a period of approximately 40 years. While it does not seem possible to design for a "lightning-proof" line specific tripout rates of the order of 0.25 have been achieved through low tower impedance to earth and effective shielding.

3.77 A reference analytical model (base case) has been derived from electrogeometrical shielding theory and used as a correlating and extrapolating device. The model incorporates features which permit the investigation of electrical and geometrical deviations from the reference configuration.

3.78 Design for effective shielding should be based on bare earth, taking into account conductor profile, leaving the effects of forestation or other surface perturbations along the right-of-way as favorable deviations.

3.79 Design for effective shielding should include provision of a reasonable (negative) margin below the critical angle determined after all known deviations have been incorporated. Present indications are that this margin should be from -5 to -10 degrees.

3.8 Recommendations

3.81 The data accumulation period should be extended through 1971 in the hope of obtaining additional data covering important low-probability events.

3.82 Analysis of the lightning performance of EHV lines (through 500 kV) afforded through cooperation between IITRI and CIGRE Working Group 01 (Lightning) should be continued to provide increased statistical correlation between Pathfinder data and actual line performance. Present correlations are largely, but not entirely, based on line performance at HV levels.

3.83 With effective shielding achievable, attention may well be redirected to the design and performance of the tower and tower grounding systems. While some new work has been done along these lines, the results require further study.

3.84 Additional research is needed in the general area of "lightning severity" measures. Among these are:

3.841 Thunderstorm days (T.D.) (Poor)
3.842 Thunderstorm hours (T.H.) (Better)
3.843 Ground flash density (G.F.D.) (Best)
3.844 Distribution of current amplitudes
3.845 Distribution of current-time wave shapes.

4.0 Discussion

4.1 Sample line identification codes

Figure 6 shows typical transmission tower-top configuration identification codes. Conductor codes are top T, middle M, and bottom B, with B used for the inner conductor in delta (triangular) or horizontal double-circuit configurations. The configuration code gives (Number of circuits)(Conductor Arrangement)(Number of ground wires). For convenience in

reference the following coding table is provided to reduce the size of tables in the appendices.

Company Code	Configuration Code	Operating Voltage-kV	Critical Impulse Spark-over-kV
A	2 V1	120	790
B	2 V1	115	690
C	2 H2	115	790
D	2 V1	345	1600
E	2 V	69/138	945
F	2 V2	138	945
G	2 V1	110	744
H	2 V1	115	690
I	2 △2	345	1600
J	2 V2	345	1600
K	2 V2	115	1100

4.2 Reference analytical model

It is important to point out that the reference analytical model has been devised to exhibit the principal features of electrogeometrical shielding theory which might be verified to a satisfactory degree in the Pathfinder field study. At the outset of this research many factors were studied and classified as "first-" "second-" or "third-order" factors.

4.21 First-order factors are observable and controllable. Among them are conductor heights and configurations, surge impedances, and impulse insulation levels.

4.22 Second-order factors may be estimated extrapolated, or calibrated from experimental results, with theory playing a guiding, rather than controlling role.

4.23 Third-order factors are those theoretically present but not directly observable or controllable. Among these are:

4.231 Influence of conductor voltage on striking distance.

4.232 Influence of "exact" electric field strengths near the leader

"tip" versus the mean values implied by striking distance and voltage.

4.233 Variability of corona filament lengths from the mean value of striking distance.

4.234 Variability of insulator impulse sparkover in the presence of ionization from near corona field.

4.235 Shielding effect of crossarm for portions of conductor very near the tower.

4.3 Deviations from the reference model

Deviations from the reference model, or base case, obviously may occur in first, second, and third order factors as outlined in the preceding section. The most important of these arise from conductor and ground wire heights. Clearly if the ground wires, phase conductors, and the earth all have the same sag from their respective elevations at the towers, their average heights above earth equal their tower values and the reference model is accurate in this respect. In practice some lines approach this situation quite closely. For flat earth the conductors are above their mean values for about 40 per cent of the span so that some attention should be given this deviation. One might consider shielding for conductor height at the quarter span points or elect to be conservative and shield for conductor height at the tower.

Second and third order factors are, by definition less tangible than first order factors and here experimental and statistical evidence must be used to assess the deviation factor K to be used with the master curves of Fig. 9. Further discussion of deviations is reserved for Appendix 7.3.

4.4 Models of the backflash mechanism

4.41 Models of the backflash mechanism are not considered in detail in this report because they have been exhaustively treated in the literature for many years. It is

appropriate, however, to indicate the status of the most recent research and to relate the results of the backflash events recorded in the field study to these models in a general way. The kinds of backflash events recorded range from single-circuit, single-conductor events to double-circuit, multiconductor events. Moreover, grounding conditions range from under five ohms for double circuit fault on a highly insulated line with very high towers (50 meters) to counterpoise grounding in gravel-like soil for double-circuit, multiconductor faults with very low towers (23 meters). Thus, virtually the whole range of possible backflash events has been recorded and these are fully consistent with past and currently-accepted models. The variables involved are even more numerous than those of shielding models and it is only recently that some progress is being made in defining wave shapes and rates of current rise. Further, new studies suggest that the lightning current distribution curve, developed during modern European and other foreign studies, may reflect substantially higher current values than the older "AIEE curve" developed in United States studies.

Recent studies by Popolansky (14) indicate that lightning current amplitudes follow the log-normal probability distribution. Figure 13 shows this distribution in terms of the ratio of current amplitude to the median value. Poplansky's results follow a curve with I (50%) equal to approximately 24.5 kA while the AIEE curve has a median current I (50%) approximately equal to 17 kA, also with apparent log-normal distribution.

4.42 Distributed grounding systems (continuous counterpoise) has been widely used in very high resistivity soil. While important reductions in lightning tripout rate have been achieved, the levels reached for the lines of the Pathfinder Study are entirely too high for EHV lines. Baatz in Germany

and more recently Kawaii in Japan have made field studies of the transient response of counterpoise systems including some with various terminal electrodes. This response is found to differ markedly from that of ideal distributed systems composed of inductive, conductive, and capacitive constants. (25)

Devgan and Whitehead have studied the response of distributed grounding systems analytically using modal rather than travelling wave response and have developed simplified circuit models permitting better visualization of the response and evaluation of the effects of grounding improvements. A paper is in preparation on this work. The principal finding reaffirms the value of short local grounding systems at the tower footing serving as both capacitive and conductive elements to eliminate or reduce the high initial voltage response to steep current waves. (26)

4.43 Berger has reviewed records of lightning strokes obtained at the Mount San Salvatore, Switzerland lightning laboratory and furnished amplitude and wave shape data to CIGRE Working Group 33-01 (Lightning) and to the I.E.E.E. Working Group on Methods of Estimating Lightning Performance of Transmission Lines. These and other studies comprise a cooperative effort with EEI Project RP50 and will be included to the degree possible in supplementary report on the research extension for 1971.

5.0 Acknowledgments

It is a pleasure to acknowledge the financial, technical, and supervisory support of Project RP50. The Edison Electric Institute and its member companies have furnished both the financial support and direct participation in the field investigations employing the Pathfinder instrument. Additional financial support was provided by the Bonneville Power Administration, and the cooperation of the Tennessee Valley

Authority in furnishing valuable statistical data is gratefully acknowledged.

EEI member companies participating directly in the field study are:

American Electric Power Corporation
Atlantic City Electric Company
Carolina Power and Light Company
Commonwealth Edison Company
The Detroit Edison Company
Florida Power Corporation
New England Electric System
Ohio Valley Electric Corporation
Public Service Company of Colorado
Texas Electric Service Company
Union Electric Company
Virginia Electric and Power Company

The essential support of project representatives for these companies and the cooperation of their employees in patrolling, reporting, and verifying field data are acknowledged with the greatest appreciation.

It is appropriate to acknowledge the special efforts exerted by the suppliers of the Pathfinder instrument and its current collection system in providing the degree of reliability so important to an experimental investigation of this kind. The Line Material Company Division of McGraw-Edison Industries furnished the instrument, and the Joslyn Manufacturing Company furnished the current collection system.

The Steering Committee, initially chaired by Mr. H. R. Armstrong and now chaired by Mr. D. W. Gilman, has furnished invaluable guidance at crucial points in the program and has been available at all times for advice and assistance. Current members are Mr. B. D. Miller, Mr. G. S. Haralampu, and Mr. W. S. Price. Dr. George E. Watkins, Director of Research, EEI, and

his headquarters staff have been most helpful whenever called upon to assist in administrative or operational procedures. The cooperation of many individuals; students, I.E.E.E. and CIGRE Committee members, and IITRI associates in furnishing technical information from reports and personal files is gratefully acknowledged.

6.0 Administrative Statement

The scope of EEI Research Project RP50 (IITRI Project No. E8004) for Phase III of the program included:

6.1 Receive, record and analyze Pathfinder operations reported by participating companies.

6.2 Continue such analytical and statistical studies of the transmission lines of participating companies and other cooperating organizations which are contributing to the objectives of the project.

6.3 Provide such liaison with participating companies, the I.E.E.E. Lightning and Insulator Subcommittee and CIGRE Study Committee No. 33 (Working Group 33-01 on lightning) as will bring new research results to bear on project objectives as promptly as possible.

6.4 Provide quarterly letter reports and annual summary reports.

This report summarizes the results of tasks 6.1, 6.2 and 6.3 and constitutes the final report of the formal program concluded December 31, 1970, as required under 6.4.

Respectfully submitted,
IIT RESEARCH INSTITUTE

E. R. Whitehead,
Research Engineer
Power Systems and Reliability

Approved:

E. L. Radnik
Manager
Power Systems and Reliability

Approved:

M. E. Goldberg
Assistant Director
of Research

90004240

February 16, 1971

7.0 Appendices

The following Appendices have been prepared for those who will be engaged in shielding design or who have an interest in more detailed information than has been presented in the preceding summaries.

7.1 Design Procedure for Shielding Configuration

Design procedure involves all aspects of the shielding problem as developed earlier and in subsequent appendices. The objective here, however, is on orderly procedure and reference will be made to other appendices only where necessary to assist in this procedure. Each step will be illustrated by a specific, but hypothetical, problem. See Figures 7 and 8.

Step 1

The profile of the proposed right-of-way will have dictated the profile of the phase conductors and the required preliminary tower elevations necessary for appropriate ground clearances. A single-circuit 500 kV line is to be constructed on this right-of-way classified as 40 per cent flat, 40 per cent rolling, and 20 per cent mountainous. Other data are:

Conductor height at tower	Yt	= 22m
Conductor sag	Sc	= 12m
Ground wire height at tower	Ht	= 31m
G.W. elevation above conductor	Sg	= 6m
Critical impulse sparkover	(BIL)	=2000kV
Conductor surge impedance	Z	= 360ohms

Step 2

(a) Mean heights(reference) of phase conductors and ground wires based on preliminary assumptions.

Rolling profile $\bar{Y} = Y_t = 22m$

Flat profile $\bar{Y} = Y_t - 2 S_c/3 = 14m$

Mountainous profile $\bar{Y} = 2Y_t = 44m$

Mean height for line

$\bar{Y} = 0.4 \times 22 + 0.4 \times 22 + 0.2 \times 44$

$= 17.6 + 8.8 = 26.4$ meters

$\bar{b} = (H_t - 2 S_g/3) - (Y_t - 2 S_c/3)$

$= H_t - Y_t + \frac{2}{3} (S_c - S_g)$ $\qquad b_t = H_t - Y_t$

$\bar{b} = b_t + 8 - 4 = 9 + 8 - 4 = 13$m

$\bar{H} = \bar{Y} + \bar{b} = 26.4 + 13 + 39.4$m

(b) At this point the conductor surge impedance may be recalculated if desired. Assume that this calculation confirms the estimate of 360 ohms for the purpose of this illustration. Then

Step 3

$I_c = 2 E/Z$ kA $= 2 \times 2000/360 = 11.1$kA

$I_{oc} = 1.1 \times 11.1 = 12.2$ kA

$\bar{r}_{sc} = 6.7 \times I_{oc}^{0.8} = 6.7 \times 12.2^{0.8} = 49.6$ m

$\bar{r}_{sc}$ = estimated mean striking distance from leader to ground wire or tower

Step 4

Express the mean conductor height in per unit $\bar{r}_{sc}$ (normalized $\bar{Y}$).

$\bar{Y}/\bar{r}_{sc} = 26.4/49.6 = 0.53$

Express $\bar{C}$ (estimated from $\bar{b}$) in per unit $\bar{r}_{sc}$ as

$\bar{C}/\bar{r}_{sc} = 15/49.6 = 0.3$

For reference conditions K = 1, Fig. 9 is read at $K\bar{Y}/\bar{r}_s = 0.53$ for $\bar{C}/\bar{r}_{sc} = 0.3$ Thus $\bar{\theta}_{sc} = 19°$ preliminary reference value

Step 5

Consider now the ways in which the conductor height deviates from this reference value. The most obvious approach is to revise the estimate for conductor height at the tower corresponding to uniform rolling country and as an extreme, again for conductor height corresponding to mountainous profile for the full line. These estimates become:

(a) Rolling profile (100%)

$\bar{Y}/\bar{r}_{sc} = 22/49.6 = 0.44$

$\bar{\theta}_{sc} = 25°$ This value is less conservative than the mean profile and should not be used.

(b) Mountainous profile

$\bar{Y}/\bar{r}_{sc} = 44/49.6 = 0.89$

$\bar{\theta}_{sc} = -1°$ This value is clearly quite conservative when considered for the entire line.

(c) Returning to the reference conditions of Step 4 we now consider electrical uncertainties and apply a deviation factor k = 1.2.

$1.2 \times 0.53 = 0.64$

Enter Figure 9 with $K\bar{Y}/\bar{r}_{sc} = 0.64$ and read

$\bar{\theta}_{sc} = \bar{\theta}_s = 12°$

A check of Figs. 20 and 21 verifies an extremely low risk of shielding failure for all of the line except the mountainous portion.

Applying the deviation factor of K = 1.2 to the conductor height ratio of(b) we obtain 1.2 x 0.89 = 1.07 and read from Fig. 9

$\bar{\theta}_{sc} = \bar{\theta}_s = -12°$

90004243

Step 6

Consider a tower design providing a mean shielding angle of not greater than + 12 degrees for the flat and rolling portions of the line and special construction providing -12 degrees for the mountainous portion of the line. If uniform design is more economical, use -12° as the angle for the entire line. In connection with the actual design of the towers it should be noted that the mean shielding angle is somewhat less than that at the tower if the groundwire has smaller sag than the phase conductor. This is normally the case, and for the assumption of this appendix we have, for the positive shield angle:

$\bar{\theta}_s$ = arc tan $a/\bar{b}$ = 12°

$\bar{\theta}_t$ = arc tan a/b_t = 13°

$\bar{c} = \bar{b}/\cos\bar{\theta}_s = 13/\cos 12° = 13.3$m

$a = \bar{c} \sin\bar{\theta}_s = 13.3 \times \sin 12° = 2.08$m

b_t = 9 m $a/b_t = 2.08/9 = 0.231$

7.2 The Reference Analytical Model

The analytical model consists of a few basic assumptions and relations deduced from them. The basic assumptions of the electrogeometrical theory are: (Figures 7 -12)

7.21 The "leader" of the first stroke of a lightning flash is preceded by a region of low intensity "corona" ionization, believed to consist of weakly-ionized filaments which may come into contact with one or more grounded objects as the leader approaches the line.

7.22 When corona filaments span the space from leader to earth, the shortest of these (on the average) result in "streamers" which progress both from the leader and grounded objects, complete the "last step" and thus prevent the completion of competing paths.

From electric field considerations one cannot really associate a spherical corona region in advance of the leader, but it is convenient to take the tower or ground wire as the desired target and consider all other "striking distances" with respect to this norm.

7.23 There exists a lower limit of first stroke current which can be accepted by the phase conductor without insulator sparkover, and there exists a corresponding critical "striking distance" associated with the related prospective stroke current to zero resistance ground.

$I_c = 2E/Z$ critical conductor current

$I_{oc} = 1.1 I_c$ critical prospective current

$\bar{r}_{sc} = 6.7 I_{oc}^{0.8}$ mean critical striking distance to tower or ground wire.

E = Basic insulation level or critical impulse sparkover voltage for negative polarity 1.2/50 microsecond waves.

Z = Surge impedance of phase conductor in the presence of ground wires.

(This assumption includes the further assumption that secondary phase-phase sparkover (or phase-ground) does not occur from local intense ionization. There are rare instances in which such events may have occurred.)

7.24 There exist striking distances to the phase conductor $\bar{r}_{sw}$ and to smooth earth $\bar{r}_{sg}$ which provide equal probability of completing the final path from the leader. In a limited critical region these are referred to the striking distance to the ground wire $\bar{r}_{sg}$ by the relations

$\bar{r}_{sw} = K_{sw} \bar{r}_{ss}$ for phase conductor W

$\bar{r}_{sg} = K_{sg} \bar{r}_{ss}$ for smooth earth plane

When the striking distances are associated with the critical prospective stroke current I_{oc} the values are denoted by the addition of the subscript c as in $\bar{r}_{sw_c}$ or r_{sg_c} corresponding to $\bar{r}_{ss_c}$

7.25 It is convenient to develop the main model relations assuming $\bar{r}_{sw} = \bar{r}_{ss}$ and include exceptions in a deviation analysis. If provision is made for $\bar{r}_{sg}$ to differ from $\bar{r}_{ss}$ and if all striking distances in the following development are defined to be critical mean values we can locate the ground (shield wire) such that the exposure arc is reduced to zero and

$$\sin \bar{\theta}_1 = \sin (\bar{\theta}_s + \bar{\beta}) = \frac{K_{sg}\bar{r}_{ss} - \bar{Y}}{\bar{r}_{ss}} \qquad (7.2\text{-}1)$$

$$\sin (\bar{\theta}_s + \bar{\beta} = K_{sg} - \bar{Y}/r_{ss} \qquad (7.2\text{-}2)$$

It is desirable to provide for deviations in $\bar{Y}$ (or even in $\bar{r}_{ss}$) so a deviation constant k is applied to the $\bar{Y}/\bar{r}_{ss}$ ratio to yield

$$\sin (\bar{\theta}_s + \bar{\beta}) = K_{sg} - K\bar{Y}/\bar{r}_{ss} \qquad (7.2\text{-}3)$$

$$\beta = \text{arc sin } \bar{C}/2\bar{r}_{ss} \qquad (7.2\text{-}4)$$

Then $\bar{\theta}_s = (\bar{\theta}_s + \bar{\beta}) - \bar{\beta}$ = critical shielding angle (7.2-5)

7.26 Figure 9 provides curves of equations (7.2-3), and (7.2-5) for various values of $\bar{\beta}$ through the factor $\bar{C}/\bar{r}_{sc}$ and assuming that K_{sg}=1. (This restriction and others are removed in Appendix 7.3) It is possible to use the curves of fig. 9 for a wide variety of deviations from the reference conditions assumed here by assigning an appropriate value to $K\bar{Y}/\bar{r}_s$. This figure thus assumes a key role in shielding design.

7.3 Deviation Analysis

This appendix considers three sorts of deviation from the reference analytical model; those arising from making the model itself more general, those arising from simple deviations from average geometry, and those arising from potential adjustments in basic assumptions. The last class can be considered in the nature of calibrations while retaining the usefulness of the curves of Fig. 9 pending advances in knowledge of striking distances from new theoretical or experimental studies.

7.31 The first and most important deviation to be considered arises directly from the Pathfinder data and the mean performance of samples lines over statistically significant periods of time. Since Fig. 9 shows critical shielding angles one cannot expect perfect shielding of such angles. Figure 14 shows that some shielding failures did indeed occur for small negative excess shielding angles (shielding angle margins). Approaching the margin problem from the opposite direction, Fig.15 shows that the the actual performance or the five lines of Table 7 closely parallels the estimated shielding failure rate. The difference is some combination of backflash events and exceptional shielding failure events. Taken together, these figures suggest that a shielding angle margin (negative excess-angle) between 5 and 10 degrees below the critical values of Fig. 9 should provide virtually complete freedom from shielding failure. (This conclusion assumes that all other known geometrical deviations have been included in reaching $\bar{\theta}_{sc}$). It is preferred at this time to avoid adjusting the mean striking distance relation in order to keep the various quantities as independent as possible pending further information. In the region near $\bar{Y}/\bar{r}_s = 1.00$, a deviation constant of

$K = 1.1$ provides about 6° margin

$K = 1.2$ provides about 11° margin

7.32 There are a number of possible deviations from the reference model which can influence the selection of the shielding angle. These are

7.321 Variation of conductor height above mean value

7.322 Striking distance $\bar{r}_{sw}$ / $\bar{r}_{ss}$

7.323 Striking distance $\bar{r}_{ss}$ / $\bar{r}_{sg}$

7.324 Mean ground angle $\bar{\theta}$ / 0

Since these variations are combined in various degrees in the Pathfinder field study it is impossible, in general, to separate their individual effects. In exceptional cases, however, the effects of some variations have been strikingly evident. Variations of conductor height in a single span above the mean value for the line have been responsible for some recorded shielding failures. (This important variation is discussed in Appendix 7.1). On the other hand, the presence of high trees along 70 percent of the right of way of one sample line greatly increased the effective striking distance to the reference earth so that no shielding failures have been recorded for the shielding angle of 63°. There is theoretical evidence, at least on the laboratory scale, that the striking distance from the leader to a plane earth should be about 0.8 of the striking distance to the tower or ground wire. There are two possible reasons why this effect is not evident in the Pathfinder results; (1) the earth is rarely, if ever, a smooth plane because of brush, rocks, fences, low trees, etc. and (2) the extrapolation of this difference to very large distances may not be valid. Indeed, when a value of K_{sg} = 0.9 was used to estimate shielding failure rates of existing lines the estimates proved excessive. For the present at least a value for K_{sg} of unity seems best.

Negative transverse ground angle can be an important deviation which should be taken into account to the extent justified by the proportion of the line affected. (In this case the conductors on the opposite side of the line may be favorably affected by a positive ground angle.) The simplest way to do this when the striking distances to ground wire and phase conductor are equal is to add the ground angle algebraically to the shielding angle determined for a horizental earth plane. Figure 10 shows the more general case where K_{sw} and K_{sg} are not unity.

Figure 12 shows the effect of various deviation factors relating to striking distances on the critical shielding angle. This shows that any assumed increase in the striking distance to the phase conductor calls for a decrease in the shielding angle. Such an increase could occur as a result of a single corona filament longer than the mean striking distance $\bar{r}_{ss}$. It is felt that this is an unobservable effect and that such variations can be included in the deviation factor used to determine the shielding angle margin as in Section 7.31.

7.33 The curves of figure 9 are widely applicable provided one enters them with the proper value of $K\bar{Y}/\bar{r}_{ss}$. The deviation factor K to be used depends, of course, on the nature of the values $\bar{Y}$ and $\bar{r}_{ss}$ used. As pointed out in 7.1, if $\bar{Y}$ is a highly stable number for rolling profile, or represents the maximum conductor height to be considered, then K simply accounts for unobservable effects (including variations from $\bar{r}_{ss}$) and should be assigned a value of 1.2. If, on the other hand, $\bar{Y}$ is a computed mean for the complete line, then the deviation of the maximum conductor height from its mean value can be included in the value for K. As an illustration, assume that the mean conductor height for the entire line yields a ratio $\bar{Y}/\bar{r}_{ss}$ of 0.6. Several valley and river crossings, however, bring this ratio for these spans to, say, 0.8. Then a pre-

liminary value of K from geometric considerations becomes

$$K_g = \frac{0.8}{0.6} = 1.33$$

Uncertainty of electrical considerations, including $\bar{r}_{ss}$ is included in the electrical deviation factor

$$K_e = 1.2$$

Then the final value of K to be used in entering figure 9 becomes

$$K = K_e K_g = 1.2 \times 1.33 \text{ and}$$

$$K\bar{Y}/\bar{r}_{ss} = K_e K_g \bar{Y}/\bar{r}_{ss} = 1.2 \times 1.33 \times 0.6$$

$$K\bar{Y}/\bar{r}_{ss} = 0.96$$

If the mean spacing ratio $\bar{c}/\bar{r}_{ss}$ is 0.4 the shielding angle should be approximately -10 degrees, which would accommodate the entire line. Alternatively, one might perhaps design a structure which could be readily adapted to the exceptional spans with -10 degrees shielding angle and provide the remainder of the line with a shielding angle determinined from

$$K = K_e = 1.2$$

$$K\bar{Y}/\bar{r}_{ss} = 1.2 \times 0.6 = 0.72$$

$$\bar{\theta}_s = +5 \text{ degrees.}$$

7.4 Statistical Studies

With few exceptions, the purpose of statistical studies has been to determine shielding angles associated with known superior lightning performance. Because of the large number of lines involved it has been impossible to determine the terrain and profile factors to the refinement obtainable for the individual spans involved in shielding failure events furnishing Pathfinder signals. Nevertheless, the mean conductor

heights and shielding angles of Table 3 have been estimated as carefully as possible and devided into two groups as shown below.

7.41 Parameters of Exceptional HV Lines

Item	Group 1	Group 2
Exposure in mile-years	38000	14000
Mean tripout rate*	0.17	0.25
Terrain evaluation	open or lightly wooded	lightly to moderately wooded
Mean $\bar{Y}/\bar{r}_{ss}$	0.42	0.57
Mean $\bar{c}/\bar{r}_{ss}$	0.18	0.25
Mean $\bar{\theta}_s$	21°	17°
Mean excess angle $\bar{\theta}_s - \bar{\theta}_{sc}$	-9°	-2°

*Adjusted to 40 thunderstorm days (very small adjustments involved)

These excess angles are consistent with Figures 14 and 15 and give further evidence that the basic curves of Figure 9 are useful design relations.

Table 7 shows a summary of performance for five lines of the Pathfinder study which have tower footing resistances under ten ohms. The exposure in kilometer years is sufficient to establish reasonably stable performance data which is shown in Figure 15 for the corresponding excess shielding angles. Reference has already been made to the trend shown in this figure and its use in estimating appropriate shielding angle margins.

A large scale extension of performance statistics to EHV lines, including 500 kV is needed to determine whether the data of this report can be reliably extrapolated to EHV, and ultimately to UHV lines.

7.42 Variability of Lightning Tripout Rates

It is well known that lightning tripout rates can be highly variable, yet one cannot always obtain large exposures in terms of mile-years. Figures 16 and 17 show the results of yearly, 5-year, 16-year and 25-year averages. These curves follow Poisson-like distribution curves. It seems possible to say that 5-year averages are reasonable values to use when more stable data are unavailable, but even here there is a substantial probability (20%) of actual 5-year rates from 20 to 70 percent higher than the "long-time" rate. (These data are given as illustrative of actual statitics and not as general conclusions.)

Tables 7 through 9 show detailed statistical studies for reference purposes.

7.5 Pathfinder Records

Table 10 presents a complete log of Pathfinder signals and associated data. The entire log has been very carefully reviewed with the result that a very few signals have been regrouped to change perhaps two or three interpretations. Occasionally a later report contains a signal obviously associated with a group reported earlier or inadvertently logged out of proper order.

8.0 List of References

During the course of the project, a great many references were reviewed. In addition, the results of current research by others has been drawn upon through the courtesy of other investigators. The following list includes only those specifically noted in the text or which support more general statements in this report.

1. AIEE Committee Report, "A Method of Estimating the Lightning Performance of Transmission Lines," A.I.E.E. Transactions, Vol. 69, Part II, 1950, pp 1187-96.

2. R. Lundholm, R. B. Finn, W. S. Price, "Calculation of Transmission Line Lightning Voltages by Field Concepts," AIEE Transactions, Part III (Power Apparatus and Systems), Vol. 76, 1957, pp 1271-83.

3. C. F. Wagner, A. R. Hileman "A New Approach to the Calculation of the Lightning Performance of Transmission Lines - Part III," AIEE Transactions, Part III (Power Apparatus and Systems) Vol. 79, Oct. 1960, pp 589-603.

4. R. Lundholm., "Over-voltage in a Direct Lightning Stroke to a Transmission Line Tower," Paper No. 333, CIGRE, Paris France,1958.

5. V. V. Burgsdorf,"Lightning Protection of Overhead Transmission Lines and Operating Experience in the U. S. S. R.," Paper No. 326, CIGRE, Paris, France, 1958.

6. C. J. Miller, "Anomalous Flashovers on Transmission Lines, " AIEE Transactions, Part III (Power Apparatus and Systems) Vol. 75, 1956, pp 897-907, See especially discussion by H. R. Armstrong, page 903.

7. Ohio Brass Company, Mansfield, Ohio, U. S. A., "Lightning Performance of Typical Transmission Lines" (Book) Second Edition, 1955.

8. F. Chambers, C. P. Almon, Jr., "Performance of 161 kV and 115 kV Transmission Lines," October 1962, pp 431-59. Covers 22 years and 6500 miles experience on lines of the Tennessee Valley Authority. Supplementary data for an additional five years have been privately furnished.

9. V. I. Levitov, el al, "Operational Experience on the 500 Kv Networks in the U.S.S.R.," Report No. 416, CIGRE, Paris, France, 1966.

10. G. W. Brown, E. R. Whitehead, "Field and Analytical Studies of Transmission Line Shielding - Part II" Transactions IEEE, Vol. 88, pp 617-26, May 1969.

11. J. R. Currie, Liew Ah Choy, M. Darveniza, "Monte Carlo Determination of the Frequency of Lightning Strokes and Shielding Failures on Transmission Lines, " Presented at the Winter Power Meeting of the IEEE Power Engineering Society, February 5, 1971, New York, N.Y. (To be published in the PAS Transactions).

12. R. H. Golde, K. Berger, D. J. Malan, C. F. Wagner, "Journal of the Franklin Institute," Special issue on Research on the Lightning Pheonomenon, Vol. 283, No. 6, June, 1967.

13. E. D. Sunde, "Earth Conduction Effects in Transmission Systems" (Book) Dover Publications, Inc., New York, N. Y.

14. F. Popolansky, "Measurement of Lightning Currents in Czechoslovakia and the Application of Obtained Parameters in the Prediction of Lightning Outages of EHV Transmission Lines", Paper No. 33-03 CIGRE, Paris, France, 1970.

15. M. A. Sargent, M. Darveniza, "The Calculation of Double Circuit Outage Rate of Transmission Lines," IEEE Transactions, (PA&S) Vol. 86, pp 665-78, June, 1967.

16. Liew Ah Choy, M. Darveniza, "A Sensitivity Analysis of Lightning Performance Calculations for Transmission Lines," paper 70TP615-PWR presented at the IEEE Summer Power Meeting and EHV Conference, Los Angeles, California, July 12-17, 1970.

17. J. G. Anderson, "Monte-Carlo Computer Calculation of Transmission Line Lightning Performance," IEEE Transactions (PA&S) Vol. 80, pp 414-20 August, 1961.

18. J. M. Clayton, F. S. Young "Estimating Lightning Performance of Transmission Lines" IEEE Transactions (PA&S), Vol. 83, pp 1102-10, November 1964.

19. F. S. Young, J. M. Clayton, A. R. Hileman, "Shielding of Transmission Lines," Trans. IEEE, Special Supplement, Vol. 825, pp 132-54, February, 1963.

20. R. H. Golde "The Frequency of Occurrence and Distribution of Lightning Flashes to Transmission Lines," Trans. IEEE, Vol. 64, Part III, pp 902-10 1945.

21. K. Berger, "Electric Requirements of Overhead Lines for Very High Voltages, " Bulletin S.E.V., (Zurich, Switzerland), Vol. 54, pp 749-54, 1963.

22. H. R. Armstrong, E. R. Whitehead, "Field and Analytical Studies of Transmission Line Shielding," Transaction IEEE (PA&S), Vol. 87, pp 270-81, January, 1968.

23. E. R. Whitehead, "Lighting Performance of EHV Lines" CIGRE Doc. 33-69(sc)- IWD, presented to Colleguiun of S. C. No. 33, Sydney, Australia, September, 1969.

24. A. Braunstein, "Lightning Strokes to Transmission Lines and Shielding Effects of Ground Wires," IEEE Transactions (PA&S) Vol. 89, No. 8, Nov./Dec. 1970, pp 1900-1910.

25. H. Baatz, "Der Wirksame Widestand Ausegehnter Eder bei Stossbeanspruchung," Electrotechnik, Vol. 2, No. 7, pp 185-89, July, 1948.

26. S. Devgan, "Analytical Models for Lumped and Distributed Grounding Systems" Thesis, Illinois Institute of Technology, January, 1970.

TABLE 5

GROUNDING CONDITIONS AND TYPE OF FAULT
FOR RECORDED BACKFLASH EVENTS

Pathfinder Operation Number	Single Circuit Single Conductor (ohms)	Single Circuit Multiple Conductor (ohms)	Double Circuit Multiple Conductor (ohms)	Reference Note Number
7-8-9	< 10			1
10-11			Counterpoise	2
15	2			3
16	< 10			3
18-19		4.2/6.2		1
20		250		4
21		140		4
29			37	5
33-34			Counterpoise	2
35	Counterpoise			2
36	Counterpoise			2
38	Counterpoise			2
41	X			2
42-43			X	2-6
44-45	X			2
46-47			Counterpoise	2
48	X			2
51-52			Counterpoise	2
54		< 10		3

TABLE 5 (Continued)

GROUNDING CONDITIONS AND TYPE OF FAULT
FOR RECORDED BACKFLASH EVENTS

Pathfinder Operation Number	Single Circuit Single Conductor (ohms)	Single Circuit Multiple Conductor (ohms)	Double Circuit Multiple Conductor (ohms)	Reference Note Number
63-64			Counterpoise	2
80-81			X	2
83-84			Counterpoise	2
85-86			Counterpoise	2
88-89-90	3 ohms			1
94-95			3.5 ohms	
98	< 1			
99	6			
100	8			
101	X			2
102	3.5			
104	< 10			
105-106			< 10	
109	< 10			
114-115			X	2
115	X			2
117	X			2

TABLE 5 (Continued)

GROUNDING CONDITIONS AND TYPE OF FAULT
FOR RECORDED BACKFLASH EVENTS

Pathfinder Operation Number	Single Circuit Single Conductor (ohms)	Single Circuit Multiple Conductor (ohms)	Double Circuit Multiple Conductor (ohms)	Reference Note Number
118-119			X	2
120	Counterpoise			2
121-2-3-4	Counterpoise			1-2
131			Counterpoise	
135-136			2.5	7
137-138			3.0	7

Notes:

(1) Sequential towers - probably positive polarity stroke.
(2) Individual tower resistances high but unknown.
(3) Black signal only - probably very short time current pulse.
(4) Three-conductor to ground fault (L_1 L_2 L_3 G).
(5) Second circuit flashover not on instrumented conductor.
(6) Simultaneous red signals, denoting a positive polarity stroke.
(7) Exceptional records. Double circuit tripout on 345 kV line with very low ground resistance.

TABLE 6

ELECTROGEOMETRIC DATA AND REFERENCE MODEL ANALYSIS OF RECORDED SHIELDING FAILURE EVENTS FOR $K_{sg} = K = 1.0$

Number S. F. Strokes	Co. Code	$\bar{H}$ ft.	$\bar{H}$ m	$\bar{Y}$ ft.	$\bar{Y}$ m	$\bar{C}$ ft.	$\bar{C}$ m	$\bar{r}_{sc}$ ft.	$\bar{r}_{sc}$ m	$\bar{H}/\bar{r}_{sc}$	$\bar{Y}/\bar{r}_{sc}$	$\bar{C}/\bar{r}_{sc}$	$\bar{\theta}_s$ deg.	$\bar{\theta}_{sc}$ deg.	$\bar{\theta}_s - \bar{\theta}_{sc}$ deg.
11	A	67	20.4	58	17.7	12.5	3.8	71	21.6	0.94	0.82	0.18	44	5	39
1	B	76	23.2	66	20.1	14.0	4.3	64	19.5	1.19	1.03	0.22	45	-7	52
1	D	120	36.6	95	29.0	32.0	9.7	128	39.0	0.94	0.74	0.25	33	9	24
11	D	128	39.0	101	30.5	32.0	9.7	128	39.0	1.00	0.79	0.25	33	6	27
4	D	136	41.5	110	33.6	32.0	9.7	128	39.0	1.06	0.86	0.25	33	1	32
3	D	147	45.0	118	36.0	32.0	9.7	128	39.0	1.15	0.92	0.25	33	-2	35
1	E	82	25.0	68	20.8	19.0	5.8	84	25.6	0.97	0.81	0.23	42	5	37
1	E	86	26.2	68	20.8	22.0	6.7	84	25.6	1.02	0.81	0.26	35	4	31
1	E	85	25.9	70	21.4	22.0	6.7	84	25.6	1.01	0.83	0.26	40	2	38
1	F	138	42.0	107	32.6	31.0	9.4	84	25.6	1.64	1.27	0.37	7	-28	35
1	F	126	38.4	103	31.4	23.0	7.0	84	25.6	1.50	1.23	0.27	9	-21	30
3	G	66	20.2	55	16.8	15.0	4.6	68	20.8	0.97	0.81	0.22	42	5	37
2	H	63	19.2	53	16.1	12.5	3.8	63	19.2	1.00	0.84	0.20	38	4	34
1	I	113	34.4	50	15.2	68.0	20.7	132	40.0	0.85	0.38	0.51	21	22	-1
1	J	140	42.7	81	24.7	63.0	19.2	128	39.0	1.09	0.63	0.49	22	7	15
3	K	100	30.5	75	22.8	25.0	7.6	93	28.3	1.08	0.81	0.27	0	3	-3

TABLE 7

ELECTROGEOMETRIC PARAMETERS FOR FIVE HV AND EHV LINES WITH TOWER FOOTING RESISTANCES UNDER 10 OHMS

Line Code	A	J	J	D	K
Number of Circuits	2	1	2	2	2
Line kV	120	230	345	345	120
BIL kV	790	1500	1600	1600	1100
Height $\bar{H}$ - m	20.4	27.5	43.0	43.0	30.5
Height $\bar{Y}$ - m	17.7	16.5	28.5 (2)	35.0	22.8
Spacing $\bar{C}$ - m	3.80	12.5	15.5 (2)	10.-	7.6
Striking $\bar{r}_s$ - m	19.5	37.0	39	39.0	28.0
Mean $\bar{\theta}_s$ - deg.	44	15	20 (2)	31	0.0
Mean $\bar{\theta}_{sc}$ - deg.	0	20	4	-1	4.0
No. ground wires	1	2	2	1	2
T. D. per year	37	40	43	40	85
Kilometer years	1320	5900	1573	1365	700
Actual tripout rate	5.15	0.24	3.7	5.7	2.8
Est. S.F. Rate (1)	5.0	0.0	3.3	4.5	0.0
Profile Distribution					
% Flat	100	50	50	75	100
% Rolling	--	50	50	16	--
% Mountainous	--	--	--	9	--

NOTES: (1) Estimated by interpolation or extrapolation from Figures 18-22. Tripout rate = 0.9 spark-over rate.

(2) Mean values for top and middle conductors. See Figure

90004260

TABLE 8

LIGHTNING TRIPOUTS FOR 25 YEARS

COMPANY CODE J CIGRE LINE CODE 30

Line Length - 236 km p = 0.0024 Np = 0.57 S.T.R.= 0.24

Number and Percent Equalling or Exceeding
Number of Tripouts Indicated

Number of Tripouts	One Year				Five Years			
	No.	S.T.R.	%	P%	No.	S.T.R.	%	% (P)
0	25	0.00	100	100	21	0.000	100	100
1	10	0.42	40	46	21	0.085	100	100
2	2	0.85	8	11	16	0.170	76	78
3	0	1.27	0	2	14	0.255	67	54
4	|	|	|	|	8	0.340	38	32
5	|	|	|	|	3	0.425	14	16
6	|	|	|	|	1	0.510	5	7
7	|	|	|	|	1	0.595	5	3

P = Probability of tripout for one kilometer-year
N = Number of kilometer-years
Np = Expectation of tripout for N km-years
S.T.R. - Specific tripout rate = tripouts per 100 kilometer years
%(P) Theoretical Poisson distribution

TABLE 9 LINE CODE A

Year	Trip-outs	Lightning Specific Rate Averaged for Number of Years Indicated															
		1	2	3	4	5	6	7	8	9	10	11	12	13	14	15	16
1968	5	6.05															
1967	3	3.63	4.85														
1966	2	2.42	3.04	4.00													
1965	6	7.26	4.85	4.45	4.85												
1964	2	2.42	4.85	4.00	3.94	4.36											
1963	7	8.50	5.45	6.05	5.15	4.85	5.05										
1962	3	3.63	6.05	4.85	5.45	4.85	4.64	4.85									
1961	3	3.63	3.63	5.25	4.55	5.10	4.65	4.50	4.70								
1960	4	4.85	4.25	4.00	5.15	4.60	5.05	4.68	4.55	4.70							
1959	4	4.85	4.85	4.45	4.24	5.10	4.64	5.00	4.70	4.68	4.72						
1958	2	2.42	3.63	4.05	3.94	3.9	3.64	4.35	4.70	4.45	4.36	4.50					
1957	4	4.85	3.63	4.05	4.24	4.1	4.00	4.68	4.40	.70	4.48	4.40	4.55				
1956	9	10.9	7.90	6.05	5.75	5.6	5.25	5.00	5.45	5.12	5.33	5.10	4.95	5.05			
1955	4	4.85	7.90	6.85	5.75	5.6	5.45	5.20	5.00	5.37	5.10	5.30	5.05	4.97	5.00		
1954	5	6.05	5.45	7.27	6.66	5.8	5.65	5.80	5.30	5.12	5.45	5.18	5.35	5.12	5.00	5.15	
1953	5	6.05	6.05	5.65	6.80	5.55	5.85	5.70	5.60	5.37	5.20	5.50	5.25	5.40	5.20	5.15	5.15

TABLE 10

LOG OF PATHFINDER SIGNALS AND ASSOCIATED DATA

Numbers			R or	Geometry			Signals			Tripout		Conductors			Circuits		
Signal	Stroke	Tower	C P	H̄	Ȳ	Ōs	R	G	B	Yes	No	T	M	B	1	2	Note
A 1	1	200	R< 10	67	58	44	x	-	x	x	-	x	-	-	x	-	
2	1	201	R< 10	67	58	44	x	-	x	-	-	x	-	-	x	-	
3	2	262	R< 10	67	58	44	x	-	x	x	-	x	-	-	x	-	
4	3	271	R< 10	67	58	44	x	-	x	x	-	x	-	-	x	-	
5	3	272	R< 10	67	58	44	x	-	-	x	-	x	-	-	x	-	
6	4	312	R< 10	67	58	44	x	-	-	-	x	x	-	-	x	-	
B 7	5	99	R< 10	70	58	45	x	-	x	x	-	x	-	-	x	-	
8	5	100	R< 10	70	58	45	x	-	-	x	-	x	-	-	x	-	
9	5	101	R< 10	70	58	45	x	-	x	x	-	x	-	-	x	-	
C 10	6	85	C P	65	56	63	-	x	-	x	-	x	-	-	-	x	1
11	6	85	C P	65	56	63	-	x	-	x	-	x	-	-	-	-	
D 12	7	53	1.0	129	102	33	x	-	x	x	-	x	-	-	x	-	
13	8	79	2.5	129	102	33	x	-	x	x	-	x	-	-	x	-	
14	9	106	1.5	120	102	33	x	-	x	x	-	x	-	-	x	-	
15	10	184	2.0	136	110	34	-	-	x	x	-	x	-	-	x	-	2
B 16	11	136	R< 10	78	68	45	-	-	x	x	-	x	-	-	x	-	2
17	12	81	-	82	68	42	x	-	x	x	-	x	-	-	x	-	
18	13	59	4.2	86	68	35	x	-	-	-	-	x	-	x	x	-	
19	13	61	6.2	86	68	35	x	-	x	x	-	x	-	x	x	-	
20	14	318	250	91	68	28	-	x	x	x	-	x	x	x	x	-	

TABLE 10 (Continued)

LOG OF PATHFINDER SIGNALS AND ASSOCIATED DATA

Numbers			R or	Geometry			Signals			Tripout		Con-ductors			Cir-cuits		
Signal	Stroke	Tower	C P	$\bar{H}$	$\bar{r}$	θ_s	R	G	B	Yes	No	T	M	B	1	2	Note
E 21	15	255	140	86	68	35	-	x	x	x	-	x	x	x	x	-	
B 22	16	114	-	76	66	45	x	-	-	x	-	x	-	-	x	-	
23	16	115	-	76	66	45	x	-	x	x	-	x	-	-	x	-	
F 24	17	93	4.0	138	107	7	x	-	x	x	-	x	-	-	x	-	
25	17	94	8.5	138	107	7	x	-	x	x	-	x	-	-	x	-	
A 26	18	239	R<10	67	58	44	x	-	-	x	-	x	-	-	x	-	
27	18	240	R<10	67	58	44	x	-	x	x	-	x	-	-	x	-	3
28	19	260	R<10	67	58	44	x	-	x	x	-	x	-	-	x	-	4
E 29	20	215	37	92	68	27	-	x	x	x	-	x	-	-	-	x	5
G 30	21	139	-	66	55	42	x	-	x	x	-	x	x	-	x	-	
31	21	140	-	66	55	42	x	-	-	x	-	x	x	-	x	-	
H 32	22	138	C P	63	53	38	x	-	-	-	x	x	-	-	x	-	
33	23	217	C P	63	53	38	-	x	x	x	-	x	-	-	-	x	
34	23	217	C P	63	53	38	-	x	x	x	-	x	-	-	-	-	
35	24	171	C P	63	53	38	-	x	x	x	-	x	-	-	x	-	
36	25	168	C P	63	53	38	-	x	x	x	-	x	-	-	x	-	
D 37	26	88	3.5	122	95	32	x	-	x	x	-	x	-	-	x	-	
C 38	27	227	C P	65	56	63	-	x	x	x	-	x	-	-	x	-	
A 39	28	308	R<10	67	58	44	x	-	-	-	x	x	-	-	x	-	
I 40	29	31/4	1.5	113	50	21	x	-	-	x	-	-	x	-	x	-	

TABLE 10 (Continued)

LOG OF PATHFINDER SIGNALS AND ASSOCIATED DATA

Numbers			R or	Geometry			Signals			Tripout		Conductors			Circuits		
Signal	Stroke	Tower	C P	$\bar{H}$	$\bar{Y}$	$\bar{\theta}_s$	R	G	B	Yes	No	T	M	B	1	2	Note
G 41	30	98	-	65	55	42	-	x	x	x	-	x	-	-	x	-	
42	31	19	-	65	55	42	x	-	-	x	-	x	-	-	-	x	6
43	31	19	-	65	55	42	x	-	-	x	-	x	-	-	-	-	
44	32	23	-	65	55	42	-	x	-	x	-	x	-	-	x	-	
45	32	24	-	65	55	42	-	x	x	x	-	x	-	-	x	-	
46	33	46	-	65	55	42	-	x	x	x	-	x	-	-	-	x	
47	33	46	-	65	55	42	-	x	x	x	-	x	-	-	-	-	
48	34	64	-	65	55	42	-	x	-	x	-	x	-	-	x	-	
E 49	35	29	13.2	85	70	40	x	-	-	x	-	x	x	-	x	-	
50	35	30	32.0	85	70	40	x	-	x	x	-	x	x	-	x	-	
C 51	36	231	C P	65	56	63	-	x	x	x	-	x	x	x	-	x	
52	36	231	C P	65	56	63	-	-	x	x	-	x	-	-	-	-	
A 53	37	267	R<10	67	58	44	x	-	x	x	-	x	-	-	x	-	
54	38	280	R<10	67	58	44	-	-	x	x	-	x	x	-	x	-	2
J 55	39	118	R<10	140	81	22	x	-	x	x	-	-	x	-	x	-	
56	39	119	R<10	140	81	22	x	-	-	x	-	-	x	-	x	-	
D 57	40	9	R<10	128	101	33	x	-	x	x	-	x	-	-	x	-	
58	40	10	R<10	128	101	33	x	-	x	x	-	x	-	-	x	-	
59	41	17	R<10	128	101	33	x	-	x	x	-	x	-	-	x	-	
60	41	18	R<10	128	101	33	x	-	x	x	-	x	-	-	x	-	
61	42	71	R<10	128	113	34	x	-	x	x	-	x	-	-	x	-	

TABLE 10 (Continued)

LOG OF PATHFINDER SIGNALS AND ASSOCIATED DATA

	Numbers			R or	Geometry			Signals			Tripout		Con-ductors			Cir-cuits		
	Signal	Stroke	Tower	C P	$\bar{H}$	$\bar{Y}$	θ_s	R	G	B	Yes	No	T	M	B	1	2	Note
D	62	42	72	R<10	128	113	34	x	-	-	x	-	x	-	-	x	-	
H	63	43	80	C P	63	53	38	-	x	x	x	-	x	-	-	-	x	
	64	43	80	C P	63	53	38	-	x	-	x	-	x	-	-	-	-	
D	65	44	92	2.0	128	102	34	x	-	x	x	-	x	-	-	x	-	
	66	44	93	1.5	128	102	34	x	-	-	x	-	x	-	-	x	-	
	67	45	99	2.5	128	102	34	x	-	x	x	-	x	-	-	x	-	
	68	46	103	1.5	120	102	33	x	-	-	x	-	x	-	-	x	-	
	69	46	104	2.5	120	102	33	x	-	-	x	-	x	-	-	x	-	
	70	47	117	2.0	128	102	33	x	-	-	x	-	x	-	-	x	-	
	71	47	118	2.0	128	102	33	x	-	x	x	-	x	-	-	x	-	
	72	48	165	1.5	128	102	33	x	-	x	x	-	x	-	-	x	-	
	73	48	166	1.5	128	102	33	x	-	x	x	-	x	-	-	x	-	
	74	49	204	1.0	147	118	33	-	-	x	x	-	x	-	-	x	-	
	75	49	205	3.5	147	118	33	x	-	-	x	-	x	-	-	x	-	
G	76	50	53	-	66	55	42	x	-	x	x	-	x	-	-	-	x	
	77	50	53	-	66	55	42	-	x	-	x	-	x	-	-	-	-	
	78	51	55	-	66	55	42	x	-	-	-	x	-	-	-	x	-	
	79	52	101	-	66	55	42	x	-	-	-	x	-	-	-	x	-	
	80	53	51	-	66	55	42	-	x	x	x	-	x	-	-	-	x	
	81	53	51	-	66	55	42	-	x	x	x	-	x	-	-	-	-	

TABLE 10 (Continued)

LOG OF PATHFINDER SIGNALS AND ASSOCIATED DATA

Numbers			R or	Geometry			Signals			Tripout		Conductors			Circuits		
Signal	Stroke	Tower	C P	$\bar{H}$	$\bar{Y}$	$\bar{\theta}s$	R	G	B	Yes	No	T	M	B	1	2	Note
G 82	54	50	-	66	55	42	x	x	-	?	?	x	-	-	x	-	7
C 83	55	362	C P	65	56	63	-	x	x	x	-	x	-	x	-	x	
84	55	362	C P	65	56	63	-	x	x	x	-	x	-	x	-	-	
85	56	230	C P	65	56	63	-	-	x	x	-	x	-	-	-	x	
86	56	230	C P	65	56	63	-	-	z	z	-	x	-	-	-	-	
D 87	57	267	215	138	110	33	x	-	x	x	-	x	-	-	x	-	
K 88	58	34	-	100	75	0	x	-	-	x	-	x	-	-	x	-	
89	58	35	3	100	75	0	x	-	-	x	-	x	-	-	x	-	
90	58	37	-	100	75	0	x	-	-	x	-	x	-	-	x	-	
91	59	295	-	100	75	0	x	-	-	x	-	x	-	-	x	-	
92	59	296	-	100	75	0	x	-	x	x	-	x	-	-	x	-	
93	59	297	-	100	75	0	-	-	x	x	-	x	-	-	x	-	
94	60	141	3.5	100	75	0	-	x	x	x	-	x	-	-	-	x	
95	60	141	-	100	75	0	-	x	x	x	-	x	-	-	-	-	
96	61	322	0.5	100	75	0	-	-	x	x	-	x	-	-	x	-	
97	61	321	0.5	100	75	0	x	-	x	x	-	x	-	-	x	-	
98	62	208	0.5	100	75	0	-	x	-	x	-	x	-	-	x	-	
99	63	124	6.0	100	75	0	-	x	x	x	-	x	-	-	x	-	
100	64	236	8.0	100	75	0	-	x	-	x	-	x	-	-	x	-	
G 101	65	95	-	66	55	42	-	x	x	x	-	x	-	-	x	-	

TABLE 10 (Continued)

LOG OF PATHFINDER SIGNALS AND ASSOCIATED DATA

Numbers			R or	Geometry			Signals			Tripout		Conductors			Circuits		
Signal	Stroke	Tower	C P	$\bar{H}$	$\bar{Y}$	θ_s	R	G	B	Yes	No	T	M	B	1	2	Note
K 102	66	232	-	102	73	0	x	-	-	-	x	x	-	-	x	-	
103	67	78	4.0	102	74	0	x	x	-	-	x	x	-	-	x	-	7
104	68	36	3.5	102	74	0	-	x	-	-	-	-	-	-	x	-	
105	69	140	R<10	102	74	0	-	-	x	x	-	x	-	-	-	x	
106	69	140	R<10	102	74	0	-	-	x	x	-	x	-	-	-	-	
107	70	319	R<10	102	74	0	-	-	x	x	-	x	-	-	x	-	
108	70	320	R<10	102	74	0	-	-	x	x	-	x	-	-	x	-	
109	71	19	R<10	102	74	0	-	-	x	x	-	x	-	-	x	-	
D 110	72	242	R<10	140	111	33	x	-	x	x	-	x	-	-	x	-	
111	73	263	R<10	160	131	33	x	-	x	x	-	x	-	-	x	-	
E 112	74	75	R<10	91	72	34	x	-	x	x	-	x	-	-	x	-	
113	74	74	R<10	91	72	34	x	-	-	x	-	x	-	-	x	-	
G 114	75	56	-	66	55	42	-	x	x	x	-	x	-	-	-	x	
116	75	56	-	66	55	42	-	x	x	x	-	x	-	-	-	-	
115	76	58	-	66	55	42	-	-	x	x	-	x	-	-	x	-	
117	77	60	-	66	55	42	-	x	x	x	-	x	-	-	x	-	
118	78	182	-	66	55	42	-	x	x	x	-	x	-	-	-	x	
119	78	182	-	66	55	42	-	x	x	x	-	x	-	-	-	-	
H 120	79	185	C P	63	53	38	x	-	x	x	-	x	-	-	x	-	
121	80	188	C P	63	53	38	x	-	x	-	x	-	-	-	x	-	

TABLE 10 (Continued)

LOG OF PATHFINDER SIGNALS AND ASSOCIATED DATA

	Numbers			R or	Geometry			Signals			Tripout		Con-ductors			Cir-cuits		
	Signal	Stroke	Tower	C P	$\bar{H}$	$\bar{Y}$	$\bar{\theta}s$	R	G	B	Yes	No	T	M	B	1	2	Note
H	122	80	189	C P	63	53	38	x	-	-	-	x	-	-	-	x	-	
	123	80	189	C P	63	53	38	x	-	-	-	x	-	-	-	x	-	
	124	80	191	C P	63	53	38	x	-	-	-	x	-	-	-	x	-	
	125	81	239	2.0	147	118	33	x	-	x	x	-	x	-	-	x	-	
	126	82	245	2.0	147	118	33	x	-	x	x	-	x	-	-	x	-	
	127	82	246	2.0	147	118	33	x	-	-	x	-	x	-	-	x	-	
A	128	83	234	R<10	67	58	44	x	-	x	x	-	x	-	-	x	-	
	129	83	235	R<10	67	58	44	x	-	x	x	-	x	-	-	x	-	
	130	84	203	R<10	67	58	44	x	-	x	x	-	x	-	-	x	-	
C	131	85	223	C P	65	56	63	-	-	x	x	-	x	?	?	x	-	
F	132	86	58	R<10	126	103	9	x	-	x	x	-	x	-	-	x	-	
	133	86	60	R<10	126	103	9	x	-	x	x	-	x	-	-	x	-	
D	134	87	78	R<10	130	100	33	x	-	x	x	-	x	-	-	x	-	
	135	88	98	2.5	120	102	33	-	x	x	x	-	x	-	-	-	x	
	136	88	98	2.5	120	102	33	-	x	x	x	-	x	-	-	-	-	
	137	89	100	3.0	120	102	33	-	x	x	x	-	x	-	-	-	x	
	138	89	100	3.0	120	102	33	-	x	x	x	-	x	-	-	-	-	

Please see next page for notes.

Letter code before a signal number denotes participating company.

R = Red Pathfinder Signal
G = Green Pathfinder Signal
B = Blackfinder Signal

T = Top Conductor
M = Middle Conductor
B = Bottom Conductor

NOTES

(1) Individual tower resistances
(2) Current-time area below instrument threshold for impulse signal
(3) Records unclear on breaker operation
(4) Tower identification questionable
(5) M or B Conductor on other circuit
(6) Positive polarity stroke
(7) Instrument malfunction or current reversal

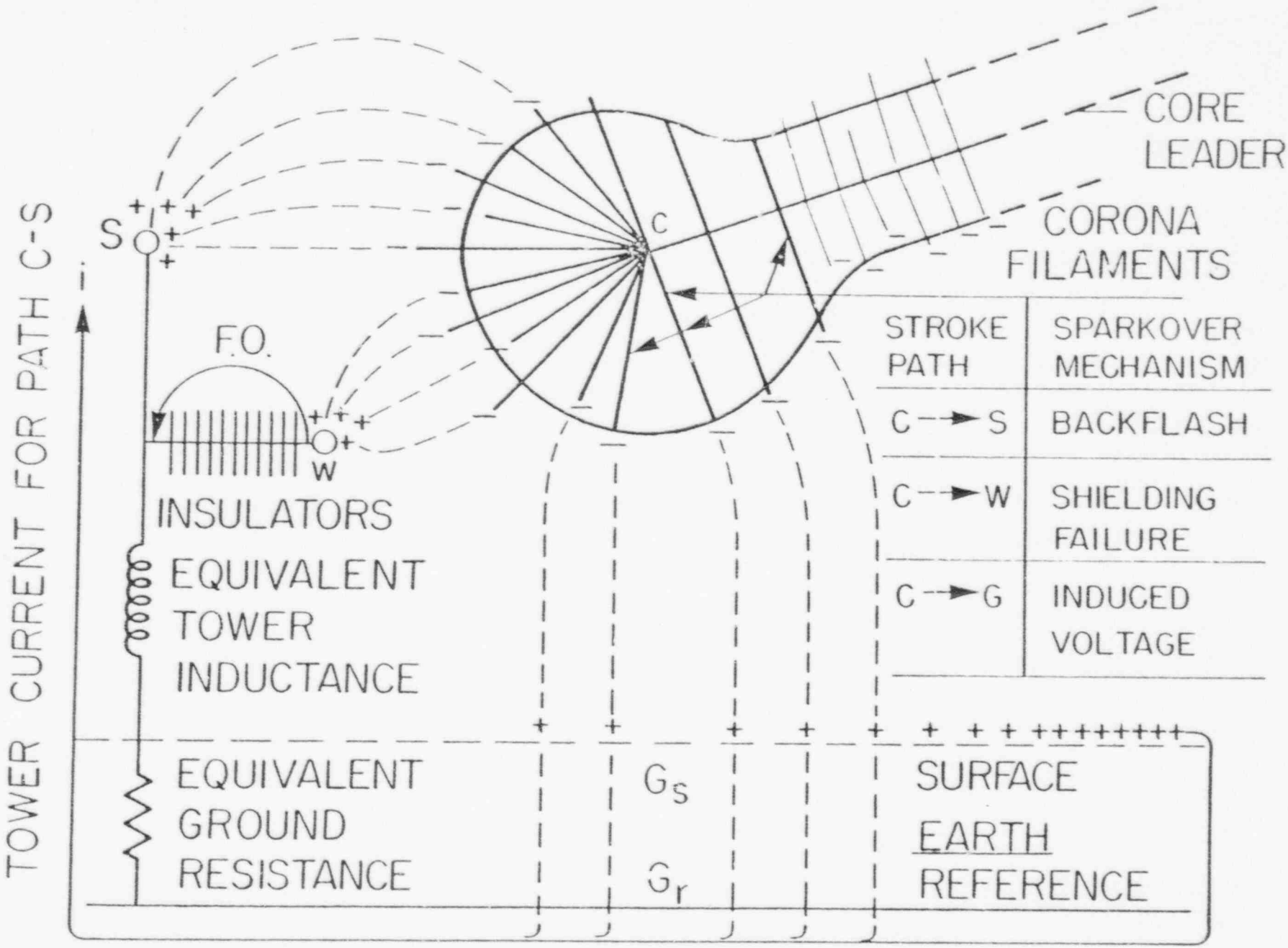

Fig. 1 MECHANISMS OF LIGHTNING SPARKOVER

STROKE TO TOWER OR GROUND WIRE - S

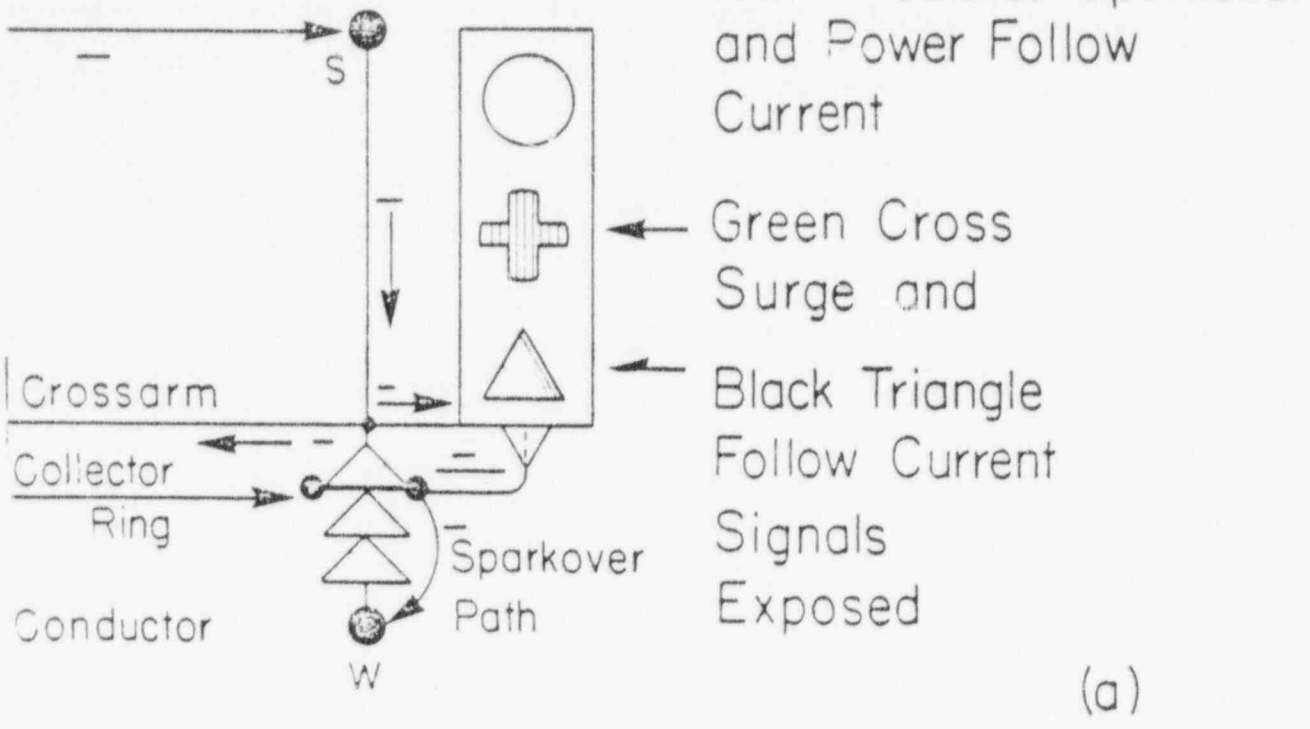

(a)

STROKE TO PHASE CONDUCTOR - W

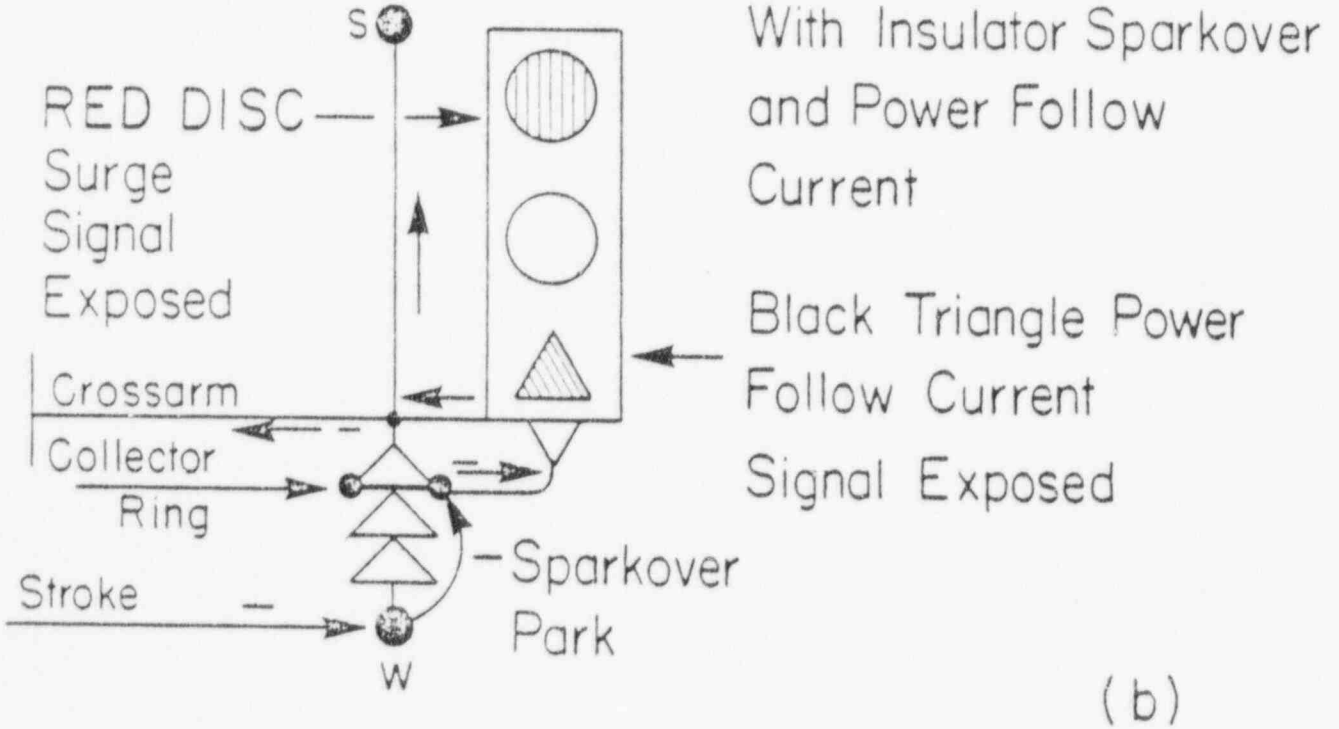

(b)

Fig. 2 CURRENT PATHS FOR INSULATOR SPARKOVER

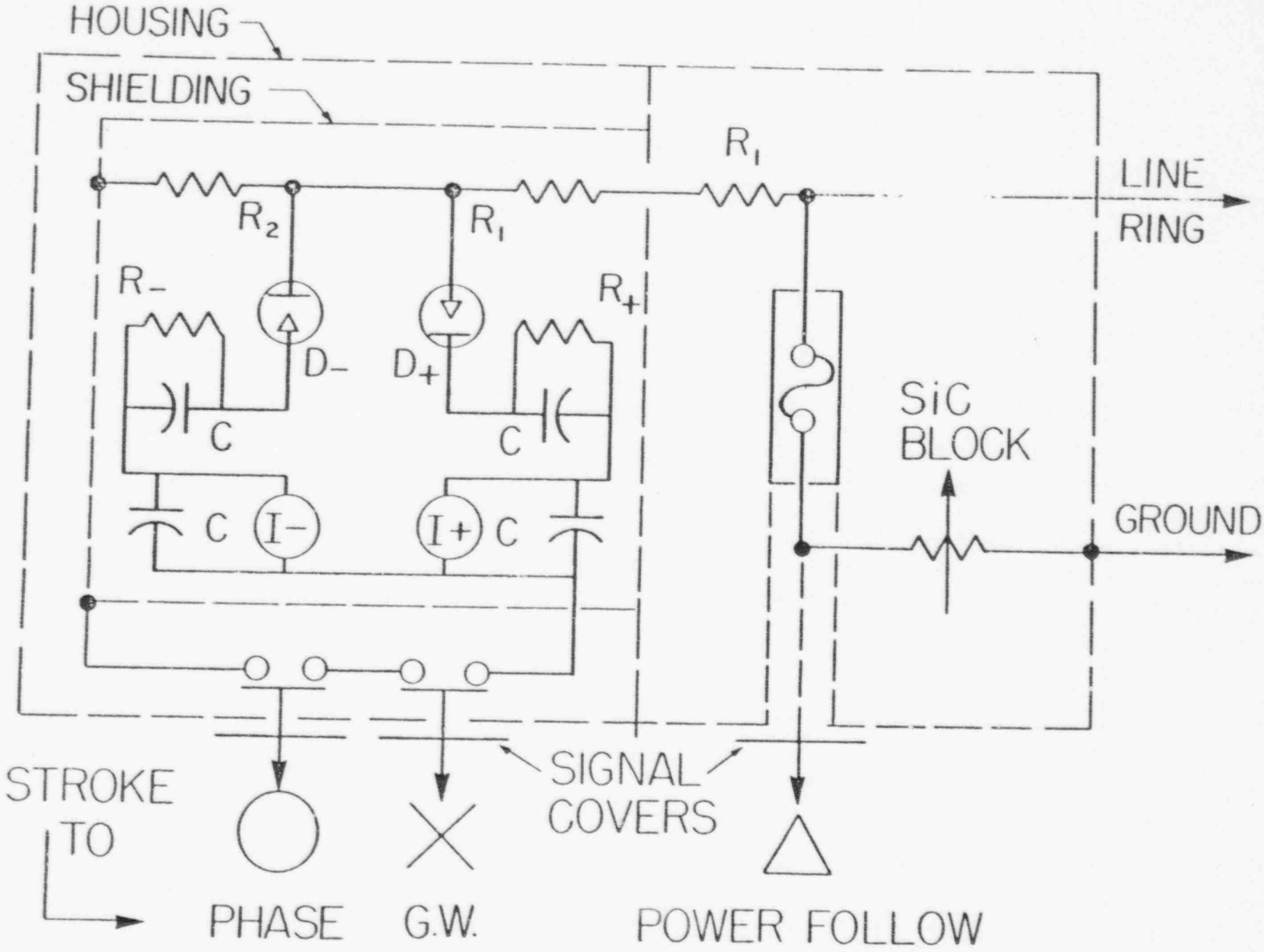

Fig. 3 PATHFINDER CIRCUIT

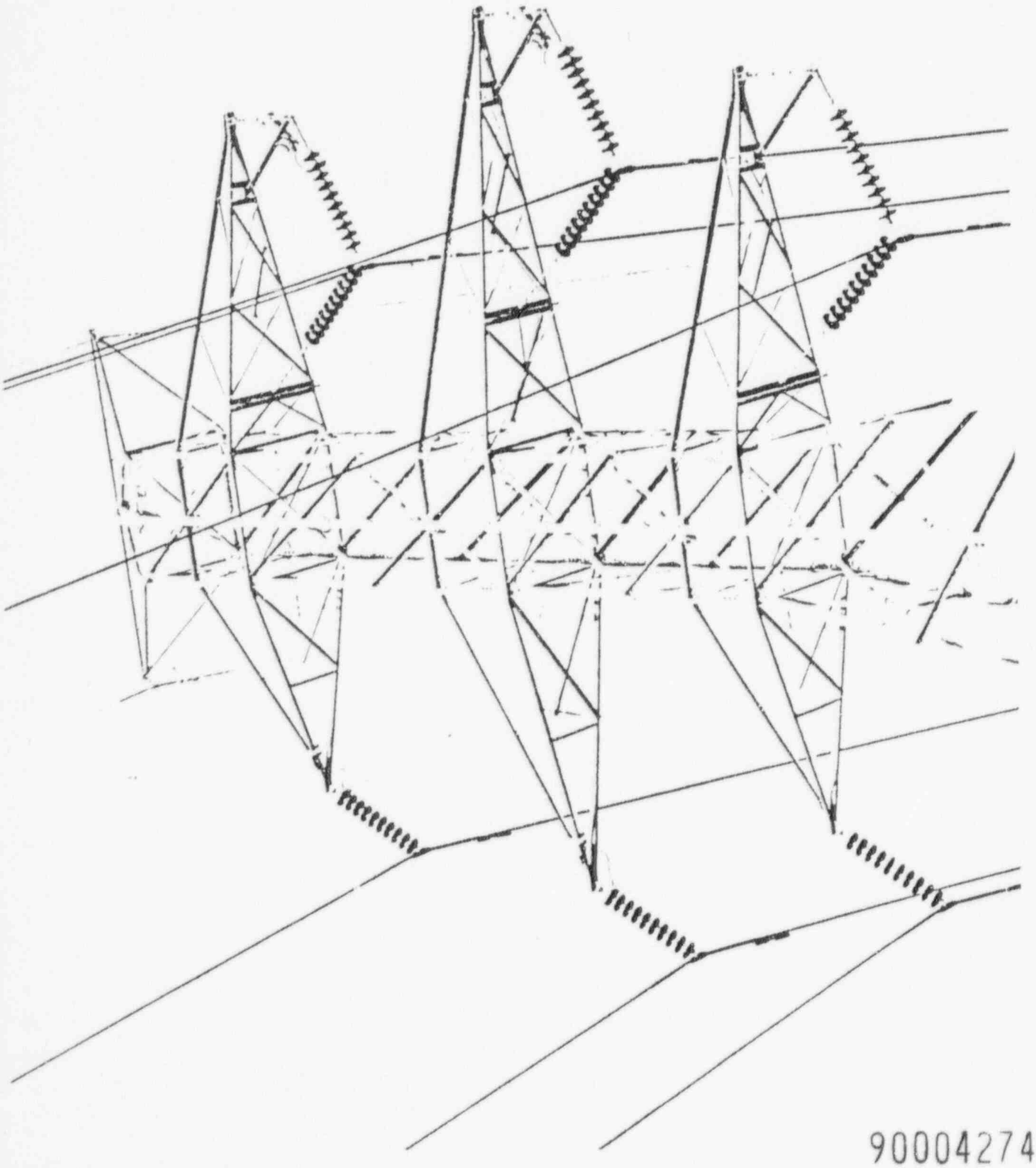

90004274

Fig. 4 PATHFINDER ON 138 kV TOWER

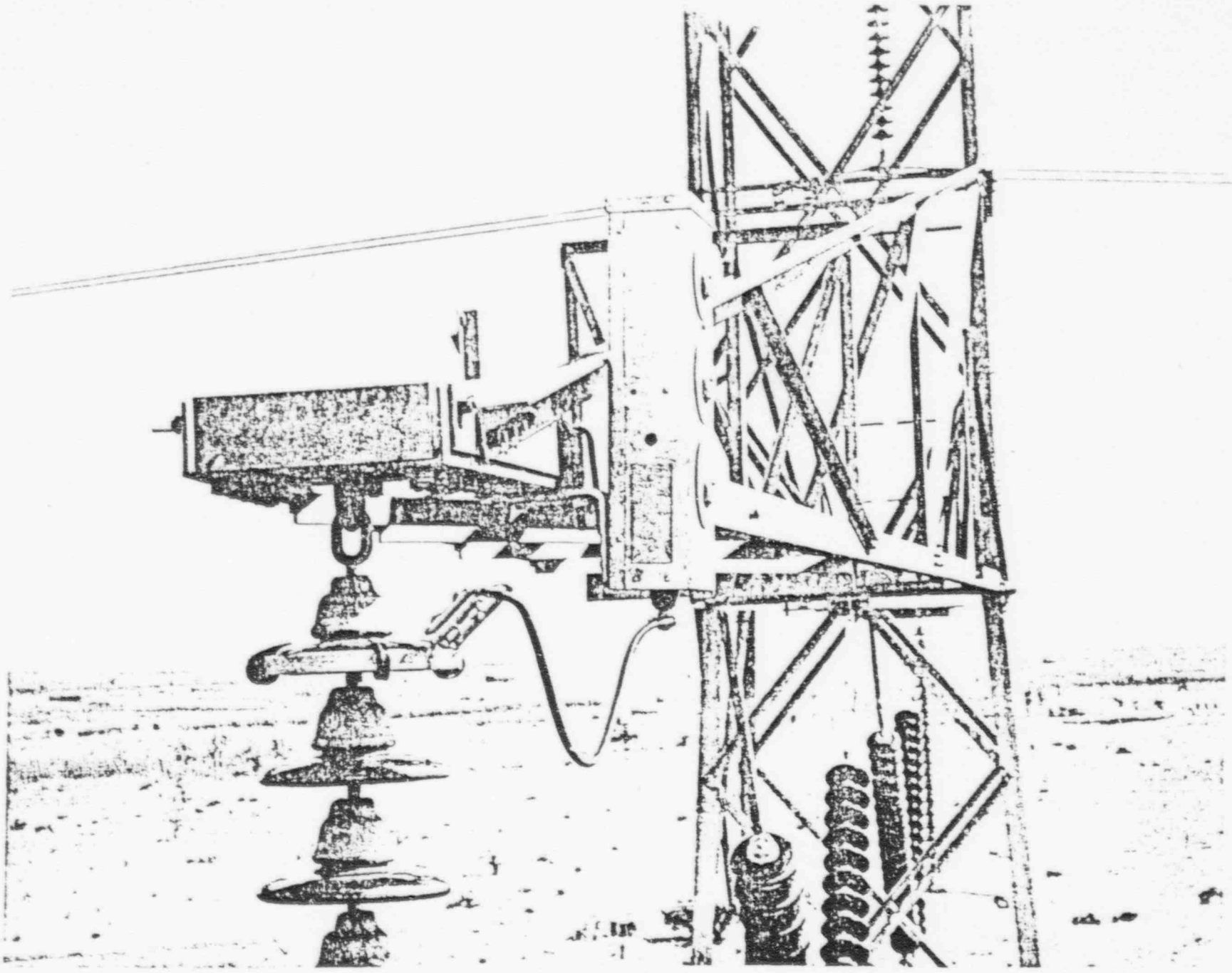

Fig. 5 PATHFINDER ON 345 kV TOWER

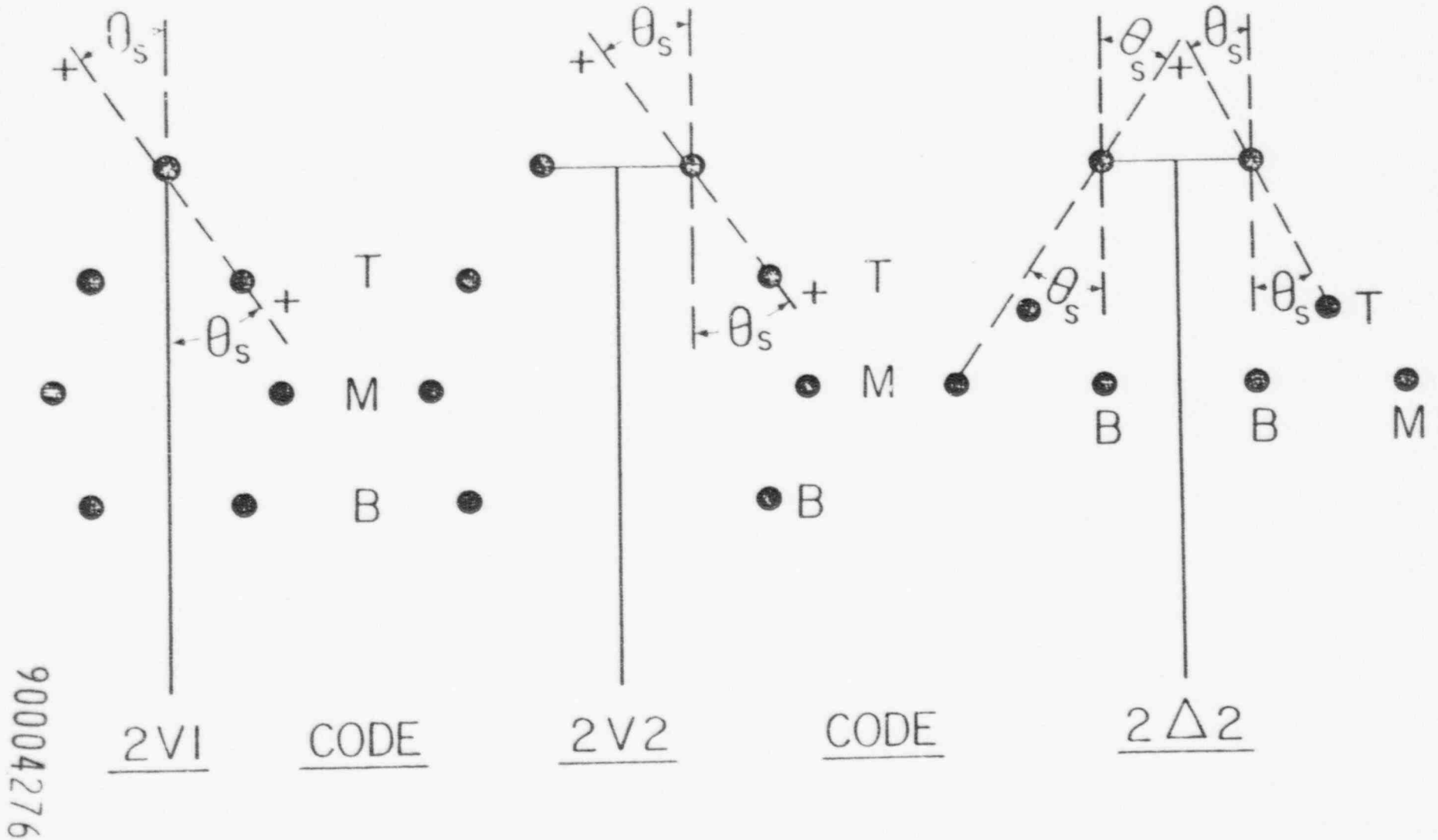

Fig. 6 TRANSMISSION LINE CONFIGURATION CODES

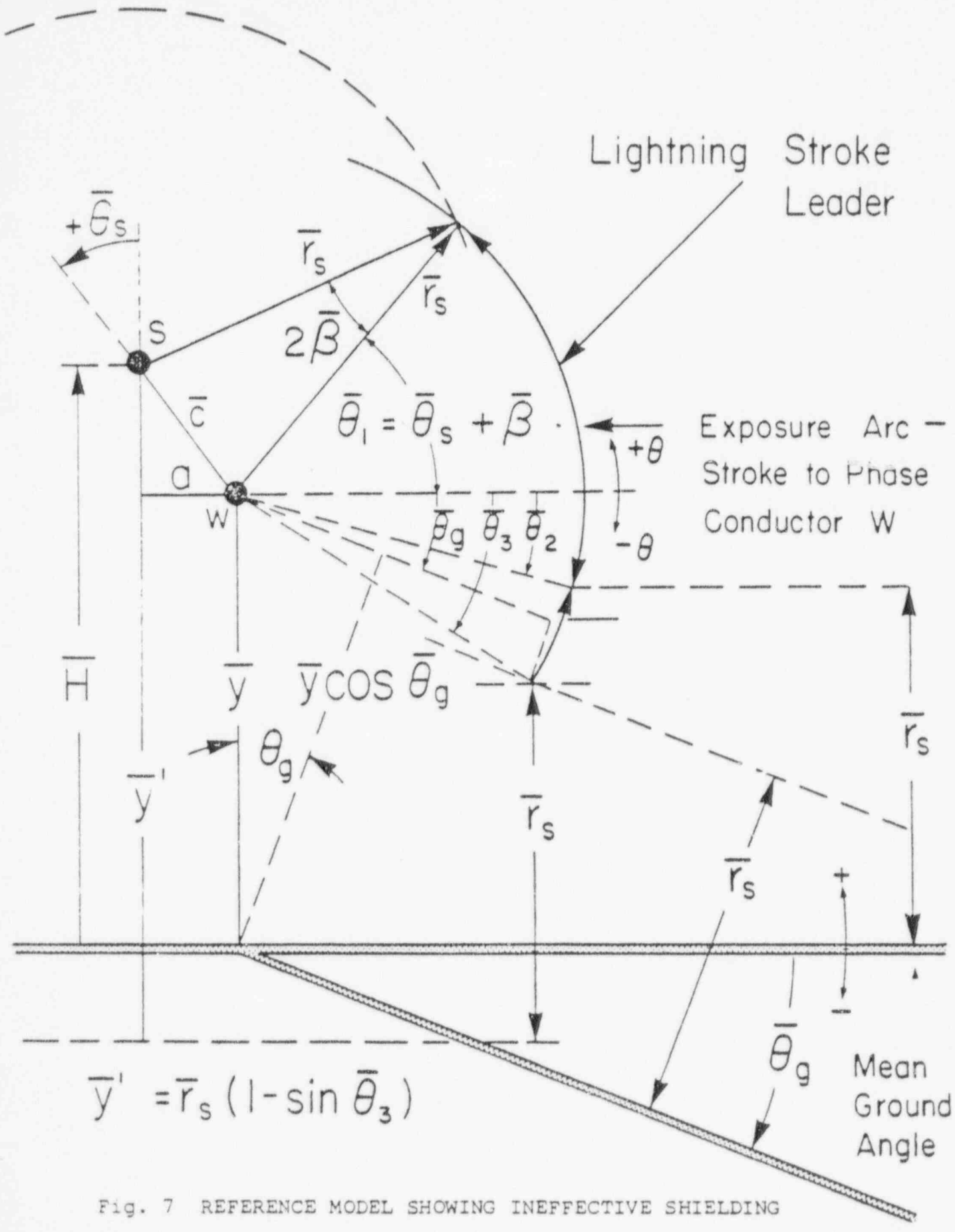

Fig. 7 REFERENCE MODEL SHOWING INEFFECTIVE SHIELDING

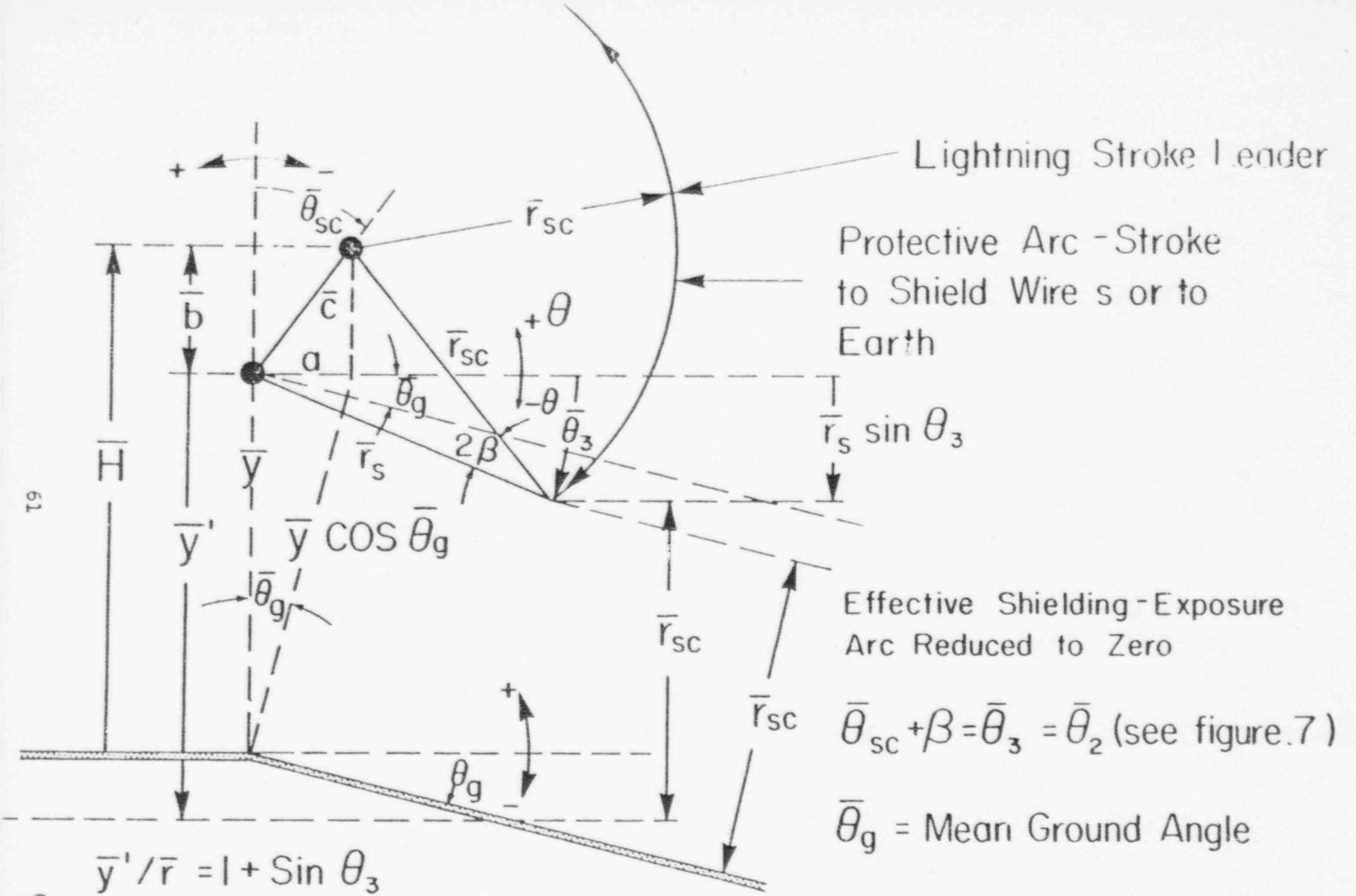

Fig. 8 REFERENCE MODEL SHOWING EFFECTIVE SHIELDING

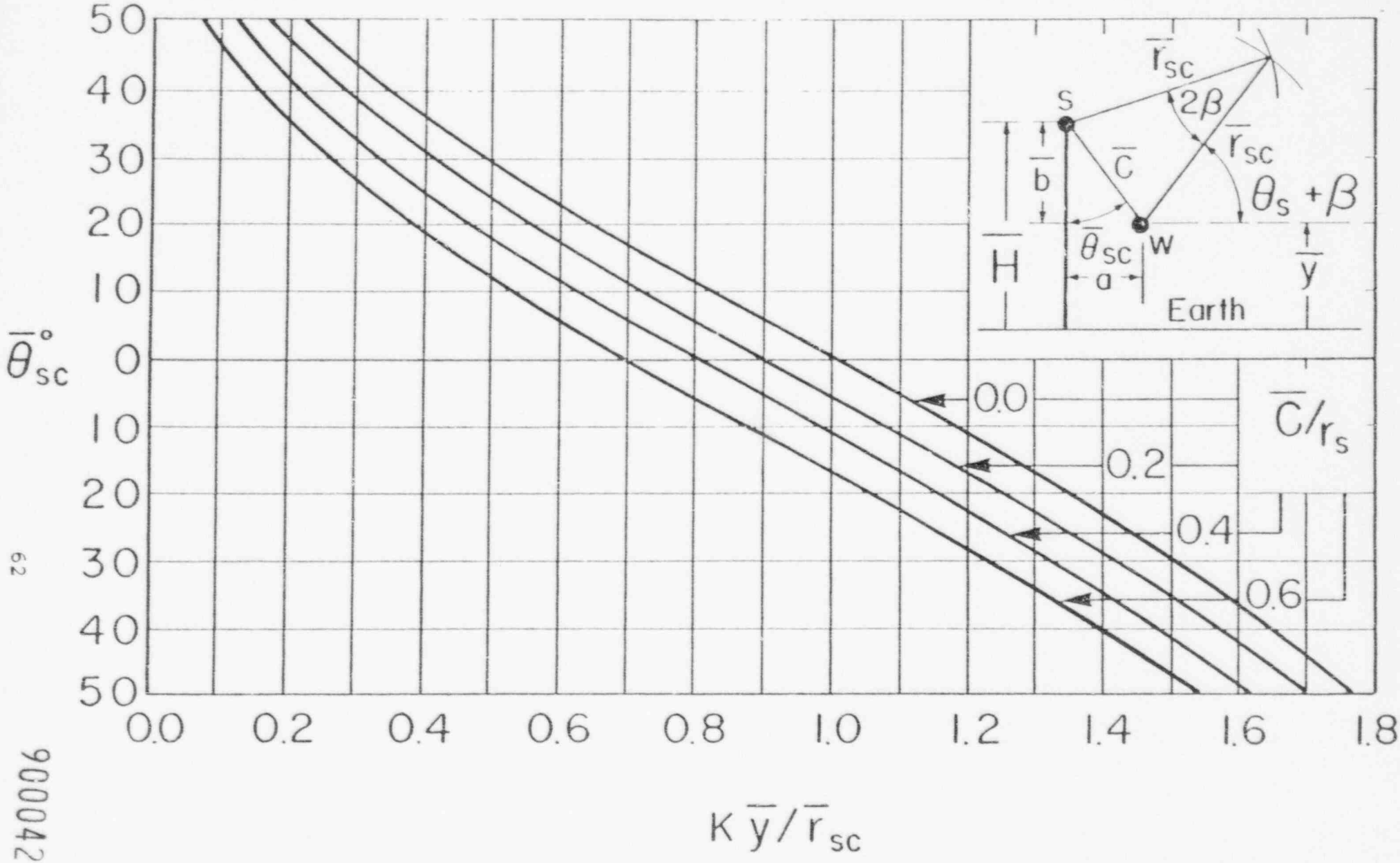

Fig. 9 CRITICAL SHIELDING ANGLE CURVES

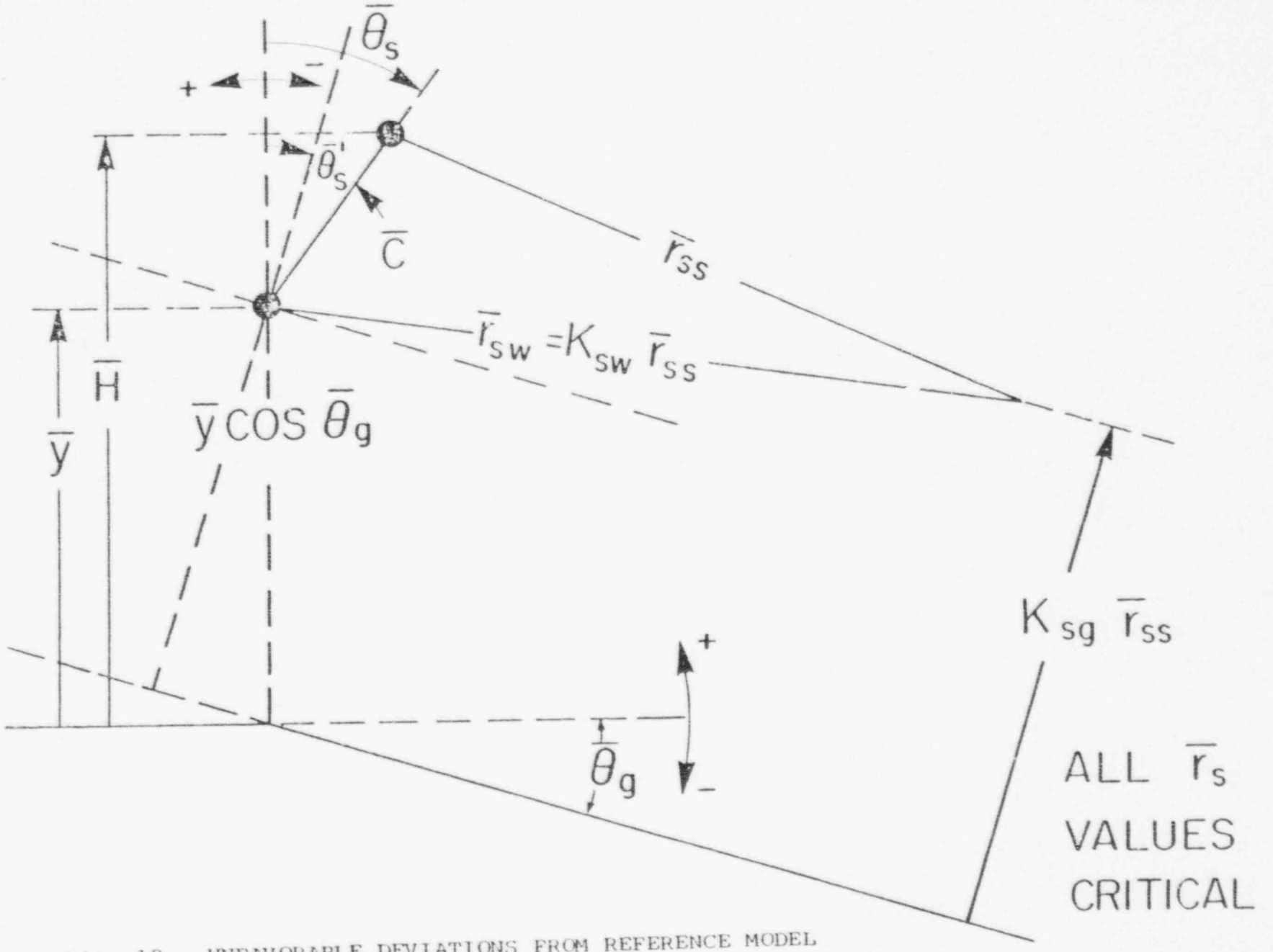

Fig. 10 UNFAVORABLE DEVIATIONS FROM REFERENCE MODEL

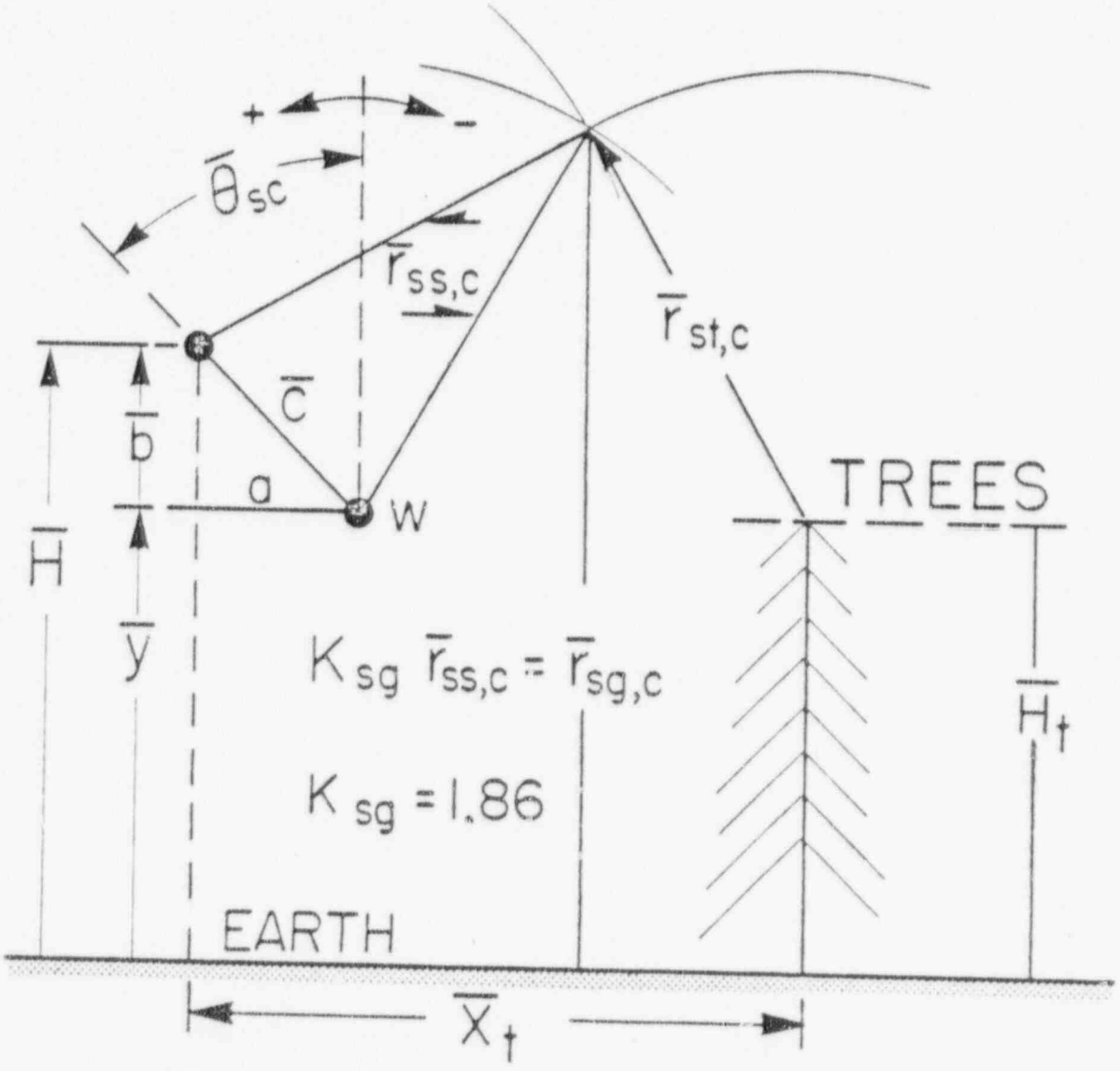

Fig. 11 FAVORABLE DEVIATION FROM REFERENCE MODEL

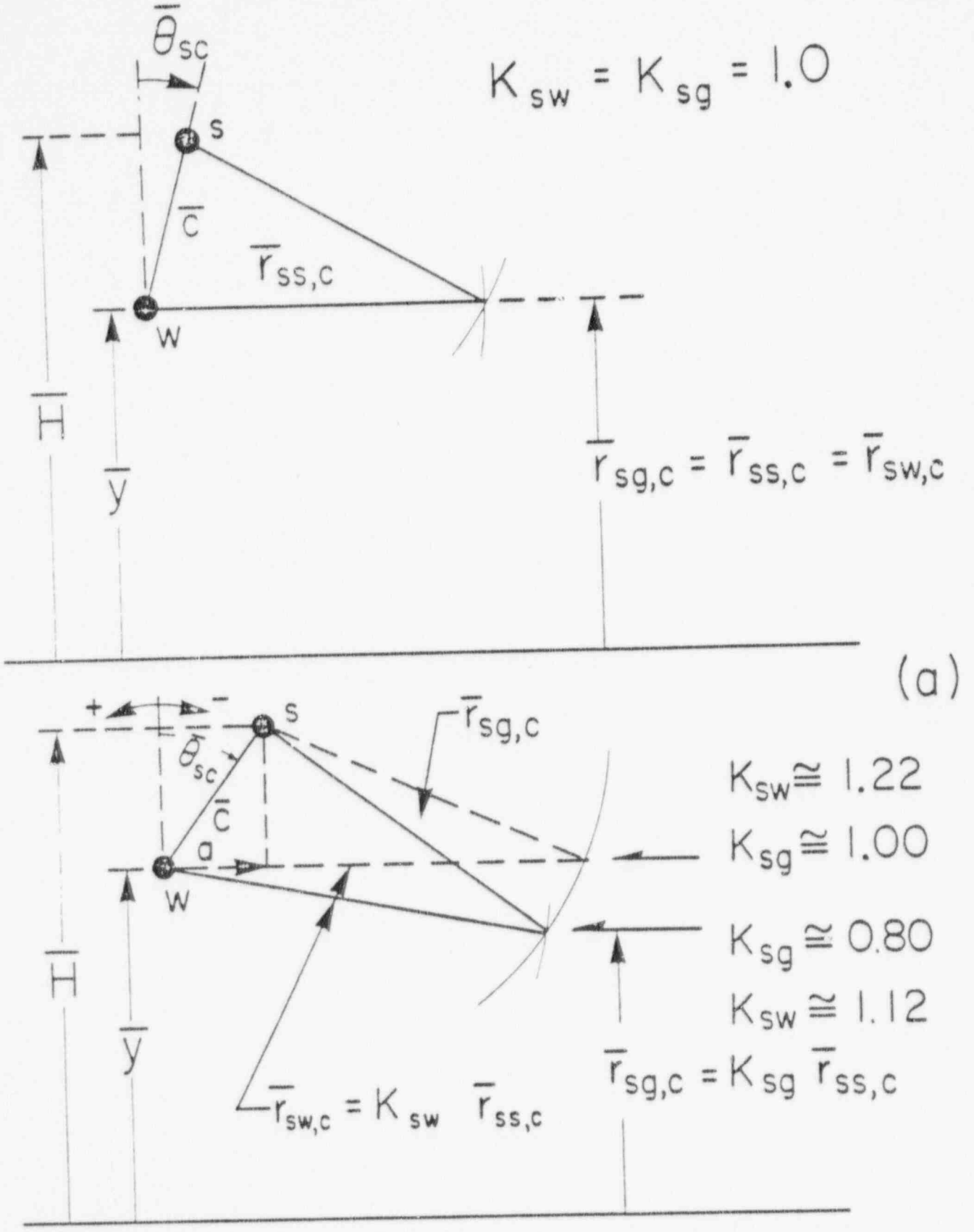

Fig. 12 EFFECT OF DIFFERING STRIKE DISTANCES

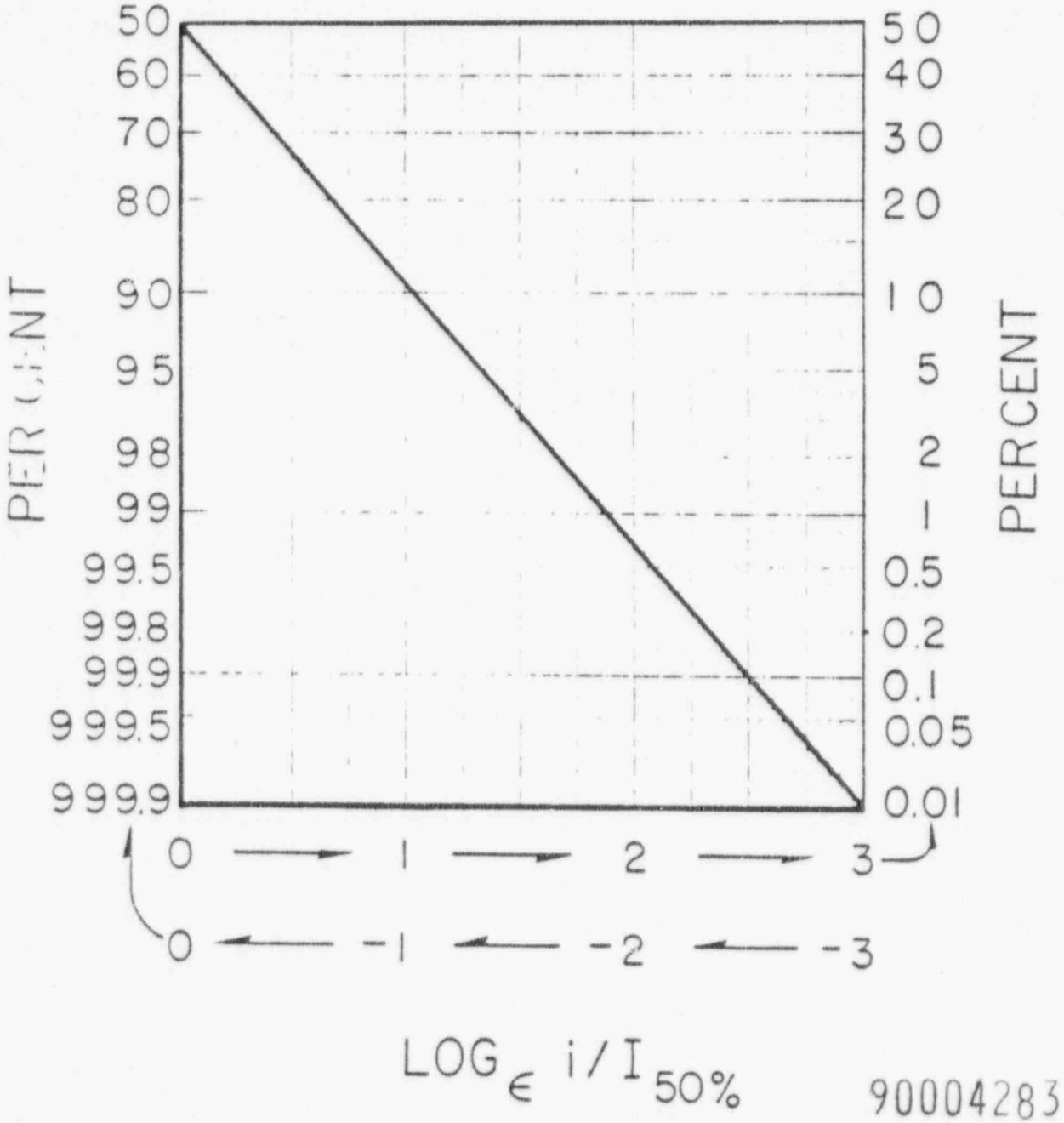

Fig. 13 LOG NORMAL CURRENT DISTRIBUTION

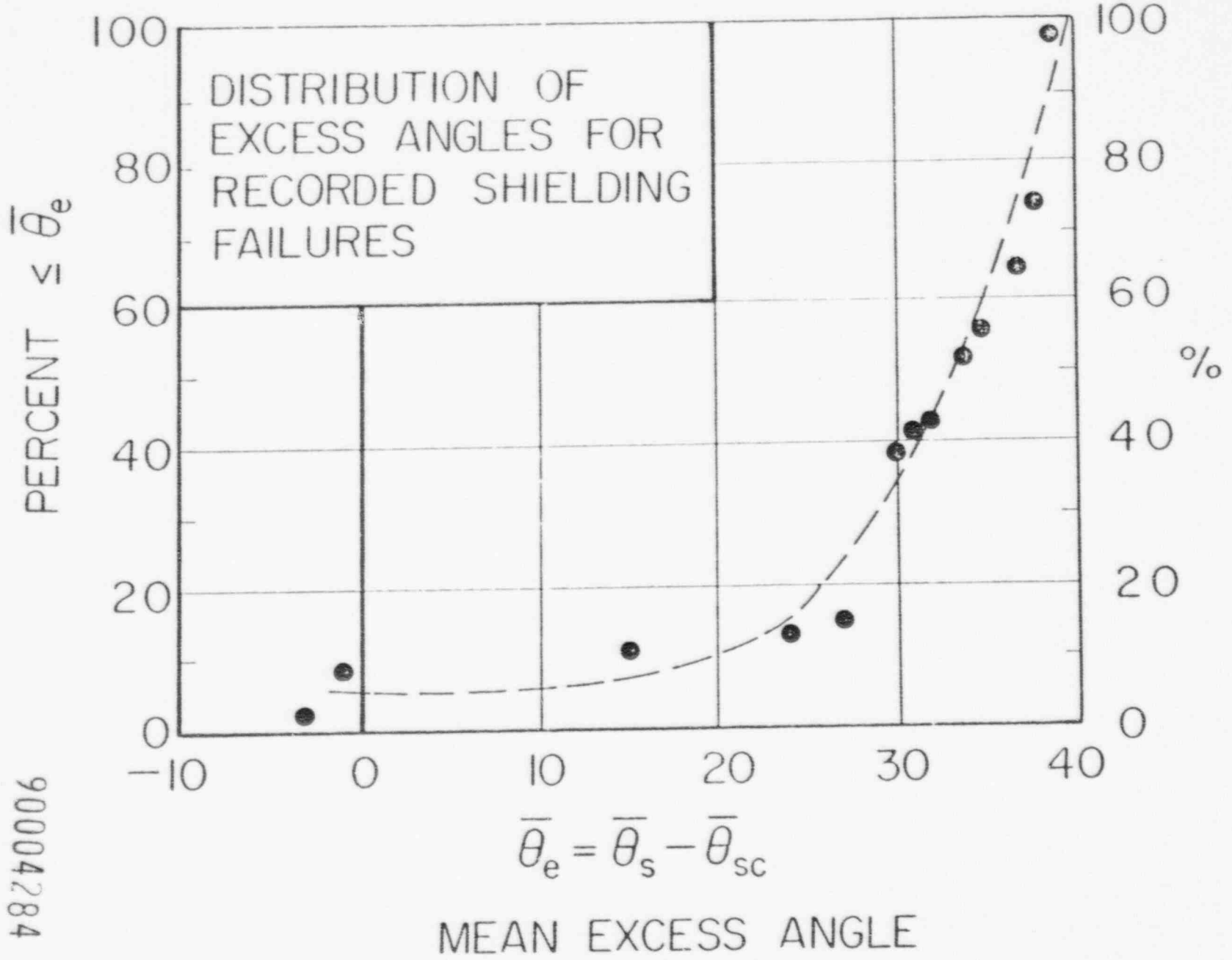

Fig. 14 MEAN EXCESS ANGLE FOR RECORDED SHIELDING FAILURES

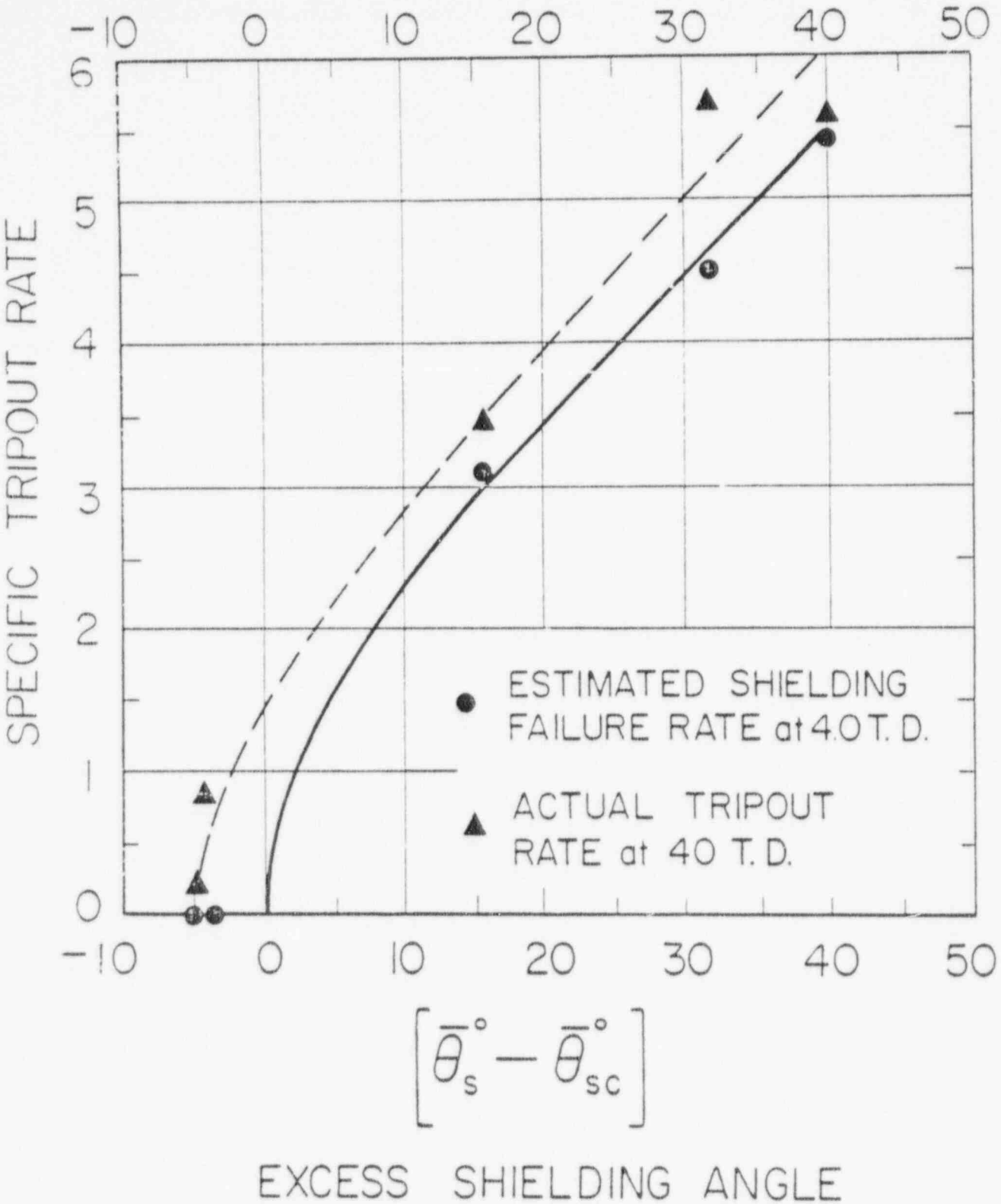

Fig. 15 MEAN EXCESS SHIELDING ANGLES FOR FIVE HV AND EHV LINES WITH TOWER FOOTING RESISTANCE UNDER 10 OHMS

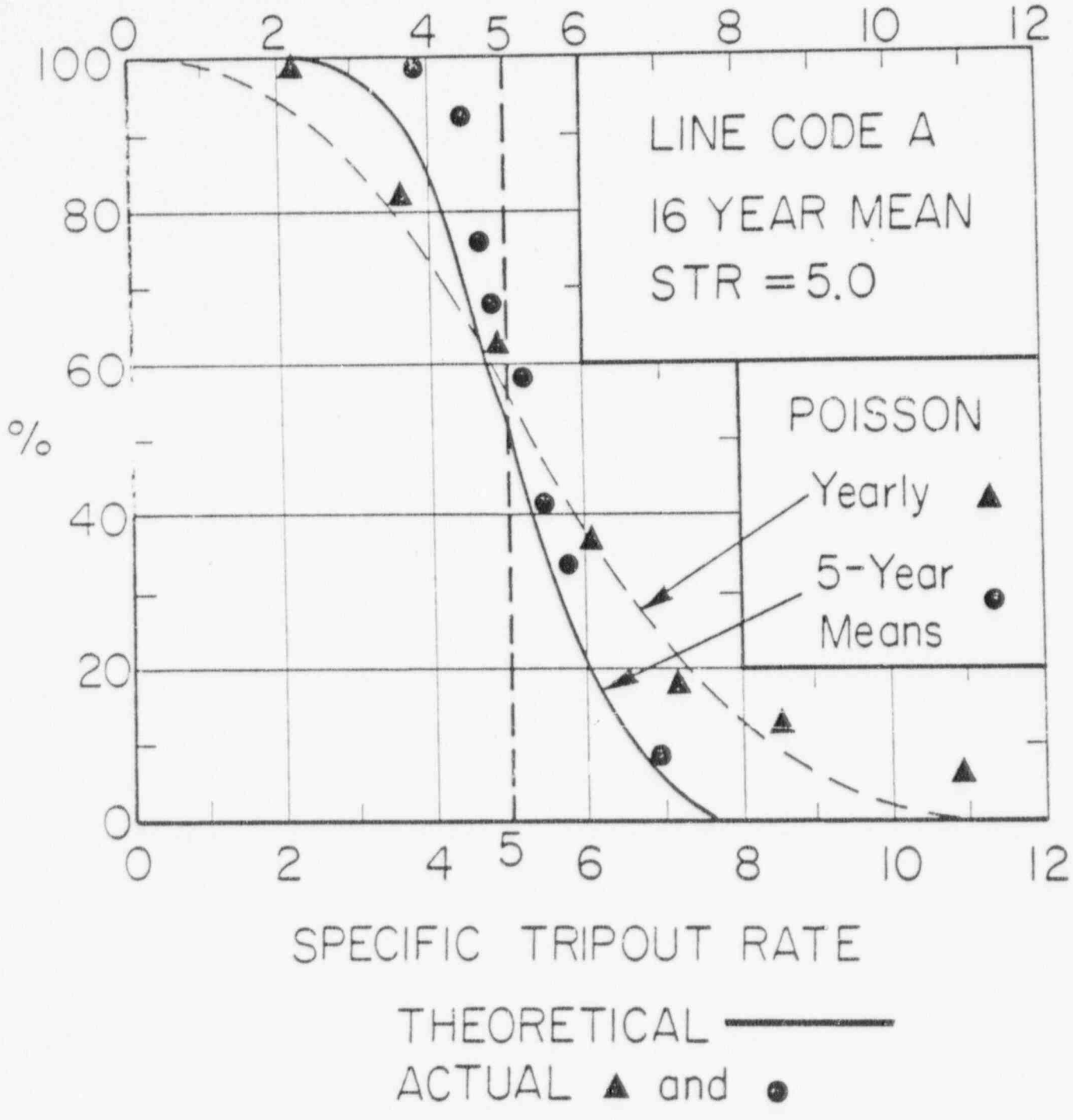

Fig. 16 DISTRIBUTION OF 1-YEAR, 5-YEAR, AND 16-YEAR LIGHTNING TRIPOUT RATES FOR 120 kV LINES

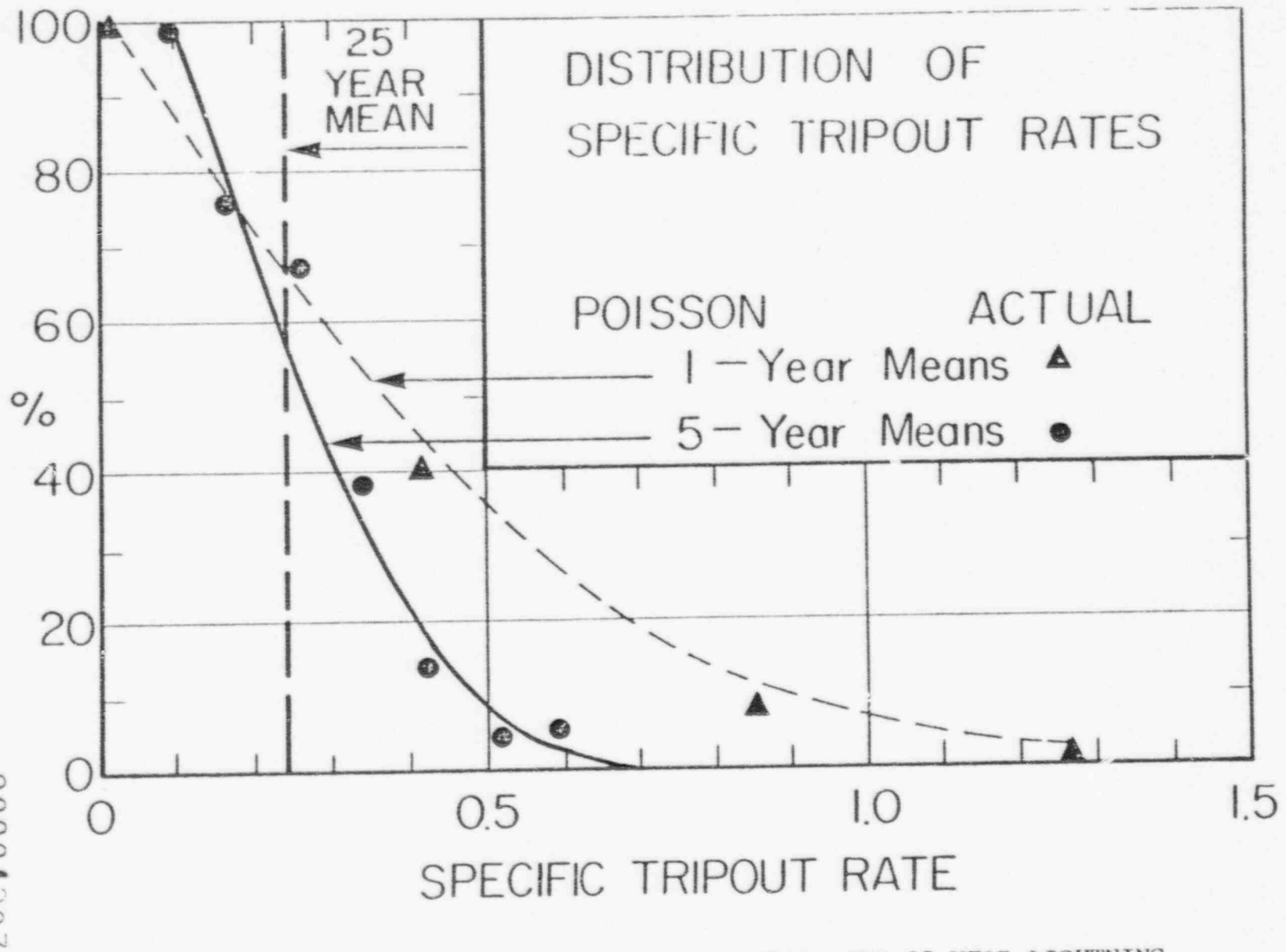

Fig. 17 DISTRIBUTION OF 1-YEAR, 5-YEAR, AND 25-YEAR LIGHTNING TRIPOUT RATES FOR 230 kV LINE

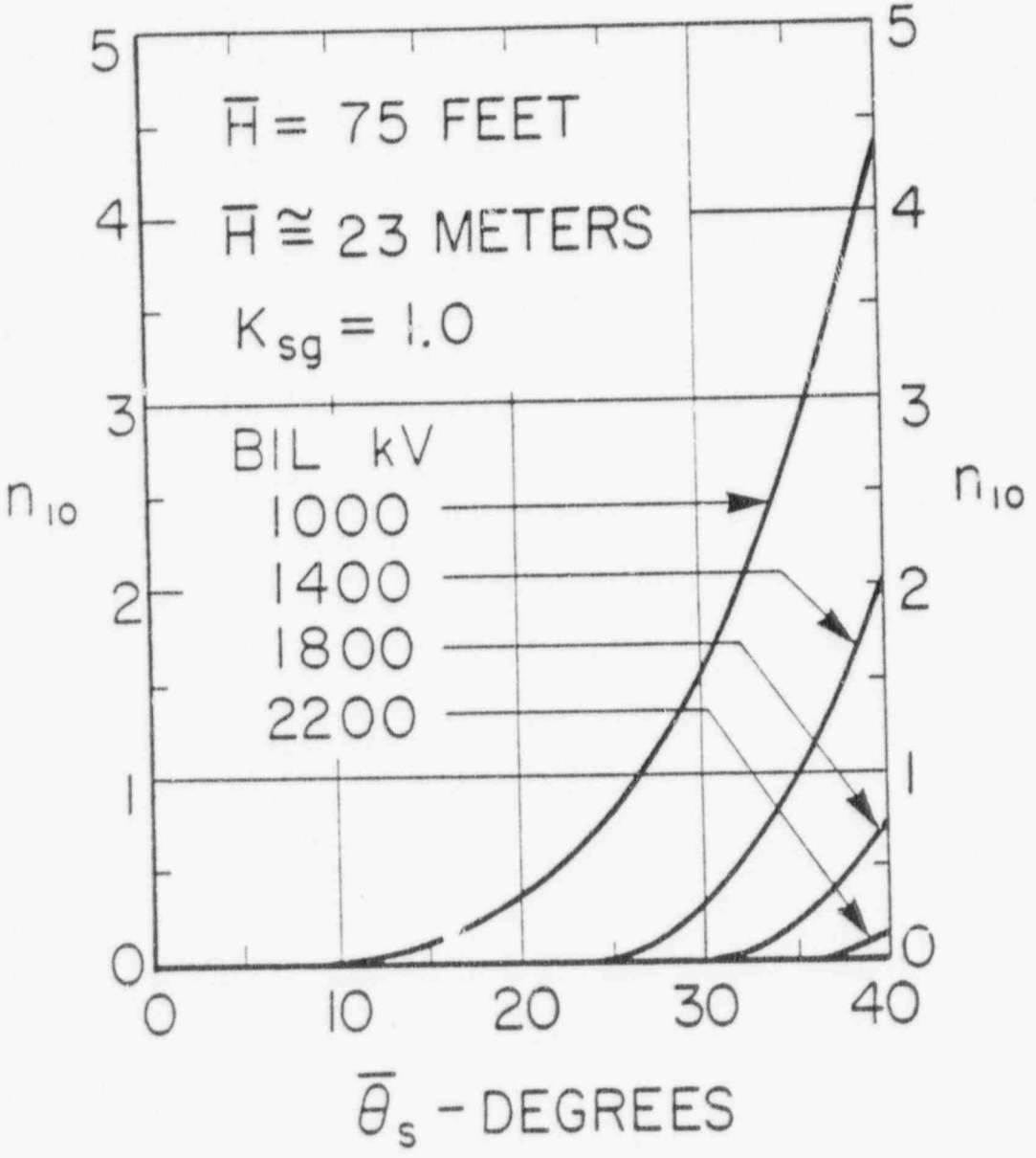

Fig. 18

90004288

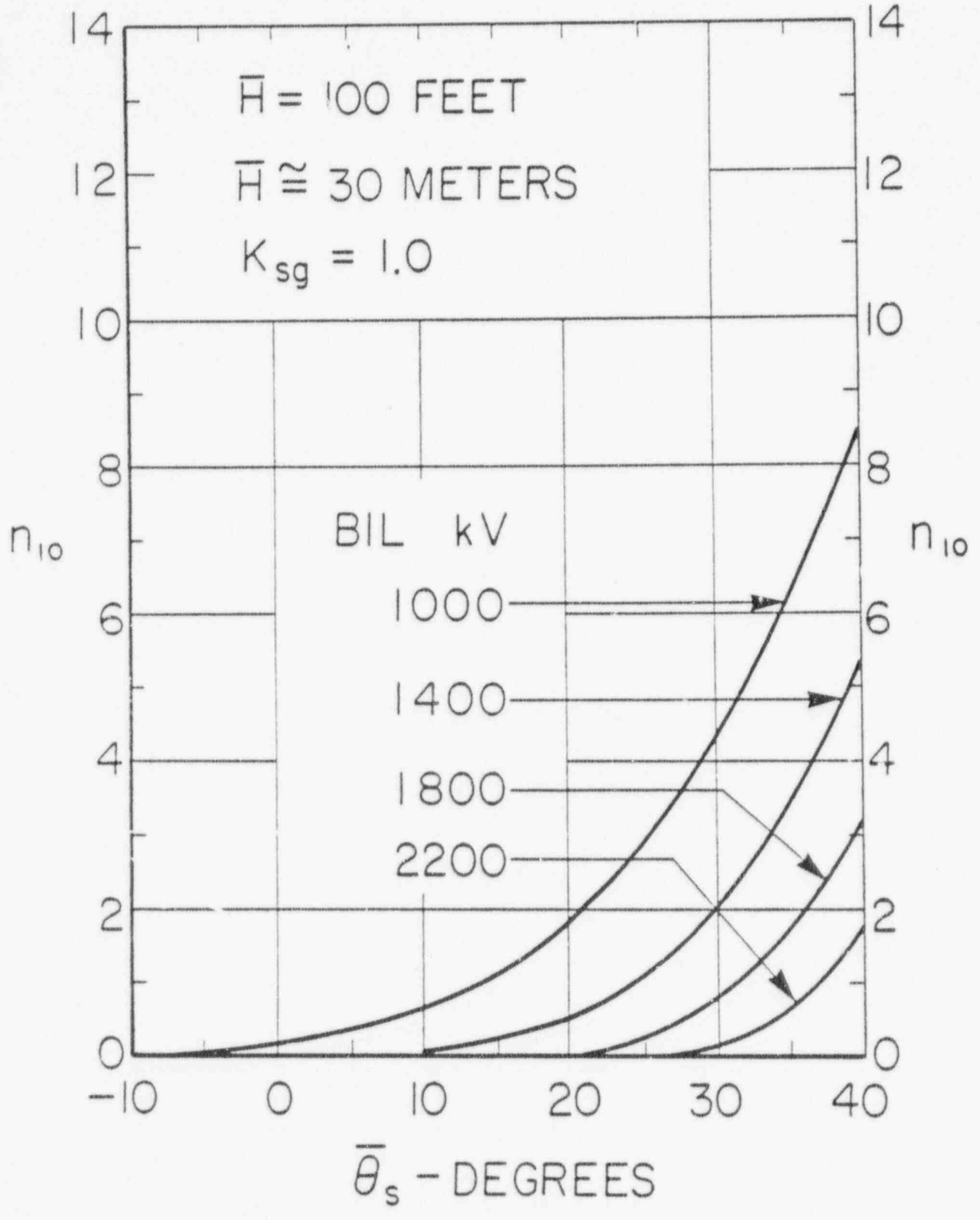

90004289

Fig. 19

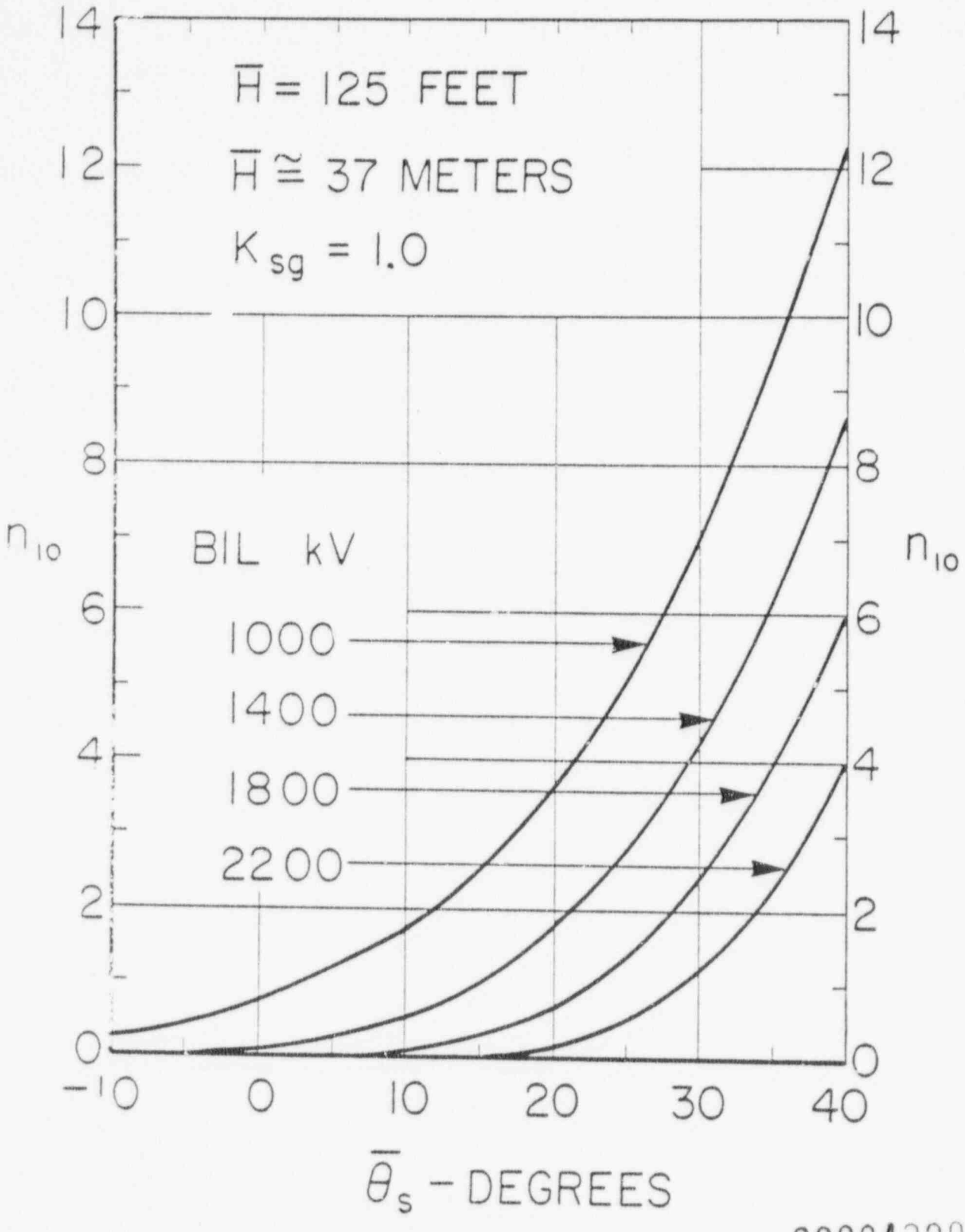
$\bar{H}$ = 125 FEET
$\bar{H} \cong$ 37 METERS
K_{sg} = 1.0
BIL kV
1000
1400
1800
2200
n_{10}
n_{10}
14
12
10
8
6
4
2
0
−10
0
10
20
30
40
$\bar{\theta}_s$ – DEGREES
90004290

Fig. 20

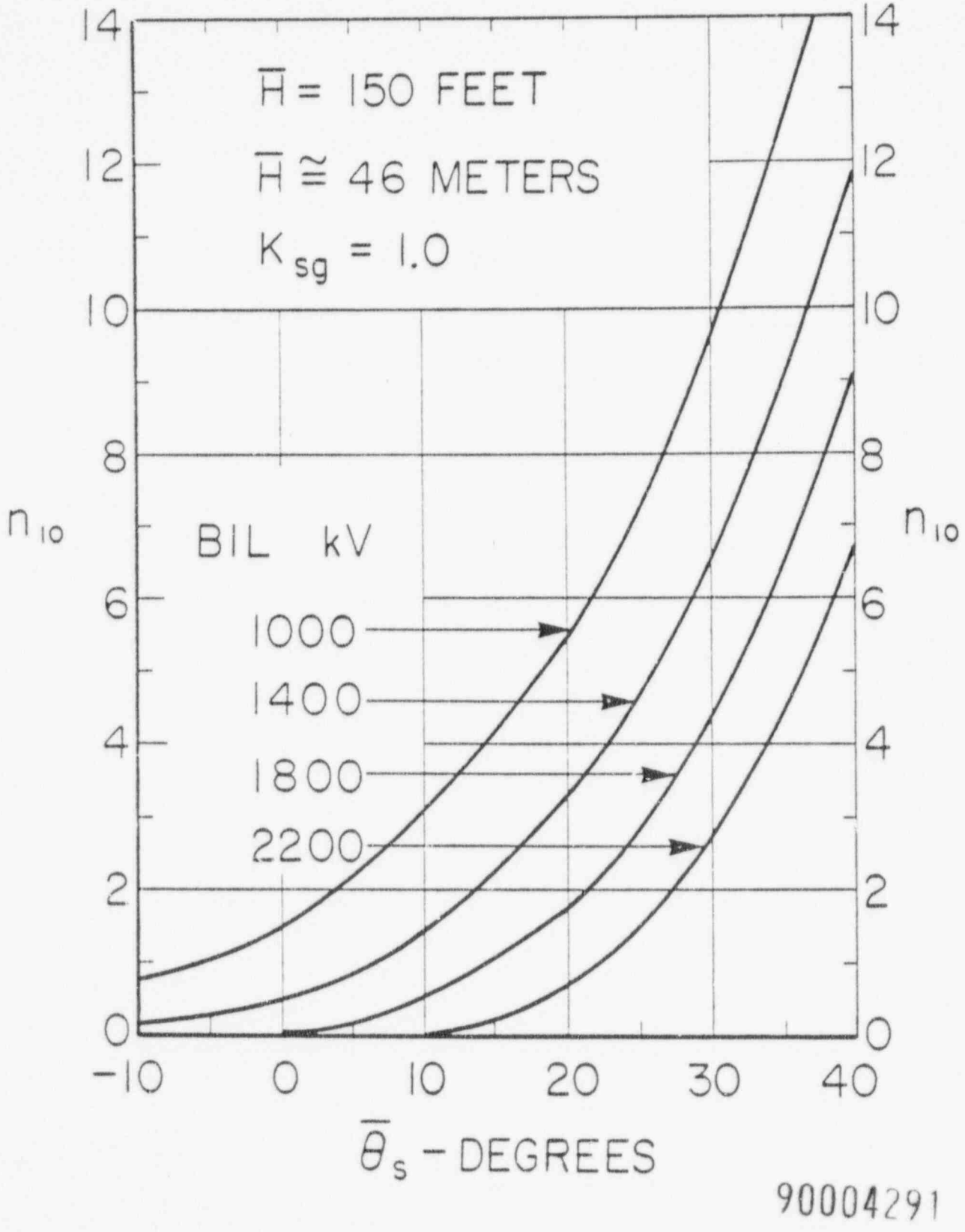
$\bar{H}$ = 150 FEET
$\bar{H} \cong$ 46 METERS
K_{sg} = 1.0
BIL kV
1000
1400
1800
2200
n_{10}
n_{10}
$\bar{\theta}_s$ - DEGREES
0
2
4
6
8
10
12
14
-10
0
10
20
30
40
90004291

Fig. 21

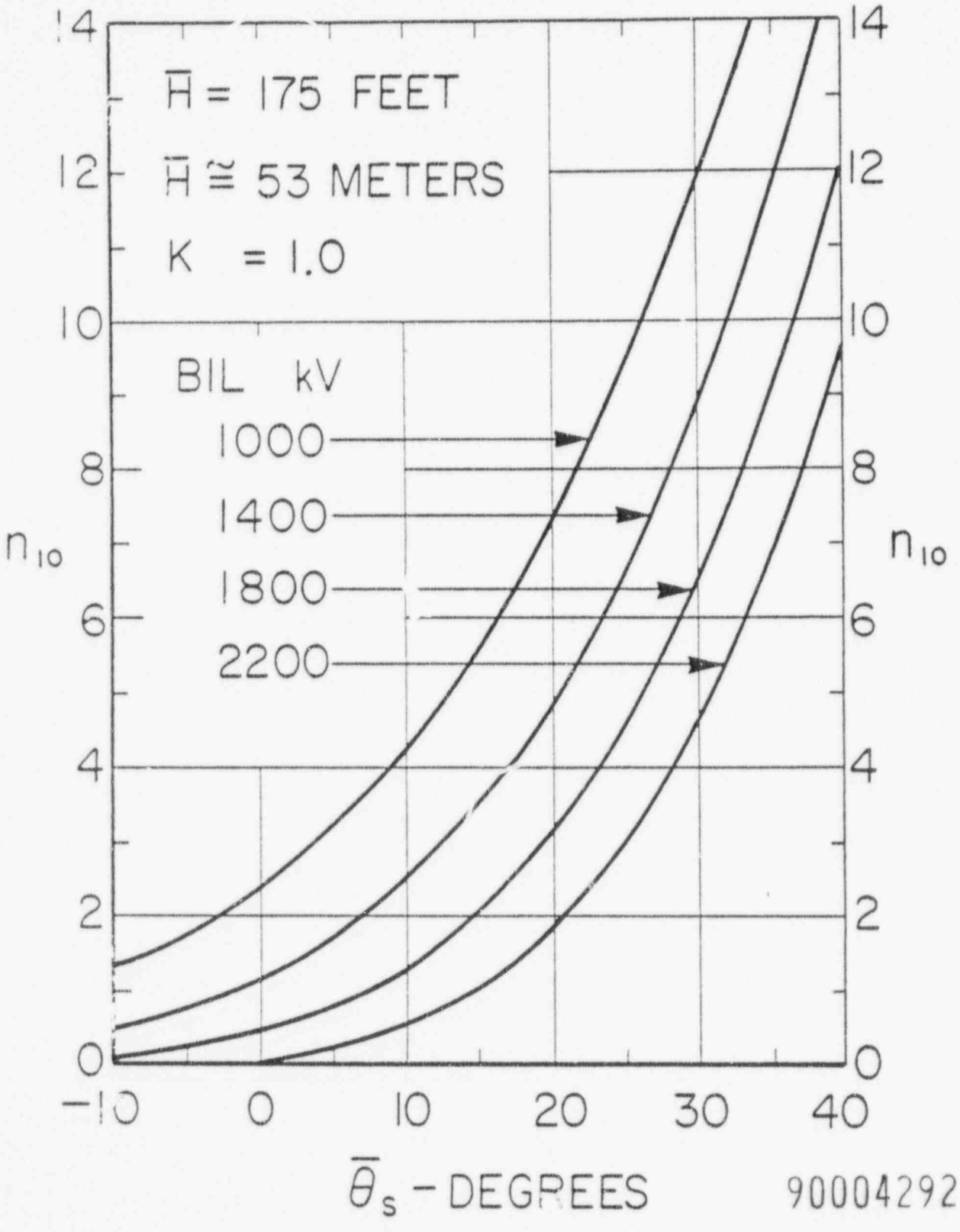
$\bar{H}$ = 175 FEET
$\bar{H} \cong$ 53 METERS
K = 1.0
BIL kV
1000
1400
1800
2200
n_{10}
n_{10}
14
12
10
8
6
4
2
0
−10
0
10
20
30
40
$\bar{\theta}_s$ - DEGREES
90004292

Fig. 22

ATT (3)

IEEE Transactions on Power Apparatus and Systems, Vol. PAS-95, no. 5, September/October 1976

REF. 21

FREQUENCY OF DISTRIBUTION ARRESTER DISCHARGE CURRENTS DUE TO DIRECT STROKES

Gordon W. Brown
Consultant, Joslyn Mfg. Co.
Chicago, Illinois

Steven Thunander
Joslyn Mfg. Co.
Chicago, Illinois

ABSTRACT

The "Electrogeometric" Theory, developed for transmission line lightning performance calculations, is applied to distribution systems as a means of predicting arrester discharge currents. The resulting rates of occurrence and frequency distributions compare favorably with presently available information. The effect of stroke location on arrester current is explained and shown to be significant. Predischarge and pole reflections are shown to have similar effects, and do not significantly affect crest current. Footing resistance is accounted for. Indirect strokes are treated briefly and shown to produce minimal arrester current.

INTRODUCTION

Over the past decade, there has been increasing interest in and concern over distribution system failures caused by lightning. Interest has centered on arresters and the duty they are likely to see. Also within the past 10 years, major advances have been made in the ability to predict the occurrences of lightning to transmission lines. In particular, the "Electrogeometric Theory," or Brown-Whitehead model, has now been extensively used and abundantly verified for HV and EHV systems. (Refs. 1 through 7.) Especially important, Sargent in Ref. 7 makes an impressive argument both for the theory and his proposed distribution of stroke currents to level ground. Using the Brown-Whitehead model and knowing the geometry of tall structures for which data is available, he inferred what the distribution to level ground had to be. Doing so, he was able to very nearly eliminate discrepancies in field data from various investigators, including those used on the "AIEE curve."[8] Sargent's synthetic distribution to level ground is shown in Figure 1.

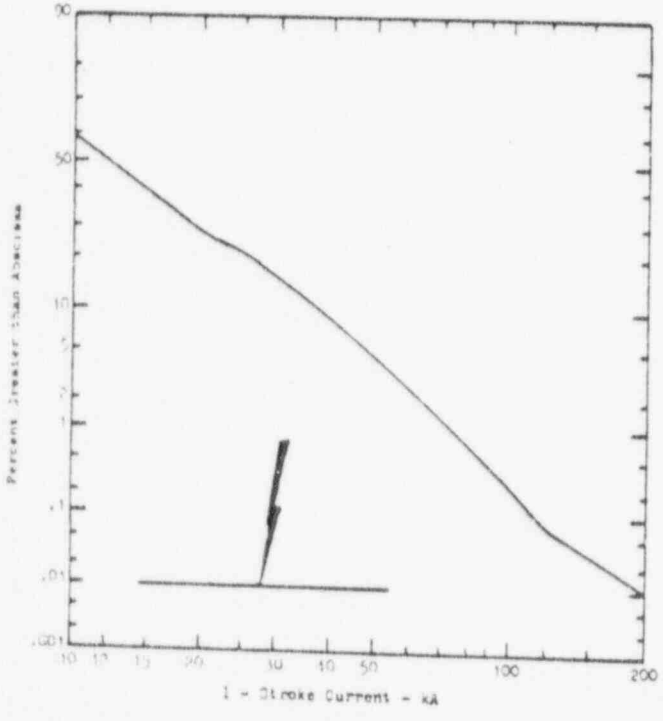

Figure 1. Frequency of Strokes to Level Ground (log-normal graph)

Paper F 76 160-2, recommended and approved by the IEEE Surge Protective Devices Committee of the IEEE Power Engineering Society for presentation at the IEEE PES Winter Meeting & Tesla Symposium, New York, N.Y., January 25-30, 1976. Manuscript submitted July 31, 1975, made available for printing November 14, 1975.

In the following, after (I) briefly dispensing with indirect strokes, we will (II) develop the frequency of direct stroke currents to distribution LINES. This will precede (III) relating stroke currents to arrester currents, following which (IV) the desired frequency distribution of arrester discharge currents will be developed. As the first stage in the development, we show that indirect strokes may be dispensed with.

I. INDIRECT STROKES

The electrogeometric theory indicates that a leader tip which will cause an indirect surge cannot be closer than the strike distance. (Fig. 2)

$$E \approx \frac{q}{2\pi\epsilon\sqrt{r_s^2 + 2r_s h - h^2}}$$

(Reference 13)

q = coul/m of leader

r_s = strike distance

$= 7.1\, I^{.75}$

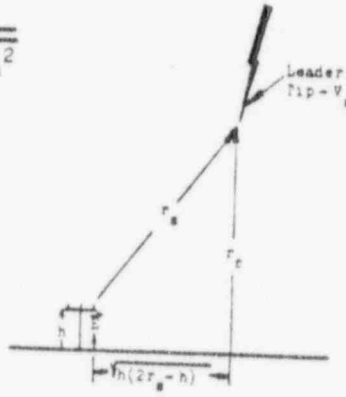

Figure 2. Geometry of Closest Approach of Indirect Stroke

Referring to Figure 2, the voltage induced in the conductor is approximately hE. Were the charge on the leader instantly collapsed by striking some other earthed point, this voltage would split in two equal surges travelling down the conductor in opposite directions. The strike distance is a function of leader voltage, which is in turn a function of the charge per unit length of the leader channel. (See References 1 and 2) The equations of the electrogeometric model suggest a capacitance to earth of the leader channel of (very) approximately 7.8 pf/m, and a leader voltage of (crudely) $0.76\, r_s^{.83}$ MV. Coupling this with the information of Fig. 2 allows rough determination of the maximum surge voltage and current as shown in Table I. Although this analysis is only a rough approximation, it is clear that surges due to indirect strokes produce minimal line and even smaller arrester currents. It is noted that the currents of Table I

Table I

Maximum Arrester Current Due to Indirect Strokes Assuming a Line 10m High with 400Ω Surge Impedance

I Stroke Current kA	Leader Closest Approach m	Maximum Possible Arrester Current amps
10	40	1120
50	135	1100
100	225	1080

are consistent with field data (e.g. Refs. 11 and 12).

II. FREQUENCY OF DIRECT STROKE CURRENTS TO DISTRIBUTION LINES

Before examining arrester currents, consider the problem of determining the frequency of stroke currents to a line.

(A) "Electrogeometric" Model

The geometry of conductor exposure is a function of strike distance (and thus current). At each strike distance, there is an exposed circular arc as shown in Fig. 3a. Note that there is a maximum strike distance (and thus current) for a given shielding configuration as in Fig. 3b. For larger strike distances, the stroke will always be closer to either shield or earth than to conductor, and cannot, therefore, strike the line.

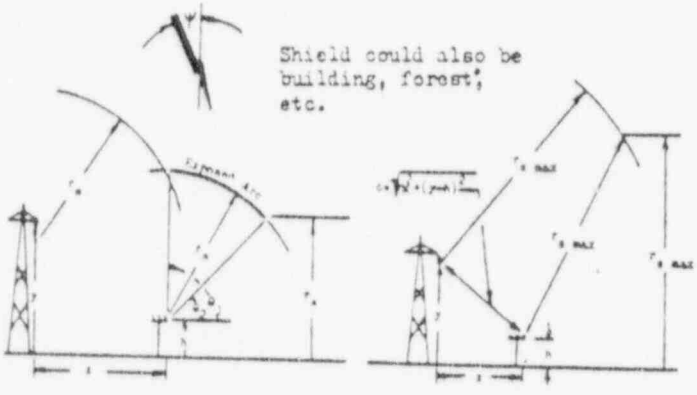

(a) Exposed Conductor (b) Maximum Strike Distance

Figure 3. Geometry of a Line Exposure to a Stroke with Strike Distance r_s.

As shown in Refs. 1 and 2, the number of strokes hitting the line is

$$n = N_o \int_0^\infty X f(I) dI \qquad (1)$$

In this equation, the parameters are as follows:

- n = strokes per unit length and time to the line
- N_o = stroke density (strokes/unit area/yr)
- X = swath (effective exposed width, as in Ref. 1. Related directly to exposed arc of Fig. 3.)
- $f(I)$ = frequency distribution of stroke current magnitudes to level ground (Fig. 1)

The effective swath, X, is a function of the distribution stroke-approach angles (Ψ in Fig. 3a). Again from Ref. 1:

$$X = \frac{2r_s}{\pi} \int_{\theta_2}^{\theta_1} \int_{\Psi_2}^{\Psi_1} \sin(\theta - \Psi)\cos\Psi \, d\Psi \, d\theta \qquad (2)$$

θ_1 and θ_2 are as in Fig. 3a; Ψ_1 and Ψ_2 are the limits on the approach angle (e.g. Ψ_2 is often $-\pi/2$). [It is noted that recent works (e.g. Ref. 4) suggest slightly different equations for the strike distance. They also suggest a difference between strike distance to ground and to conductor. However, in order to use these, the distribution of Fig. 1 must be redetermined. The distribution of strokes to level ground based on other equations was not available at this writing. In any case, experience with transmission systems shows that the differences in overall performance are not significant.]

(B) Results for Shielded and Unshielded Lines

The rates of occurrence of strokes to lines, for various configurations, are shown in Fig. 4 (unshielded lines) and Fig. 5 (shielded lines). Though the rate for shielded lines is not easily normalized, use of an abscissa of $x/(h+10)$ makes interpretation easier. Note that rates for forested lines can be inferred from the data. For example, for a 10 meter (vertical configuration) high line with a 10m high forest 20m on either side of the line:

From Fig. 4, 60 str./100km-yr (at 10 strokes per sq.km. and yr.).

From Fig. 5, at $x/(h+10) = 20/20 = 1$ and $y/h = 1$, the rate would be reduced to 65% of 60 = 39, were the "forest" on one side of the line. Being on both sides, it is reduced to 2(39 - 60/2) = 18 strokes per 100 km and year.

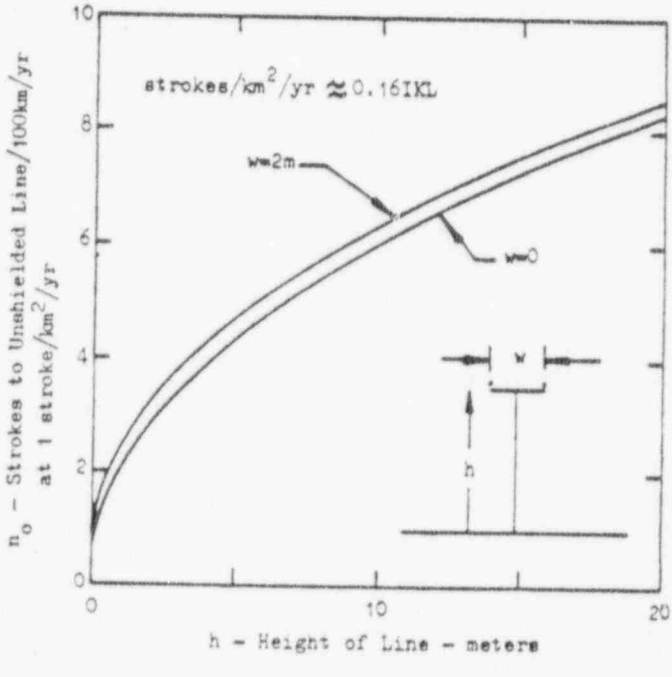

Figure 4. Number of Strokes to an Unshielded Distribution Line per 100 km and Year

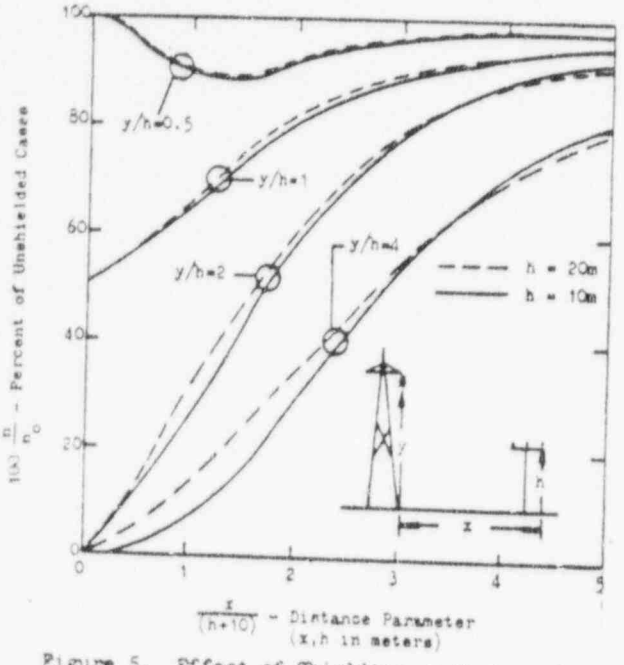

Figure 5. Effect of Shielding on Number of Strokes to the Line

This approach is valid for tree heights less than or equal to line height. For higher levels, maximum strike distance will likely be very small and the line will be effectively shielded, except for very low current strokes.

From Eq. 1, we can write the frequency function of stroke currents hitting the line as

$$f_L(I) = \frac{Xf(I)}{\int_0^\infty Xf(I)dI} \qquad (3)$$

And in turn the distribution function is found:

$$\text{Probability that current} > I_o = F_L(I_o) = \int_{I_o}^\infty f_L(I)dI \qquad (4)$$

The results are shown in Fig. 6. One set of curves is accurate for all reasonable distribution line configurations. There would be slight differences at transmission tower heights.

The frequency of strokes through arresters can be determined if line current and arrester current magnitudes can be related. This is done in the following section.

III. RELATING LINE AND ARRESTER CURRENTS

(A) Effect of Stroke Location

Consider, as in Fig. 7a, a line with arrester spacing T (measured in surge travel time), and a direct stroke impinging at ρT from the arrester being considered. (Though arresters are assumed at each grounded pole, it is only necessary that there be flashovers at the grounded poles.)

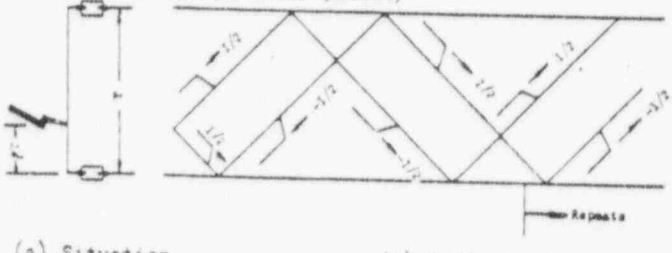

(a) Situation (b) Reflections

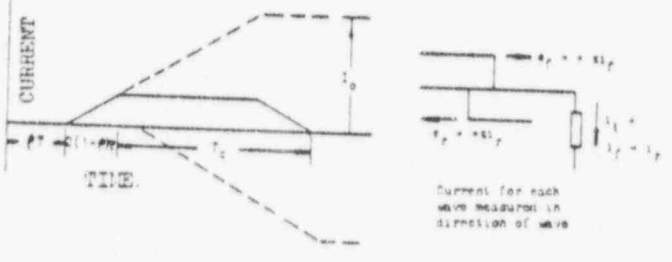

(c) A "Block" of Arrester Current (d) Convention for Travelling Waves

Figure 7. Effect of Stroke Location

Note that in the reflection diagram (Fig. 7b), the analysis of the effects of the surge may be considered as repeated blocks of surge current, the block being the effect of the first wave and the first reflection from the other end. The block is illustrated in Fig. 7c. The wave form is considered as a ramp to a flat crest, I_o. (Note the convention used for travelling wave signs in Fig. 7d. It is not the usual approach, but the authors believe it to be a better one. Regardless of the origin of a wave, if current is measured in the direction of travel, v = +zi!)

(B) Effective Arrester Current

For the stroke wave form assumed (constant ramp to I_o at time-to-crest T_c), the amount of current-time area added by the "block" is

$$\int i dt = \frac{I_o}{T_c} r 2(1-\rho)T]T_c$$

Since a new "block" is added every 2T, the average cur-

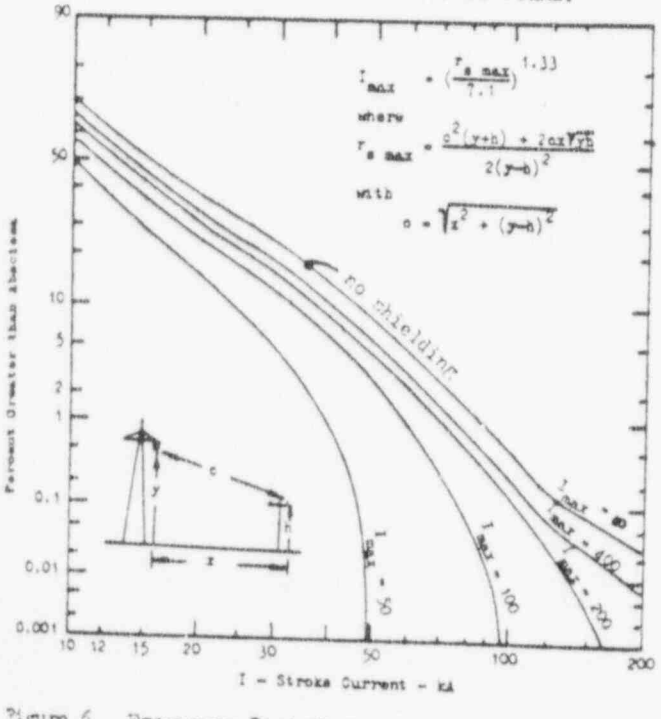

Figure 6. Frequency Distribution of Strokes to Lines (log-normal graph)

rent (i.e., the average crest current) in the arrester is $I_a = (1-\beta)I_o$, as illustrated in Fig. 8.

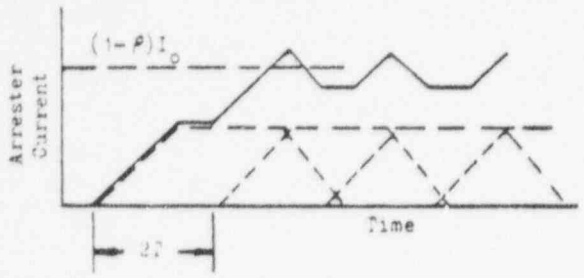

Figure 8. Illustration of Effect of Stroke Location on Arrester Crest Current Magnitude

Although the actual crest will be higher, it is of far shorter duration than the bulk of the wave, and short duration surges through an arrester probably produce smaller gap etchings than long duration surges. To the order of accuracy presently available, it is therefore assumed that the effective arrester current due to a stroke with current I_o is given by $(1-\beta)I_o$. To be sure, strokes with fronts faster than the travel time between the arresters will produce short duration spikes, repeated every 2T, but (1) in most situations will involve strokes with fronts much longer than twice travel time, (2) the effect of such duty in comparison with more "normal" waveforms is unclear, though (3) it is certainly less severe than a full steady wave of I_o. Finally, (4) since the statistics of tail form of strokes (and particularly its dependence on other stroke parameters) are unclear, $(1-\beta)I_o$ is still appropriate as the effective current.

(1) Prodischarge. As indicated in Refs. 14-16, prodischarge currents will flow between the struck conductor and nearby conductors to relieve the stress between them. The lines near the point of impact act much like a high discharge voltage (about 186kV per foot of spacing) arrester. As soon as the first reflection from the other grounded pole, prodischarge current is eliminated. Thereafter, the current flows as if prodischarge had not occurred. The initial (prodischarge) "blocks" of current are sufficient to insure that the voltage will not again exceed the prodischarge level of the line. In extreme cases, this can represent a significant reduction in rate of rise of arrester current (e.g. where time-to-crest is significantly shorter than travel time between grounded poles). However, this doesn't represent a significant fraction of the statistics, and doesn't affect average crest current at all. Hence, the effect of prodischarge on arrester current is ignored.

(2) Footing Resistance. High footing resistance will reduce arrester currents. The effect is illustrated in Fig. 9. (Recall the convention of Fig. 7d.) For example, with 200 ohm footing resistance and top phase protection, the arrester current would be 70% of its value with no footing resistance. (cf. Fig. 9c) It will be even closer for three-phase protection as shown in Fig. 9d.

(3) Reflections Down (and Up) the Pole. The above ignores the effect of waves travelling up and down the pole. It is relatively easy (but laborious) to show that such reflections do not affect the magnitude of the effective crest. The effect is illustrated in Fig. 10.

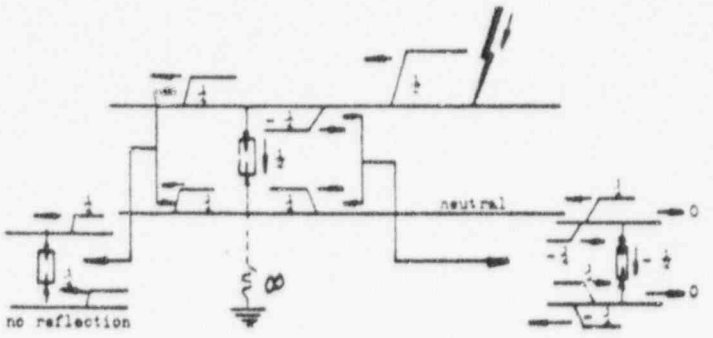

(a) High Footing Resistance

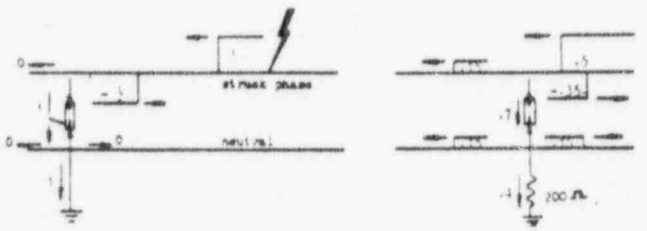

(b) Low Footing Resistance (c) 200Ω Footing Resistance

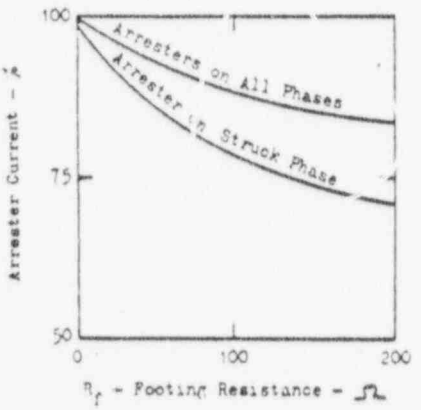

(d) Overall Effect (Approximate)

Figure 9. Effect of Footing Resistance on Arrester Current

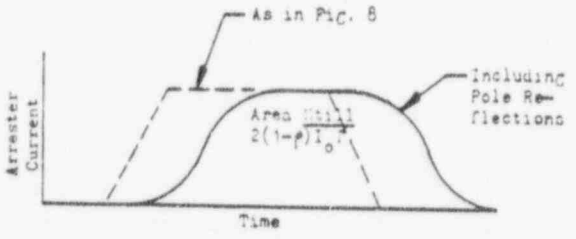

Figure 10. Effect of Pole Reflections on a "Block" of Arrester Current (cf. Fig. 8)

As with prodischarge, the effect is to siphon off a single, small block of charge early (e.g. small fraction of a microsecond), to delay the crest, and to smooth the wave. This adds to the case for using $(1-\beta)I_o$ as the effective crest.

IV. FREQUENCY OF ARRESTER CURRENTS

(A) Strokes to Poles

As just seen, arrester current is a function of stroke location. The Brown-Whitehead model predicts that for lines with significant sag angles, some strokes will hit towers directly. However, for sags found on distribution lines, the strokes will be evenly distributed without regard to poles. This is illustrated in Fig. 11.

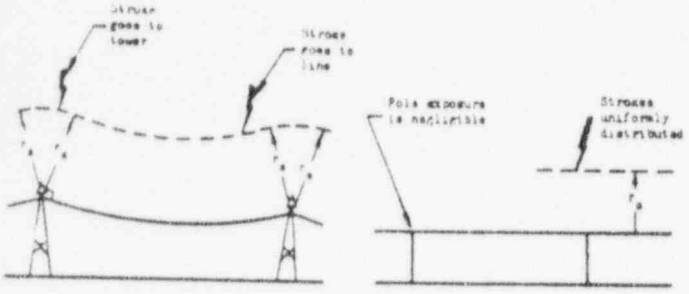

(a) Transmission Line (b) Distribution Line

Figure 11. Effect of Sag on Stroke Location

(B) Strokes to the Line

In the Appendix it is shown that the frequency function of arrester currents is

$$f_A(I_a) = \int_{I_a}^{\infty} \frac{f_L(I)}{I}\, dI$$

where $f_L(I)$ is as in Eq. 3. Finally, the distribution function is

$$F_A(I_a) = \begin{matrix}\text{Probability that} \\ \text{Arrester Current} \\ \text{Is Greater than } I_a\end{matrix} = \int_{I_a}^{\infty} f_A(I)\,dI$$

This has been performed numerically. The results are shown in Fig. 12.

(C) Example

Find the number of arrester operations on the distribution line illustrated in Fig. 13, if the stroke density is 10 strokes/sq.km/yr (corresponding to an IKL of about 60). Also, find the number of arrester operations greater than 65kA.

From Figs. 4 and 5, with 2m outer phase spacing, with $y/h = 3$ and $x/(h+10) = 2.50$, we read

n = # strokes to unshielded line
= 6.25x10 = 62.5 strokes/100km/yr.

$n/n_o \approx 0.55$

Thus, there are 0.55*62.5=35 strokes/100km/yr. to the line. Each produces 2 arrester operations. From Fig. 12:

$$r_{s\,max} = \frac{(53.85)^2(30+10) + 2(53.85)50\sqrt{30(10)}}{2(30-10)^2}$$

= 262m and

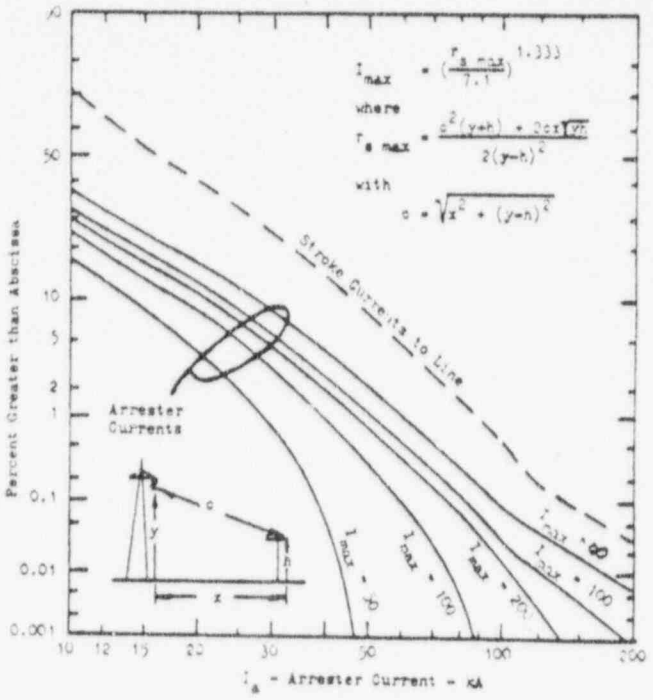

Figure 12. Frequency Distribution of Arrester Currents (log-normal graph)

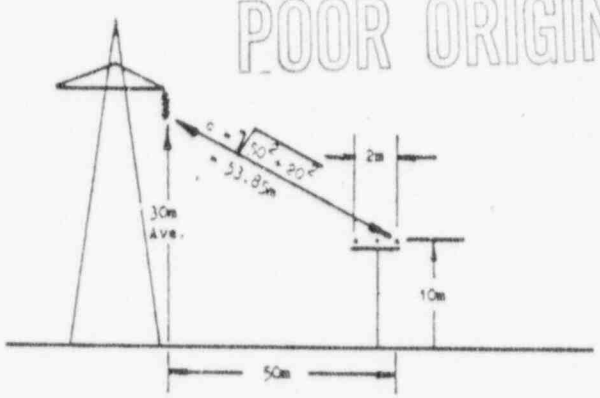

Figure 13. Flat Construction Example

$$I_{max} = \left(\frac{262}{7.1}\right)^{1.33..} = 123\text{kA}$$

Thus (Fig.12) approximately 0.25% will be greater than 65kA. This represents 0.0025x35x2 = 0.2 arrester operations per 100km/yr. This is compared with about 0.75% greater than 65kA for an unshielded line, representing 0.0075(62.5)(2) ≈ 1 arrester operation per 100 km per year. For a 30-year lifetime, this represents about one operation for each 3 miles of span.

This calculation assumed arresters on the struck line at every grounded pole, as would be the case with top phase protection or arresters on all phases. If this is not the case, the approach is more complex. If there are arresters at every other grounded pole, for example, it could be assumed that there will be only one arrester operation per stroke. This will be the case if there is an insulation failure at the grounded pole (possible, since the insulation voltage will be at prodischarge levels for at least twice the travel time between stroke impact and arrester). In the event the voltage is low enough not to flashover the insulation, we lose little by not considering the resulting arrester operation. This is illustrated in Fig. 14.

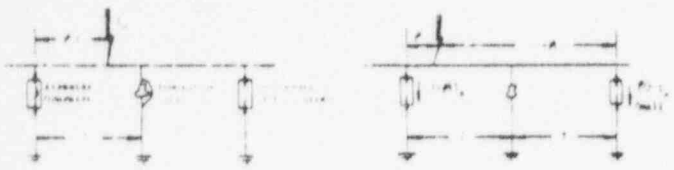

(a) Insulation Fails (b) Insulation Holds

Figure 14. Interpretation of the Number of Arrester Operations per Stroke

For this case, the number of arrester operations exceeding 65kA would be halved. Similar arguments could be made for considering each stroke to produce fractional arrester operations for more distant arrester placement (e.g. 2 significant operations for every 3 strokes with arresters every third grounded pole).

(D) Multiple Strokes

The effect of multiple strokes is unclear. McCann and Deck[12] suggest that only 30% of arrester operations show multiple components. However, all field data (e.g. Refs. 12, 18, 19) suggest that subsequent components are more than ample to cause arrester operation. On the other hand, the average of the highest of subsequent components is roughly half that of the first component. Hence, calculations of numbers of actual occurrences of arrester currents greater than some given current well above the mean (e.g. 20kA) will not be seriously in error due to multiple components, while those below the mean will almost certainly be low. In essence, we are determining the statistics of the maximum or first component.

(E) Comparison with Existing Information

There is much information in the literature regarding "suggested" distributions of line and arrester currents. As noted earlier (page 1) AIEE recommendations correlate with near perfection our estimates of frequency distributions of strokes to the line. Typical of suggested frequency distributions of arrester currents is found in Ref. 20, shown in Fig. 15 (largely extrapolated). Since this includes incidents due to direct strokes and indirect strokes, and gives no indication of footing resistance, this curve should be lower than our prediction perhaps by as much as a factor of 4. If shielding was present (even to the extent of a wooded area less than the height of the line), the reduction would be even greater. For crude illustration, the curve is also shown redrawn with a multiplier of 5. While the extrapolation is rather extreme, it suggests that the approach given here is appropriate. At the other extreme, Ref. 21 gives data for a test line with arresters apparently particularly susceptible to high currents. A rough approximation suggests the two data points also shown in Fig. 15.

Clearly, much remains to be done in our understanding of distribution arrester currents. It is believed that the present paper will be an aid to those seeking field records in the near future, and ultimately in the application and design of arresters.

CONCLUSIONS

1. The "Electrogeometric Theory" of lightning performance has been extended to distribution systems, and frequency distributions of line and arrester currents due to direct strokes have been predicted. Rates of strokes to distribution lines of various heights are also predicted.

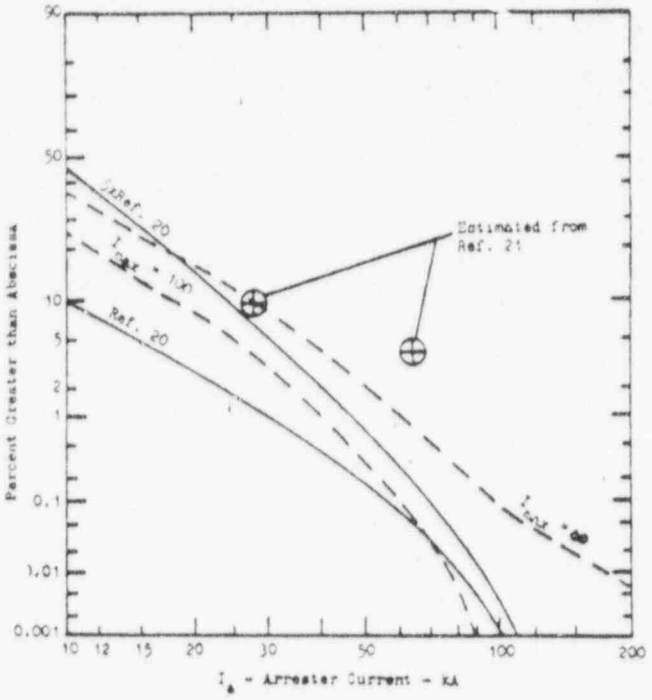

Figure 15. Comparison with Existing Information

2. Indirect strokes are shown to produce minimal (of order 1 kA max) line and arrester currents.

3. The effect of shielding by nearby structures (e.g. HV lines, buildings) and natural shielding is shown. Such effects reduce the number of strokes to the line and increase the frequency distribution of those strokes that do hit.

4. The effect of stroke location on arrester current magnitude is analyzed. It reduces the frequency distribution of currents markedly compared with strokes to the line. An effective arrester current of $(1-\rho)I_o$ is suggested, where ρ is the stroke location measured as a fraction of the distance between stroke discharge points.

5. Effects of footing resistance, predischarge, pole reflections, and multiple strokes are considered and illustrated. Predischarge and pole reflection is not expected to significantly affect arrester crest current magnitude.

6. The results are compared with existing information, and the analysis is shown to be quite reasonable. It is clear, however, that much field work remains to be done for full verification.

APPENDIX

FREQUENCY DISTRIBUTION OF ARRESTER CURRENTS

It was shown that a stroke of current I at location ρ produces an arrester current $(1-\rho)I_o$ as shown previously.

Since stroke location is random, the frequency function of is

$$f(\rho) = \begin{cases} 1, & 0 \leq \rho \leq 1 \\ 0 & \text{elsewhere} \end{cases}$$

Now, $f_1(I)$, the frequency of strokes to the line, can be readily found, as shown previously. Finally, I and

ρ are independent. Thus

$$f_A(I_a)dI_a = \int f_L(I) f_\rho(\rho) d\rho\, dI$$

where the integration may be performed over either variable, maintaining I_a by

$$I_a = (1-\rho)I$$

The most convenient is to integrate over I:

$$dI_a = -I d\rho \qquad \text{or} \qquad |d\rho| = +\frac{dI_a}{I}$$

$$f_A(I_a)dI_a = +\left[\int \frac{f_L(I)}{I}\, dI\right] dI_a$$

The limits are governed by the fact that I cannot be less than I_a:

$$f_A(I_a) = +\int_{I_a}^{\infty} \frac{f_L(I)}{I}\, dI$$

Finally, the distribution function is

$$F_A(I_a) = \int_{I_a}^{\infty} f_A(I_a) dI_a$$

The alternative form of the frequency function is

$$f_A(I_a) = \int_0^1 \frac{f_L\left(\frac{I_a}{1-\rho}\right)}{1-\rho}\, d\rho$$

REFERENCES

(1) Brown, G. M. and E. R. Whitehead, "Field and Analytical Studies of Transmission Line Shielding: Part II," IEEE PAS, May 1969, pp. 617-620.

(2) Brown, G. M., The Electrogeometry of Shielding Against Lightning, Ph.D. Thesis, IIT, June 1967.

(3) Gilman, D. E. and E. R. Whitehead, "The Mechanism of Lightning Flashover on High Voltage and Extra High Voltage Transmission Lines," Electra, March 1973, pp. 65-96.

(4) Whitehead, E. R., "CIGRE Survey of the Lightning Performance of Extra High Voltage Transmission Lines," Electra, March 1974, pp. 63-89.

(5) Currie, J. R., Liew Ah Choy, and M.Darveniza, "Monte Carlo Determination of the Frequency of Lightning Strokes and Shielding Failures of Transmission Lines," IEEE PAS, Sept./Oct. 1971, pp. 2305-12.

(6) Sargent, Michael A. and M.Darveniza, "Lightning Performance of Double Circuit Transmission Lines," IEEE PAS, May/June 1970, pp. 913-925.

(7) Sargent, M. A., "The Frequency Distribution of Current Magnitudes of Lightning Strokes to Tall Structures," IEEE PAS, Sept./Oct. 1972, pp. 2224-29.

(8) AIEE Committee Report, "A Method of Estimating Lightning Performance of Transmission Lines," AIEE Transactions, Pt. II, 1950, pp. 1187-96.

(9) Poplansky, F., "Measurement of Lightning Currents in Czechoslovakia....," CIGRE 33-03, 1970.

(10) Golde, R. H., "Lightning Surges on Overhead Distribution Lines Caused by Indirect and Direct Lightning Strokes," AIEE PAS, June 1954, pp. 437-447.

(11) Hylten-Cavalius, N. and Ake Stromberg, ASEA Research #8, "Field Measurements of Lightning Currents," 1964.

(12) McCann, G. E. and E. Beck, "Field Research on Lightning Arrester Discharges," AIEE PAS, 1947, pp. 625-629.

(13) Weber, E., Electromagnetic Fields, Volume I, Wiley, 1950, pp. 111-115.

(14) Wagner, C. F. and A. R. Hileman, "Effect of Prediscbarge Currents upon Line Performance," AIEE PAS, April 1963, pp. 117-131.

(15) Wagner, C.F. and A.R. Hileman, "Prodischarge Current Characteristics of Parallel Electrode Gaps," AIEE PAS, Dec. 1964, pp. 1236-42.

(16) Industry Task Force, "Investigation & Evaluation of Lightning Protective Methods for Distribution Circuits, Part I: Model Study and Analysis," IEEE PAS, Aug. 1969, pp. 1232-38.

(17) Industry Task Force, "Investigation & Evaluation of Lightning Protective Methods for Distribution Circuits, Part II: Application and Evaluation," IEEE PAS, Aug. 1969, pp. 1239-47.

(18) McCann, G. E., "The Measurement of Lightning Currents in Direct Strokes," AIEE PAS, 1944, pp. 1157-74.

(19) Berger, K. and E. Vogelsanger, "Messungen und Resultate der Blitzforschung der Jahre 1955...1963 auf dem Monte San Salvatore," Schwizerischer Electrotechnische Vereins, Bulletin, January 1965, pp. 2-22.

(20) IEEE Committee Report, "Surge Protection of Cable Connected Distribution Equipment on Underground Systems," IEEE PAS, Feb. 1970, pp. 263-267.

(21) Mambuca, J. A., "Lightning Problems on Distribution Systems," IEEE T&D Meeting, Oct. 12, 1972.

Discussion

Ernest A. Goodman (Ernest A. Goodman, Inc., Pittsburgh, PA): This is a very fine paper, based on an expansion of Dr. Brown's doctoral thesis, and subsequent work largely applicable to transmission lines. However, as the paper states, the theories apply equally to distribution lines with their arresters. Hence, the paper is a welcome and useful theoretical and mathematical analysis of distribution line and distribution arrester lightning performance.

Verification and substantiation of these theories and calculations, by determination of actual distribution arrester discharge currents, is an expansive undertaking which must involve many thousands of arrester service years in order to be statistically valid. An I.E.E.E., P.E.S. Surge Protective Devices Committee Working Group is presently engaged in organizing such a study, which would involve thousands of distribution arrester with an average service of 10 years from more than a dozen major utilities. It is the objective of that Working Group to determine, with reasonable accuracy, actual numbers and magnitudes of lightning discharge currents through these distribution arresters, to gain a better understanding of the performance required of such arresters on present-day distribution systems with their typical operating voltages, load densities (i.e. arrester spacings), shielding, and grounding.

Reference (22) below should be included among significant, pertinent references.

This paper is a useful, mathematical treatment of the very real practical problem of establishing discharge current capabilities and IR voltage limitations required of today's and tomorrow's distribution arresters.

REFERENCE

(22) Westrom, A.C., "Circuit Protection Requires Direct Stroke Analysis", I.E.E. Transmission and Distribution Committee Meeting, May 8-9, 1975, Minneapolis, Minnesota.

Manuscript received January 27, 1976.

A.C. Westrom (Kearney Division, Kearney-National, Inc., Atlanta, GA): Your calculations include interesting relationships deserving of further study and correlation with field work. My own more simplified calculations suggest a more severe direct stroke duty for distribution surge arresters.* They show for example that 7% of the arresters installed on a typical 15KV class single phase distribution line located in a TD-60 area would discharge 65kA or greater surges in a 30 year lifetime. This percentage bears substantial relationship to a 1975 field study with early reporting in the reference and final reporting in an additional paper (co-authored) to be presented at the 1976 Underground Transmission and Distribution Conference. Distribution arresters are indeed direct stroke interceptors when applied to exposed circuits.

It is believed that 7% of the population is motivational relative to product design and application. I would like to solicit additional field studies where good results can be obtained as reasonable cost by inspecting the gap parts of suitable arrester designs returned from field duty.

REFERENCE

*Westrom, A.C., "Circuit Protection Requires Direct Stroke Analysis," I.E.E. T&D Committee Meeting May 8-9, 1975, Minneapolis, Minnesota.

Manuscript received February 4, 1976.

Edwin R. Whitehead (Consultant, Colorado): This paper is a significant contribution to the research on surge arrester currents on distribution systems. As distribution voltages reach levels formerly associated with the subtransmission system, protective margins of transformer windings may be lowered. Effective coordination of insulation levels with voltage levels of the arrester and its grounding/bonding system require more information on the actual lightning currents to which the arrester may be subjected under direct-stroke conditions. Large-scale field investigations using sophisticated measurement techniques have been proposed to obtain this information. In such investigations, great care should be used to select line routes and instrumented points so as to maximize data yield. In the planning stages, this paper may prove valuable in assessing the shielding effects of adjacent high-voltage lines or wooded areas.

The authors cite Sargent's paper, "The Frequency Distribution of Current Magnitudes of Lightning Strokes to Tall Structures" as one of several references verifying the "electrogeometric" theory. It should be remarked parenthetically that Armstrong and Whitehead (1968) coined this term to mean any of the several approaches to the problems of shielding or stroke incidence in which the "striking distance" element of the geometry is found from the electrical properties of the leader. Since current research on an extension of this theory will utilize newly-defined entities, but not a new "theory", it is hoped that this generalized intent will be recognized. Sargent made additional and important contributions in showing the dependence of the current-amplitude distribution on the structure height and deducing a reference amplitude distribution for zero height or flat earth. Often overlooked, however, is Linck's discussion showing that the analytical model used was not equally successful in predicting the observed numbers of strokes to tall communication towers as a function of height. He suggested that the discrepancy might be due to some factor not included in the model as used and that further study of striking distance and leader angle distribution might be required when the structure geometry was other than that of the transmission line. Such studies are now in progress by both Linck and Whitehead in which a new entity, the "attractive range" is defined as consisting of two or more terms of which only the first is independent of the structure height. One measure of the attraction between the leader and the structure is a parameter defining the leader approach angle probability density function, this parameter being a function of both tower height and prospective current to earth. For the heights of the distribution lines involved, only the first term of the "attractive range" seems applicable so that the methods used by the authors would be unaffected.

Manuscript received February 11, 1976.

J.L. Koepfinger (Duquesne Light Co., Pittsburgh, PA): This paper provides a better understanding of the effects that lightning has upon distribution circuits. Is is significant to note that figure 15, which relates past data on arrester current to calculations, indicated that arrester currents in excess of 65kA are unusual. Also indicated is the fact that arrester currents in excess of 20kA can be expected quite frequently. This is in contrast to data compiled by K.B. McEachron and W.A. McMorris, AIEE Transaction Vol. 57, 1938 page 307, which indicates that 1% of the distribution arrester currents are greater than 20KA.

As the authors indicate, there is a strong need for further modern field data to establish the existence of a high frequency of arrester currents in excess of 20kA.

Manuscript received February 11, 1976.

G.W. Brown and S.L. Thunander: Many thanks to the discussors for their kind remarks. Dr. Whitehead rightly notes concern for strokes to higher transmission lines. It is the authors' opinion that this is largely due to lack of accurate knowledge of localized Isokeraunic Level (IKL), so only time and data will tell. It is clear that Sargent's frequency distribution is highly predictive, even for high structures. One would expect the distribution to change with a height dependent "attractive range." Recent work by the authors (Ref. #23) suggests that the numbers of strokes to EHV lines are still adequately predicted by the model of the present paper. Again, only time and more data will be definitive.

Mr. Koepfinger notes that arrester current in excess of 20kA can occur "quite frequently." Consider this example: an arrester on the outer phase of a horizontal unshielded distribution line in a treeless terrain with very low footing resistance and 200 meters (650 feet) between grounded poles in a region with an IKL of 60, would experience an average of one stroke above 20kA every forty years. Since treeless areas and good footing resistance don't generally go hand in hand, this number represents a "worst case." Further, (as noted in the text) the data of Figure 15 show very much lower frequencies than suggested by Reference 21. Later data from the same source suggest much lowered frequencies. In terms of *arrester* failure, the present study does not support concern.

With respect to protected *equipment* failures, it must be noted that discharge voltage is much less a function of crest current, rather, it is the function of current rate-of-rise.

Presently there is a great deal of interest in the industry concerning the levels of surge current distribution arresters actually experience. We certainly agree with the discussors that there is a definite need for field work to accumulate data in this area. A field study conducted under controlled conditions that could be compared against the theoretical model would certainly benefit the entire industry. Utility companies across the country would be able to develop their standards with regards to the level of lightning protection they desire while equipment manufacturers would have a base from which to establish design levels. It is the authors' hope that this paper will serve as the impetus and guideline for such studies.

Once again, we wish to thank the discussors.

REFERENCE

(23) G.W. Brown, "Lightning Performance I-Shielding Failures Simplified," submitted to IEEE for presentation at Winter Power Meeting, January 1977.

Manuscript received June 17, 1976.

IEEE Transactions on Power Apparatus and Systems, Vol. PAS-97, no. 1, January/February 1978

LIGHTNING PERFORMANCE II
UPDATING BACKFLASH CALCULATIONS

REF. 22

Gordon W. Brown, Senior Member

U. S. Energy Research and Development Administration
Washington, D. C.

ABSTRACT AND CONCLUSIONS

An updated method of determining the backflash performance of transmission lines is thoroughly presented, using a step-by-step example. At each stage, sufficient information is given to apply the method to any system. Incorporated in the analysis are revised effects of corona and bound charge; effect of stroke location along the span; joint distribution of stroke current rate of rise and crest magnitude; frequency distributions of footing resistance, terrain type, stroke location, and system voltage.

One of the significant results is the understanding of tower top voltage as a function of rate of rise of current. This enables easy formal calculation of probabilities and greatly simplifies the testing (or computation) to determine tower top voltage. Only one ramp at each desired stroke location is needed to develop the necessary voltage information.

Second components of lightning events, characterized by lower magnitudes and higher rates of rise, are shown to have an insignificant effect on backflash performance.

As might be expected, for an exponential distribution of footing resistance, applicable resistance is much higher than average resistance (a factor of 1.8 for the sample 500kV line). Accurate characterization of the footing resistance distribution of the line is thus essential for any degree of accuracy in backflash calculations.

It is important to note that the method is straightforward. Any or all of the parts can be more easily done with aid of a computer, but Monte Carlo techniques are not necessary. There is not the frustration of a "zero backflash" result with no suggestion of order of magnitude. For the sample 500kV line, with 60% Flat, 30% Rolling, and 10% Mountainous terrain and an overall average footing resistance of about 12 ohms, the calculated backflash outage rate is 0.23 per 100km-yr (at an IKL of 40). This is quite comparable to recent estimates based on field surveys.

INTRODUCTION

(A) The Method Outlined

The method is to be envisioned in the following 5 stages:

I. Establishing Line Parameters (including corona)
II. Establishing the Tower Top Voltage Required for Flashover (as a function of time to flashover)
III. Establishing the Stroke Rate of Rise and Magnitude Required for Flashover (as a function of time to flashover)
IV. Establishing the Probability of Backflashover as a Function of Line Configuration, Footing Resistance, CFO for a Random Stroke to the Tower or Span
V. Line Backflash Outage Rate (accounting for variations in line configuration, footing resistance, and line voltage)

(B) The Sample Line Studied

The following are the assumed characteristics of the line for which backflash performance will be determined.

For All Terrain:

Ground wires: 1 cm OD
Spacing between ground wires: 15m(49')
Phase conductor bundle: 2x1.5cm(1.5")OD, 45cm(18") centers
Spacing between phases: 10m(33')
Insulators: 25 (positive impulse CFO=2000kV)
Line voltage: 500kV

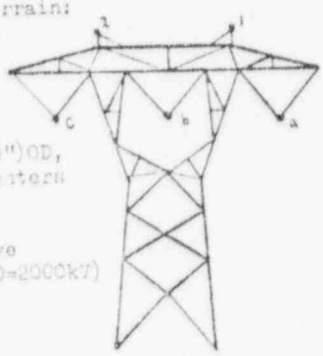

Figure 1. Sample Line

10% Mountainous Terrain

$\bar{R}_f$ = 30Ω, exponentially distributed
Span = 600m (1968 feet)
Z_t = 160Ω
Ground wire height at tower = 50m (164 feet)
Sag = 14m
Average heights: Ground wire: h = 60m
Phase conductor: y = 50m

30% Rolling Terrain

$\bar{R}_f$ = 15Ω, exponentially distributed
Span = 500m (1640 feet)
Z_t = 150Ω
Ground wire height at tower = 40m (130 feet)
Sag = 11m
Average heights: Ground wire: h = 40m
Phase conductor: y = 30m

60% Flat Terrain

$\bar{R}_f$ = 7Ω, exponentially distributed
Span = 400m (1302 feet)
Z_t = 140Ω
Ground wire height at tower = 30m (98 feet)
Sag = 8m
Average heights: Ground wire: h = 25m
Phase conductor: y = 15m

I. ESTABLISHING THE LINE PARAMETERS (INCLUDING CORONA EFFECTS)

The impedances unaffected by corona are determined first. Conductor notations are as follows.

F 77 016-9. A paper recommended and approved by the IEEE Transmission and Distribution Committee of the IEEE Power Engineering Society for presentation at the IEEE PES Winter Meeting, New York, N.Y., January 30-February 4, 1977. Manuscript submitted July 21, 1976; made available for printing October 28, 1976.

0018-9510/78/0100-0039$00.75 ©1978 IEEE

(A) Mutual Impedances

Corona doesn't affect the mutual impedances, and the average values are (M, R, and F refer to Mountainous, Rolling, and Flat terrain respectively):

$$z_{1a} = 60 \ln \frac{D_{1a}}{d_{1a}} = \begin{matrix} 142\Omega, M \\ 115\Omega, R \\ 81\Omega, F \end{matrix}$$

$$z_{2a} = 60 \ln \frac{D_{2a}}{d_{2a}} = \begin{matrix} 103\Omega, M \\ 77\Omega, R \\ 46\Omega, F \end{matrix}$$

$$z_{12} = 60 \ln \frac{D_{12}}{d_{12}} = \begin{matrix} 125\Omega, M \\ 101\Omega, R \\ 75\Omega, F \end{matrix}$$

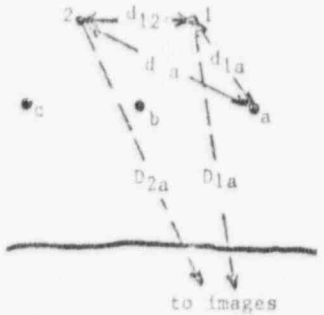

Figure 2. Mutual Impedances

(B) Ground Wire Surge Impedance and the Coupling Factor

Under corona, both ground wire surge impedance and coupling factor are affected by the increased effective radius of the conductor. The ground wire self-impedance is

$$z_{11} = vL_{11} = \frac{v}{v_o} 60 \ln \frac{2h}{r_1} \qquad (v_o = 300 m/\mu s)$$

where v is the corona-reduced velocity, and r_1 is the ground wire radius. Using R for the corona radius

$$\frac{v}{v_o} = \sqrt{\frac{\ln \frac{2h}{R}}{\ln \frac{2h}{r_1}}} \quad \text{and} \quad z_{11} = z_{22} = 60 \sqrt{\ln \frac{2h}{R} \ln \frac{2h}{r_1}}$$

For a given effective corona voltage, the corona radius is as in Figure 3 (see Appendix I). For the specific line considered, ground wire surge impedance and coupling factor are as in Figure 4.

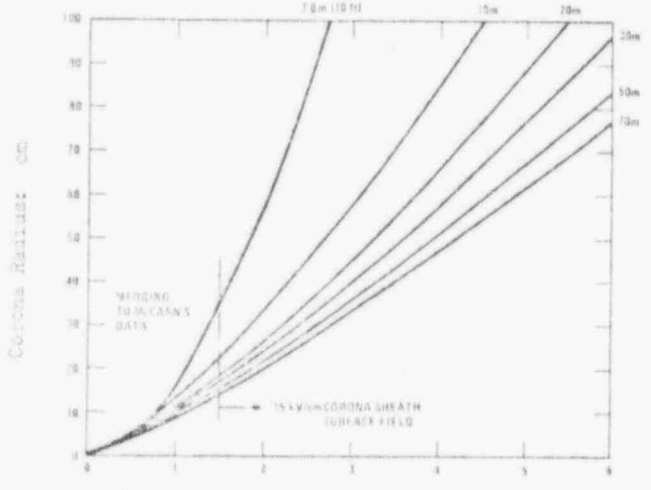

Figure 3. Effective Corona Radius

Corona radius is a function of the charge on the ground wire, which is a function of the tower voltage, bound charge, and potential coefficients. The "Effective Corona Voltage" of Figure 4 is developed next.

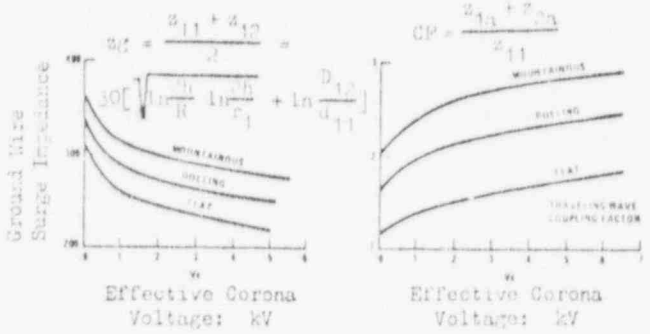

Figure 4. Surge Impedance and Coupling Factor for Sample Line

(C) Effective Corona Voltage

Bound charge act's to reduce the total charge on the ground wire. For a ground wire of given height, bound charge can be expressed in terms of the voltage which such a charge would, by itself, produce on the line. This voltage is termed V_h. Because strike distance (i.e., proximity of leader charge) increases with current, and leader charge increases with current, the net effect is that this voltage is relatively independent of stroke current. The result is shown in Figure 5.

It is noted that it is assumed that bound charge does not produce a significant tower voltage (cf. the discussions in Reference 1. Further, charges of the final streamers from leader and from tower are not likely to have as much charge as the main leader charge, though this is commonly assumed. Lower streamer charges further reduce the effect.)

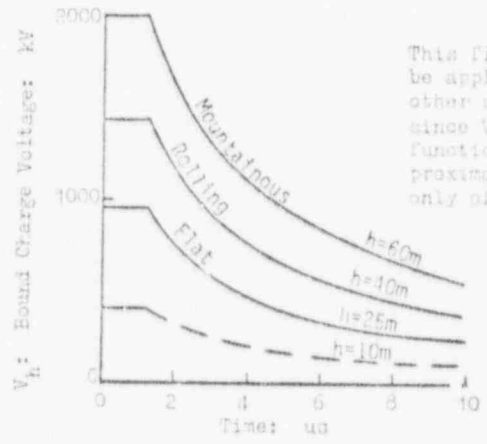

This figure can be applied to other situations, since V_h is a function (approximately) only of height.

Figure 5. Equivalent Reduction of Ground Wire Voltage Due to Bound Charge

1. Single Ground Wire. For a single ground wire, V_h is subtracted from the actual tower top voltage (V_t) to yield V_{e1}, the single ground wire effective corona voltage:

$$V_{e1} = (V_t - V_h)$$

2. Two Ground Wires. For two ground wires, the charge, q, required on the ground wire to produce a given ground wire potential is reduced. Hence, to find the proper coupling factor and effective ground wire surge impedance, one must enter the abscissa ("Effective Corona Voltage" axis) of Figure 4 with

$$V_{c2} = V_{c1} \cdot \frac{q \text{ for two wires}}{q \text{ for one wire}} = \frac{60 \ln \frac{2h}{R}}{60 \ln \frac{2h}{R} + z_{12}} V_{c1}$$

For rigor, the multiplier should be found at each step, but it varies very slowly with corona radius.

Example 1: For the Rolling terrain case, at a corona radius of 25cm, the ratio is

$$\frac{V_{c2}}{V_{c1}} = \frac{\ln \frac{8000}{20}}{\ln \frac{8000}{20} + \ln \frac{81.4}{15}} = .78$$

At R = 40cm, this becomes .76.

For the system at hand, we approximate by using .74, .77, and .81 for the Mountainous, Rolling, and Flat cases respectively.

II. ESTABLISHING TOWER TOP VOLTAGE NECESSARY FOR FLASHOVER

The volt-time curve for standard insulators (Reference 2) is shown in Figure 6.

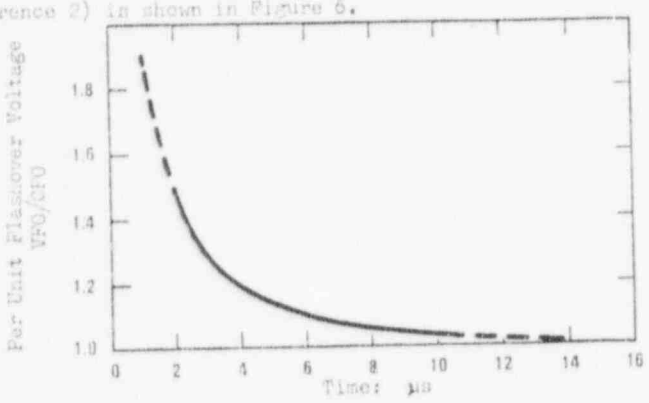

Figure 6. Insulation Positive Impulse Volt-Time Curve (Reference 2)

This represents, of course, the required voltage from phase conductor to tower top. A very brief iteration yields the tower top voltage, $V_t FO$ required to produce flashover, at a given time.

$$V_t FO = \frac{VFO}{1-CF}, \quad \text{where}$$

CF = coupling factor, a function of $(V_t - V_h)$ from Figures 4 and 5

VFO = flashover voltage, as in Figure 6

Example 2: At t=1μs for the Mountainous case,

Trial	VFO	V_n	$V_t FO$	$V_t - V_h$	$\frac{V_{c2}}{V_{c1}}(V_t - V_h)$	CF
1	2400	1100	3000	1900	1410	.25
2	2400	1100	3200	2100	1550	.252
3	2400	1100	3210	2110	1560	.252

The overall results are as follows (T_s = span travel time) for the sample line.

Table I

Tower Voltage Required for Flashover

t	Mountainous		Rolling		Flat	
	t(μs)	$V_t FO$(kV)	t(μs)	$V_t FO$(kV)	t(μs)	$V_t FO$(kV)
T_s	2	4010	1.67	4090	1.33	4100
$2T_s$	4	3210	3.33	3200	2.67	3180
$4T_s$	8	2830	6.67	2730	5.33	2600
$6T_s$	12	2780	10.00	2660	8.00	2490
$8T_s$	16	2720	13.33	2610	10.67	2450

III. STROKE RATE OF RISE AND MAGNITUDE REQUIRED FOR FLASHOVER

One of the key insights which came in the course of the present work was the recognition that only a ramp stroke current is required to define the stroke current and rate of rise required for flashover. In Figure 7 it is seen that for a given rate of rise, flashover will occur at a specific time, provided crest current is sufficiently high. This approach

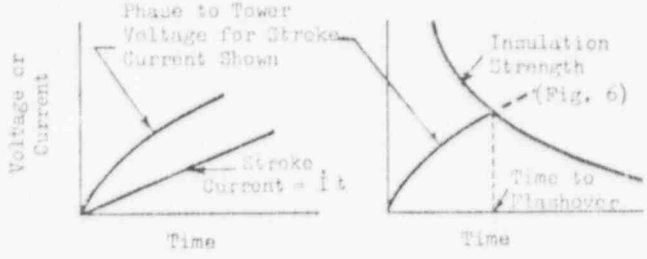

Figure 7. Illustration that Fixed Ramp of Current Leads to Known Time to Flashover

(tower voltage as a function of rate of rise rather than crest current) makes formal calculation of the probability rather easy. It also suggests that in order to determine the voltage for a stroke at a given location (e.g., at the tower), only one test need be made; namely, a ramp of current at that location! Such a test could be made either digitally, or on models, or by hand as illustrated next.

(A) Tower Top Voltage as a Function of dI/dt

1. Stroke to Tower. For a stroke to the tower, quite simple but very accurate approximations to tower top voltage can be developed assuming a ramp of stroke current (Appendix II). The results are summarized below and in Figure 8.

$$V_t = B_{oo} V_{oo} + B_o \dot{I}_o t$$

$$V_{oo} = + \frac{Z_t^2 (Z_t^2 - R_f^2)}{2Z_t (Z_t + 2R_f)} 2T_t \dot{I} \quad (T_t = \text{tower travel time one way})$$

$$\dot{V}_o = \frac{R_f Z_t}{2R_f + Z_t} \dot{I}$$

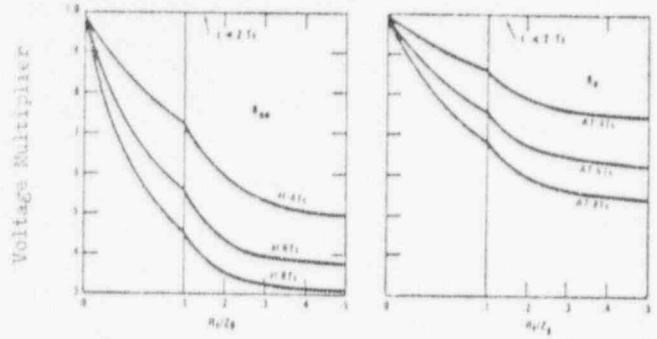

Figure 8. Parameters for Determining Tower Voltage for a Stroke to Tower

Example 3: For the Mountainous case, with $R_f = 30\Omega$, $2T_t = .328$ μs. Z_g (Figure 4) varies between 300 and 308. $Z_g = 304$ is assumed. $Z_t = 160\Omega$. $T_n = 2$ μs. Hence

$$V_{oo} = \frac{(304)^2(160^2 - 30^2)}{2(160)(304 + 30)^2}(.328)\dot{I} = 17.7\,\dot{I}$$

$$V_o = \frac{30(304)}{30+304} = 25.0\,\dot{I}$$

At, for example, $t = 12$ μs (or $6T_g$), with $R_f/Z_g = 30/295 = .102$,

$$B_{oo} = .56 \text{ and } B_o = .76$$

Thus,

$$V_t = .56(17.7)\dot{I} + .76(25.0)(12)\dot{I}$$

$$= 237.9\,\dot{I}$$

The summary is as follows. Calculations are made for $R_f = \bar{R}_f$, $2\bar{R}_f$ and $3\bar{R}_f$.

Table II

Tower Voltage vs. Time

For the Sample Line

t	Mountainous V_t/I: kV/(kA/μs)				Rolling V_t/I				Flat V_t/I			
	t(μs)	R_f=30	60	90	t(μs)	R_f=15	30	45	t(μs)	R_f=7	14	21
$2T_g$	2	67	77	100	1.67	39	54	67	1.33	21	28	34
$3T_g$	4	117	170	232	3.33	63	95	121	2.67	30	45	58
$4T_g$	8	178	245	348	6.67	97	150	197	5.33	45	70	92
$5T_g$	10	231	312	454	10.00	124	194	261	8.00	58	91	119
$6T_g$	12	278	361	510	11.33	140	223	308	10.67	70	110	141

B. Stroke to the Span. For a stroke to the span, the voltage is the same as a stroke to the tower, until the first reflection arrives, after which it is reduced (Appendix II). The net effect is that the V_t/I is reduced by the multiplier:

$$\frac{(V_t/\dot{I}) \text{ for stroke to span}}{(V_t/\dot{I}) \text{ for stroke to tower}} = \begin{cases} 1, & t < t_{ko} \\ \dfrac{V_{tko} + (1-k)(V_t - V_{tko})}{V_t} \end{cases}$$

where

$V_{tko} = V_t$ (for stroke to tower) at $t_{ko} = 2(1-k)T_g$

k = distance from tower to stroke as a fraction of the span

T_g = span travel time

Example 4: For the Mountainous case, $R_f = 30\Omega$, at mid-span:

$k = \frac{1}{2}$, $t_{ko} = 2(1 - .5)(2\mu s)$

$= 2\mu s$ at which (Table II)

$V_{tko} = 67\,\dot{I}$

Consider the voltage 16μs after incidence of surge at the tower:

$V_t = 278\,\dot{I}$

$$\frac{(V_t/\dot{I}) \text{ stroke to span}}{(V_t/\dot{I}) \text{ stroke to tower}} = \frac{67 + .5(278-67)}{278} = .62$$

(B) Stroke Current Rate of Rise and Crest Magnitude Required for Flashover

Table I (V_tFO) and Table II are readily utilized to determine the minimum $\dot{I}$(= dI/dt) and I(crest) required to produce flashover at a given time.

Example 5: At t = 8μs, Mountainous case, $R_f = 30\Omega$,

$V_tFO = 2830$kV (from Table I)

$V_t/\dot{I} = 174$kV/(kA/μs) (Table II)

Hence

$$\dot{I} = \frac{2830}{174} = 16.3\text{kA/μs}$$

At this rate, I must be at least

$$I_{min} = (16.3\text{kA/μs}) \times 8\mu s = 130\text{kA}$$

The results corresponding to Table II are shown in Table III.

Table III

$\dot{I}$ and I_{min} Required for Flashover Stroke to Tower

t	Mountainous R_f=30		60		90		Rolling 15		30		45		Flat 7		14		21	
	$\dot{I}$	I_{min}	$\dot{I}$	I_{min}	$\dot{I}$	I_{min}	$\dot{I}$	I_{min}	$\dot{I}$	I_{min}	$\dot{I}$	I_{min}	$\dot{I}$	I_{min}	$\dot{I}$	I_{min}	$\dot{I}$	I_{min}
$2T_g$	60	120	42	83	34	67	105	210	74	150	61	124	106	212	84	170	67	134
$3T_g$	27	110	18	70	14	55	57	172	38	114	29	86	42	126	29	87	23	68
$4T_g$	16	129	11	91	8	65	29	232	18	144	14	112	20	160	13	104	10	80
$5T_g$	10	142	8	79	5	70	18	234	11	143	8	104	11	143	7	91	5	70
$6T_g$	10	157	7	110	5	78	17	268	11	174	8	126	10	158	7	110	5	78

For a stroke to the span, I and I_{min} for flashover will increase since $V_t/\dot{I}$ is reduced (Example 4, above).

IV. PROBABILITY OF BACKFLASHOVER AT SPECIFIC FOOTING RESISTANCE, SOIL TYPICAL

(A) Probability of Flashover for a Stroke to Tower

In Reference 3, the joint character of the distributions of current magnitude and rate of rise are discussed. With $f(I,\dot{I})$ being the joint frequency distribution, the probability of flashover can be written

$$PFO = \int_0^\infty \int_{I_{min} \text{ at } \dot{I}}^\infty f(I,\dot{I})\,dI\,d\dot{I} = \int_0^\infty g[\dot{I}, I_{min}(\dot{I})]\,d\dot{I}$$

The function $g(\dot{I}, I_{min})$ is shown in Figure 9.

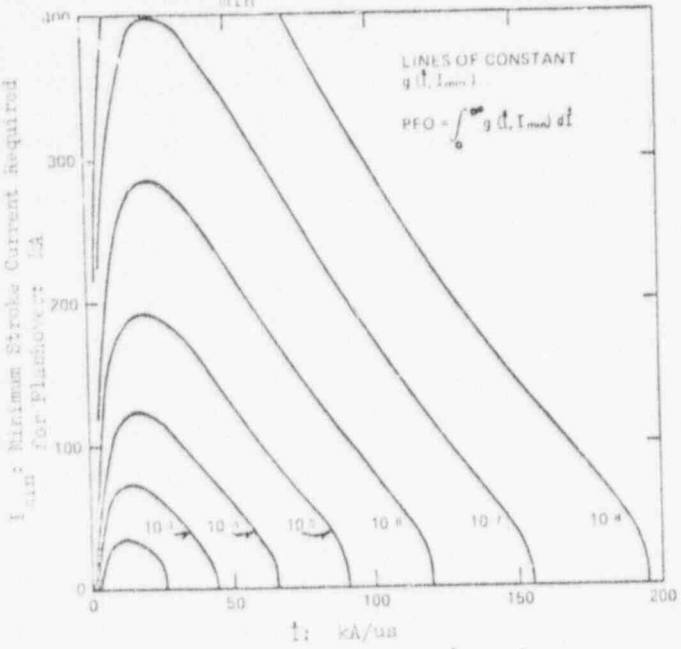

Figure 9. The Function $g(\dot{I}, I_{min})$

By plotting $\dot{I}$ vs. I_{min} on Figure 9, $g(\dot{I}, I_{min})$ as a function of $\dot{I}$ can be easily found and integrated, as in Figure 10.

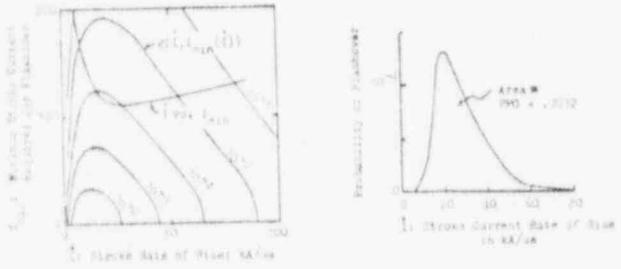

Figure 10. Calculation of PFO for the Mountainous Case, $R_f = 30$

The parameters upon which Figure 9 is based are as follows.[3]

The crest stroke current to lines has a mean of 16kA. The standard deviation of the natural logarithm of the crest current is 0.69. The corresponding values for the rate of rise are 12kA/μs and 0.55 respectively. The correlation factor between ln(I) and ln(dI/dt) is 0.369.

(B) Second Components

Because second components of strokes generally have much higher rates of rise, it was thought they might produce significant backflash failures. However, the crest magnitudes are smaller, and more significantly, magnitude and rate of rise are negatively correlated.[4] This results in $g(\dot{I}, I_{min})$ for second components being roughly two orders of magnitude smaller in the region of interest. To illustrate, first and second components are compared for $g(\dot{I}, I_{min}) = 10^{-6}$ in Figure 11 below. Clearly, second components can be ignored in backflash calculations.

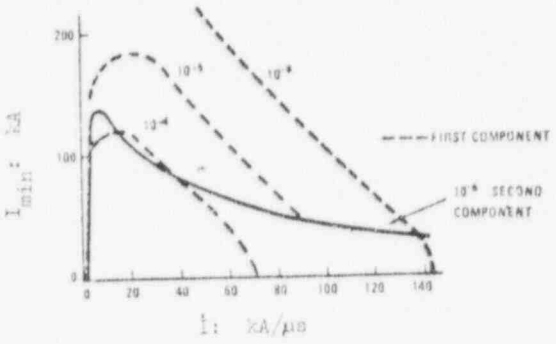

Figure 11. Negligible Effect of Second Components

(C) Probability for Stroke to the Span

As noted above, $\dot{I}$ and I_{min} required for flashover are increased since $V_f/\dot{I}$ is reduced (cf. Example 4). Figure 12 illustrates the values for a stroke to the midspan ($k = 0.5$), for which the probability of flashover is calculated to be .0020.

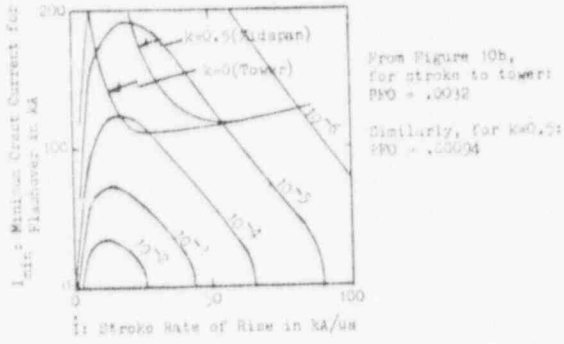

Figure 12. Probability of Flashover for Stroke to Midspan (Mountainous Terrain: $R_f = 30$)

(D) Expected Stroke Location

1. Strokes Directly to Tower. The "Brown-Whitehead" model enables estimates of the proportion of strokes to the tower, as in Figure 13.

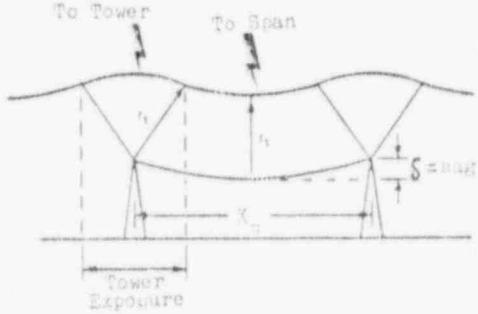

$r_s = 7.1 I^{.75}$

Figure 13. Exposure of Tower to Strokes

It is readily shown that the fraction of strokes to the tower is, closely,

$$P_t \simeq \frac{8\delta\, r_s}{X_n^2} = \frac{56.8\delta\, I^{.75}}{X_n^2}$$

δ = sag in meters
X_n = span length in meters

Example 6: For the Mountainous terrain case ($R_f = 30\Omega$) considered in the example of Figures 10 and 12, the appropriate percentage to the tower is near the peak of $g(I, I_{min})$. In this region (Figure 9) I is of order 120kA, for which

$$P_t = \frac{56.8(10)(120)^{.75}}{(500)^2} = .082$$

2. Strokes to the Span. From Figure 13, it is reasonable to consider the strokes to the line to be linearly distributed along the line. (For the above example, this is the remaining 1 - .082 or 91.8% of the strokes.)

(E) OVERALL PROBABILITY OF FLASHOVER FOR A RANDOM STROKE

A sketch of the probability of flashover versus the number of strokes is shown in Figure 14 (in per unit of the total).

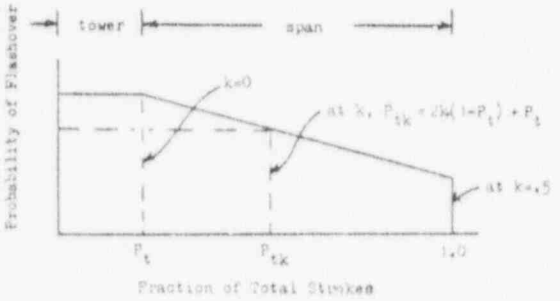

Figure 14. Distribution of Flashover Probability Along the Line

P_{tk} is the fraction of the total strokes for which the probability of flashover is that at k. The overall probability of flashover for a random stroke to the line is readily estimated as the area under the curve of Figure 14. The example of Figures 10 and 12 and Example 4 is continued in Figure 15.

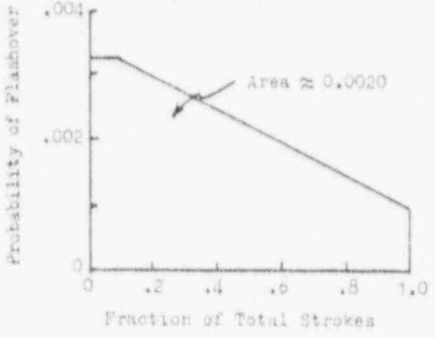

Figure 15. Distribution of Probability of Flashover (Mountainous Terrain: $R_f = 30$)

Thus for that case, the probability of flashover for a random stroke to the line is about .002. The results for the cases studied are shown in Figure 16. For the sample line chosen, the PFO is (apparently) approximately a function only of footing resistance. Smoothing the values of the three terrains, and repeating the calculations for 1500kV and 2500kV CFO, the results are plotted in Figure 17.

IV. LINE BACKFLASH OUTAGE RATE

(A) Footing Resistance Distribution

The distribution of footing resistances for the

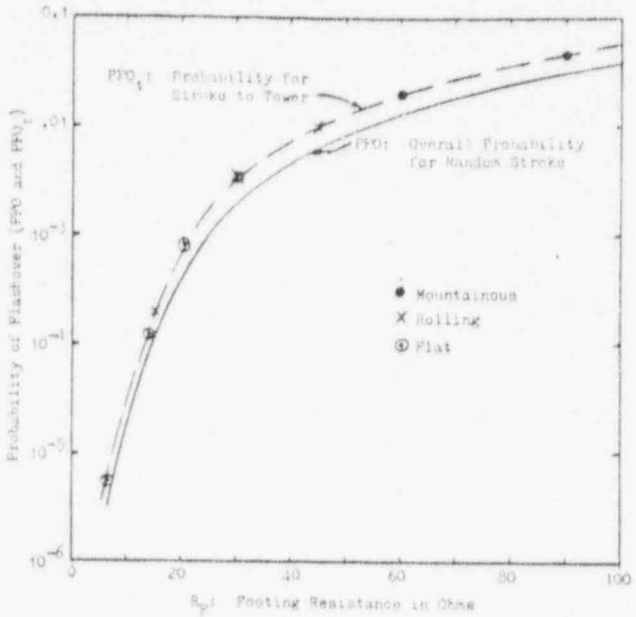

Figure 16. Probability of Line Flashover (CFO = 2000)

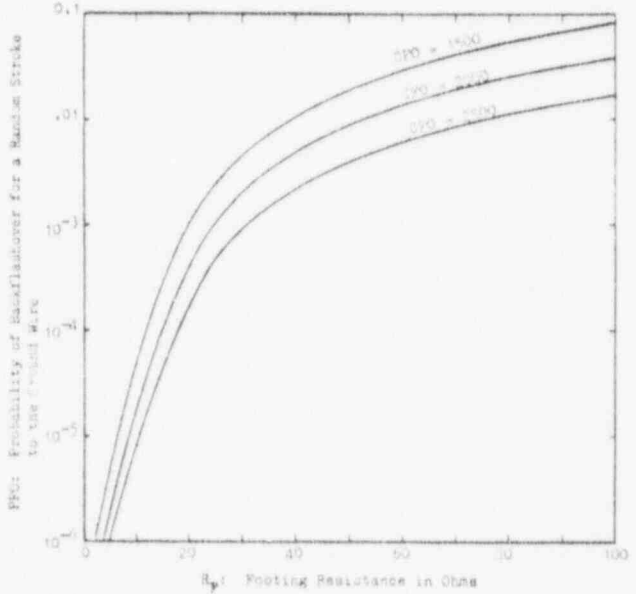

Figure 17. Overall Probability of Line Flashover as a Function of Footing Resistance and CFO

sample line postulated was exponential. This choice was based on an approximate fit to the distribution given in Reference 6. For such a distribution, the probability for the line is higher than that found by using the average footing resistance. The overall probability is thus

$$PFO^* = \int_0^\infty PFO \; e^{-R_f/\bar{R}_f} \frac{R_f}{\bar{R}_f}$$

PFO^* = overall probability of flashover for a line with average footing resistance $\bar{R}_f$, and an exponential distribution

PFO = probability of flashover for a line with all footing resistances = R_f (i.e., Figure 16)

It is readily shown that an effective footing resistance, R_f^*, can be found which will have the same probability of flashover as the line. That is,

$$PFO(R_f^*) = PFO^*$$

It is also readily shown that if PFO can be approximated as a power of R_f, a single relation between R_f^* and $\bar{R}_f$ results, as shown in Figure 18.

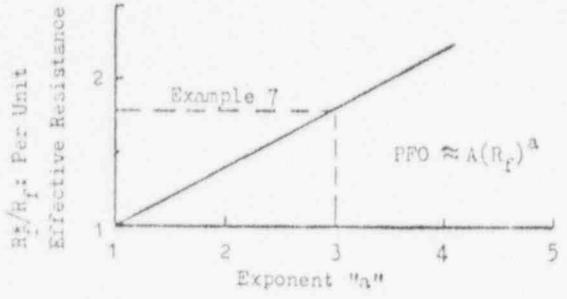

Figure 18. Multiple of Average Footing Resistance to Yield Actual Probability of Flashover

Example 7: A good fit is provided to the curves of Figure 17 by relations of the form

$$PFO \approx A R_f^3$$

suggesting $R_f^* = 1.8\bar{R}_f$ (Figure 18). This suggests the following overall probabilities from Figure 17.

PFO at R_f^*

Terrain	1500 CFO	2000 CFO	2500 CFO
Mountainous ($\bar{R}_f = 30, R_f^* = 54$)	.022	.010	.0049
Rolling ($\bar{R}_f = 15, R_f^* = 27$)	.0034	.0015	.00069
Flat ($\bar{R}_f = 7, R_f^* = 12.1$)	.00013	4.7×10^{-5}	2.4×10^{-5}

(B) Distribution of Line Voltage

Although for rigor, coupling factor differences between center and outer phases would have to be considered, we here assumed that all phases are the same. The A.C. voltage on at least one phase is at least 50% of crest, of opposite polarity to the stroke (cf., for example, Reference 7). The frequency distribution of voltage is most easily expressed as a frequency distribution of θ, since any value between 30° and 150° is equally likely, and the distribution is thus of constant magnitude as in Figure 19. (From symmetry, we need consider only from θ = 30° to 90°.)

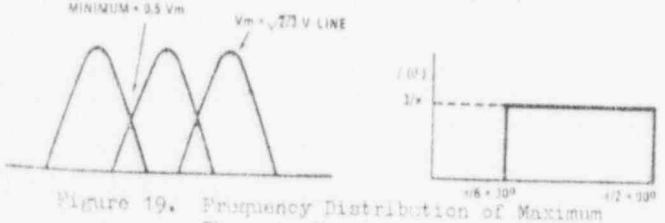

Figure 19. Frequency Distribution of Maximum Phase to Tower Voltage

Now the CFO is a function (presently unknown) of the line or "bias" voltage. Though there are indications that the effect is small,[10] we will be pessimistic and assume that the CFO is reduced by the line voltage present. Thus the "next stage" flashover probability becomes

$$\overline{PFO} = \int_{\pi/6}^{\pi/2} PFO^* f(\theta) d\theta$$

where PFO* is a function of R_f^* and CFO, the latter reduced by $V(\theta) = V_m \sin\theta$. Finding (Figure 17) PFO* vs θ:

PFO* (Figure 17)

θ	V	CFO-V	Mountainous	Rolling	Flat
30	204	1796	.016	.0022	7.5×10^{-5}
50	313	1687	.018	.0025	8.4×10^{-5}
70	384	1616	.020	.0027	9.4×10^{-5}
90	408	1592	.021	.0030	.00010

The indicated integration is performed in Figure 20 for the Mountainous case. For the Rolling and Flat terrain cases, the overall probabilities are .0026 and 8.6×10^{-5} respectively.

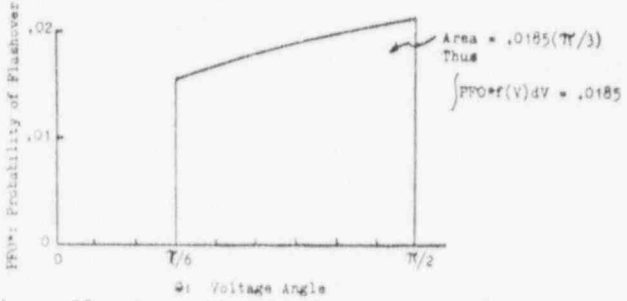

Figure 20. Accounting for Distribution of Voltages

(C) Number of Strokes to the Line

The number of strokes to the line is, of course, a function of height. The "Brown-Whitehead" model has been used to determine this number. The results are given in Figure 21.

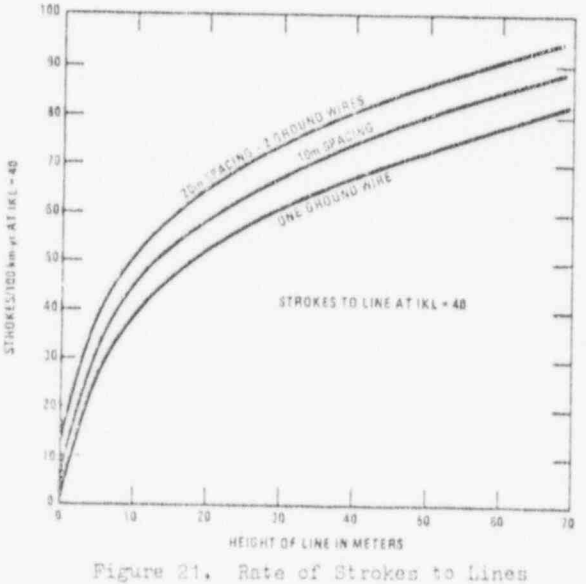

Figure 21. Rate of Strokes to Lines

Using Figure 21, we have (for 15m ground wire spacing) 88, 78 and 67 strokes/100km-yr to the line for the 60, 40 and 25m heights respectively.

(D) AT LAST!

With 10% Mountainous, 30% Rolling, and 60% Flat terrain, the backflashover rate (BFO) for this line is, at a CFO of 2000

$$BFO = [.1(88)(.0185)+.3(78)(.0026)+.6(67)(8.6\times10^{-5})]$$

= 0.23 outages per 100km-yr

It is noted that this is quite comparable with experience. Table VI of Reference 11, for example, reports an average DFO of 0.26 (normalized to an IKL of 40) for a CIGRE study of EHV lines similar to the above sample line.

APPENDIX I: Corona Radius

McCann[8] provided experimental data on coupling factors, for voltages to about 1.7MV. However, his extrapolations of corona radius to higher voltage have seemed to many to call for radii that are too large.

As McCann notes, the assumption of a field of 30kV/cm at the corona surface was far too high. Yet McCann's extrapolations call for continually reducing fields and are inconsistent with respect to height. In attempting to resolve these problems, the writer turned to the q-V data of Wagner and Lloyd.[9]

Wagner's q-V curves were obtained by applying measurements proportional to voltage and charge simultaneously to the x and y axes of an oscillograph during applications of impulse voltages. His results for a 0.927" (2.35cm) diameter conductor 10ft above a ground plane are shown in Figure 22.

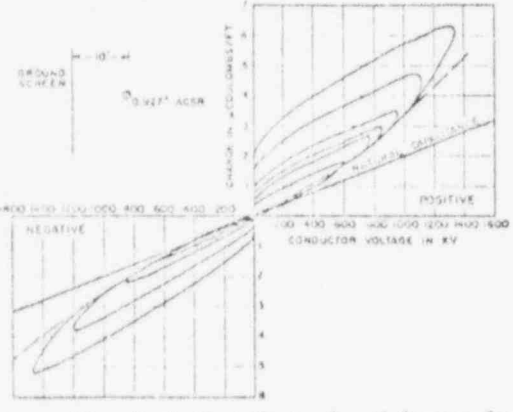

Figure 22. Replotted Most of q-V Curves for a 0.927" ACSR Conductor (Ref. 9)

As one examines this curve, a problem becomes apparent. The "natural capacitance" should be

$$C = \frac{2\pi\epsilon}{\ln\frac{2h}{r}} = 8.89\ \text{pf/m} = 8.89\ \frac{\mu\ \text{coul/m}}{\text{MV}}$$

At 1600kV, this calls for 14.2 μ coul/m, or 4.34 μ coul/ft. But Figure 22 shows about 3.2 μ coul/ft. Further, on at least the negative portion, there appears to be a trace falling (impossibly) below the "natural capacitance" line. Evidently there is a scaling error, which is most likely in the measurement of charge.

Drawing on McCann's results, we find a predicted radius of 10" of 25.4cm at 1500kV. Accepting this figure as valid, since it is in the actual measured range of his data, this would "force" a conclusion that the q scale of Figure 22 is low by a factor of 1.455.

The appropriate point on the q-V curve, in determining corona radius, is the point at which dq/dV = 0 (the horizontal tangent). Taking the locus of points at dq/dV = 0 from Figure 22 yields a corona sheath surface electrostatic field as shown in Figure 23. Irrespective of the correction to q, the salient feature is the rapid flattening at about 1200kV (negative) and less than 800kV (positive). If we reduce McCann's

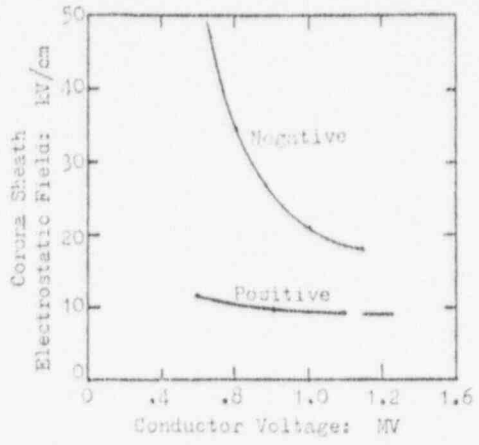

Figure 23. Re-evaluation of Wagner-Lloyd Data (Ref. 9)

data (Figures 4 and 5 of Reference 1) to corona sheath surface field, the results are as in Figure 24. Because of the scatter, it is more difficult to predict the sharp bend, but in light of Figure 4, it seems reasonable to presume a limiting electrostatic field of

15kV/cm for negative voltages and

10kV/cm for positive voltages

This enables much more confident extrapolation of corona radius for higher voltages. The results for negative surges are shown in Figure 3 of the text.

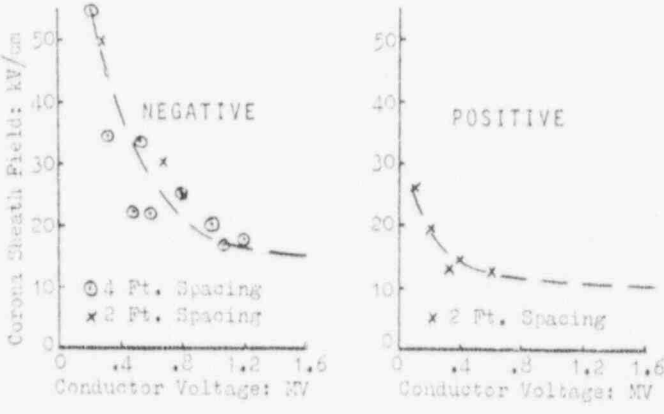

Figure 24. McCann's Data for 10ft Height (Ref. 8)

APPENDIX II: Tower Top Voltage

(A) Stroke to Tower

The reflection factors for determining the surge voltage sent down the lines (i.e., injected into the system) are shown in Figure 25. Assuming a ramp of stroke current, I, this injected voltage (at tower top without reflections from other towers) is

$$V = It\left(\frac{Z_t Z_y}{Z_g + 2Z_t}\right)\left\{1 + \frac{(1+\rho_t)\rho_f}{(1-\rho_t\rho_f)}\left[\frac{n-1}{1} - \rho_t\rho_f + \frac{(\rho_t\rho_f)^n}{n}\right]\right\}$$

In this equation, n is the multiple of (one way) tower travel time. For all practical purposes, the last term may be ignored (with great accuracy at times of interest), and the injected voltage becomes

$$V_2 = \dot{V}_o t + V_{oo}$$

where $\dot{V}_o$ and V_{oo} are as given with Figure 8 of the text.

The constant term is significant for the first several microseconds. Reflection lattice calculations for the effect of the first three towers on either side of the struck tower have been made. For the above injected voltage, the tower top voltage at the arrival of each reflection is given as

$$V_t = B_o V_{ot} + B_{oo} V_{oo}$$

B_o and B_{oo} are as shown in Figure 8 of the text.

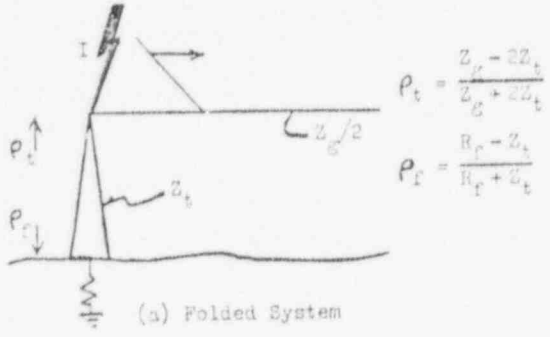

(a) Folded System

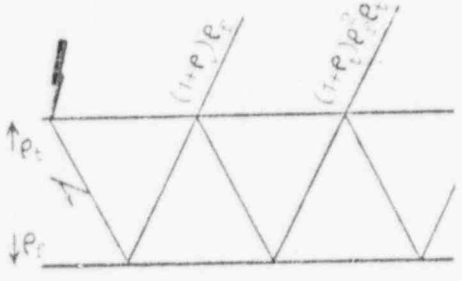

(b) Tower Lattice

Figure 25. System for Determining Injected Voltage

(B) Stroke to Span

Though the argument is for arrester discharge currents, it is readily seen from Reference 12 that the long-time average current down the tower, for a stroke a fraction, k, of the span travel away from the tower, will be (1 - k) times the stroke current. It is also readily shown that the tower top voltage will rise at the same rate as for a stroke to the tower until the first reflection arrives. Coupling these two concepts suggests that, to a first order, the tower top voltage for a stroke to the span (V_{tk}) may be approximated by

$$V_{tk} = \begin{cases} V_t & t < 2(1-k)T_s \\ V_{tko} + (1-k)(V_t - V_{tko}) & \end{cases}$$

This approximation is compared (in Figure 26) against calculations for a 500kV line with a (one way) span travel of 1.2μs and a 20 ohm footing resistance. The approximation is close to an upper bound, and thus slightly conservative.

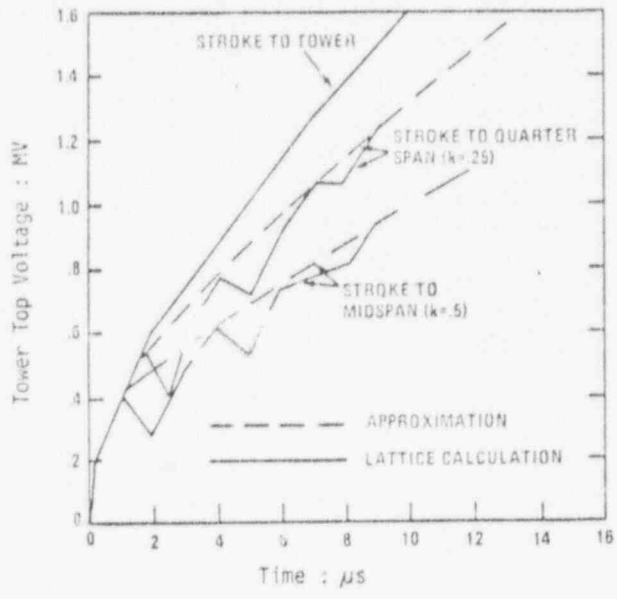

Figure 26. Example: Voltage at Stroke to Span

ACKNOWLEDGEMENTS

Grateful acknowledgement is made to Dr. John C. Cronin and Percy Cheats of ITE Imperial and to Dr. R.C. Colclaser of the University of Pittsburgh for verifying the voltage lattice calculations, both for tower and span strokes, using an independent computer model.

REFERENCES

1. M. Darveniza and Liew Ah Choy, "A Sensitivity Analysis of Lightning Performance Calculations for Transmission Lines," IEEE PAS, July/August, 1971, pp. 1443-51.
2. Edison Electric Institute, EHV TRANSMISSION REFERENCE BOOK, 1968.
3. G. W. Brown, "Joint Frequency Distribution of Stroke Current Rates of Rise and Crest Magnitude to Transmission Lines," submitted to IEEE.
4. K. Berger, R. B. Anderson and H. Kroninger, "Parameters of Lightning Flashes," ELECTRA, July, 1975, pp. 23-38.
5. E. R. Whitehead and G. W. Brown, "Field and Analytical Studies of Transmission Line Shielding II," IEEE PAS, May, 1969, pp. 617-20.
6. M. A. Sargent and M. Darveniza, "The Calculation of the Double Circuit Outage Rates of Transmission Lines," IEEE PAS, June, 1967, pp. 665-78.
7. Electric Power Research Institute, TRANSMISSION LINE/345kV AND ABOVE, 1975.
8. G. D. McCann, "The Effect of Corona on Coupling Factors Between Ground Wires and Phase Conductors," AIEE PAS, 1943, Vol. 62, pp. 818-26, Disc. 940-42.
9. C. F. Wagner and B. L. Lloyd, "Effects of Corona on Travelling Waves," AIEE PAS, October, 1955, pp. 858-72.
10. J. K. Hepworth, R. C. Klewe, R. H. Lobley and B.A. Tozer, "The Effect of A. C. Bias Fields on the Impulse Strength of Point-Plane and Sphere-Plane Gaps," IEEE PAS, Nov/Dec, 1973, pp. 1898-1903.
11. E. R. Whitehead, P. Poplansky and M. Darveniza, "Lightning Protection of UHV Transmission Lines," ELECTRA, July, 1975, pp. 36-89.
12. G. W. Brown and C. Thunander, "Frequency of Distribution Arrester Discharge Currents," IEEE Transactions Paper F76-160-2, presented at Winter Power Meeting, January 1976.

Combined Discussion[1, 2]

E. R. Whitehead (Consultant, Boulder, CO): This paper makes certain approximations which apparently facilitate the estimation of transmission line outages arising from shielding failures. I think it unproductive to debate these approximations, since other factors such as terrain features give rise to uncertainties of greater importance.

So far as I now know, Dr. Brown is the first investigator to make use of extensive data derived from the CIGRE Survey of the Lightning Performance of EHV Transmission Lines. [1] While correlation between estimated and actual outages attributed to shielding failure shown in his Table I is quite good, it might have been even better if terrain features such as parallel lines on and forestation along the right-of-way could have been characterized quantitatively. This table lists several examples of lines for which the estimated shielding failure outages substantially exceed the actual total outage rates. Among these are lines number 43 and 44 for which 40 percent of the right of way is heavily forested, and lines number 51 and 52 which are on a common right of way and separated by only 46 meters over 100 percent of their length. Terrain features for these and other lines of low shielding failure rate

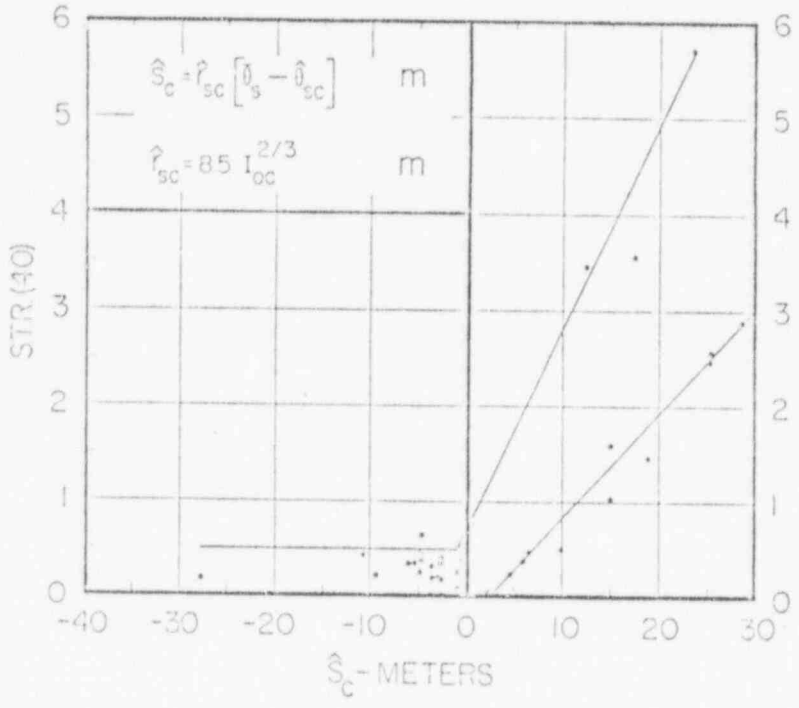

Fig. 3

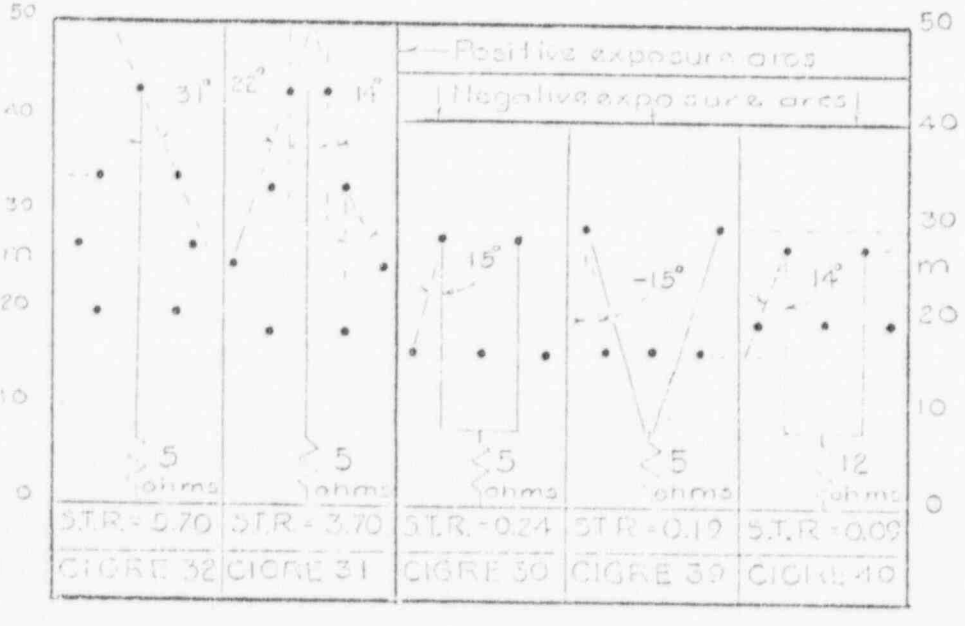

Fig. 6

[1] G. W. Brown, Lightning Performance—I Shielding Failures Simplified, this issue, pp. 33

[2] G. W. Brown, Lightning Performance—II Updating Backflash Calculations, this issue, pp. 39

Manuscript received February 22, 1977.

are listed in Table VI of the SURVEY. Figure 3 of reference [1] defines an "effective exposure arc", S, and gives the actual total outage rate as a function of this exposure index. For positive values of S the higher outage rates reflect a high shielding failure rate. Negative values of S simply represent the safety margin for shielding failures. In this region the outage rate is largely made up of "backflashovers". In the shielding

failure region upper and lower bound lines are shown. Lines having favorable terrain features, including lines 43, 44, 51 and 52, are shown on the lower bound, while lines in "open terrain" are shown on the upper bound.

Figure 6 of reference [11], augmented by the addition of two lines, is especially interesting because all lines except No. 40 are located in a geographical region for which the thunderstorm-day (TD) rate is 40–43 per year. Line No. 40 is located in a region with only a slightly lower rate of 32 TD per year, so that a very small adjustment of the specific tripout rate from 0.07 to 0.09 was required. Lines 20 and 39 were in open terrain, while the terrain for line 40 was characterized as "open to wooded". This figure illustrates, as few other data can, the striking dependence of the shielding failure tripout rate on conductor heights and shielding angle.

As a final comment, may I strongly urge that shielding for new lines be designed for an expected shielding failure rate of zero referred to bare earth. As shown in Figure 6, the results are likely to be rewarding.

REFERENCE

[11] "CIGRE Survey of the Lightning Performance of Extra-High-Voltage Transmission Lines", E. R. Whitehead, *ELECTRA*, No. 33, March 1974, pp. 63-89.

Abdul M. Mousa (Teshmont Consultants Ltd., Winnipeg, Canada): I wish to congratulate Dr. Brown for his continuing contributions to the study of the lightning performance of transmission lines, and would appreciate his response to the following comments and questions:

(1) The paper by Brown-Whitehead (Ref. 2) was written prior to the final calibration of the electrogeometric model. Ref. 2 used the preliminary calibration,

$$r_s = 7.1\, I_o^{0.75} \quad \ldots\ (1)$$

$$K_{sg} = 0.9 \quad \ldots\ (2)$$

Frequency distribution of stroke magnitudes = AIEE distribution . . (3)

Sargent [4] demonstrated that the application of the electrogeometric model partially explains the reason for the differences between the frequency distribution of stroke magnitudes measured at structures of different heights, and used a modified Brown-Whitehead model (K_{sg} = 1.0) to arrive at a tentative synthetic distribution of stroke current magnitudes to level ground. Sargent clearly indicated that his synthetic distribution will have to be revised after the finalization of the calibration of the electrogeometric model.

Later Gilman-Whitehead [5] and Whitehead (Ref. 3) finalized the calibration of the electrogeometric model based on data from the "Lightning Stroke Pathfinder Project". They offered the following equations:

$$r_s = 9.4\, I_o^{2/3} \quad \ldots\ (4)$$

$$K_{sg} = 1.0 \quad \ldots\ (5)$$

It appears to the discussor that a new synthetic frequency distribution of stroke current magnitudes to level ground based on equations no. (4) and (5) should have been first developed, then used in conjunction with equations no. (4) and (5) to calculate the shielding failure outage rates.

(2) Whitehead [6, 5] previously developed curves for the calculation of shielding failure outage rates using the equations:

$$r_s = 6.7\, I_o^{0.8} \quad \ldots\ (6)$$

$$K_{sg} = 1.0 \quad \ldots\ (7)$$

$$Z = 400 \text{ ohm} \quad \ldots\ (8)$$

Whitehead does not clearly state which frequency distribution of stroke magnitudes he used. If we enter Whitehead Figures 20 and 21 [6] by the line data given in examples 1 and 2 of the paper (after modifying the value of CFO to an equivalent 1600 kV at 400 ohm surge impedance), we get (see Figure 10),

Manuscript received February 22, 1977.

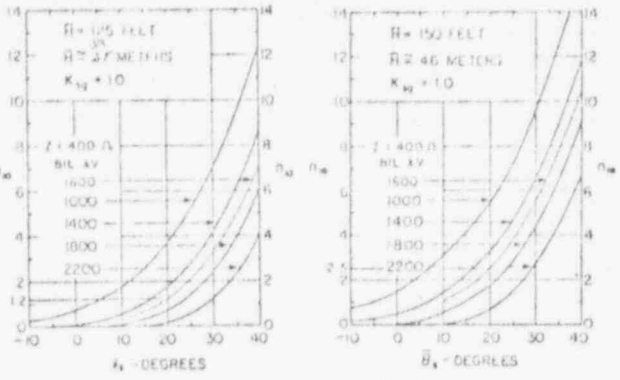

Fig. 10

at H ≅ 38 meters, n_{10} = 1.2

and at H ≅ 46 meters, n_{10} = 2.5

By interpolation, we get,

at H = 40 m, n_{10} ≅ 1.6 tripouts/100 mile-year at IKL = 25

i.e., Sfo ≅ 1.6 tripouts/100 km-year at IKL = 40

This is double the value of 0.8 given in the paper. I would like the author to confirm that his calculations are for *both* outer phases as indicated on Fig. 2 and would welcome any explanation he may offer for such differences between these two estimating methods, especially that both methods use comparable relations between r_s and I_o.

(3) The striking distance, r_s, is usually given in terms of the prospective stroke current *to zero-resistance earth*, I_o. The stroke current *to conductor* required for flashover, IFO, is related to the surge impedance of the conductor, Z, and the critical impulse flashover of the line insulation, CFO, by the equation given in the paper. According to Ref. Nos. 3, 5, 6 and 7, I_{oc} and IFO are related by the equation:

$$I_{oc} = 1.1\ IFO \quad \ldots\ (9)$$

it would be helpful if Dr. Brown states the reason for taking I_{oc} equal to IFO.

(4) The last two columns in Table I give the calculated shielding failure outage rate, sfo, and the actual specific tripout rate, STR, both being at an IKL of 40. It is to be noted that the STR values include both the actual shielding failure outage rates and the backflash rates. In Section 4.9.1 of Ref. 3, Whitehead concludes that STR values under about 0.5 have a negligible shielding failure outage component. Would the correlation in Table I be still good, if we take into consideration both Whitehead's conclusion and the fact that SFO should be less than STR?

(5) Figure 2 demonstrates the approximate adequacy of the maximum striking distance as the only parameter needed to define the annual number of strokes collected by the live conductors of a transmission line (shielding failure rate). Fig. 2 covers a range up to a maximum striking distance of 90 meters. Accordingly, the curves of Fig. 4 are identified by a single parameter; the maximum striking distance, and curves for 40, 60 and 100 m are given. It appears to the discussor that the identification by a single parameter becomes inadequate if the extreme case of an infinite maximum striking distance is considered, which physically refers to an unshielded line. Thus, the top curve in Fig. 4 becomes only valid for the conductor height for which it has been calculated, namely sixty feet above ground, and hence that curve needs a two-parameter identification:

$$r_{s\,max} = \infty \ \&\ h = 60 \text{ ft } (\cong 18 \text{m})$$

Other curves do exist for other conductor heights as shown by Sargent [4].

(6) The paper mentions Ref. No. 1 as the source of the exact relation between $r_{s\,max}$ and the transmission line geometrical parameters c, x, y and h. In Ref. No. 1 the situation is slightly different, namely that of a distribution circuit shielded by the conductors of an adjacent transmission line. To avoid a cross reference which may be confusing, I suggest that the distances c and x be indicated on Fig. 1.

(7) There appears to be two typographical errors in the paper,

i) In the exact equation for $r_{s\,max}$ in terms of c, x, y, and h, which follows Fig. 2, the denominator should read $2(h-y)^2$, rather than $x(h-y)^2$.

ii) In Section III (c) "Sample Calculations — Low Shielding Failure Rate", the second line should read CFO = 1600 kV, rather than CFO = 1800 kV, in order to be in agreement with subsequent calculations.

(8) The term "striking distance" rather than "strike distance" has been used in previous technical papers and appears to be more widely accepted.

REFERENCES

[4] Michael A. Sargent, "The Frequency Distribution of Current Magnitudes of Lightning Strokes to Tall Structures", *IEEE Trans.*, Vol. PAS-91, pp. 2224-2229, September/October 1972.

[5] D. W. Gilman and E. R. Whitehead, "The Mechanism of Lightning Flashover on High-Voltage and Extra-High-Voltage Transmission Lines", *Electra* No. 27, pp. 65-96, March 1973.

[6] E. R. Whitehead, "Final Report of Edison Electric Institute – Mechanism of Lightning Flashover Research Project", *EEI Publication*, No. 72-900.

[7] H. R. Armstrong and E. R. Whitehead, "Field and Analytical Studies of Transmission Line Shielding", *IEEE Trans.*, Vol. PAS-87, pp. 270-281, January 1968.

E. R. Whitehead (Consultant, Boulder, CO): This paper is much more involved than that treating shielding failures so I will confine my remarks to a few general areas in which the developments may have been somewhat over simplified. In a discussion of Sargent's [1] 1972 paper on "The Frequency Distribution of Current Magnitudes of Lightning Strokes to Tall Structures", H. Linck pointed out that the so-called Brown-Whitehead "electrogeometric model" does not adequately predict the *number* of strokes to (or *from*) such structures. This is hardly surprising, since the calibration of the "striking distance" was based specifically on known shielding failure events as well as statistically-postulated shielding failure events. Moreover, the heights of towers and shield (ground) wires for lines involved in the studies reported by Whitehead [2] were much lower than those commonly found for radio and television towers as considered by Linck and Sargent. A hint that something *might* be amiss for the higher transmission lines surfaced in a comparison of mean backflash outage rates as found in the CIGRE [3] and LEI surveys. Table 1 of this discussion presents statistics summarizing only those outages thought to be *caused only by backflash events*.

Table 1

Parameter or Statistics		Survey HV (FEI)	Survey EHV (CIGRE)
Line voltage – kV	Mean	155	390
	Maximum	230	735
Line sample size kilometer – years	Mean	1625	1940
	Maximum	10460	5900
Thunderstorm days TD	Mean	52	35
	Maximum	67	98
Critical impulse flashover voltage	Mean	1385 (1)	1727
	Maximum	1685 (1)	2880
Low voltage measured ground resistance	Mean	23	26
	Maximum	94	110
Shielding angle-line mean in degrees	Mean	18	19
	Maximum	39	30
Mean shield wire height H	Mean	21	27
	Maximum	34	45
Specific tripout (2) rate at 40 TD per year	Mean	0.125	0.290
	Maximum	0.470	0.640
Total sample size in kilometer years		84,000	65,300

NOTE (1): These data reflect a substantial amount of wood pole construction.

NOTE (2): Tripouts per 100 kilometers per year.

Study of this table indicates that the parameters and statistics for the EHV lines are either comparable with or in favor of a lower tripout rate for the EHV lines, *with the exception of mean shield wire height H*. This has led to some concern regarding the effect of height, particularly in connection with the design of proposed UHV lines.

Recent studies by Eriksson [4], Linck [5], Bazelyan [6] and Whitehead [7] suggest that the concept of "striking distance" will have to be supplemented to include the increasing effect of upward streamers, leader orientation, and finally a "triggering" component giving rise to upward leaders. The leader orientation toward the tower and the upward streamer mechanism are difficult to separate analytically or even photographically, but both lead to increased incidence of flashes to tall structures. In the case of the "triggering" mechanism, the tower "strikes to the cloud" before downward leader conditions are fully developed, so that one might expect the median current for negative polarity to decrease with height. Recent data furnished by Popolansky [8] in an internal working document for the CIGRE working group on lightning shows that this is indeed the case. Preliminary engineering models by this discussor indicate that the median current is a function of height which rises from a reference value for flat earth to a maximum for relatively low heights and thereafter falls slowly to a limiting value of zero as the height increases without limit. The height at which the maximum occurs is much larger for positive flashes than for negative flashes, perhaps by a factor of two. These models must be regarded as speculative until more studies are completed.

A final point of concern is that of the critical flashover voltage for non-standard wave shapes. The author bases his insulation strength on the wave shape of voltage which results from a ramp current. Voltage waves of quite different form can cause insulator flashover if the critical value for a specific wave shape is reached or exceeded.

Caldwell and Darveniza [9] have studied selected non-standard wave shapes of the type likely to be found on transmission lines and determined quite accurate critical flashover voltages by innovative laboratory techniques. Whitehead has developed an empirical procedure which enables these critical voltages to be found from impulse flashover curves based on the standard 1.2/50 microsecond voltage wave.

REFERENCES

[1] Sargent, M. A. (1972), "The Frequency Distribution of Current Magnitudes of Strokes to Tall Structures", Trans. IEEE, PA&S-91, pp. 2224-2229.

[2] Whitehead, E. R. (1972), "Final Report on Edison Electric Institute Research Project NO RP-50, Mechanism of Lightning Flashover on Transmission Lines", No. 72-900, EEI, 90 Park Ave., New York, N.Y. 10017.

[3] Whitehead, E. R. (1974), "CIGRE Survey of the Lightning Performance of Extra-High-Voltage Transmission Lines", *ELECTRA*, 33, pp. 63-89.

[4] Eriksson, A. J. (1974), "The Striking Distance of the Lightning Flash", NEER-CSIR, Special Report, Pretoria, Republic of South Africa.

[5] Linck, H. (1976), "Questions Concerning an Improved Model Technique for Simulation of the Lightning Exposure of Tall Structures", An internal working document, IWD 12, SC 33, WG [illegible].

[6] Bazelyan, E. M. (1974), "Selecting Points for Lightning Strokes", Electrical Technology (Elektrichestvo) No. 10, pp. 15-19.

[7] Whitehead, E. R. (1976), "Analytical Speculations on Improved Electrogeometric Models of the Lightning Flash and Transmission Line Environment", with Addendum and Appendix. IWD 12 and 12 a SC33, WG 33.01.

[8] Popolansky, F. (1976), "Preliminary Report on Lightning Observations in CSSR", IWD 24, SC 33, WG 33.01. (To be published in Czech with an English Summary.)

[9] Caldwell, R. O. and Darveniza, M. (1973), "Experimental and Analytical Studies of the Effect of Non-Standard Wave Shapes on the Impulse Strength of External Insulation", Trans. IEEE, PA&S-92, pp. 1420-1428.

J. J. LaForest (General Electric Company, Schenectady, NY): The author here has presented a detailed method of assessing backflashover performance, and two observations are in order. First, any of the calculation methods require a knowledge of the tower response to stroke current. The author uses tower travel time of (T_t) and tower impedance (Z_t) to indicate tower response and for the example given, uses $T_t = 0.328/2\mu s$ and 160. ohms, respectively. For some line designs, the designer may consider a choice between lattice or steel pole designs and knowledge of tower response for these cases is required. Would the author comment on source data for these design variations and that for the example? Our calculations for backflashover have been augmented by nano-second model tests where specific line and tower designs have been analyzed for response to stroke current. [1]

The second observation is that besides isokeraunic level, the effects of other weather factors are not discussed, such as windswing where tangent strings are employed. For this case, the probability of flashover should be considered in the light of windswing reducing the air gap during the storm.

REFERENCE

[1] TRANSMISSION LINE REFERENCE BOOK 345 kV AND ABOVE, Fred Weidner & Son Printers, Inc., New York, NY.

Manuscript received February 15, 1977.

Manuscript received February 17, 1977.

Gordon W. Brown, Paper F77015-1: Many thanks to the discussors for their most thought-provoking comments.

First, in response to Dr. Whitehead, his comments on forestation forced me back to my original notes. I had taken a cursory look at the effect of inclusion of forestation parameters, but it rapidly became apparent that it wouldn't be helpful at this stage. Clearly, forestation has the effect of making the line lower in height (i.e., raising the ground plane). How great the effect is will depend upon height and type of trees, possibly season of the year, soil moisture, and perhaps other unknowns. Even assuming that the forestation of lines 43 and 44 (cited by Whitehead) completely eliminates shielding failures, only 40% of the line is so forested, and the difference must remain as yet unexplained. Further, assuming a reduction due to forestation is counter productive on several lines, particularly lines 105 to 109. My opinion is that we do not understand the effects of forestation well enough to be included at the present time.

Regarding the remainder of Dr. Whitehead's comments, I certainly agree that shielding design should aim towards zero shielding failures. With respect to the parameters he cites (and the host of other parameters in the CIGRE articles), I am not convinced of the necessity of the rather large array of parameters. Indeed, it was my desire to seek for simplification of parameters which, in large measure, prompted me to write the present article.

I will respond to Mr. Mousa's discussion using his numbers.

(1) Well over two years ago, I was aware that new ground frequency distributions had to be made. In fact, I was concerned that Sargent's frequency distribution was being used *unmodified* with new strike distance equations. In private conversations with Dr. Whitehead, I raised this concern and was assured that the "raw" Berger data was part of an overall computer program which made shielding and backflash calculations, calculating frequency distributions internal to the program. I urged at that time that these frequency distributions be made public. As yet, they have not been. Since (a) my primary interest was in determining whether my "hunch" about the importance of terrain shape was correct, (b) knowing that the modified equations would have little effect for shielding, and (c) that the work in repeating what others had done would be as much if not more than my primary interest, I used Sargent's frequency distributions. Of course, I had to use the same model. The results, I believe, suggest that at least for shielding, the simpler model can be used.

(2) The results you show are indeed surprising. I went back to my Ph.D. thesis, where similar curves were developed using $r_s = 7.11 \cdot 75$. There are significant differences in places. Not unexpectedly, I agree with myself! (I.e., my original calculations from 1967 yield results close to that of the present paper). The method used was different. The same model was used. In my more youthful exuberance, I made (horribly complex) explicit integrations for shielding failures. In trying to explain these to my colleagues for the present study, I discovered (a) a few (minor) errors and (b) that it was far easier and more reliable to allow the computer to perform numerical integrations on the basic model. However, the two methods gave similar results. Some of the differences undoubtedly involve assumptions about the height of the conductor, which may be different. The frequency distribution used is, in the CIGRE article, not that of Sargent, but based on earlier assumptions. That too, is undoubtedly part of the difference. Other than that, I haven't enough information to pursue the problem. To answer your main question: Yes, the failure rates are *for both* outer phases.

(3) The reason for using I_{0c} = 1FO is twofold. The decisive reason is that this is what Sargent used in developing his frequency distribution, and I was thus forced to use it if I was to use his frequency distribution. The second reason is that the factor of 1.1 is, as I understand it, an educated guess, and I again felt that other estimable parameters were far more important (again, terrain). In this spirit I feel it is important to maintain the model at the simplest possible level until we can demonstrate that a given parameter is important.

(4) To say that STR values under 0.5 have negligible shielding failure components is a bit sweeping. It seems clear that some of the lines of Table I indeed involve backflash. This almost certainly is true for lines 88 to 99. Also, as noted in the article, the STR is higher than the SFO rate. Eliminating the high SFO lines (31, 32, 85, 86, and 105 to 109) for which statistical variation could swamp information from the lower rate lines, and eliminating the puzzling lines 44 and 45, the remaining 29 lines yield an average calculated SFO of 0.19 (s.d. = .19). It seems quite plausible to believe that the difference is accounted for by backflash.

(5) Calculations of frequency distribution were made for a wide *range* of heights from 5 meters to 50 meters. While there is a gradual change, the difference for lines above 25 meters is of the order of a few thicknesses of the line drawn on Figure 4, and the difference decreases for higher lines. What Sargent's work reveals is that the type of structure is far more important than its height, and that the variation with height for towers is more than that for lines. In any case, the variation due to height is even less for shielding failure frequency distributions, and the "$r_s = \infty$" line is shown more for comparative purposes.

(6) I didn't want to clutter up Figure 1 with too many parameters. The parameters "c" and "x" are fully defined by the equations alone, but for completeness, their physical significance is

"c" is the actual straight line distance between ground wire and phase wire.

"x" is the horizontal distance between ground wire and phase wire.

(7) Many thanks for pointing out two important typographical errors! They have been corrected in the text.

(8) The term "striking distance" is more common in CIGRE publications, while "strike distance" is found more frequently in the IEEE Transactions. I personally prefer the shorter term.

Manuscript received April 25, 1977.

Gordon W. Brown, Paper F77016-9: Dr. Whitehead raises a considerable number of provocative questions and concerns. He points to Linck's criticism of Sargent's paper, suggesting that the model used is a poor predictor of number of incidents. However, it is my view that Sargent effectively responded to those criticisms in his closure. The table comparing HV and EHV lines is indeed suggestive that something is amiss. While I agree that there will certainly be attractive effects for higher structures, I find it difficult to accept, at present, that such effects account for the bulk of the discrepancy. The *difference* in mean heights is quite modest. I've got a nagging feeling that the difference lies in the actual distribution of footing resistances, particularly the upper end of the distribution. Very substantial effects can occur if the footing resistance distribution is in any way differently skewed, even though reported means and maxima are accurate. It is to be noted, too, that in the table, footing resistance is higher for the EHV lines. Figure 17 of the present article suggests that a 3 ohm difference in footing resistance in the neighborhood of 25 ohms is just about equivalent to a difference of 350kV in CFO. These are the differences indicated in Dr. Whitehead's Table I in his discussion.

The impact of the larger number of wood pole lines in the HV study also raises uncertainties. Other factors which may play a part are line sags, differences in terrain and larger cleared rights of way for EHV lines.

I have seen Eriksson's publication analyzing a single stroke. There are several junctures in his photograph which could plausibly be called the proper strike distance. It is, I submit (as does Eriksson), difficult to be in any way definitive. I am anxious to see any further analyses he has. Unfortunately, I have not seen Bazelyan's article, and Linck's is not publicly available. Poptansky's data is also not publicly available. Until this information is fully available for scrutiny, I must remain a friendly skeptic.

Regarding non-standard waveshapes, consider the following qualitative argument. The stroke current on the line is engaged in battle. It is "fighting" to backflashover the line insulation. Countering its attempts are the "relentless" effects of ground. If the stroke current even begins to relax (i.e., the rate of rise slackens), the stroke will lose the battle. Even though stroke current may have a long duration near crest, tower top potential are characterized by relatively sharp rises and drops, with sawtooth oscillations on the front due to span and tower reflections. Qualitatively, it is the front that counts. Looking at it another way, suppose we knew the CFO for a given waveshape. *Most* of the strokes having that (or similar) waveshape and causing backflashover will have a higher voltage, and for these we are concerned with front of wave flashover. In other words, there will not be great error using a ramp approximation. Certainly there are other, far more important factors, namely, footing resistance. In any case, I eagerly await publication of Dr. Whitehead's models for review.

Dr. LaForest raises two questions. Concerning tower impedance, I was infinitely more concerned with developing an overall algorithm for backflashover calculations and confronting new aspects of that algorithm (as well as reviewing the question of corona effects). I simply chose a reasonable surge impedance value for the type of tower used as the example. It's difficult to recall, but I probably started assessing the choice using Sargent's 1969 article, "Tower Surge Impedance" (*IEEE PAS*, May, 1969, pp. 1680-87). I know that I also discussed the choice with several other investigators engaged in calculations of wave reflections on groundwire systems. Also, it is to be noted that tower surge impedance, while significant, is not dominant, and errors in tower surge impedance measured in tens of percent can be tolerated without marked effect in backflashover rate. This is readily seen in the (approximate)

Manuscript received April 25, 1977.

equations for tower top potential at the end of page 3 and top of page 4, in which only the constant term is a function of tower surge impedance and travel-time.

Regarding tangent strings, I toyed with the idea of incorporating modification for such a line (i.e., windswing reduction of strength), but dropped it as detracting from what I felt were more important elements. It would have entailed far too much additional discussion (including an entire *new* example) in an already lengthy article. It would certainly have to be included in studying actual situations where tangent strings are employed. Conceptually, it is straightforward. However, I am glad the subject was raised. Thank you for bringing it into focus through the discussion.

IEEE Transactions on Power Apparatus and Systems, Vol. PAS-97, no. 1, January/February 1978

JOINT FREQUENCY DISTRIBUTIONS OF STROKE CURRENT RATES OF RISE AND CREST MAGNITUDE TO TRANSMISSION LINES

REF. 23

Gordon W. Brown, Senior Member

U. S. Energy Research and Development Administration
Washington, D. C.

ABSTRACT AND CONCLUSIONS

Since strike distance is a function of stroke current magnitude, it is shown that the frequency distribution of rates of rise of stroke current to any structure can be readily determined. The most important of these is that for negative first components to transmission lines. For any realistic line configuration, the distribution is approximately log-normal with a mean of 12kA/μs. The standard deviation of the natural logarithm of the ratio of dI/dt to the mean is approximately 0.55 (i.e., 2 standard deviations from the mean, the rate of rise is 36kA/μs).

INTRODUCTION

Many essential aspects of transmission and distribution system design hinge on knowledge of the expected rates of rise of stroke currents to transmission lines. Until recently, this knowledge has had to rest on intelligent judgement based on limited field data. However, with the increasing verification of the "Electrogeometric" or "Brown-Whitehead" model[1] for stroke behavior relative to transmission line performance, it seemed appropriate to consider the implications of that theory on stroke rates of rise.

FREQUENCY DISTRIBUTIONS OF STROKE CURRENT RATES OF RISE

(A) Setting the Stage - Berger and Sargent

In 1972, Sargent[2] developed a remarkably predictive frequency distribution of strokes to level ground (Figure 1). This distribution is well approximated by a log-normal probability with median ($\bar{I}$) and σ of

$$\bar{I} = 13\text{kA} \text{ (that is, 50\% of strokes are expected to be} > \bar{I})$$

$$\sigma_{\ln I} = 0.74 \text{ [= standard deviation of } \ln(I/\bar{I})]$$

With this distribution, he was able to predict distribution data obtained by several investigators on different structures,[3-5] using the "Brown - Whitehead" model.[1] These distributions are shown in Figure 2. In particular, the distribution and model are highly predictive of Berger's results published in 1975.[5]

Berger found a mean of 30kA. The standard deviation he estimates is about 0.6. However, Sargent's prediction of Berger's data, which provides an excellent fit to the data (Figure 3) - as well as that of others and the earlier Berger data, as noted - has a standard deviation of 0.68. This latter figure is assumed to be the most appropriate. That is, it is assumed that

$$\bar{I}_B = 30\text{kA}$$

$$(\sigma_{\ln I})_B = 0.68$$

where the subscript "B" indicates Berger's structure.

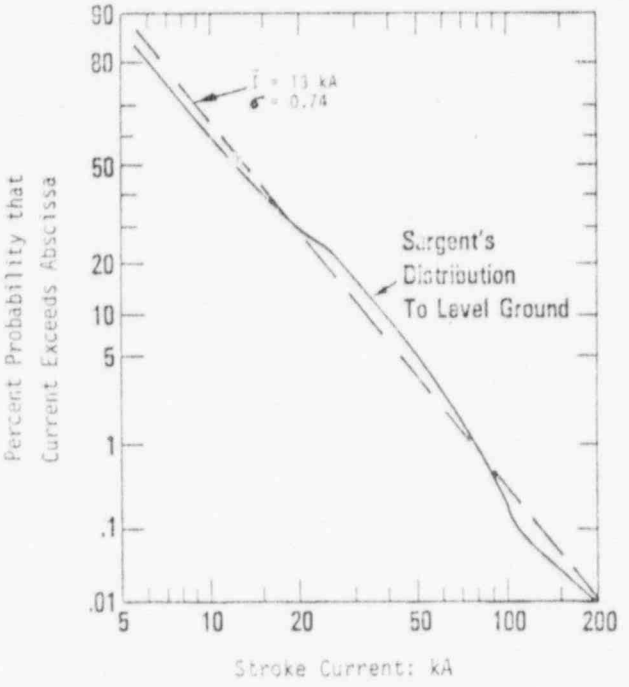

Figure 1. Sargent's Distribution of Stroke Current Magnitude to Level Ground

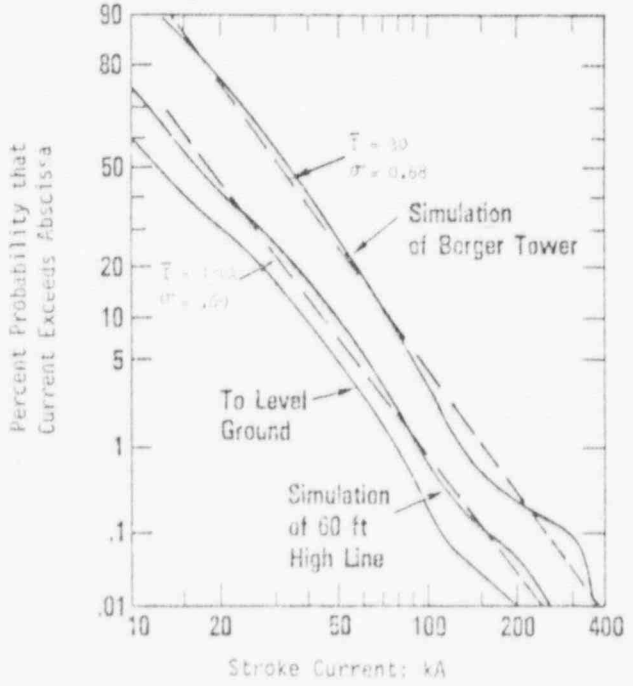

Figure 2. Predicted Distributions

78 017-7. A paper recommended and approved by the IEEE Transmission and Distribution Committee of the IEEE Power Engineering Society for presentation at the IEEE PES Winter Meeting, New York, N.Y., January 30-February 4, 1977. Manuscript submitted July 8, 1976; made available for printing October 28, 1976.

0018-9510/78/0100-0053$00.75 ©1978 IEEE

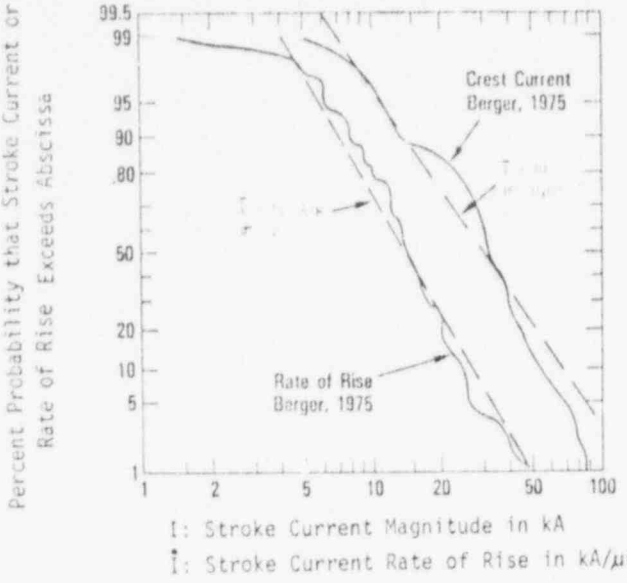

Figure 3. Berger's Data (Tower)

The data of Table 1 of Reference 6 (Berger) for dI/dt is not self-consistent. The graphical data is redrawn in Figure 3 and the median and standard deviation for I is estimated to be 14kA/μs and 0.55 respectively. (I signifies dI/dt.) (Mild emphasis is given to the higher rates of rise, greater than 5kA/μs, since these will have greater importance in lightning design.) This is assumed to be the appropriate figure for rates of rise. Berger found a correlation coefficient of 0.36.

It is assumed, then, that the distribution of stroke magnitudes and rates of rise to a structure similar to that of Berger's is

$$f_B(x_B, y_B) = \frac{e^{-\frac{x_B^2 - 2\rho x_B y_B + y_B^2}{2(1-\rho_B^2)}}}{2\pi\sqrt{1-\rho_B^2}}$$

$$x_B = \frac{\ln(I/\bar{I}_B)}{(\sigma_{\ln I})_B} \qquad y_B = \frac{\ln(\dot{I}/\bar{\dot{I}}_B)}{(\sigma_{\ln \dot{I}})_B}$$

with

$$\bar{I}_B = 30\text{kA} \qquad (\sigma_{\ln I})_B = .68$$

$$\bar{\dot{I}}_B = 14\text{kA}/\mu\text{s} \qquad (\sigma_{\ln \dot{I}})_B = .55$$

$$\rho_B = .36$$

(B) The Distribution

It is shown in the Appendix that if the median and standard deviation of current magnitudes (I) to any structure are known and can be approximated by a log-normal distribution, then the mean and standard deviation of the distribution of rates of rise (İ) can be predicted, and will be log-normal. Specifically, it is shown that the standard deviation of İ is the same for any structure. The expected correlation coefficient will change in proportion to the standard deviation of current magnitude. With Berger's structure as the "known," from Equation A9

$$\bar{\dot{I}} = \bar{\dot{I}}_B (\bar{I}/\bar{I}_B)^{(\sigma_{\ln \dot{I}})_B/(\sigma_{\ln I})_B} = 14(\frac{I}{30})^{.81/.68}$$

$$= 14(\frac{I}{30})^{.29}$$

From Equation A11

$$\sigma_{\ln \dot{I}} = (\sigma_{\ln \dot{I}})_B = .55$$

$$\rho = \rho_B \frac{\sigma_{\ln I}}{(\sigma_{\ln I})_B} = \frac{.36\sigma_{\ln I}}{.68} = .529\sigma_{\ln I}$$

1. Strokes to Level Ground. From Sargent's work we have, to level ground,

$$\bar{I} \approx 13\text{kA}, \qquad \sigma_{\ln I} \approx 0.74$$

Hence

$$\bar{\dot{I}} = 14(\frac{13}{30})^{.29} = 11\text{kA}/\mu\text{s}$$

$$\sigma_{\ln \dot{I}} = .55$$

$$\rho = .529(.74) = .39$$

2. Strokes to Lines. In studies for other investigations,[1,2] it was found with application of the "Electrogeometric" theory to lines from heights of 5m to 60m (and no indications that there would be a significant difference at greater heights) that the parameters of the current magnitude distribution were (Figure 4)

$$\bar{I} = 18$$

$$\sigma_{\ln I} = 0.69$$

Thus, we expect the following distribution for İ:

$$\bar{\dot{I}} = 14(\frac{18}{30})^{.29} = 12\text{kA}/\mu\text{s}$$

$$\sigma_{\ln \dot{I}} = .55$$

$$\rho = .529(.69) = .365$$

This is also shown in Figure 4.

3. Application to Any Structure. Since the distributions to level ground are known, the "Brown-Whitehead" model can be used to determine the frequency distribution of current magnitudes to any structure, as was done by Sargent for towers. (For full details see References 1 and 2.) Once $\bar{I}_s$ is known for the structure (hence the subscript "s"),

$$\bar{\dot{I}}_s = 14(\frac{\bar{I}_s}{30})^{.29}$$

$$(\sigma_{\ln \dot{I}})_s = 0.55$$

Thus the parameters of the distribution of dI/dt are immediately available.

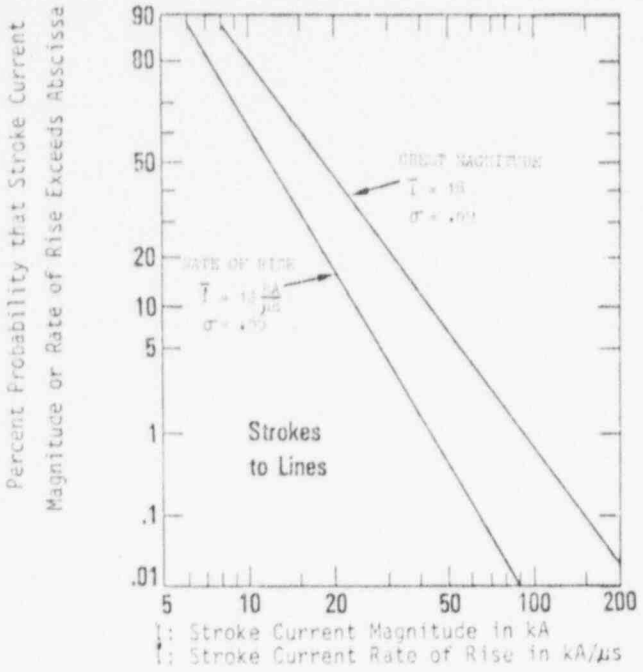

Figure 4. Distributions of Magnitude for Rates of Rise to Transmission Lines

APPENDIX

(A) Independence of dI/dt at Given I

Any text on statistics (e.g. Reference 7) will show the following relationship for two jointly distributed functions:

$$f(I,\dot{I}) = f(\dot{I}|I)f(I) \qquad A1$$

where

$f(I,\dot{I})$ is the full joint frequency distribution.
$f(\dot{I}|I)$ is the frequency distribution of $\dot{I}(=dI/dt)$ given a specific value of I.
$f(I)$ is the frequency distribution of I for random strokes without worrying about $\dot{I}$.

We will let the functions without subscripts refer to distributions to level ground. With subscript "L," the distributions are those to Lines. (An identical argument holds for any structure.)

Reference 1 shows that the frequency distribution of strokes to a line is

$$f_L(I) = \frac{X(I)f(I)}{\int_0^\infty X(I)f(I)dI} \qquad A2$$

where X(I) is the "effective swath" at a given current as defined in Reference 1. Since the "swath," X(I), is a function only of I, we could have written

$$f_L(I,\dot{I}) = \frac{X(I)f(I,\dot{I})}{\int_0^\infty X(I)f(I)dI} \qquad A3$$

Since we can also write (Equation A1)

$$f_L(I,\dot{I}) = f_L(\dot{I}|I)f_L(I)$$

comparing Equations A2 and A3, we have

$$f_L(\dot{I}|I) = f(\dot{I}|I)$$

This is quite expected. Consider "all" the strokes striking a line in a narrow band $I \pm \Delta I/2$. Since the line "reaches" for these strokes with the same strike distance $r_s(I)$, a function only of stroke current, we expect the distribution of $\dot{I}$ to be the same as that to level ground.

Hence

$$f_L(I,\dot{I}) = f(\dot{I}|I)f_L(I)$$

Similarly, for any structure,

$$f_s(I,\dot{I}) = f(\dot{I}|I)f_s(I)$$

(B) The Explicit Distributions - Correlation

We have held that Berger's data are characterized by log-normal distributions with

$$\bar{I} = 30, \qquad \sigma_{\ln I} = 0.68$$
$$\bar{\dot{I}} = 14, \qquad \sigma_{\ln \dot{I}} = .55$$

The frequency distribution is, therefore,

$$f_s(x_s,y_s) = \frac{e^{-(x_s^2-2\rho_s x_s y_s+y_s^2)/2(1-\rho_s^2)}}{2\pi\sqrt{1-\rho_s^2}} \qquad A4$$

$$x_s = \frac{\ln(I/\bar{I})}{\sigma_{\ln I}} = \frac{\ln(I/30)}{.68}$$

$$y_s = \frac{\ln(\dot{I}/\bar{\dot{I}})}{\sigma_{\ln \dot{I}}} = \frac{\ln(\dot{I}/14)}{.55}$$

$$\rho_s = .36$$

(The correlation coefficient applies to the logarithms of the currents and rates of rise.)

Seeking $f(\dot{I}|I)$, we pursue

$$f_s(y_s|x_s) = \frac{f_s(x_s,y_s)}{f_s(x_s)}$$

Since

$$f_s(x) = \frac{e^{-x^2/2}}{\sqrt{2\pi}}$$

it is readily shown[1] that

$$f_s(y_s|x_s) = \frac{e^{-(y_s-\rho_s x_s)^2/2(1-\rho_s^2)}}{\sqrt{2\pi}\sqrt{1-\rho_s^2}} \qquad A5$$

It is this expression which is invariant when considering level ground or any structure:

$$f(y|x) = f_s(y_s|x_s) = f_L(y_L|x_L) \qquad A6$$

Note the regression equation for the mean of $\dot{I}$, given I:

$$\mu_{y_B|x_B} = \rho_B x_B$$

or

$$\mu_{\ln\dot{I}} = \ln\bar{I} + \rho_B \frac{\sigma_{\ln I}}{\sigma_{\ln I}} \ln(I/\bar{I})$$

From which, with ρ and the standard deviations above,

$$\bar{I}(\text{given } I) = \bar{I}(I/\bar{I})^{\rho_B \frac{\sigma_{\ln\dot{I}}}{\sigma_{\ln I}}} \qquad A7$$

What remains is

(C) Standard Deviation of $\dot{I}$ Under Transformation

As noted, Equation A5 is invariant and holds on level ground, lines or structures. Consider the argument, which is

$$y_B - \rho x_B = \frac{\ln(\dot{I}/\bar{\dot{I}}_B)}{(\sigma_{\ln\dot{I}})_B} - \rho\frac{\ln(I/\bar{I}_B)}{(\sigma_{\ln I})_B}$$

We proceed to transform this

$$y_B - \rho x_B = \frac{\ln(\dot{I}/\bar{\dot{I}}_B)}{(\sigma_{\ln\dot{I}})_B} - \rho\left[\frac{\ln(I/\bar{I}) - \ln(\bar{I}_B/\bar{I})}{(\sigma_{\ln I})_B}\right]$$

$$= \frac{\ln(\dot{I}/\bar{\dot{I}}_B)}{(\sigma_{\ln\dot{I}})_B} + \rho\frac{\ln(\bar{I}_B/\bar{I})}{(\sigma_{\ln I})_B} - \rho\frac{\ln(I/\bar{I})}{(\sigma_{\ln I})_B}$$

$$= \frac{\ln(\dot{I}/\bar{\dot{I}})}{(\sigma_{\ln\dot{I}})_B} - \rho\frac{\ln(I/\bar{I})}{(\sigma_{\ln I})_B} \qquad A8$$

where

$$\bar{\dot{I}} = \bar{\dot{I}}_B(\bar{I}/\bar{I}_B)^{\rho\frac{\sigma_{\ln\dot{I}}}{\sigma_{\ln I}}} = \mu_{\dot{I}|\bar{I}_B} \qquad A9$$

Finally

$$y_B - \rho_B x_B = \frac{\ln(\dot{I}/\bar{\dot{I}})}{(\sigma_{\ln\dot{I}})_B} - \rho_B\frac{(\sigma_{\ln I})}{(\sigma_{\ln I})_B}\frac{(\ln(I/\bar{I}))}{(\sigma_{\ln I})}$$

$$y_B - \rho_B x_B = \frac{(\sigma_{\ln\dot{I}})}{(\sigma_{\ln\dot{I}})_B}\frac{\ln(\dot{I}/\bar{\dot{I}})}{(\sigma_{\ln\dot{I}})} - \rho_B\frac{(\sigma_{\ln I})}{(\sigma_{\ln I})_B}X$$

$$= \frac{(\sigma_{\ln\dot{I}})}{(\sigma_{\ln\dot{I}})_B}y - \rho_B\frac{(\sigma_{\ln I})}{(\sigma_{\ln I})_B}X \qquad A10$$

In order to maintain the invariance, then

$$\sigma_{\ln\dot{I}} = (\sigma_{\ln\dot{I}})_B$$

$$\rho = \rho_B\frac{(\sigma_{\ln I})}{(\sigma_{\ln I})_B} \qquad A11$$

REFERENCES

1. Whitehead, E. R. and G. W. Brown, "Field and Analytical Studies of Transmission Line Shielding — Part II," IEEE PAS, May 1969, pp. 617–26.

2. Sargent, M. A. "The Frequency Distribution of Current Magnitudes to Tall Structures," IEEE PAS, September/October 1972, pp. 2224–9.

3. Berger, K. and E. Vogelsanger, "Messungen und Resultate der BlitzForschung der Jahre 1965–1963 auf dem Monte San Salvatore," Bulletin des Schwizerischen Electrotechnischen Vereins, Bd 56, 1965, p. 2–22.

4. Poplansky, F. "Measurement of Lightning Currents in Czechoslovakia and the Application of Obtained Parameters in the Prediction of Lightning Outages of EHV Transmission Lines," CIGRE 1970, Report 33–03.

5. AIEE Committee Report, "A Method of Estimating the Lightning Performance of Transmission Lines," AIEE PAS, 1950, pp. 1187–96.

6. Berger, K., Andersen, R. B., and H.Kroninger, "Parameters of Lightning Flashes," ELECTRA, No. 41, July 1975, pp. 23–37.

7. Hoel, P. G., Introduction to Mathematical Statistics, Wiley, 1962.

Discussion

Abdul M. Mousa (Teshmont Consultants Ltd., Winnipeg, Canada): I wish to congratulate Dr. Brown for his continuing contributions to the study of the lightning performance of transmission lines, and would appreciate his response to the following comments:

1. Dr. Brown approximated Sargent's simulation of Berger's towers by a straight line (log-log scale), estimated the corresponding standard deviation to be 0.68 and held this figure to be more appropriate than the 0.60 standard deviation estimated by Berger himself. It appears to the discussor that this assumption is not justified in view of the historical development of the electrogeometric model for HV and EHV lines which went on as follows:
   i) The first models were tentatively calibrated based on line tripout data, because data about the individual shielding failure outage and backflash outage components was not available. To overcome this difficulty, Armstrong-Whitehead (8) initiated the "Lightning Stroke Pathfinder Project" with a data collection period of over 5 years. In the meantime, a preliminary calibration of the model for effectively shielded line was proposed by Armstrong-Whitehead (9), and a preliminary calibration of the model for partially shielded lines was proposed by Brown-Whitehead[1]. Brown-Whitehead used the following equations:

$$r_s = 7.1\, I_o^{0.75} \quad \ldots\ldots(1)$$

$$K_{sg} = 0.9 \quad \ldots\ldots(2)$$

   ii) Measurement of the properties of lightning, namely the frequency distribution of magnitudes and rates of rise, was being undertaken at different places:
      a) At Monte San Salvatore using *two* television towers of *different* heights[2,9]. Berger-Vogelsanger published the results of measurements for the period 1955-1963[3], later Berger published the results for the period 1963-1971[10], and finally Berger et al[9] published a summary of *all* results including a computer-aided analysis of the cummulative distributions.
      b) In Czechoslovakia where Poplansky[4] collected the measurements of lightning properties taken on a *large number* of tall objects.
      c) An AIEE committee report[5] proposed a curve for the frequency distribution of stroke magnitudes based on earlier observations on a *large number of objects* of different heights.
   iii) Sargent[6] discovered that the electrogeometric model theory partially explains the reason for the differences between the frequency distribution of stroke magnitudes measured at structures of different heights. Sargent then used a modified Brown-Whitehead model[1] (K_{sg} = 1.0) and the results of the 1955-1963 measurements at Monte San Salvatore[3] to work out a synthetic frequency distribution of stroke magnitudes to level ground, which if applied in conjunction with the modified Brown-Whitehead model, to a tower having the *average height* of the two Berger towers, would approximately yield the Berger data[3]. Sargent also found that he can approximately obtain the AIEE curve by applying his method to a 60-foot high tower, and that applying his method to two towers of 150 and 250 foot heights would yield an average which approximates Poplansky's distribution. Sargent stated that his synthetic distribution will have to be revised after finalization of the calibration of the electrogeometric model.
   iv) Later Gilman-Whitehead (11) and Whitehead (12) finalized the calibration of the electrogeometric model for HV and EHV lines. They proposed the following equations:

$$r_s = 9.4\, I_o^{2/3} \quad \ldots\ldots(3)$$

$$K_{sg} = 1.0 \quad \ldots\ldots(4)$$

The above review shows that Sargent's synthetic distribution was constructed so that using it in conjunction with the *preliminary* calibration of the electrogeometric model would *approximately* yield the *raw* results of Monte San Salvatore Station (period 1955-1963 only). However, it appears to the discussor that Sargent's results cannot be used to simulate the distribution on Berger towers) more accurately than the real Berger measurements[6], which covered the whole 1955-1971 period.

It is to be noted that there is significant differences between the striking distances given by the preliminary equation (1) and the final equation (3). Fig. 5 shows the ratio of the final/preliminary striking distances versus stroke current magnitudes.

Manuscript received February 22, 1977.

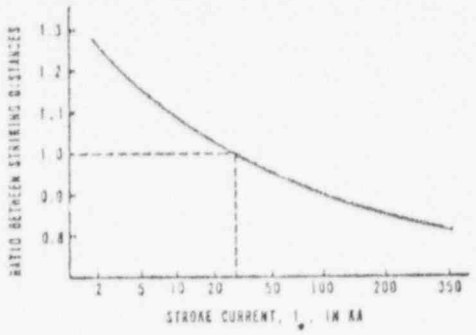

Fig. 5. Ratio between final[12] and preliminary[1] striking distances.

Based on the above, the discussor suggests that a new frequency distribution of stroke magnitudes to level ground should be developed based on equations (3) and (4) and the latest Berger data[9]. In doing so, the geometrical factor mentioned below should be also taken into consideration. Thereafter, the calculations of this paper may be repeated.

2. The discussor has noted that the frequency distribution of current magnitudes to a structure is affected, not only by the type and height of the structure, but also by its proximity to other objects. This can be explained as follows:

   If we consider two towers of equal height, h, located in a horizontal plane at a distance x from each other (which is of the order of the height, h), it will be noted that (See Fig. 6):

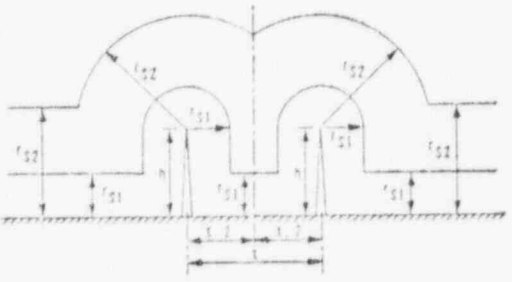

Fig. 6. Effect of striking distance on swath in case of two close towers.

   i) For low currents, the towers will have no shielding effect on each other, and hence the annual number of low current strokes collected by the two towers will be equal to *double* the annual number of strokes collected by a single tower of height h, located alone in a horizontal plane.
   ii) For high currents, the towers will have a shielding effect on each other, and hence the annual number of high current strokes collected by the two towers will be *less than double* the annual number of strokes collected by a single tower of the same height, located alone in a horizontal plane.
   iii) Thus, the frequency distribution of stroke magnitudes measured on the two towers, as compared to the distribution measured on a single tower of the same height will be as shown in Fig. 7.

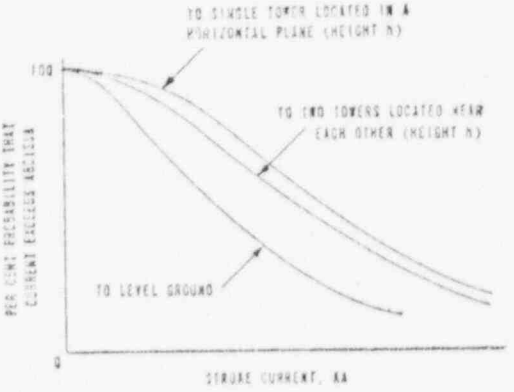

Fig. 7. Effect of proximity of other objects on the frequency distribution of stroke currents to a tower

(iv) The same phenomenon exists when the heights of the two towers are different, except that the corresponding geometry will be more complex than that of Fig. 6.

Now the Monte San Salvatore station has two television towers of different heights located at some distance from each other, with lightning records being taken on both towers. Sargent simulated the station by a single tower located alone in a horizontal plane, and having a height equal to the average heights of the two Berger towers. This approach entails a second approximation in addition to the approximation resulting from the use of a preliminary calibration of the electrogeometric model.

3. In the section entitled "Strokes to Lines", the author states that Sargent's simulation of a 60 foot high line does represent the frequency distribution of stroke currents to lines from heights of 5 m to 60 m, and that there is no indication that there would be a significant difference at greater heights. This statement appears to be in contradiction with Sargent's main finding, namely that height is the main factor affecting the frequency distribution of the stroke magnitudes to different objects of the same type (either towers or ground wires).
4. There appears to be a typographical error in the last equation in Section (A) of the Appendix, which should read,

$$f_s(I, \dot{I}) = f(\dot{I}|I)\, f_s(I)$$

REFERENCES

(8) H. R. Armstrong and E. R. Whitehead, "A Lightning Stroke Pathfinder", *IEEE Trans.*, Vol. PAS-83, pp. 1223-1227, December 1964.

(9) H. R. Armstrong and E. R. Whitehead, "Field and Analytical Studies of Transmission Line Shielding", *IEEE Trans.*, Vol. PAS-87, pp. 270-281, January 1968.

(10) K. Berger, "Methoden und Resultate der Blitzforschung auf dem Monte San Salvatore bei Lugano in den Jahren 1963-1971", Bull. SEV, Bd. 63 (1972), no. 24, pp. 1403-1422.

(11) D. W. Gilman and E. R. Whitehead, "The Mechanism of Lightning Flashover on High-Voltage and Extra-High-Voltage Transmission Lines", *Electra* no. 27, pp. 65-96, March 1973.

(12) E. R. Whitehead, "CIGRE Survey of the Lightning Performance of EHV Transmission Lines", *Electra* no. 33, pp. 63-89, March 1974.

Gordon W. Brown: Many thanks to Mr. Mousa for his thoughtful, perceptive comments and questions. Mr. Mousa raised many similar questions in regard to a related paper ("Lightning Performance – I-Shielding Failures Simplified") and the reader is referred to that discussion and closure for further development, particularly relating to the use of the strike distance-stroke current relationship. In Mr. Mousa's discussion, item 1 (iv), he raised the question of refinements in the model. I am afraid that I find the basis for the refinements a bit elusive. Tracking the relation $r_s = 9.41 I^{0.73}$ back to its original source, I am afraid I still find the justification for modifying the equations a bit elusive. Further, although the maximum differences in strike distances are only about 10 percent over the most important range (5 to 100 kA), such differences result in very small differences in outage rates. While they may result in significant differences for backflash outages, there are far more important factors (footing resistance).

Regarding Sargent's treatment of data and my own interpretation of Berger's published results, two comments are in order. First, concerning Sargent's use of the AIEE data, the AIEE distribution was the result of extensive investigation and based on the carefully considered judgement of leaders in the field, and thought to be representative of that for strokes to the transmission lines of the day. For such lines, a height of 60 feet was typical. Sargent found that, indeed, his synthetic curve reproduced the AIEE distribution, assuming it to be a 60 ft. high line (I assume the 60 ft. high "tower" in Mr. Mousa's discussion rather than "line" was unintended). Second, regarding Berger's data, I was forced to reconsider his stated parameters, since his data were not self-consistent in some cases. The standard deviation as found from his 5 percent and 50 percent figures is not the same as that found from the figures for 95 percent and 50 percent.

Further, in discussor's Reference 6, it is stated that "*some* of the data collected over the period 1963-1971 were analyzed in more detail." The meaning of "some" was unclear. Also, the method of fit used in discussor's Reference 6 was "least squares". For such data, maximum likelihood methods (which is not least squares for this case) are almost certainly better. Since Sargent's data were based on several sets of data, I felt that it was most sound to use Sargent's estimate and verify that Berger's most recent data was still consistent. Though the fit of Figure 3 is not perfect, I submit it is still consistent. Further, any synthesis must rely on more than data from one location, not just from Berger's data, as the discussor suggests. I certainly have no doubt that as the industry gathers more and better information, that the values of the parameters of the statistical distributions will change. I look forward to such efforts. In discussor's section 2, he raises the valid point that nearby structures can affect the frequency distribution. For discussor's Figure 6 a further point is worth noting. Usually, we are concerned with *either* shielding failure *or* backflash failure calculations. For shielding failures, the currents of interest are quite low, and the portion of the frequency distribution of interest will yield the same numerical results as a full, accurate frequency distribution. Similarly, for backflash, currents of concern are generally quite high, and numerical results will again be the same if we assume half the strokes to each line, and the same frequency distribution.

The fact that Sargent simulated the two towers at San Salvatore by a single tower should not introduce substantial error, though it would be great if a more accurate synthesis were done. We are, indeed, due for it.

Discussor's section 3 is answered in the discussion and closure mentioned earlier.

Finally, it is rare to find a discussor who so thoroughly reads and studies an article as Mr. Mousa has done. I have the highest admiration for (and envy of) his thoughtfulness and thoroughness. Many, many thanks!

Manuscript received April 25, 1977.

IEEE Transactions on Power Apparatus and Systems, Vol. PAS-97, no. 1, January/February 1978

LIGHTNING PERFORMANCE - I
SHIELDING FAILURES SIMPLIFIED

Gordon W. Brown, Senior Member

U. S. Energy Research and Development Administration
Washington, D. C.

ABSTRACT AND CONCLUSIONS

A radically simplified method for determining shielding failure and shielding failure outage rates is presented. The method is shown to have excellent correlation with over 120,000 km-yrs of actual line outage rates (1974 CIGRE Survey). For lines of realistic design, total shielding failure rate is found to be a function dependent only on the maximum strike distance, which is governed by line configuration and height. Shielding failure outage rate depends on line configuration and CFO, and depends heavily on the statistical distribution of heights along the line. Methodology is developed to utilize or to approximate such distributions.

INTRODUCTION

In a previous paper (Reference 1) it was shown that for shielded situations the frequency distribution of stroke current magnitudes was dependent only on the maximum strike distance, $r_{s\,max}$, for which a stroke could hit the phase wire. This is illustrated in Figure 1.

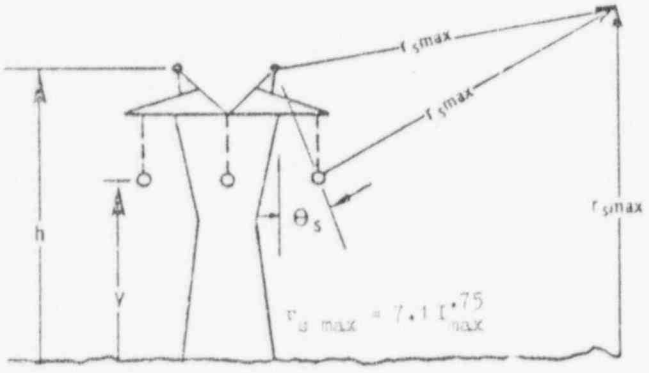

Figure 1. Shielding Parameters

The calculations of Reference 1 were, however, for distribution lines shielded by nearby transmission lines or structures. The present work extends the calculations for distances and heights typical of HV, EHV and UHV transmission lines. Frequency distributions are still found to be a function only of $r_{s\,max}$.

I. SHIELDING FAILURE RATE AND FREQUENCY DISTRIBUTION

(A) Rate of Shielding Failures

The term "shielding failures" here means all those strokes which "sneak by" the shield wires, whether or not they cause outages. It was discovered that, to a good approximation, the number of shielding failures is a function only of the maximum strike distance. This is true for all realistic transmission line structures. Calculations were made for heights to 50m and shielding angles to 45, and a variety of conductor to ground wire distances. Parameter variations were smooth, and height extrapolations to 75m are realistic with little or no additional error expected. Results are given in Figure 2. Stroke angles are assumed distributed according to $\cos^m$, with m=2 (cf. References 1-3).

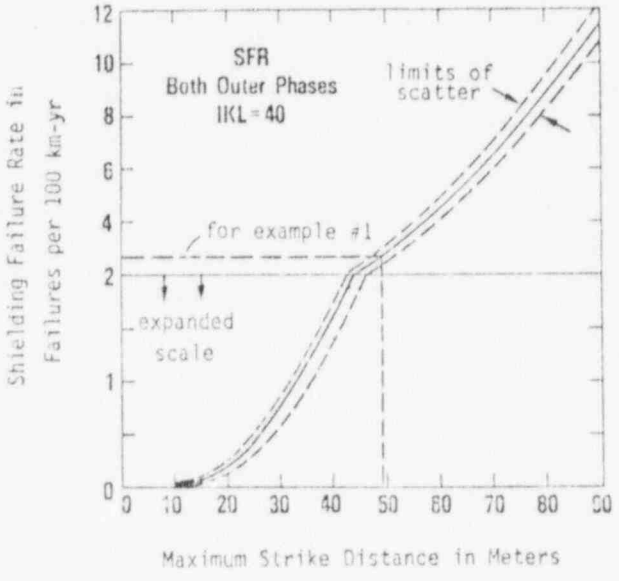

Figure 2. Shielding Failure Rate: SFR (Includes both outer phases)

The calculations were made for an isokeraunic level (IKL) of 40, and assumes a stroke density of

$$N_g = 0.16\ \text{IKL strokes/(sq.km-yr)}$$

Reference 1 gives the correct expression for $r_{s\,max}$ as a function of line parameters:

$$r_{s\,max} = \frac{c^2(y+h) + 2cx\sqrt{yh}}{2(h-y)^2}, \quad x = c\sin\theta_s$$

$$c = \sqrt{x^2 + (y-h)^2}$$

Fortunately, a much simpler expression has been found. Though an approximation, it is excellent over the entire range of possible parameters. The formula and its basis are shown in Figure 3.

Example 1: $h = 40m$, $y = 25m$, $\theta_s = 20^\circ$

$$r_{s\,max} = \frac{40+25}{2(1-\sin 20)} = 49m$$

For this $r_{s\,max}$, the number of shielding

90004 21

F 77 015-1. A paper recommended and approved by the IEEE Transmission and Distribution Committee of the IEEE Power Engineering Society for presentation at the IEEE PES Winter Meeting, New York, N.Y., January 30-February 4, 1977. Manuscript submitted July 9, 1976; made available for printing October 28, 1976.

0018-9510/78/0100-0033$00.75 ©1978 IEEE

failures is (Figure 2)

SFR = 2.7 failures/100km-yr.

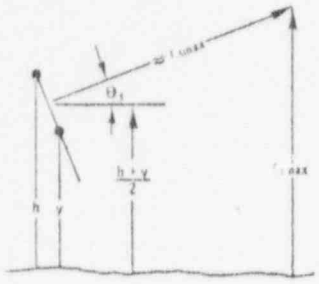

Error is significant only if h-y is greater than about $r_s/2$.

$$r_{s\,max} \cong \frac{h+y}{2(1-\sin\theta_s)}$$

Figure 3. Approximation to Maximum Strike Distance

The other major need for determination of shielding failure outage rate is the frequency distribution of the shielding failure stroke currents.

(B) Frequency Distribution of Shielding Failure Currents

As noted, the distribution is a function only of $r_{s\,max}$ (or I_{max}), and is extremely insensitive to variation of other parameters. The overall results are shown in Figure 4.

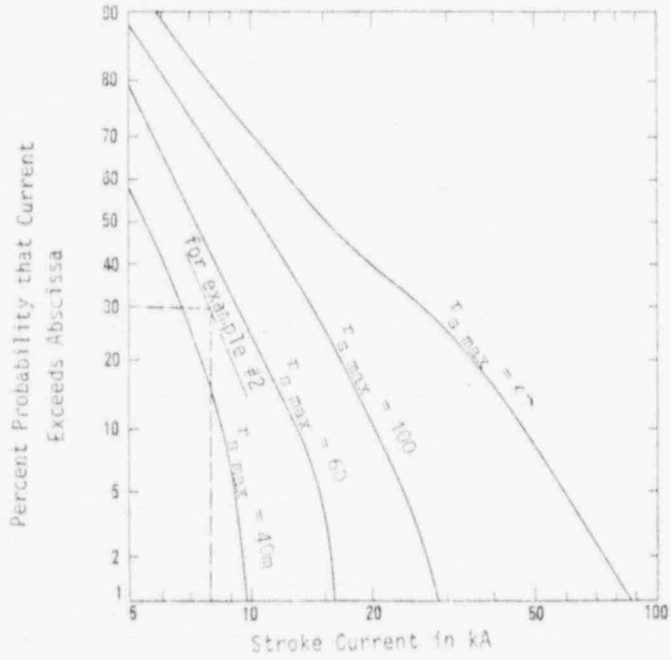

Figure 4. Frequency Distribution of Shielding Failure Stroke Currents

II. SHIELDING FAILURE OUTAGE RATE

(A) Current Required for Flashover

If the maximum current to the line, I_{max}, is greater than the stroke current required for flashover, IFO, then an outage occurs.

$$IFO = \frac{2 \cdot CFO}{Z}$$

where

IFO = stroke current required for flashover
CFO = critical flashover voltage
Z = surge impedance for a surge on the phase conductor.

Example 2: For the previous example, there were 2.7 shielding failures per 100km-yr for an $r_{s\,max}$ of 40m.

Suppose the CFO were 1500kV, and the surge impedance 375. Then

$$IFO = \frac{2 \cdot CFO}{Z} = \frac{3000}{375} = 8.0kA$$

From Figure 4 (dashed lines), for $r_{s\,max}$ = 49m, about 30% of the shielding failures are over 8kA. Thus the shielding failure outage rate is

sfo = 30% of 2.7
= 0.8 outages per 100km-yr.

(B) The Outage Rate Improved

Since both the shielding failure rate and I_{max} are functions of $r_{s\,max}$, Figures 2 and 4 can be combined. This is done in Figure 5.

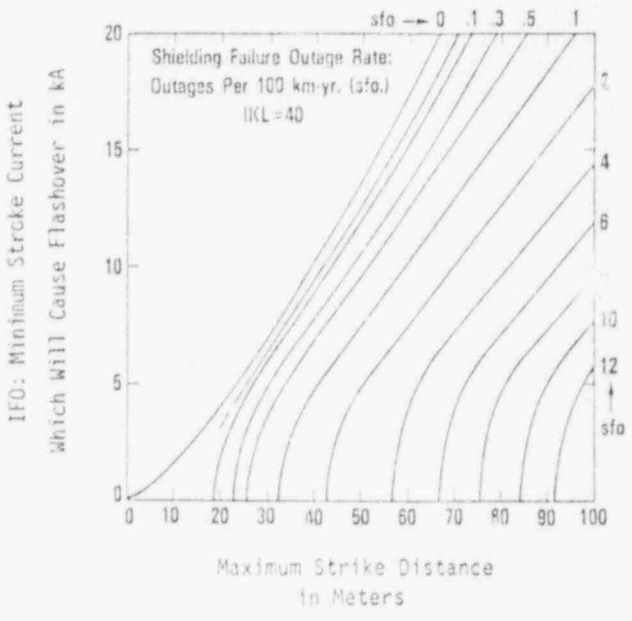

Figure 5. Shielding Failure Outage Rate

(C) The Problem of Maximum Strike Distance

As we proceed along a line, heights vary with terrain. One is tempted to use the average height to calculate the SFO rate. Ideally, we desire a full distribution of heights along the line. If the frequency distribution of ground wire height h, and conductor height y, is known, then a distribution of strike distances can be found. Let that distribution be

$f(r_{s\,max})$ = frequency distribution of maximum strike distances along the line.

Then the shielding failure rate is

$$SFO = \int_0^\infty sfo\, f(r_{s\,max})\, dr_{s\,max}$$

For a given $r_{s\,max}$ and IFO, the rate is sfo. Note that sfo is zero for $r_{s\,max}$ less than

$$R_{FO} = 7.1(IFO)^{.75}$$

Also, there is, for any line, some absolute maximum strike distance, R_{max}. (There would also be some finite minimum.) Hence we can write

$$SFO = \int_{R_{FO}}^{R_{max}} sfo\ f(r_{s\,max})dr_{s\,max}$$

Consider, as in Figure 6, a hypothetical distribution of strike distances. The illustration is chosen for a case of low shielding failure rate.

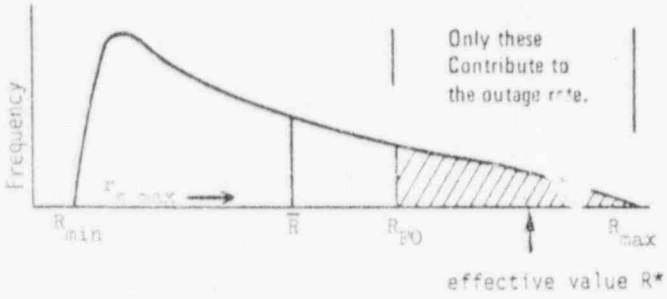

Figure 6. Frequency Distribution of Maximum Strike Distances

It is clear that if some "effective" maximum strike distance (R*) is to be used, it must lie between R_{FO} and R_{max}. It is suggested that the following procedure be used to determine the SFO rate.

(B) Recommended Calculation Procedure

1. Estimate the frequency distribution of $r_{s\,max}$:

(a) Determine the values of maximum strike distance under the following conditions: the smallest value (R_{min}), the value at the tower (R_t), and the maximum value (R_{max}).

R_{min} = $r_{s\,max}$ at midspan for flat terrain

R_t = $r_{s\,max}$ at tower dimensions

R_{max} = maximum of all $r_{s\,max}$ ("worst" or greatest conductor heights)

(Note: An approximate method for determining R_{max} is given in Section III A) following.)

(b) Estimate the shape of the distribution (i.e., histogram) of $r_{s\,max}$. It should closely parallel the distribution (histogram) of height. In particular, estimate $\bar{R}$, the average. (Note: An approximation for determining $\bar{R}$ is given in part III(A) following.)

Typical estimated shapes of the frequency distributions of maximum strike distances for flat, rolling, and mountainous terrain are illustrated in Figure 7.

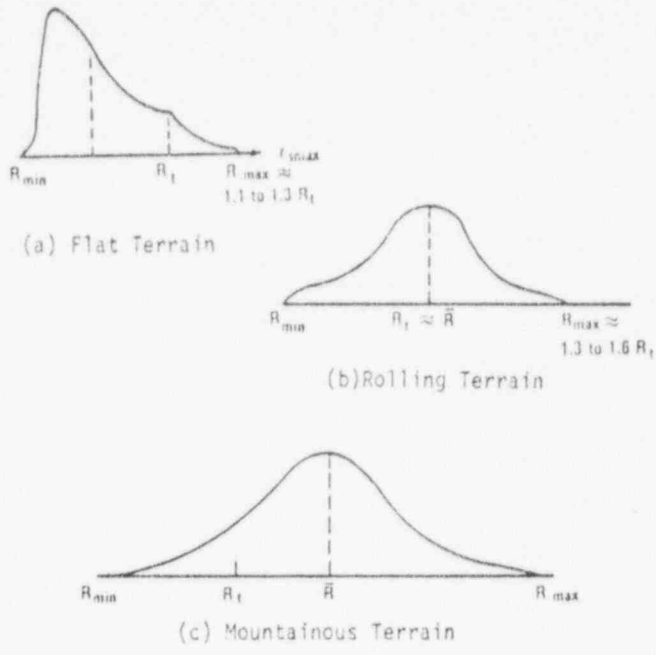

Figure 7. Estimated Form of Frequency Distribution

2. Determine R_{FO}, R*:

(a) Determine $IFO = \frac{2GFO}{2}$

and $R_{FO} = 7.1(IFO)^{.75}$

which is the minimum strike distance for which flashover can occur.

(b) Estimate R*, placing it near, but slightly greater than, the mean value of those $r_{s\,max}$ lying between R_{FO} and R_{max}.

3. Determine the outage rate:

(a) Estimate the fraction ϕ_{FO} of all strike distances between R_{FO} and R_{max}.

$$\phi_{FO} = \frac{\text{shaded area, Figure 6}}{\text{total area, Figure 6}}$$

(b) The outage rate is then

$$SFO = \phi_{FO}\ sfo^*$$

where sfo* = sfo at R* (from Figure 5). (Note: Approximate methods for estimating R* and ϕ_{FO} from R_{min}, R_{max}, $\bar{R}$ and R_{FO} are given in III (A) following.)

III. COMPARISON WITH REALITY

In the March 1974 issue of ELECTRA, E. R. Whitehead[3] reported a CIGRE Survey of EHV Transmission Line Outage Rates. Calculations have been made for each of the "11 representative reporting units" of Table III of that article.

(A) Treatment of the "Input" Data

1. $\bar{R}$: Sufficient information was available in the table to determine R_t and R_{min}. Terrain percentages were also given. Let the fractions of the line

under flat, rolling, and mountainous conditions be f_F, f_R, and f_M respectively. The average of $r_{s\ max}$, called $\overline{R}$, for the line, was approximated as

$$\overline{R} = f_F\overline{R}_F + f_R\overline{R}_R + f_M\overline{R}_M$$

with

$$\overline{R}_F \approx 1.05\left(\frac{2}{3}R_{min} + \frac{1}{3}R_t\right)$$

$$\overline{R}_R \approx R_t$$

$$\overline{R}_M \approx 1.5R_t$$

The 1.05 in $\overline{R}_F$ attempts to account for the fact that no terrain is "flat," and the tendency would be to build from hill to hill, however slight.

2. R_{max}: For purposes of estimating the distribution, R_{max} for flat, rolling, and mountainous terrain were estimated at

$$R_{F\ max} = 1.2\,R_t$$

$$R_{R\ max} = 1.4\,R_t$$

$$R_{M\ max} = 1.8\,R_t$$

With mixed terrain, the value used for the distribution was the square root of the squared sums, or

$$R_{max} = R_t\sqrt{1.44f_F + 1.96f_R + 3.28f_M}$$

This is likely to be less than actual R_{max} (such as for a case with all flat terrain plus one deep valley). In terms of estimating the shielding failures, however, something like the above approximation would be more appropriate than the actual value, unless the entire histogram of heights were used.

3. The outage rate: The shapes of the frequency distributions were then estimated for each line. Two examples are shown in Figure 8.

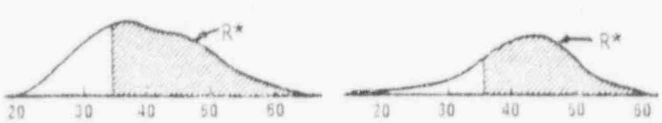

Figure 8. Frequency Distribution for Lines No. 52 and 80

After estimating all the frequency distributions, patterns were sought for approximating R* and ρ_{FO} from the other strike distances. The following were found to give excellent results:

(a) R*: First the average ($\overline{R}$*) of all $r_{s\ max}$ above R_{FO} is estimated:

$$\overline{R}^* \approx \begin{cases} \overline{R}, & R_{FO} < R_{min} \\ \overline{R} + \left(\dfrac{R_{FO} - R_{min}}{R_{max} - R_{min}}\right)(R_{max} - \overline{R}) \end{cases}$$

Then a point slightly above $\overline{R}$* is used for R*:

$$R^* = \overline{R}^* + \frac{R_{max} - \overline{R}^*}{10}$$

(b) ρ_{FO}:

$$\rho_{FO} \approx \begin{cases} 1 - \dfrac{(R_{FO} - R_{min})^2}{(\overline{R}-R_{min})(R_{max}-R_{min})}, & \text{if } R_{FO} < \overline{R} \\ \dfrac{(R_{max} - R_{FO})^2}{(R_{max}-\overline{R})(R_{max}-R_{min})}, & \text{if } R_{FO} > \overline{R} \end{cases}$$

(B) The Results

The results are shown in Table I. It seems clear that the correlation between calculation and actual data is remarkably good, with few exceptions (notably, lines #43 and 44).

Table I

Comparison of Calculated SFO Rate vs. Actual Total Outage Rate (cf. Table III of Reference 3) (both at an IKL of 40)

Line #	f_F	f_R	f_M	R_{min}	R_t	R_{max}	R_{FO}	$\overline{R}$	R*	IFO	ρ_{FO}	CALC SFO	ACTUAL STR
30	.50	.50	0	16.2	36.1	47.1	38.2	[illegible]	30.0	[illegible]	.45	.18	.24
31	.50	.50	0	16.4	[illegible]	[illegible]	[illegible]	[illegible]	[illegible]	8.0	1.00	2.5	3.4
32	[illegible]	.16	[illegible]	[illegible]	[illegible]	[illegible]	[illegible]	[illegible]	[illegible]	[illegible]	1.00	7.2	5.7
33	.33	.47	.25	21.0	41.1	[illegible]	45.1	45.3	[illegible]	11.8	.5	.15	.24
34	[illegible]	.15	.43	21.2	[illegible]	[illegible]	45.3	[illegible]	[illegible]	[illegible]	.7	.34	.33
35	.36	.14	0	21.2	[illegible]	[illegible]	45.3	[illegible]	43.0	[illegible]	.11	.013	0
36	.30	.40	.30	24.2	41.1	[illegible]	45.1	47.2	[illegible]	11.5	.65	.23	.28
39	1.00	0	0	16.2	[illegible]	27.6	36.5	—	—	[illegible]	—	0	.14
40	0	1.00	0	17.1	[illegible]	[illegible]	33.5	[illegible]	[illegible]	[illegible]	.4	.072	[illegible]
43	.20	.70	.10	13.7	43.0	[illegible]	36.1	47.0	[illegible]	[illegible]	.72	.72	0
44	[illegible]	.15	.15	13.7	43.0	[illegible]	[illegible]	47.3	58.0	[illegible]	.72	.72	0
45	.20	.75	.05	16.8	[illegible]	[illegible]	[illegible]	[illegible]	[illegible]	[illegible]	.70	.14	0
51	[illegible]	.19	.22	20.8	[illegible]	[illegible]	34.1	45.0	[illegible]	[illegible]	.18	.58	.47
52	.11	.39	.11	20.8	[illegible]	[illegible]	34.1	[illegible]	47.0	[illegible]	.23	.45	.84
56	1.00	0	0	20.7	[illegible]	[illegible]	[illegible]	[illegible]	44.0	[illegible]	.4	.17	.34
57	.80	[illegible]	.07	20.3	[illegible]	54.1	[illegible]	37.5	45.0	[illegible]	.4	.18	.19
58	[illegible]	.11	.06	20.8	[illegible]	51.5	[illegible]	38.7	45.0	[illegible]	.4	.13	.13
64	.10	.40	.50	15.4	[illegible]	[illegible]	[illegible]	58.7	[illegible]	[illegible]	.9	.69	.5
65	.10	[illegible]	[illegible]	15.4	[illegible]	57.4	[illegible]	[illegible]	46.5	[illegible]	.7	.21	.4
66	.10	.90	0	15.4	[illegible]	[illegible]	[illegible]	[illegible]	[illegible]	[illegible]	.7	.20	.19
67	.10	.90	0	15.4	[illegible]	[illegible]	[illegible]	[illegible]	[illegible]	[illegible]	.7	.20	.36
70	[illegible]	[illegible]	[illegible]	[illegible]	[illegible]	[illegible]	[illegible]	[illegible]	[illegible]	[illegible]	.22	.22	.23
71	.60	[illegible]	[illegible]	[illegible]	[illegible]	[illegible]	[illegible]	[illegible]	[illegible]	[illegible]	.13	.21	.51
75	0	1.00	0	[illegible]	[illegible]	[illegible]	[illegible]	[illegible]	[illegible]	[illegible]	1.00	1.3	1.04
76	0	1.00	0	[illegible]	[illegible]	[illegible]	[illegible]	[illegible]	[illegible]	[illegible]	1.00	1.3	1.60
77	0	1.00	0	23.9	[illegible]	[illegible]	[illegible]	[illegible]	[illegible]	14.0	.075	.02	0
88	.50	.50	0	14.5	[illegible]	[illegible]	[illegible]	[illegible]	[illegible]	[illegible]	.15	.05	.20
89	.50	.50	0	16.5	[illegible]	[illegible]	[illegible]	[illegible]	[illegible]	[illegible]	.15	.05	.11
92	.80	[illegible]	0	16.0	[illegible]	[illegible]	[illegible]	[illegible]	47.0	[illegible]	.15	.01	.21
93	.70	.23	.10	[illegible]	[illegible]	[illegible]	[illegible]	[illegible]	[illegible]	9.7	[illegible]	.08	.12
94	[illegible]	[illegible]	.05	23.6	44.9	[illegible]	[illegible]	[illegible]	[illegible]	9.7	[illegible]	.04	.45
95	.70	.20	.10	[illegible]	[illegible]	[illegible]	[illegible]	[illegible]	[illegible]	[illegible]	.1	.09	.19
96	.60	.30	.10	[illegible]	[illegible]	[illegible]	[illegible]	[illegible]	[illegible]	[illegible]	.5	.25	0
97	.60	.30	.10	[illegible]	[illegible]	[illegible]	[illegible]	[illegible]	[illegible]	9.7	.5	.25	.38
98	.80	.20	0	[illegible]	17.1	[illegible]	[illegible]	[illegible]	[illegible]	9.7	.4	.14	.64
99	.80	.20	0	[illegible]	17.1	[illegible]	[illegible]	[illegible]	48.0	9.7	.4	.14	.40
105	.24	[illegible]	.61	[illegible]	[illegible]	[illegible]	[illegible]	[illegible]	[illegible]	[illegible]	1.00	2.2	2.47
106	[illegible]	.22	.61	[illegible]	[illegible]	[illegible]	[illegible]	[illegible]	[illegible]	[illegible]	1.00	1.5	1.48
107	.34	.54	[illegible]	[illegible]	[illegible]	[illegible]	[illegible]	[illegible]	[illegible]	[illegible]	1.00	2.2	2.57
108	[illegible]	[illegible]	[illegible]	27.8	[illegible]	[illegible]	[illegible]	57.1	[illegible]	[illegible]	1.00	2.1	2.03
109	.08	.92	0	50.7	70.1	[illegible]	[illegible]	84.5	[illegible]	[illegible]	1.00	2.8	3.55

In addition to the high correlation, in 28 out of 41 cases the calculated shielding failure rate is less than the "STR" or total outage rate for the line. This is well within the bounds of reason.

(C) Sample Calculations - Low Shielding Failure Rate

Consider a 345kV line with the following data:

CFO = 1600kV
Z = 360Ω
θ_{st} = 5 degrees at tower
h_t = 34m (at tower), sag = 7m
y_t = 27m (at tower), sag = 17.3m
Terrain: 50% Flat, 50% Rolling
h_{max} = estimated to be 50m at several crossings
y_{max} = 43m

90004324

(h_{max} and y_{max} were deliberately chosen a bit higher than might be normal for purposes of illustration.)

Rolling Terrain assumes the qualitative definition that the terrain "typically" follows conductor sag. (see, e.g., Reference 3)

1. Calculation of strike distances:

(a) R_{min}:

$$h_{min} = h_t - sag = 2.7m$$
$$y_{min} = y_t - sag = 12.7m$$

θ_s at midspan is calculated from the tower angle (θ_s) and sag data:

$$x = (h_t - y_t)\tan\theta = 7\tan 5^\circ = .612m$$

At midspan, then,

$$\tan\theta_m = \frac{.612}{27-12.7} = .043, \text{ or } \theta_s = 2.45^\circ$$

Thus

$$R_{min} = \frac{h_{min} + y_{min}}{2(1-\sin\theta\sin)} = 20.7m$$

(b) R_{max}: Since R_{max} likely occurs at a tower, we use θ_{st}.

$$R_{max} = \frac{50+43}{2(1-\sin 5^\circ)} = 51m$$

(c) $R_t = \frac{34+27}{2(1-\sin 5^\circ)} = 33.4$

(d) $R_{FO} = 7.1(IFO)^{.75}$

With $IFO = \frac{2(1600)}{300} = 8.9ka$,

$$R_{FO} = 36.6m$$

2. Method using frequency distribution (histogram) of tower heights. Starting with an estimated histogram of tower heights, assuming the frequency distribution of $r_{s\,max}$ to have the same shape, and "smoothing," yields the sketch below.

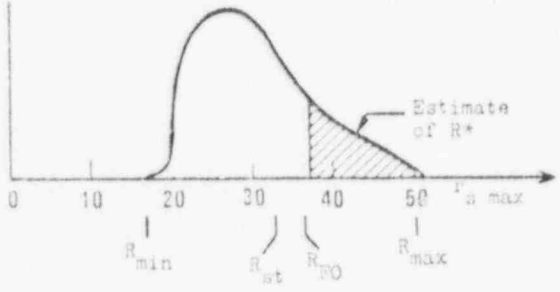

Figure 9. Estimated Frequency of Maximum Strike Distances for the Sample Calculations

The shaded area is estimated at 25% of the total. Thus

$$P_{FO} \approx 0.25$$

R* is estimated at 43m.

Entering Figure 5 with

$$r_{s\,max} = R^* = 43$$

$$IFO = 8.9kA$$

yields $sfo^* = .25$ and

$$SFO = P_{FO}sfo^* = .25(.25) = .063$$

Had the average value of $r_{s\,max}$ (about 32 or 33m from Figure 9) been used, a rate of zero would have been determined.

3. Method using estimated R*. Estimating

$$\overline{R}_F = 1.05[\tfrac{2}{3}(2.07) + \tfrac{1}{3}(33.4)] = 26.2$$

$$\overline{R}_R = 33.4$$

with $f_F = .5$, $f_R = .5$

$$\overline{R} \approx .5(26.2) + .5(33.4) = 29.8$$

Since R_{max} is known (50m), we estimate

$$\overline{R}^* = 29.8 + \frac{36.6-20.7}{50-20.7}(50-29.8) = 40.8$$

and

$$R^* = 40.8 + \frac{50-40.8}{10} = 42m$$

and

$$P_{FO} = \frac{50-36.6}{(50-29.8)(50-20.7)} = .30$$

From Figure 5, with IFO = 8.9kA,

$$sfo^* = 0.2$$

$$SFO = .30(0.2) = .06$$

Had R_{max} been calculated as done for the table, (i.e., the erroneous R_{max} used), the results would be

$$R_{max} = \sqrt{33.4 \cdot .5(1.44)+.5(1.96)} = 44m$$

$$\overline{R}^* = 29.8 + \frac{36.6-20.7}{44-20.7}(44-29.8) = 39.5$$

and

$$R^* = 39.5 + \frac{44-39.5}{10} = 40$$

and

$$P_{FO} = \frac{(44-36.6)^2}{(44-29.8)(44-20.7)} = .17$$

at R* = 40, sfo* = 0.1.

So that

$$SFO \approx .17(.1) \approx .02$$

This example illustrates that for accuracy at low shielding failure rates, it is particularly important to know the distribution of heights (strike distances).

ACKNOWLEDGEMENT

The author wishes to acknowledge the generous help of his former colleague and co-author (Reference 1) at Joslyn Mfg. Co., Mr. Steven Thunander. He carried out the necessary computations to verify that the frequency

distributions were not significantly a function of height of a line, and to calculate shielding failure rates for realistic transmission shielding configurations.

REFERENCES

1. Brown, Gordon W. and Steven Thunander, "Frequency of Distribution Arrester Discharge Currents," IEEE Transactions, presented at Winter Power Meeting, January 1976.

2. Whitehead, E. R. and G. W. Brown, "Field and Analytical Studies of Transmission Line Shielding: Part II," IEEE PAS Transactions, May 1969, pp. 617-20.

3. Whitehead, E. R., "CIGRE Survey of the Lightning Performance of EHV Transmission Lines," ELECTRA, March 1974, pp. 63-89.

For Combined Discussion see page 48

LE MÉCANISME DES AMORÇAGES DUS A LA FOUDRE SUR LES LIGNES DE TRANSPORT A HAUTE TENSION ET A ULTRA-HAUTE TENSION

par D.W. Gilman et E.R. Whitehead

Rapport présenté au Comité d'Etudes n° 33
(Surtensions et coordination de l'isolement)
et publié à la demande de son Président
M.V. Palva

Résumé.

Ce rapport présente les résultats d'une étude en trois étapes expérimentale statistique et analytique des mécanismes des coups de foudre et des contournements d'isolateurs se produisant sur les lignes de transport à haute tension et à très haute tension. Il décrit en même temps un dispositif appelé le « détecteur de cheminement », mis au point au cours de la première étape de l'étude avec l'interprétation de ses signaux et le tableau associé concernant l'interprétation des phénomènes d'« amorçage secondaire » ou de « défaillance de l'effet d'écran ». Des études expérimentales pour lesquelles furent utilisés environ 4 600 détecteurs de cheminement sur 400 miles de lignes ont permis d'obtenir 167 fonctionnements portant sur 111 coups de foudre distincts parmi lesquels 51 provoquèrent des défaillances d'effet d'écran et 52 provoquèrent des phénomènes d'amorçage secondaire. Huit coups de foudre conduisirent à des fonctionnements qu'il n'a pas été possible d'interpréter d'une façon satisfaisante. Ces études statistiques portent sur une expérience de plus de 140 000 km/ans sur des lignes dont les tensions allaient de 69 kV à 500 kV.

On a trouvé que les contournements d'isolateurs peuvent être le résultat à la fois de coups de foudre directs sur le conducteur de phase : c'est le mécanisme de « défaillance de l'effet d'écran » ; et le coup de foudre sur le pylône ou le câble de garde : c'est le mécanisme d' «amorçage secondaire ». C'est le mécanisme de défaillance de l'effet d'écran qui prédomine lorsque des angles importants de la zone protégée (par effet d'écran) se trouvent associés à des pylônes élevés et à des valeurs faibles de la résistance de mise à la terre du pied du pylône. Le mécanisme d'amorçage secondaire est le plus fréquent lorsque des valeurs élevées de la résistance de mise à la terre des pieds du pylône se trouvent associées à de faibles hauteurs de pylône et de faibles niveaux d'isolement.

THE MECHANISM OF LIGHTNING FLASHOVER ON HIGH-VOLTAGE AND EXTRA-HIGH-VOLTAGE TRANSMISSION LINES

by D.W. Gilman and E.R. Whitehead

Paper presented at Committee No 33
(Overvoltages and insulation co-ordination)
and published at the request of the Chairman
Mr. V. Palva

Abstract.

The results of a three-phase experimental, statistical, and analytical study of the mechanisms of lightning strokes to, and insulation flashover on, HV and EHV transmission lines are presented. A device called the « Pathfinder », developed during the initial phase of the study, is described together with its signal code and associated interpretation table of « backflash » or « shielding failure » events. Experimental studies using approximately 4600 Pathfinder instruments on 400 miles of line yielded 167 operations on 111 separate strokes, of which 51 caused shielding failures and 52 caused backflash events. Eight strokes resulted in operations which could not be conclusively interpreted. Statistical studies covered over 140,000 kilometer-years experience on lines from 69 kV to 500 kV voltage rating.

It is found that insulator flashovers occur both as a result of strokes directly to the phase conductor, the "shielding failure" mechanism, and as a result of strokes to the tower or shielding ground wire, the "backflash" mechanism. The shielding failure mechanism predominates when large shielding (protective) angles are associated with high towers and low tower footing resistances to ground. The backflash mechanism predominates when high tower footing resistances are associated with low tower heights and low insulation levels.

Des modèles analytiques basés sur la connaissance moderne des processus de foudre sont utiles pour rassembler les valeurs expérimentales concernant les défaillances d'effet d'écran, pour prévoir le comportement des lignes insuffisamment protégées, et pour déterminer des recommandations pour la mise au point d'un dispositif d'écran efficace. Les fondements théoriques du mécanisme d'amorçage secondaire sont bien connus et se prêtent bien à l'explication des résultats de cette étude. La conclusion est qu'avec des lignes convenablement protégées, il est possible de concevoir des lignes à haute tension et à ultra-haute tension pour des taux moyens de déclenchement d'environ 0,25 pour 100 km/an avec une densité de journées d'orage de 40 par an. Des études préliminaires des projets de lignes de transport à ultra-haute tension protégés montrent que, dans des conditions analogues, on pourrait rendre le taux de déclenchement par coup de foudre inférieur à 0,025.

Analytical models based on modern knowledge of lightning stroke processes are found useful in correlating experimental data on shielding failures, predicting performance of ineffectively shielded lines, and in providing guidelines for the design of effective shielding. The theoretical foundations of the backflash mechanism are well known and are adequate to explain the results of this study. It is concluded that, with properly shielded lines, HV and EHV lines can be designed for trip-out rates averaging approximately 0.25 per 100 kilometer-years at a thunderstorm-day level of 40 per year. Current preliminary studies of proposed UHV transmission line designs suggest that, under comparable conditions, the lightning trip-out rate many be less than 0.025.

Liste des Symboles

- a Espacement horizontal entre le conducteur de phase et le câble de garde.
- b_t Espacement vertical entre le conducteur de phase et le câble de garde au droit du pylône.
- $\bar{b}$ Distance verticale moyenne entre le conducteur de phase et le câble de garde.
- $\bar{C}$ Distance moyenne entre le conducteur de phase et le câble de garde.
- $\bar{y}$ Hauteur moyenne du conducteur de phase au-dessus du sol.
- $\bar{y}'$ Hauteur moyenne équivalente du conducteur avec un angle de sol différents de zéro.
- $\bar{H}$ Hauteur moyenne du câble de garde au-dessus du sol.
- $\bar{r}_{sc}$ Distance moyenne d'amorçage définie par l'équation (5) pour un amorçage entre le cœur de l'éclair et le câble de garde ou le pylône.
- $\bar{r}_{sg}$ Distance moyenne d'amorçage entre le cœur de l'éclair et la terre (sol).
- r_{sc} Distance moyenne d'amorçage entre le cœur de l'éclair et le conducteur de phase.
- K_{sg} Rapport $\bar{r}_{sg}/\bar{r}_{sc}$.
- K_{sc} Rapport $\bar{r}_{sc}/\bar{r}_{sc}$.
- $\hat{r}_{sc}$ Distance effective d'amorçage définie par l'équation (7) pour un amorçage entre le cœur de l'éclair et le câble de garde ou le pylône. Voir figure 8.
- I_c Courant critique de foudre dans le conducteur de phase défini par l'équation (6).
- I_{oc} Courant critique de foudre dans un sol de résistance nulle $I_{oc} = 1{,}1\ I_c$.
- *ICFO* Tension critique d'amorçage au choc (Polarité négative).
- Z Impédance caractéristique du conducteur de phase.

List of Symbols

- a *horizontal spacing between phase conductor and ground wire.*
- b_t *vertical spacing between phase conductor and ground wire at the tower.*
- $\bar{b}$ *mean vertical spacing between phase conductor and ground wire.*
- $\bar{C}$ *mean spacing between phase conductor and ground wire.*
- $\bar{y}$ *mean height of phase conductor above earth.*
- $\bar{y}'$ *equivalent mean conductor height with ground angle non-zero.*
- $\bar{H}$ *mean height of ground wire above earth.*
- $\bar{r}_{sc}$ *mean striking distance defined by equation (5) for stroke from leader core to ground wire or tower.*
- $\bar{r}_{sg}$ *mean striking distance from leader core to ground (earth).*
- r_{sc} *mean striking distance from leader core to phase conductor.*
- K_{sg} *ratio $\bar{r}_{sg}/\bar{r}_{sc}$.*
- K_{sc} *ratio $\bar{r}_{sc}/\bar{r}_{sc}$*
- $\hat{r}_{sc}$ *effective striking distance defined by equation (7) for stroke from leader core to ground wire of tower. See Figure 8.*
- I_c *critical lightning current to phase conductor defined by equation (6).*
- I_{oc} *critical lightning current to zero-resistance earth $I_{oc} = 1.1\ I_c$.*
- *ICFO* *impulse critical flashover voltage (negative polarity).*
- Z *surge impedance of phase conductor.*

$\bar{\theta}_{sc}$ Angle de protection réduisant l'arc d'exposition moyen à zéro.

$\hat{\theta}_{sc}$ Angle de protection réduisant l'arc effectif d'exposition à zéro.

$\bar{\theta}_g$ Angle de sol transversal moyen.

$\bar{\theta}_1$, $\bar{\theta}_2$, $\bar{\theta}_3$ Angles définis dans les figures 5 et 6.

2β et $2\beta'$ Angles associés à $\bar{C}$ et aux distances d'amorçage.

$\bar{S}_c$ et $\hat{S}_c$ Arcs d'exposition définis par les équations (8) et (9).

K Facteur d'écart.

n_{10} Nombre de déclenchements dus à des défaillances de l'effet d'écran par 100 miles et par an pour une densité de coups de foudre de 10 par mile carré et par an. Voir figure 14 - 18.

n'_{10} Nombre de déclenchements dus à des défaillances de l'effet d'écran par 100 kilomètres et par an une densité de coup de foudre de *10 par mile carré* et par an ou de *3,86 par kilomètre carré et* par an. Voir Figures 14 - 18.

TD Nombre de journées d'orage par an.

$\bar{r}_{ss}$ Distance générale d'amorçage entre le cœur de l'éclair et le câble de protection S (de garde). $\bar{r}_{sc} = \bar{r}_{ss}$ pour le courant critique d'amorçage I_{sc}).

$\bar{\theta}_{sc}$ *shielding angle reducing mean exposure arc to zero.*

$\hat{\theta}_{sc}$ *shielding angle reducing effective exposure arc to zero.*

$\bar{\theta}_g$ *mean transverse ground angle.*

$\bar{\theta}_1$, $\bar{\theta}_2$, $\bar{\theta}_3$ *angles defined in Figures 5 and 6.*

2β and $2\beta'$ *angles associated with* $\bar{C}$ *and striking distances.*

$\bar{S}_c$ *and* $\hat{S}_c$ *exposure arcs defined by equations (8) and (9).*

K *deviation factor.*

n_{10} *shielding failure trip-outs per 100 miles per year for stroke density of 10 per square mile per year. See Figures 14-18.*

n'_{10} *shielding failure trip-outs per 100 kilometers per year for stroke density of* 10 per square mile *per year or* 3.86 per square kilometer per year. *See Figures 14-18.*

TD *thunderstorm days per year.*

$\bar{r}_{ss}$ *general striking distance from leader core to shield (ground) wire* S ($\bar{r}_{sc} = \bar{r}_{ss}$ *for the critical stroke current* I_{sc}).

1. — Introduction.

En 1930, le Sous-Comité de l'AIEE (IEEE) s'occupant des coups de foudre et des isolateurs, a publié un rapport du Groupe de Travail [1] intitulé « Méthode d'estimation du comportement à la foudre des lignes de transport ». Les premières lignes à ultra-haute tension (345 kV) conçues selon les principes présentés dans ce rapport firent apparaître des taux de déclenchements sur coup de foudre 10 à 15 fois plus élevés que ceux prévus. Il était clair que, ou bien une nouvelle dimension du problème de la foudre était apparue, ou bien une ancienne avait été mal estimée. Dans le but de définir le problème, il semblait évident que le contournement des isolateurs de ligne était déterminé par des conditions ou des mécanismes en relation avec le chemin final suivi par la foudre jusqu'à la terre. La figure 1 définit les trois chemins possibles. Pour chacun de ces chemins, il est possible d'associer des comportements correspondants de l'isolement soumis à la tension. Pour le chemin allant directement à la terre, il est possible d'associer un mécanisme de contournement par « tension induite ». En ce qui concerne le coup de foudre sur le conducteur de phase, il est commode de définir un mécanisme de « défaillance de l'effet d'écran ». De façon analogue, et conformément à l'usage, on utilise le terme mécanique d'« amorçage secondaire » pour un c
de foudre sur le pylône ou sur le câble de

Seuls les mécanismes d'« amorçage s
et de « défaillance de l'effet d'écran
significatifs pour les lignes à ha

1. — Introduction.

In 1930 the AIEE (IEEE) Lightning and Insulator Subcommittee published a Working Group Report [1] "A Method of Estimati g the Lightning Performance of Transmission Lines". Early EHV (345 kV) lines designed in accordance with the principles presented in this report experienced lighning trip-out rates 10 to 15 times those estimated. It was clear that either a new dimension had been added to the lightning problem or an old one had been inadequately evaluated. For the purpose of problem definition, it seemed evident that the spe kover of line insulation was determined by c ons or mechanisms connected with the fi t the lightning stroke to earth. Figure ree possible paths. With these pe e corresponding responses insulation. For the pat associate an "induce For the stroke t nient to defi Similarly, the terr to c

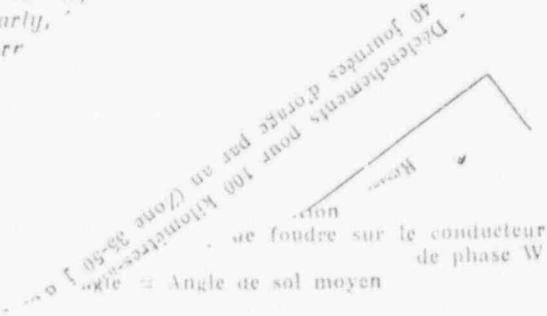

de foudre sur le conducteur de phase W

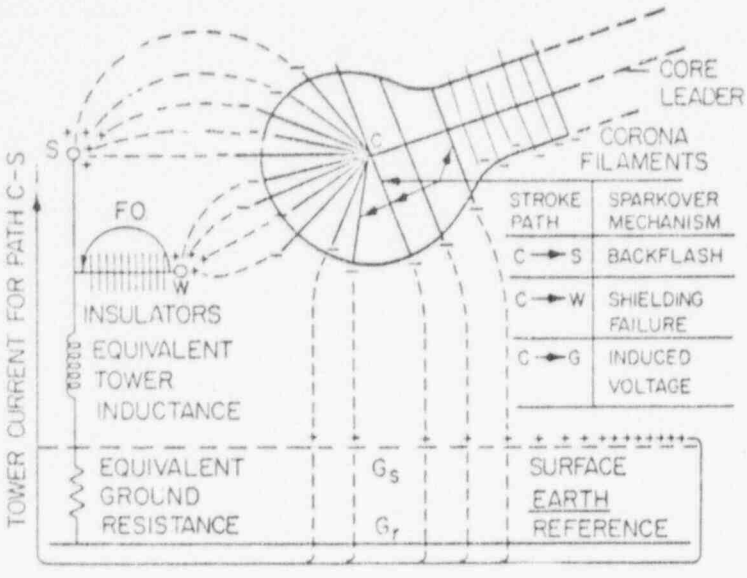

FIG. 1

Mécanisme de l'amorçage dû à la foudre

Mechanisms of lightning sparkover

Tower current for paths C-S = Courant dans le pylône pour le chemin C-S
F.O. = Contournement
Insulators = Isolateurs
Equivalent tower inductance = Conductance du pylône équivalent
Equivalent ground resistance = Résistance de sol équivalente
Core leader = Cœur de l'éclair
Corona filaments = Filaments d'effet couronne
Stroke path = Cheminement de l'amorçage
Sparkover mechanism = Mécanisme d'amorçage
Backflash = Amorçage secondaire
Shielding failure = Défaillance de l'effet d'écran
Induced voltage = Tension induite
Surface = Surface du sol
Earth reference = Terre de référence

ultra-haute tension à fort isolement. Si le contournement des isolateurs conduit à un courant de défaut à la fréquence du réseau, le phénomène est défini comme étant un contournement d'isolateur. (Etant donné qu'environ 85 % des contournements conduisent à des déclenchements, on utilisera le terme « contournement » lorsqu'aucune confusion n'est possible).

Un Groupe de Travail formé par l'Edison Electric Institute a proposé un projet de recherche pour déterminer le « mécanisme des amorçages par coup de foudre ». Après une recherche préliminaire, le Groupe de Travail s'est converti en un Comité Guide destiné à superviser un programme en 3 étapes dans lequel la mise en œuvre de chaque étape dépendait de l'accomplissement réussi de l'étape précédente. Ces étapes furent (1) la recherche de l'appareillage et la mise au point de l'étude réelle, (2) la construction et l'installation des appareils de commande, ainsi que la sollicitation et le choix des sociétés participantes, et (3) l'installation en grandeur réelle du « détecteur de cheminement » pour une période minimum de rassemblement de données et d'analyses de 5 ans. Le programme entier a duré en tout 8 ans et a été prolongé d'un an.

Ce rapport décrit le programme de recherche, résume les principaux résultats, tire des conclusions concernant le rôle relatif des mécanismes d'amorçage sur coup de foudre et présente des recommandations pour utiliser ces résultats pour la conception pratique des dispositifs de protection. La référence [2] donne les valeurs de détail sur le fonctionnement sur place du « dispositif de recherche de cheminement » ainsi que les données géométriques et électriques appliquables à la zone réellement affectée par chaque coup de foudre. Ces valeurs ont été mises à la disposition du Groupe de Travail 33.01 de la CIGRE (Foudre) sous une forme habituelle et globale grâce à l'amabilité de l'Edison Electric Institute.

insulation results in system-frequency fault current, the event is defined as an insulator flashover. (Since approximately 85 per cent of the sparkovers result in trip-outs, the term "flashover" will be used where no confusion results).

A Task Force established by the Edison Electric Institute recommended a research project to determine "The Mechanism of Lightning Flashover". Following a preliminary investigation, the Task Force was converted to a Steering Committee to supervise a three-stage program with the implementation of each stage dependent upon successful completion of the preceding one. These stages were (1) instrumentation research and design of the field study, (2) pilot instrument manufacture and installation, and sollicitation and selection of participating companies, and (3) full scale installation of the "Pathfinder" instrument for a minimum five-year data gathering and analysis period. The total duration of the full program with a one-year extension was eight years.

This paper describes the plan of research, summarizes the principal results, draws conclusions regarding the relative role of the lightning flashover mechanisms and presents guidelines for using the results in the practical design of shielding systems. Reference [2] contains all detailed data on field operations of the Pathfinder device together with the geometrical and electrical data applicable to the actual span affected by each stroke. These data have been made available to CIGRE Working Group 33.01 (Lightning) on a current and cumulative basis through the courtesy of the Edison Electric Institute.

Overhead Lines – Faster Planning, Design and Construction

A digital computer evaluates the data obtained by surveying in the field and calculates technical details of towers and foundations.

Results:

- ☐ Table with technical data regarding the profile and the crossings.
- ☐ Recording of the profile on microfilm.
- ☐ Optimizing the siting, types and heights of towers. The calculation of the tower allocation includes tower and line data, terrain conditions, as well as costs of towers, foundations and right-of-way.
- ☐ Calculation of conductor clearances to ground and crossings. All conductor conditions are exactly taken into account.
- ☐ Dimensions of tower members and foundations. The most economical design of each member in the tower is calculated. Foundation forces are also analyzed.

Our digital calculation programs enable overhead lines to be planned more quickly, more reliably, more economically.

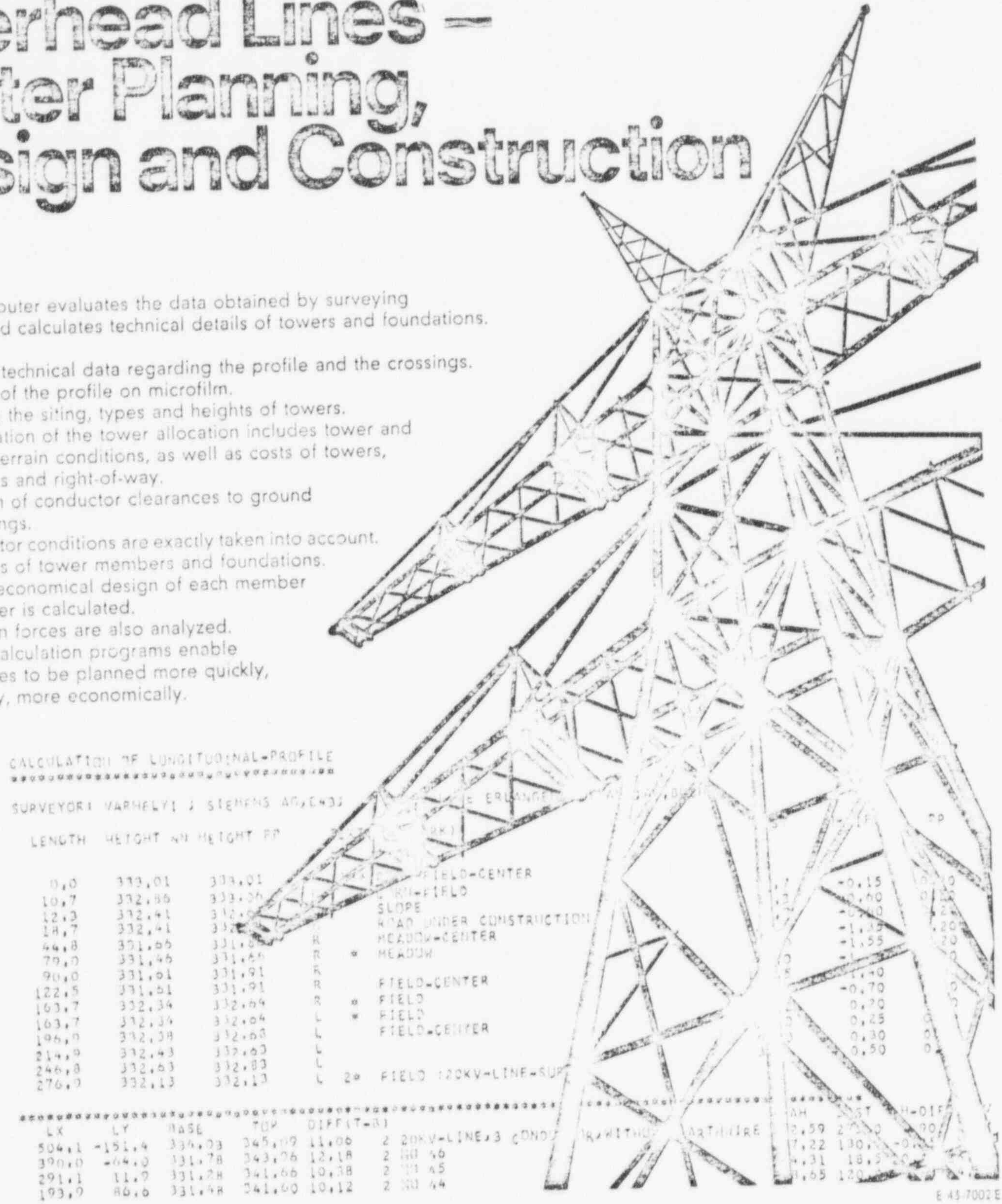

E 43-7002 E

Siemens Optimize Overhead Line Construction with the Computer

90004 531

2. — Plan de recherche.

Le plan de recherche pour la troisième étape du programme a été divisé en trois phases distinctes mais néanmoins reliées entre elles :

2.1. *Etudes expérimentales.*

Analyse d'un ensemble prévu d'au moins 100 fonctionnements du détecteur de cheminement pour faire une discrimination entre les coups de foudre sur le pylône ou le câble de garde, mécanisme d'« amorçage secondaire », et les coups de foudre sur un conducteur de phase, mécanisme de « défaillance de l'effet d'écran ». L'essai réel comportait la mise en place de 4 600 appareils « détecteurs de cheminement » sur 640 km de lignes de 110 kV à 345 kV appartenant à 12 compagnies membres de l'EEI situées de la Floride au Vermont, du Missouri au Michigan et du Texas au Colorado. *L'importance de cette phase est la connaissance détaillée des phénomènes individuels.*

2.2. *Etudes statistiques.*

Recherche statistique sur une grande échelle du comportement à la foudre des lignes existantes avec leur disposition de conducteurs, leur profil de ligne, leur conditions de terrain et de mise à la terre des pylônes. *L'importance de cette phase est représentée par les valeurs statistiques significatives rassemblées d'une façon qui se prête à l'analyse.*

2.3. *Modèle analytique.*

Mise au point du modèle analytique le plus simple présentant les caractéristiques principales de comportement à la foudre trouvées dans les phases 2.1 et 2.2, et servant par conséquent à faire une *extrapolation* du comportement connu des lignes existantes à celui des dispositifs proposés pour des lignes nouvelles. *L'importance de cette phase porte sur des recommandations concernant les projets de lignes, tandis qu'un intérêt secondaire repose dans une estimation améliorée des caractéristiques aux coups de foudre.*

Si on les considère séparément, les phases constitutives du plan de recherche conduisent à des questions cruciales irrésolues. Si on les prend dans leur ensemble, elles conduisent à des conclusions pratiques importantes et font ressortir certaines voies de recherche. Après que les « détecteurs de cheminement » aient été mis en place et que le premier fonctionnement ait montré la discrimination satisfaisante entre les mécanismes d'amorçage à la foudre, on a pratiquement réalisé ensemble les trois phases de la recherche.

2. — Plan of research.

The plan of research for Stage 3 of the program was divided into three distinct, though related, phases :

2.1. Experimental studies.

The analysis of an expected total of at least 100 Pathfinder operations to discriminate between strokes to the tower or ground wire, the "backflash" mechanism, or strokes to the phase conductor, the "shielding failure" mechanism. The field sample encompassed 4600 Pathfinder instruments on 640 km of line from 110 kV to 345 kV line voltage, owned by 12 EEI member companies located from Florida to Vermont, Missouri to Michigan and Texas to Colorado. The emphasis of this phase is on detailed knowledge of individual events.

2.2. *Statistical studies.*

A large-scale statistical investigation of the lightning performance of existing lines together with their conductor configurations, line profile, terrain and tower grounding conditions. The emphasis of this phase is on significant statistics appropriately grouped for analysis.

2.3. The analytical model.

The development of the simplest analytical model which exibits the principal features of lightning performance found in phases 2.1 and 2.2, and which thereby serves to extrapolate the known performance of existing lines to that of proposed designs for new lines. The emphasis of this phase is on design guidelines, though secondary benefits lie in improved estimates of lightning stroke characteristics.

Taken separately, the component phases of the plan of research would leave crucial questions unresolved. Taken together, they lead to important practical conclusions and sharpen the focus on remaining avenues of investigation. After the Pathfinder devices were in place and the initial operation indicated the satisfactory discrimination of the lightning flashover mechanisms, the three research phases were conducted essentially concurrently.

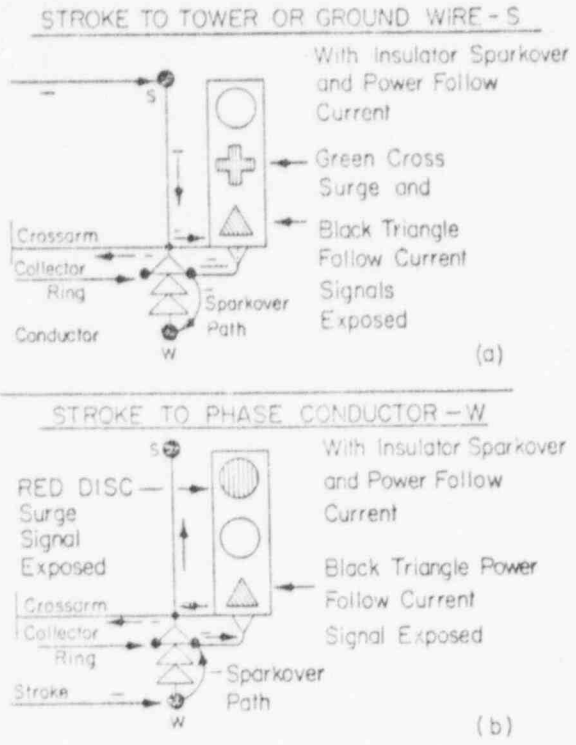

Fig. 2

Chemin suivi par le courant d'après le détecteur de cheminement pour le contournement d'un isolateur

Pathfinder current paths for insulator sparkover

Stroke to tower or ground wire S = Coup de foudre sur le pylône ou le câble de garde

a

With insulator sparkover and power follow current = Avec contournement d'isolateur et courant de suite
Green cross : surge = Croix verte : surtension
Black triangle : follow current = Triangle noir : courant de suite
Signals exposed = Signaux visibles
Crossarm = Bras du pylône
Collector ring = Anneau de garde
Conductor = Conducteur
Sparkover path = Contournement

b

Stroke to phase conductor — W = Coup de foudre sur le conducteur de phase — W

Red disc = Disque rouge
Surge = Surtension
Signal exposed = Signal visible
Crossarm = Bras du pylône
Collector ring = Anneau de garde
Stroke = Coup de foudre
Sparkover path = Contournement
With insulator sparkover and power follow current = Avec contournement d'isolateur et courant de suite
Black triangle : power follow current = Triangle noir : courant de suite
Signal exposed = Signal visible

3. — Résumé des résultats.

3.1. *Fonctionnement du détecteur de cheminement.*

La figure 2 montre les signaux du détecteur de cheminement correspondant à des coups de foudre sur le pylône ou sur le câble de garde et à des coups de foudre directs sur un conducteur de phase. La flèche indique l'écoulement des électrons au lieu du courant conventionnel. La figure 3 montre les circuits internes de l'appareil. le tableau 1 donne des interprétations probables pour 11 signaux pos-

3. — Summary of results.

3.1 Operation of the Pathfinder instrument.

Figure 2 shows the pathfinder signals which are exposed for strokes to the tower or ground wire and for strokes directly to the phase conductor. The current arrows indicate electron flow instead of conventional current. Figure 3 shows the internal circuits of the instrument. Table 1 gives the probable interpretations for eleven possible signal, line fault and stroke polarity combinations. Table 2

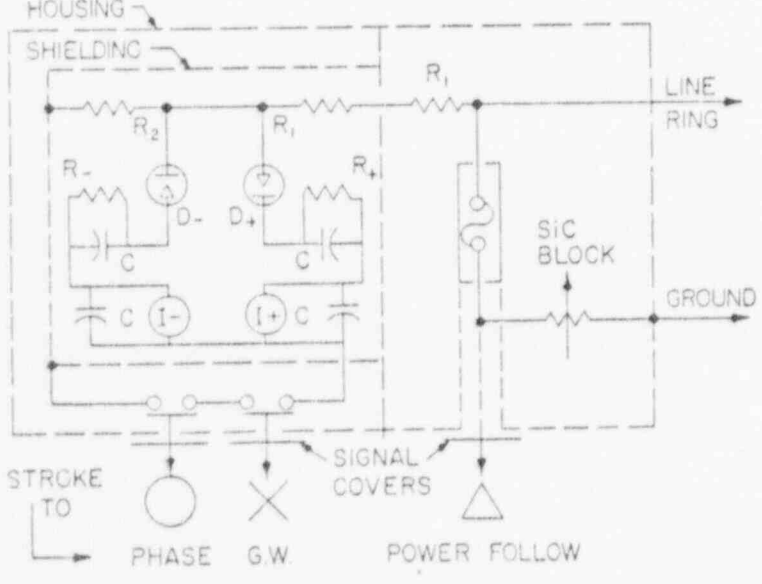

Fig. 3

Circuit du détecteur de cheminement

Pathfinder circuit

Housing = Enveloppe
Shielding = Ecran
Stroke to phase = Coup de foudre sur conducteur de phase
G.W. = Câble de garde
Signal covers = Signaux
Power follow = Courant de suite
SiC block = Barrière de SiC
Line ring = Anneau de garde côté ligne
Ground = Terre

TABLEAU 1 — TABLE 1

Codification des signaux de détecteur de cheminement et interprétations probables (2)

Pathfinder signal code with probable interpretations (2)

Signal *Signal* Circuit *circuit*	Rond rouge *Red Disc* 1 2	Croix verte *Green Cross* 1 2	Triangle noir *Black Triangle* 1 2	Interprétations probables *Probable Interpretations*		
				Coup de foudre sur *Stroke to*	Polarité *Polarity*	Type de défaut *Type of Fault*
	x			le conducteur *conductor*	–	aucun *none*
	x		x	le conducteur *conductor*	–	phase-terre *line-to-ground*
		x		le câble de garde *ground wire*	–	aucun *none*
		x	x	le câble de garde *ground wire*	–	phase-terre *line-to-ground*
		x	x	le câble de garde *ground wire*	–	Note 1
		x	x x	le câble de garde *ground wire*	–	circuit double *double circuit*
			x	le câble de garde *ground wire*	–	Note 2
	x	x		le conducteur *conductor*	–	Note 3
	x	x	x x	le conducteur *conductor*	–	Note 4
	x x			le câble de garde *ground wire*	+	Note 1
	x x		x x	le câble de garde *ground wire*	+	circuit double *double circuit* Note 5

Notes :

1. Contournement à double circuit sans puissance de suite. *Double circuit sparkover without power follow.*
2. Coup de foudre sur le câble de garde. Courbe temps-intensité en dessous du niveau d'activation. *Stroke to ground wire. Current-time curve below activation level.*
3. Coup de foudre sur le circuit (1), amorçage secondaire sur le circuit (2) sans puissance de suite. *Stroke to circuit (1), backflash on circuit (2) without power follow.*
4. Coup de foudre sur le circuit (1) amorçage secondaire sur le circuit (2) avec puissance de suite. *Stroke to circuit (1) backflash on circuit (2) with power follow.*
5. Les défauts polyphasés intéressent souvent les conducteurs sur lesquels ne sont pas raccordés les appareils. *Multiple-conductor faults frequently involve conductors wich do not have instruments connected.*

sibles, pour des combinaisons de défaut en ligne et de la polarité des coups de foudre. Le tableau 2 résume les valeurs et les interprétations correspondant à 167 fonctionnements de l'appareil obtenus d'après 111 coups de foudre distincts. Etant donné que les échantillons de lignes furent spécialement choisis d'après certaines catégories d'angles de protection, de profils de ligne et de conditions de mise à la terre, *on ne peut pas* considérer les lignes 5 et 12 de ce résumé comme la mise en évidence d'un partage général des amorçages à la foudre d'une façon égale entre « défaillance de l'effet d'écran » et « amorçage secondaire ». La figure 4 montre un détecteur de cheminement installé sur un pylône d'une ligne 345 kV en double delta. Le détail du signal, les données géométriques et toutes les données correspondant au défaut se trouvent, pour tous les fonctionnements, dans la référence [2].

summarizes the data and interpretations for 167 instrument operations obtained from 111 separate lightning strokes. Since the line samples were especially selected for certain classes of shielding angle, line profile and grounding conditions, data lines 5 and 12 of this summary cannot be taken as indicating a general division of lightning flashovers into "shielding failure" and "backflash" events on an equal basis. Figure 4 shows a pathfinder instrument mounted on a tower of a 345 kV line of double-delta configuration. Detailed signal, geometrical and fault data will be found for all operations in reference [2].

TABLEAU 2 — TABLE 2

Résumé des fonctionnements du détecteur de cheminement au 1er janvier 1972

Summary of pathfinder operations as of January 1, 1972

Numéro de la ligne *Line Number*	Désignation des valeurs *Data description*		Valeurs Numériques *Numerical Data*
1	Fonctionnements du détecteur de cheminement – *Pathfinder instrument operations*		167
2	Nombre de coups de foudre distincts – *Number of separate lightning strokes*		111
3	Nombre de coups de foudre ayant provoqué un déclenchement – *Number of strokes causing trip-out*		94
4	Pourcentage de coups de foudre ayant provoqué un déclenchement – *Per cent strokes causing trip-out*		85
5	Nombre de coups de foudre ayant provoqué des défaillances d'effet d'écran – *Number of strokes causing shielding failures*		51
6	Type de défaut à la suite d'une défaillance* de l'effet d'écran – *Type of fault from shielding failure**	Nombre *Number*	
7	Déclenchements monophasés sur le conducteur supérieur – *Top single-conductor trip-outs*	39	
8	Déclenchements monophasés sur le conducteur médian – *Middle single-conductor trip-outs*	2	
9	Déclenchements polyphasés – *Multi-conductor trip-outs*	3	
10	Déclenchements à double circuit – *Double-circuit trip-outs*	1	
11	Pas de déclenchement – *No trip-out*	6	
12	Nombre de coups de foudre ayant provoqué des phénomènes d'amorçage secondaire – *Number of strokes causing backflash events*		52
13	Type de défaut à la suite d'amorçages secondaires* – *Type of fault from backflash events**	Nombre *Number*	
14	Déclenchements monophasés sur le conducteur supérieur – *Top single-conductor trip-outs*	21	
15	Déclenchements polyphasés – *Multiple-conductor trip-outs*	5	
16	Déclenchements à double circuit** – *Double-circuit trip-outs***	20	
17	Pas de déclenchement – *No trip-out*	6	
18	Nombre affiché de coups de foudre de polarité négative – *Indicated number of negative polarity strokes*		103
19	Pourcentage affiché de coups de foudre négatifs – *Indicated per cent negative strokes*		93
20	Mauvais fonctionnements de l'appareil ou inversion du courant – *Instrument malfunction or current reversal*		8

Remarques :

* Configuration en double circuit vertical ou en double triangle.

** Les déclenchements à double circuit peuvent aussi être polyphasés sur l'un des circuits ou sur les deux.

Notes :

* *Double-circuit vertical or double triangle conductor configuration.*

** *Double-circuit trip-outs may also be multiconductor on one or both circuits.*

3.2. *Résumés des résultats statistiques portant sur les comportements à la foudre.*

Les tableaux 3 et 4 donnent des valeurs de comportement à la foudre et des paramètres de ligne pour plus de 120 000 km/an de comportement dans des zones fortement foudroyées. Une hypothèse de base de la présente recherche est qu'il faut que ces lignes soient effectivement protégées. Une conclusion secondaire, en accord avec de nombreuses autres études, est que des lignes construites avec une rigidité d'isolement normale au choc critique, et avec des résistances nominales de mise à la terre de 25 Ω ou inférieures peuvent avoir un bon comportement moyen à la foudre.

Des études statistiques supplémentaires ont été effectuées grâce aux efforts communs du projet de recherche RP 50 [2] de l'Institut d'Electricité Edison et de l'étude générale des performances à la

3.2. Summaries of statistical data on lightning performance.

Tables 3 and 4 give lightning performance data and line parameters for over 120,000 km -years of superior lightning performance. A basic assumption of the present research is that these lines must be effectively shielded. A secondary conclusion, in agreement with many other studies, is that lines designed with normal critical impulse insulation strength and with nominal ground resistances of 25 ohms or less can give good average lightning performance.

Additional statistical studies have been conducted through co-operative efforts of the Edison Electric Institute Research Project RP 50 [2] and the Survey of the Lightning Performance of EHV Lines by

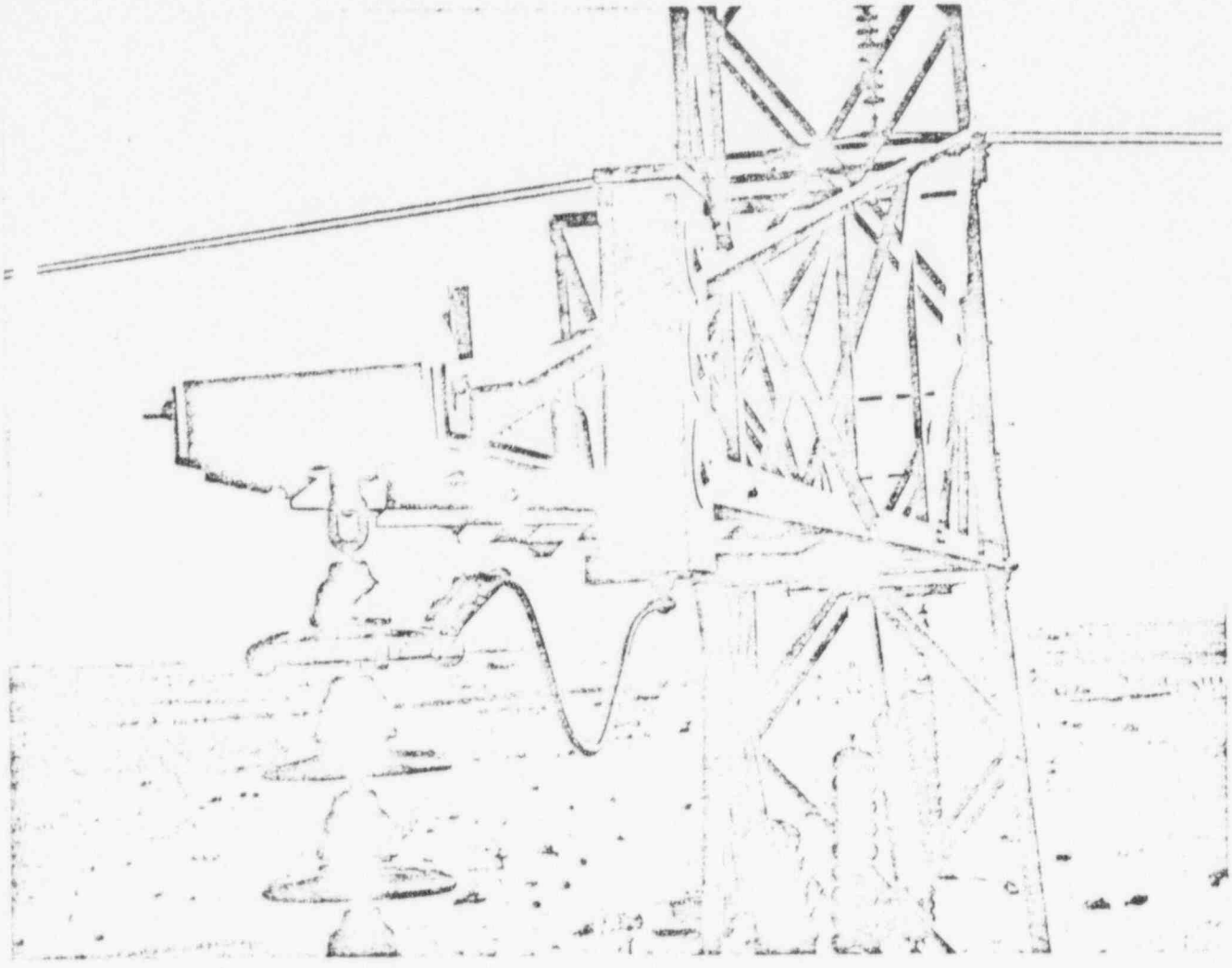

FIG. 4
Appareil détecteur de cheminement installé sur un pylône 345 kV
Pathfinder instrument mounted on 345 kV tower

TABLEAU 3 — TABLE 3

Comportement aux coups de foudre de 50 lignes de transport de 115 kV à 230 kV pour 84 000 kilomètres-années (3,4)

Lightning performance of 50 transmission lines 115 kV to 230 kV for 84 000 kilometer-years (3,4)

Caractéristiques *Characteristics*	Minimum une ligne *Minimum one line*	Moyenne ensemble des lignes *Average all lines*	Maximum une ligne *Maximum one line*
Déclenchements spécifiques* – *Specific trip-outs**	0.00	0.11	0.31
Kilomètres-années – *Kilometer-years*	338	1675	10460
Niveau critique au choc (kV) – *Critical impulse level (kV)*	950	1300	1625
Hauteur moyenne du câble de garde $\overline{H}$ (m) – *Mean ground wire height* $\overline{H}$ (m)	13	21	34
Angle de protection moyen $\overline{\theta}_s$ (deg) – *Mean shielding angle* $\overline{\theta}_s$ (deg)	−6	18	39
Résistance de terre moyenne (ohms) – *Mean ground resistance (ohms)*	2	23	94

* Déclenchements pour 100 kilomètres-années basés sur 40 journées d'orage par an (Zone 35-50 j d'orage/an).

* *Trip-outs per 100 kilometers-years adjusted to 40 T.D. (thunderstorm days) per year. (Range 35-50 T.D./year).*

TABLEAU 4 — TABLE 4

Comportement aux coups de foudre pour des lignes 500 kV en URSS pour 37 780 kilomètres-années (5)

Lightning performance for 500 kV lines in URSS for 37 780 kilometer-years (5)

Caractéristiques *Characteristics*	Moyenne pour toutes les lignes *Average for all lines*
Déclenchements spécifiques basés sur 40 j. d'orage* – *Specific trip-outs adjusted to 40 T.D.**	0.23
Niveau critique au choc (kV) – *Critical impulse level (kV)*	1800
Hauteur moyenne du câble de garde $\bar{H}$ (m) – *Mean ground wire height $\bar{H}$ (meters)*	inférieur à/*under* 30
Angle de protection moyen $\bar{\theta}_s$ (deg) – *Mean shielding angle $\bar{\theta}_s$ (degrees)*	20
Angle de protection maximum (deg) – *Maximum shielding angle (degrees)*	30
Résistance de terre moyenne (ohms) – *Mean ground resistance (ohms)*	inférieur à/*under* 5

* Basé sur la relation :
Déclenchements spécifiques = K (jours d'orage)$^{1.5}$.

* *Adjusted by the relation :*
Specific trip-outs = K (T.D.)$^{1.5}$.

foudre des lignes à ultra-haute tension faite par le Groupe de Travail 33-01 du Comité d'Etude n° 33 de la CIGRE [8]. On se servira dans un chapitre ultérieur de données choisies tirées de ces études.

CIGRE Working Group 33-01 of Study Committee No. 33 [8]. Selected data drawn from these studies will be used in a later section.

3.3. *Modèle analytique de référence.*

Le *modèle analytique de référence* est un ensemble électro-géométrique présentant les principales caractéristiques que l'on trouve aux paragraphes 3.1 et 3.2. Dans sa forme de base, il donne la géométrie physique moyenne du pylône et des conducteurs et les distances d'amorçage moyennes estimées dérivées de l'électro-géométrie du coup de foudre par des considérations d'équilibre d'énergie [6] [7]. La figure 5 montre le modèle déterminé pour l'hypothèse de distances d'amorçage égales depuis l'extrémité du cœur de l'arc de foudre jusqu'au câble de garde S, au conducteur de phase W et à la terre ou au sol. Bien que dans la forme de base soit incluse

3.3. *The reference analytical model.*

The reference analytical model *is an electrogeometrical concept which exhibits the principal performance features found in sections 3.1 and 3.2. In its basic form it provides for the mean physical geometry of the tower and conductors and for mean estimated striking distances derived from the electrogeometry of the lightning stroke from energy balance considerations [6, 7]. Figure 5 shows the model drawn for the assumption of equal striking distance from the tip of the stroke leader core to the shield wire S, the phase conductor W and the earth or ground. Although the basic form includes the assumption of a flat ground plane, Figure 5 also*

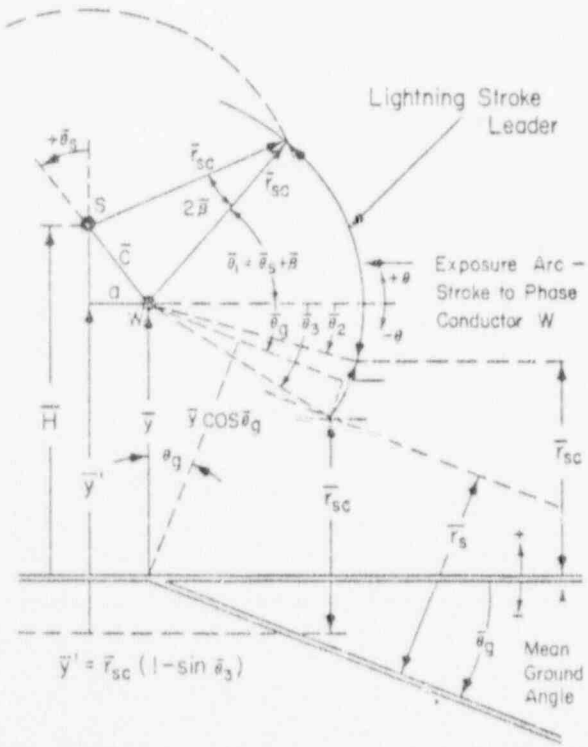

FIG. 5

Modèle de référence représentant une protection inefficace

Reference model illustrating ineffective shielding

Lightning stroke leader = Eclair
Exposure arc = Arc d'exposition
Stroke to phase conductor W = Coup de foudre sur le conducteur de phase W
Mean ground angle = Angle de sol moyen

l'hypothèse d'un sol plat, la figure 5 englobe également l'influence d'un écart du plan de sol par rapport à l'horizontale selon un angle négatif $\bar{\theta}_g$. La configuration indiquée sur cette figure illustre un *effet d'écran inefficace* avec un angle d'exposition de référence allant de $\bar{\theta}_2$ (ou $\bar{\theta}_3$) à $\bar{\theta}_1$.

Si l'on diminue la valeur $\bar{\theta}_s$ de l'angle de protection jusqu'à une valeur qui élimine l'angle d'exposition, on définit l'angle de protection $\bar{\theta}_{sc}$, angle de protection critique moyen, ou de référence. Dans cette condition, $\bar{\theta}_1$ devient égal à $\bar{\theta}_2$ pour un sol de niveau ou $\bar{\theta}_3$ pour l'angle de sol négatif indiqué. La géométrie de la figure 6 se trouve résumée par les équations (1) — (4).

includes the effect of a deviation of the ground plane from the horizontal by a negative angle $\bar{\theta}_g$. The configuration shown in this figure illustrates ineffective shielding *with a reference exposure arc from $\bar{\theta}_2$ (or $\bar{\theta}_3$) to $\bar{\theta}_1$.*

If the shielding angle $\bar{\theta}_s$ is reduced to a value which eliminates the exposure arc, the shielding angle is defined as $\bar{\theta}_{sc}$, the mean critical, or reference, shielding angle. Under this condition, $\bar{\theta}_1$ becomes equal to $\bar{\theta}_2$ for level ground or $\bar{\theta}_3$ for the negative ground angle indicated. The geometry of Figure 6 is summarized by the equations (1) - (4).

$$\bar{\theta}_{sc} = \bar{\theta}_g - \beta - \arcsin\left[(\bar{y}/\bar{r}_{sc})\cos\bar{\theta}_g - 1\right] \quad (1)$$

$$\beta = \arcsin\left(\bar{C}/2\,\bar{r}_{sc}\right) \quad (2)$$

Il est commode de définir deux relations auxiliaires supplémentaires

It will be convenient to define two additional auxiliary relations

$$\bar{\theta}_3 = \bar{\theta}_g - \arcsin\left[(\bar{y}/\bar{r}_{sc})\cos\bar{\theta}_g - 1\right] \quad (3)$$

$$\bar{y}'/\bar{r}_{sc} = 1 - \sin\bar{\theta}_3 \quad (4)$$

où $\bar{y}'$ est la hauteur équivalente du conducteur au-dessus du niveau du sol permettant d'obtenir le même angle d'écran qu'avec un angle de sol de $\bar{\theta}_g$. L'équation (4) est utile lorsqu'on la rapproche des courbes estimatives de la figure 7.

where $\bar{y}'$ is the equivalent conductor height above level ground to require the same shielding angle as a ground angle of $\bar{\theta}_g$. Equation (4) is useful in connection with the estimating curves of Figure 7.

La figure 7 donne des courbes estimatives de l'angle d'écran de référence $\bar{\theta}_{sc}$ en fonction de la hauteur relative du conducteur (normalisée) $\bar{y}$ et de l'espacement $\bar{C}$ en prenant comme valeur de base ou de référence la distance d'amorçage $\bar{r}_{sc}$. Ces courbes sont calculées d'après les équations (1) et (2) en prenant le facteur K égal à l'unité. Ce facteur permet de tenir compte dans le choix final d'un angle d'écran de différentes variations par rapport au modèle de référence de la figure 6.

Figure 7 provides estimating curves for the reference shielding angle $\bar{\theta}_{sc}$ in terms of the per unit (normalized) conductor height $\bar{y}$ and spacing $\bar{C}$ with the striking distance $\bar{r}_{sc}$ as base or reference value. These curves are calculated from equations (1) and (2) with the factor K set equal to unity. This factor permits various deviations from the reference model of Figure 6 to be taken into account in the final selection of a shielding angle.

L'électro-géométrie du modèle analytique est expliquée en détail à la référence [6] dans laquelle on souligne qu'il n'est possible de déterminer des estimations valables des distances d'amorçage que par comparaison d'un modèle analytique convenable avec des valeurs provenant d'essais réels. On dispose maintenant de suffisamment de données pour essayer utilement d'améliorer les concepts retenus initialement en ce qui concerne la distance d'amorçage. Du point de vue expérimental, les valeurs détaillées concernant les hauteurs du conducteur médian du câble de garde dans les cas où l'on avait enregistré des défaillances de l'effet d'écran, ainsi que la tension critique d'amorçage et l'impédance caractéristique permettent le calcul des angles d'exposition de référence pour tous les cas de défaillance de l'effet d'écran. Il est bien entendu nécessaire dans ce but de fixer une distance d'amorçage à la terre pour le courant critique de foudre dans chacun des cas. Cependant, avant de faire cela, il est souhaitable de rappeler que les distances d'amorçage sont répétées statistiquement autour de leur valeur moyenne comme cela est indiqué sur la figure 8. Etant donné que des distances d'amorçage plus faibles nécessitent un angle d'écran plus petit

The electrogeometry of the analytical model is developed in detail in reference [6] wherein it is pointed out that valid estimates of striking distances can be determined only from comparison of a suitable analytical model with data from field experience. Sufficient data are now available to make a useful attempt to improve the concepts initially adopted in respect to striking distance. From the experimental point of view, the detailed data on mean conductor and ground wire heights for the spans in which shielding failures were recorded, together with the critical flashover voltage and surge impedance, permit the calculation of reference exposure arcs for all shielding failure events. For this purpose it is, of course, necessary to assign a striking distance to the critical lightning current to earth for each event. Before doing so, however, it is desirable to recall that the striking distances are statistically distributed about their mean value as conceptually indicated in Figure 8. Since shorter striking distances require a smaller shielding angle for elimination of the reference exposure arc, one should expect occasional shielding failures to occur if the exposure arc and shielding angle are determined on the basis of the mean striking distance.

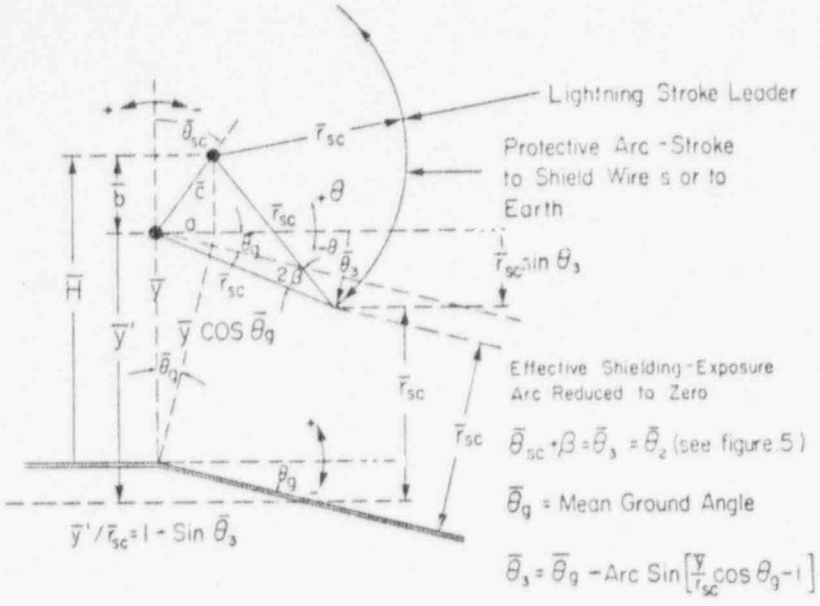

Fig. 6

Modèle de référence représentant une protection efficace

Reference model illustrating effective shielding

Lightning stroke leader = Eclair
Protective arc-stroke to shield wire s or to earth = Arc de protection – Coup de foudre sur le câble de garde s ou la terre
Effective shielding-exposure arc reduced to zero = Protection efficace – Arc d'exposition réduit à zéro
Mean ground angle = Angle de sol moyen

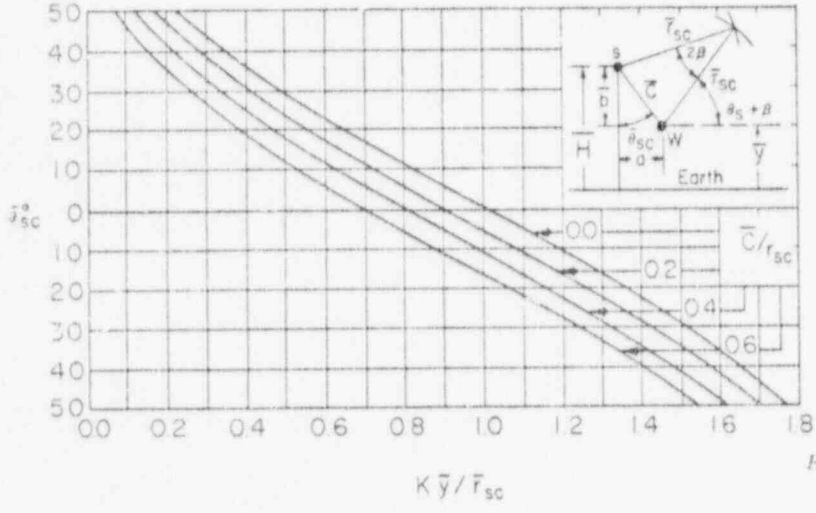

Fig. 7

Courbes d'estimation correspondant à un angle de protection de référence θ_s

Estimating curves for reference shielding angle θ_s

Earth = Sol

pour éliminer l'angle d'exposition de référence, il faut s'attendre à ce que des défaillances occasionnelles de l'effet d'écran se produisent si l'angle d'exposition et l'angle d'écran sont déterminés en se basant sur la distance d'amorçage *moyenne*. La figure 9 montre la répartition des angles d'exposition pour 51 cas d'enregistrement de défaillance de l'effet d'écran, déterminés à l'aide de la distance d'amorçage *moyenne*. Cela montre qu'environ 6 % de ces phénomènes se sont produits pour des arcs d'exposition égaux ou inférieurs à — 1 m. Bien que l'écart-type des distances d'amorçage comme l'in-

Figure 9 shows the distribution of exposure arcs for 51 recorded shielding failure events determined by the mean striking distance. It is shown that about 6 % of these events occurred for exposure arcs equal to or less than one negative meter. Although the standard deviation for striking distances as indicated in Figure 8 is unknown, it is possible to assign the reasonable value of 10 % and recalculate the exposure arcs on this basis. The effect of such a recalculation is shown in Figure 10 where all the exposure arcs are positive, with the minimum value nearly two meters.

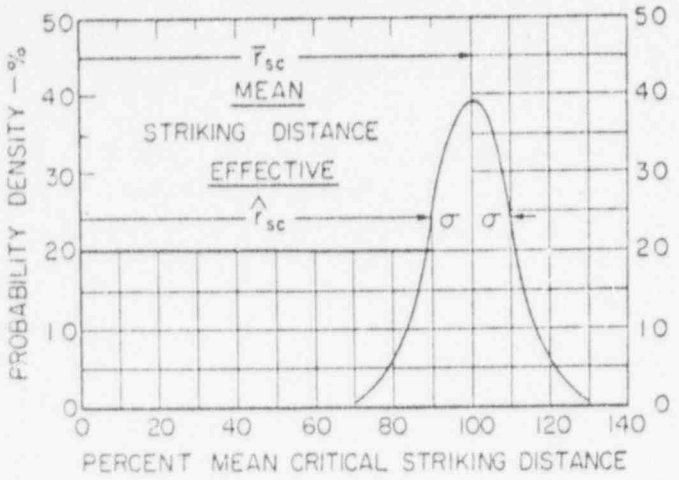

FIG. 8

Illustration des concepts de distances moyenne et effective d'amorçage

Illustrating the concepts of mean and effective striking distances

Percent mean critical striking distance = Distance d'amorçage critique moyenne en %
Probability density = Densité statistique
Mean = Moyenne
Effective striking distance = Distance d'amorçage effective

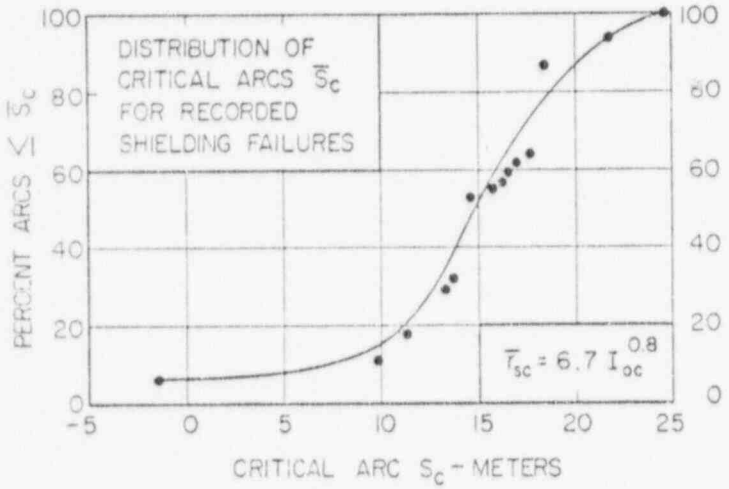

FIG. 9

Répartition des arcs d'exposition de référence en se servant des distances moyennes d'amorçage

Distribution of reference exposure arcs using mean striking distances

Critical arc $\bar{S}_c$-meters = Arc critique $\bar{S}_c$-mètres
Percent arcs = Pourcentage d'arcs
Distribution of critical arcs $\bar{S}_c$ for recorded shield failures = Répartition des arcs critiques $\bar{S}_c$ pour des défaillances enregistrées de l'effet d'écran.

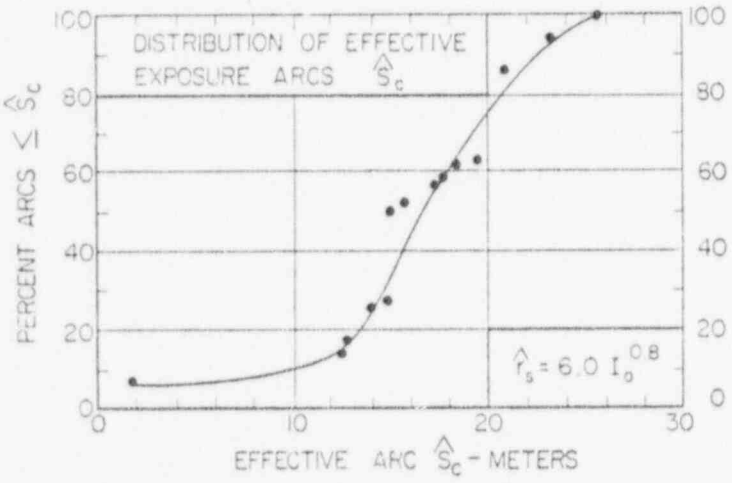

FIG. 10

Répartition des arcs d'exposition en se servant des distances effectives d'amorçage

Distribution of exposures arcs using effective striking distances

Effective arc $\hat{S}_c$ meters = Arc effectif $\hat{S}_c$-mètres
Percent arcs = Pourcentages d'arcs
Distribution of effective exposure arcs = Répartition des arcs effectifs d'exposition

dique la figure 8 soit inconnu, il est possible de fixer la valeur raisonnable de 10 % et de recalculer les arcs d'exposition sur cette base. L'influence d'un tel calcul est indiquée à la figure 10. Ici, tous les arcs d'exposition sont positifs, avec une valeur minimale d'environ 2 mètres.

Il est possible de faire une approximation de ce problème d'étalonnage d'après un procédé indépen-

It is possible to approach this calibration problem from an independent direction, if a sufficient

TABLEAU 5 — TABLE 5

Référence CIGRE [8]	Niveau critique du contournement au choc kV	Kilomètres-ans	Nombre moyen de journées d'orage par an	Résistance moyenne en ohms	Données concernant le profil			Mètres		Déclenchements spécifiques réels par 40 j d'orage	
CIGRE [8] Number	*ICFO kV*	*Kilometer years*	*Mean TD/Year*	*Mean Ohms*	*Profile Data*			*Meters*		*Specific Trip-out*	
					% F	*% R*	*% M*	$\bar{S}_e$	$\hat{S}_e$	*Actual*	*At 40TD*
30	1500	5 960	40	5	50	50	–	– 3.0	–1.75	0.24	0.24
31	1600	1 570	43	5	50	50	–	11.0	13.4	3.70	3.30
32	1600	1 760	40	5	75	16	9	22.0	24.4	5.70	5.70
33	2130	790	40	25–	35	40	25	– 4.3	– 0.8	0.25	0.25
35	2130	590	40	25–	86	14	–	–17.5	–13.4	0.00	0.00
36	2130	660	40	25–	30	40	30	– 0.8	3.3	0.76	0.76
39	1600	3 140	40	5	100	–	–	–23.0	–18.3	0.19	0.19
40	1580	4 460	32	12	–	100	–	– 6.0	– 2.4	0.07	0.10
66	1570	1 280	30	20	10	90	–	0.9	3.8	0.16	0.25
67	1570	1 320	30	20	10	90	–	0.9	3.8	0.30	0.46
69	1570	590	30	20	30	70		– 1.0	1.9	0.17	0.26
84	1619	3 000	31.5	10	60	30	10	0.0	2.5	0.40	0.57
	Total	25 060									

dant. Si l'on peut trouver un nombre suffisant de lignes de transport avec des expositions très comparables et une résistance de terre suffisamment faible pour minimiser les cas de déclenchements par « amorçages secondaires », on peut relever leurs arcs d'exposition en fonction de l'enregistrement de leurs déclenchements par coups de foudre. Le tableau 5 présente la liste de 12 lignes pour lesquelles ces conditions strictes semblent être convenablement remplies. On espère bien entendu que des données supplémentaires de qualité comparable pourront être obtenues d'après le travail cité à la référence [8].

number of transmission lines can be found with closely comparable exposure and sufficiently low ground resistance to minimize "backflash" trip-outs, their exposure arcs may be plotted against their lightning trip-out record. Table 5 lists 12 lines for which these strict requirements appear to be adequately met. It is, of course, hoped that additional data of comparable quality can be developed from the work of reference [8].

Les références [2] et [6] définissent la distance d'amorçage critique de référence $\bar{r}_{ac}$ par rapport au pylône ou au câble de garde de la façon suivante :

References [2] and [6] define the reference critical striking distance $\bar{r}_{ac}$ to the tower or ground wire as :

$$\bar{r}_{ac} = \bar{K}_{ac} I_{oc}^{0.8} = 6.7\, I_{oc}^{0.8} \quad \text{mètres pour } I_{oc} \text{ en kA.} \quad \textit{metres for } I_{oc} \textit{ in kA.} \tag{5}$$

où *where* $I_{oc} = 1.1\, I_c$ kiloampères *kiloamperes*

et *and* $I_c = 2\,E/Z = 2\,(\text{ICFO})$ (6)

Impédance caractéristique du conducteur *Surge impedance of conductor*

ICFO = tension critique d'amorçage au choc en polarité négative *impulse critical flashover voltage, negative polarity*

Les références [8] et [9] définissent aussi une distance d'amorçage « effective » par rapport au pylône ou au câble de garde de la façon suivante

References [8] and [9] also define an "effective" striking distance r_{ac} to the tower or ground wire as

$$\bar{r}_{ac} = \bar{K}_{ac} I_{oc}^{0.8} = 6.0\, I_{oc}^{0.8} \quad \text{mètres } \textit{metres} \tag{7}$$

en supposant que l'écart-type σ de la figure 8 est environ 10 % de la distance d'amorçage critique. Dans les équations (5) et (7) le courant I_{oc} repré-

assuming that the standard deviation σ of Figure 8 is approximately 10 % of the critical striking distance. In equations (5) and (7) the current I_{oc}

sente le courant de foudre prévu s'écoulant dans une terre de résistivité nulle correspondant au courant critique I_c dans le conducteur. Toute mobilité de la tension ICFO est supposée incluse dans σ.

Il est maintenant possible de donner une définition des « arcs d'exposition de référence critiques moyens » et des « arcs d'exposition de référence critiques effectifs » de la façon suivante

$$\bar{S}_c = \bar{r}_{sc}\,(\bar{\theta}_s - \bar{\theta}_{sc}) \quad \frac{\text{mètres}}{\text{metres}} \tag{8}$$

et/and

$$\hat{S}_c = \hat{r}_{sc}\,(\hat{\theta}_s - \hat{\theta}_{sc}) \quad \frac{\text{mètres}}{\text{metres}} \tag{9}$$

Dans les équations (8) et (9) $\bar{\theta}_s$ est l'angle d'écran moyen réel de la ligne. $\bar{\theta}_{sc}$ est l'angle d'écran critique moyen trouvé d'après la figure 7 en prenant K égal à l'unité et en utilisant la distance d'amorçage moyenne $\bar{r}_{sc}$ pour déterminer les rapports d'entrée $\bar{y}/\bar{r}_{sc}$ et $\bar{C}/\bar{r}_{sc}$. D'une façon analogue, on trouve $\hat{\theta}_{sc}$ d'après la même figure en se servant de $\hat{r}_{sc}$ pour déterminer les rapports dentrée correspondants.

La figure 11 montre les taux de déclenchements par coup de foudre en prenant comme référence 40 jours d'orage par an, pour les lignes du tableau 5. Il faut remarquer que la plupart des lignes ont des expositions strictement comparables tandis que pour les autres, seule une correction minime est nécessaire. Cette figure porte également à penser qu'il faudrait se servir de la relation concernant la distance d'amorçage moyenne avec $\bar{K}_{si} = 6{,}7$ pour des études dont le but est de prévoir le taux de défaillance d'effet d'écran d'une ligne, mais qu'une relation correspondant à la distance d'amorçage effective avec $\hat{K}_{si} = 6{,}0$ est plus utile dans la conception de lignes « effectivement protégées ». Tandis que des données complémentaires satisfaisant aux normes de comparaison du tableau 5 seront recherchées à la CIGRE dans le cadre des performances des lignes à ultra-haute tension, il ne semble pas vraisemblable que l'on atteigne par des techniques statistiques une précision beaucoup plus grande dans les relations concernant la distance d'amorçage. Il faudrait souligner que les équations en grande partie empiriques (5) et (7) ont été déterminées d'après

represents the prospective stroke current to earth of zero resistivity corresponding to the critical current to the conductor I_c. Any variability in the ICFO voltage is assumed to be included in σ.

It is now possible to define "mean critical reference exposure arcs" and "effective critical reference exposure arcs" as

In equations (8) and (9) $\bar{\theta}_s$ is the actual mean shielding angle of the line. $\bar{\theta}_{sc}$ is the mean critical shielding angle found from Figure 7 with K set equal to unity and the mean striking distance $\bar{r}_{sc}$ used to determine the entry ratios $\bar{y}/\bar{r}_{sc}$ and $\bar{C}/\bar{r}_{sc}$. Similarly, $\hat{\theta}_{sc}$ is found from the same figure using $\hat{r}_{sc}$ to determine the corresponding entry ratios.

Figure 11 shows the lightning trip-out rates, referred to 40 thunderstorm days per year, for the lines of Table 5. It should be noted that most of the lines have strictly comparable exposure while only minimal correction is required for the remainder. This figure also suggests that the mean striking distance relation with $\bar{K}_{si} = 6.7$ should be used for studies whose objective is the prediction of the shielding failure rate of a line, but that the effective striking distance relation with $\hat{K}_{si} = 6.0$ is more useful for the design of "effectively-shielded" proposed lines. While additional data meeting the comparability standards of Table 5 will be sought in the CIGRE EHV line performance survey, it seems unlikely that much greater precision in the striking distance relations will be attained by statistical techniques. It should be stressed that the essentially empirical equations (5) and (7) have been developed from experiments on and statistics of lines having ICFO levels from about 700 kV to 2130 kV and are probably adequate up to perhaps 3000 kV. Additional careful investigation of the theoretical base for these equations should be undertaken before applying

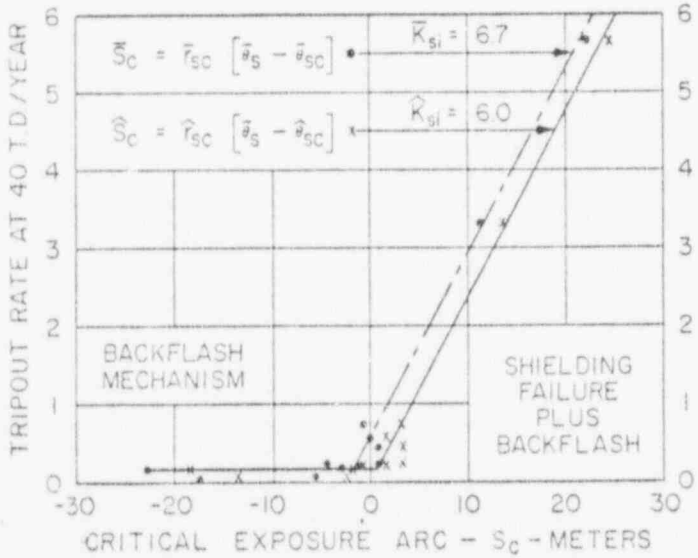

90004542

FIG. 11

Déclenchements spécifiques et arcs critiques d'exposition pour les lignes du tableau 5

Secific trip-outs and critical exposure arcs for the lines of Table 5

Critical exposure arc $-S_c-$ meters	= Arc d'exposition critique S_c-mètres
Trip-out rate at 40 T.D./ Years	= Taux de déclenchement pour 40 jours d'orage par an
Blackflash mechanism	= Mécanisme d'amorçage secondaire
Shielding failure plus blacktlash	= Défaillance de l'effet d'écran plus amorçage secondaire

A la Foire de la technique, Trafo Union s'oriente vers les puissances-limites

Tout utilisateur de transformateurs se renseigne sur les nouvelles idées et cherche un partenaire sérieux.

Trafo Union met à la disposition des utilisateurs de nouvelles puissances-limites, la Société livre des transformateurs pour les tensions les plus élevées.

Celui qui désire dépasser les limites d'hier est tenu à de nouvelles dimensions afin de maîtriser les puissances et les masses les plus élevées, ce qui permettra de trouver de nouveaux domaines d'utilisation pour les projets d'aujourd'hui et les exigences de demain.

Trafo Union est la Société allemande qui possède le plus grand potentiel d'expansion dans le domaine des transformateurs.

De nombreux preneurs de licences dans plusieurs parties du monde en tirent profit.

Trafo Union possède des plateformes d'essai pour transformateurs les plus modernes d'Allemagne.

Trafo Union innove continuellement dans la technique de fabrication des gros transformateurs et offre en outre une gamme de transformateurs de distribution parfaitement étudiés.

Trafo Union représente pour vous l'éventail complet de matériel depuis le commutateur de prise en charge jusqu'aux transformateurs pour la transmission par courant continu des très hautes tensions.

Trafo Union, c'est le sigle de la technique de pointe également dans les détails. Cela va du commutateur à thyristors pour transformateurs sur locomotives à la maîtrise de la technique des enroulements à feuilles d'aluminium utilisés sur les transformateurs du type GEAFOL.

Trafo Union, c'est votre partenaire sur le Marché international comme sur le marché allemand. Soyez persuadés de la capacité technique de Trafo Union.

Transformatoren Union AG
7 Stuttgart 50, Deckerstraße 5
République Federale de l'Allemagne

Foire d'Hannover 1973
Sujet: limite de puissance des transformateurs
Pavillon 14/24
entre hall 11 et 12

Trafo-Union

Fondée par le groupe AEG
et la maison SIEMENS

90004343

des expériences et des statistiques portant sur des lignes ayant des niveaux ICFO d'environ 700 kV à 2 130 kV et qu'elles conviennent probablement peut-être jusqu'à 3 000 kV. Il faudrait entreprendre d'autres recherches sérieuses portant sur la base théorique de ces équations avant d'appliquer ces relations simples aux niveaux ICFO ultra-haute tension de 4 000 à 5 000 kV. Il est possible que certains perfectionnements soient nécessaires dans les relations concernant la distance d'amorçage.

these simple relations to the UHV ICFO levels of 4000 to 5000 kV. It is possible that moderate refinements will be required in the striking distance relations.

4. — Discussion.

4. — Discussion.

Cette partie présente une brève discussion concernant un certain nombre de points particuliers considérés plus en détail à la référence [2] et quelques relations analytiques qui n'apparaissent pas dans les références [2] ou [9] sont ajoutées. Au début de la recherche en 1963, on effectua une étude de toutes les publications disponibles traitant de l'approximation électro-geométrique de l'effet d'écran des lignes de transport. Des facteurs qui semblaient intéressants pour ce problème furent classés selon les trois groupes suivants :

This section presents a brief discussion of a number of topics considered in greater detail in reference [2] and a few analytical relations are added which do not appear in references [2] or [9]. At the outset of the research in 1963 a study was made of all available publications dealing with the electro-geometrical approach to transmission line shielding. Factors apparently affecting the problem were classified into three groups as follows :

4.1. *Facteurs de premier ordre.*

4.1. First-order factors.

Les facteurs de premier ordre sont ceux que l'on peut observer, mesurer et contrôler. On distingue parmi eux :

First-order factors are those which are observable, measurable and controllable. Among them are :

4.11. Les dimensions, les hauteurs et la géométrie des conducteurs, et le profil de la ligne.

4.11. Conductor sizes, heights and geometry, and line profile.

4.12. L'impédance caractéristique du conducteur.

4.12. Conductor surge impedance.

4.13. Les niveaux d'isolement au choc.

4.13. Impulse insulation levels.

4.2. *Facteurs de second ordre.*

4.2. Second-order factors.

Les facteurs de second ordre sont ceux que l'on peut estimer, extrapoler ou dont on peut donner un ordre de grandeur d'après des résultats expérimentaux ou des données statistiques concernant les performances de la ligne, la théorie jouant un rôle de guide. Parmi eux :

Second-order factors are those that may be estimated, extrapolated or calibrated from experimental results or statistical line performance data, with theory playing a guiding role. Among these are :

4.21. Les tensions de foudre associées aux courants de foudre prévus.

4.21. Stroke voltages associated with prospective stroke current.

4.22. Les distances d'amorçage associées aux tensions de foudre.

4.22. Striking distances associated with stroke voltages.

4.3. *Facteurs de troisième ordre.*

4.3. Third-order factors.

Les facteurs de troisième ordre sont ceux qui sont présents théoriquement mais que l'on ne peut pas observer ou contrôler directement. On distingue parmi eux :

Third-order factors are those which are theoretically present, but not directly observable or controllable. Among them are :

4.31. Des différences entre les distances *moyennes* d'amorçage entre le cœur de l'éclair et le pylône, le câble de garde, le conducteur de phase et la terre.

4.31. Differences between mean striking distances from the leader core to the tower, shield wire, phase conductor and earth.

4.32. Les écarts-types des distances d'amorçage par rapport à leur valeur moyenne.

4.33. L'influence de la tension à la fréquence du réseau du conducteur sur la distance d'amorçage.

4.34. L'influence de la répartition des charges correspondant à l'effet couronne sur les rigidités diélectriques « exactes » et sur les distances d'amorçage.

4.35. L'influence de l'effet couronne autour de l'éclair sur la rigidité au choc de la chaîne d'isolateurs.

4.36. L'effet d'écran des bras du pylône pour les parties du conducteur voisines du pylône.

Le *modèle analytique de référence* est conçu d'après les facteurs de premier et de second ordre. L'influence possible des facteurs de troisième ordre ne peut être mise en évidence dans l'état actuel de nos connaissances, qu'en supposant qu'ils contribuent à des écarts par rapport au modèle de référence, en imposant des variations quantitatives convenables des facteurs de premier ou de second ordre et en déterminant analytiquement les influences de telles variations. Si les effets de la variation sont favorables, ce n'est pas la peine de modifier quoi que ce soit. Si les effets de la variation sont défavorables, il devrait être possible d'obtenir une petite marge dans la valeur finale de l'angle d'écran pour tenir compte de l'incertitude correspondante.

4.32. Standard deviations of striking distances from their means.

4.33. Effect of conductor system-frequency voltage on striking distance.

4.34. Effect of corona-filament charge distribution on "exact" electric field strengths and on the striking distances.

4.35. Effect of stroke corona on impulse strength of the insulator string.

4.36. Shielding effect of tower crossarm for portions of conductor near the tower.

The reference analytical model *is developed from first and second-order factors. The possible influence of third order factors can, with the present state of our knowledge, be exhibited only by assuming them to contribute to* deviations *from the reference model, assigning reasonable quantitative deviations in first or second-order factors and determining the effects of such deviations analytically. If the effects of the deviation are favorable, no design action needs to be taken. If the effect of the deviation are unfavorable, it should be possible to provide a small margin in the final shielding angle to take account of the uncertainty involved.*

5. — Analyse des variations.

5.1. *Angle de sol différent de zéro.*

Les courbes estimatives de la figure 7 sont basées sur un angle de sol nul et calculées pour des valeurs déterminées de la hauteur et des rapports d'espacement $\bar{y}/\bar{r}_{sc}$ et $\bar{C}/\bar{r}_{sc}$ en prenant le facteur de variation K égal à l'unité. Pour un angle de sol $\bar{\theta}_g$ différent de zéro, l'équation (1) permet un calcul direct de $\bar{\theta}_{sc}$ si l'on se sert de $\bar{r}_{sc}$, et de $\hat{\theta}_{sc}$ si l'on se sert de $\hat{r}_{sc}$. On peut alternativement se servir de la figure 7 avec les rapports donnés par l'équation (4) et l'équation (3). Les deux résultats devraient concorder aux erreurs de lecture près de la figure 7. Prenons à titre d'exemple

5. — Deviation analysis.

5.1. Non-zero ground angle.

The estimating curves of Figure 7 are based on zero ground angle and calculated for assigned values of the height and spacing ratios $\bar{y}/\bar{r}_{sc}$ and $\bar{C}/\bar{r}_{sc}$ with the deviation factor K set equal to unity. For a non-zero ground angle of $\bar{\theta}_g$, equation (1) permits direct calculation of $\bar{\theta}_{sc}$ if $\bar{r}_{sc}$ is used and of $\hat{\theta}_{sc}$ if $\hat{r}_{sc}$ is used. Alternatively, Figure 7 may be entered with the ratio given by equation (4) and equation (3). The two results should agree within reading errors of Figure 7. As an illustrative example, let

$$\bar{\theta}_g = -30°$$

$$\bar{y}/\bar{r}_{sc} = 1.0$$

$$\bar{C}/\bar{r}_{sc} = 0.4$$

Il résulte alors

Then there results

$$\beta = \arcsin 0.2 = 11.5°$$

$$\bar{\theta}_3 = \arcsin (1.0 - 1.0 \times 0.366) - 30° = 22.3°$$

$$\sin \bar{\theta}_3 = -0.38$$

$$\bar{y}'/\bar{r}_{sc} = 1.0 - (-0.38) = 1.38$$

$$\bar{\theta}_{sc} = -34° \text{ d'après la figure 7}$$

from figure 7

Par un calcul direct d'après l'équation (1), on trouve que

By direct calculation from equation (1) it is found that

$$\bar{\theta}_{sc} = -33.8°$$

5.2. *Distances d'amorçage inégales.*

Les modèles des figures 5 et 6 sont basés sur des distances d'amorçage moyennes entre l'extrémité du cœur de l'éclair et le câble de garde S, le conducteur de phase W et la terre G égales entre elles. On peut exprimer l'écart par rapport à cette condition de référence comme suit en fonction ed la distance de base $\bar{r}_{ss}$, distance d'amorçage au câble de garde :

5.2. Unequal striking distances.

The models of Figures 5 and 6 are based upon equal mean striking distances from the tip of the leader core to the shield wire S, the phase conductor W and the earth G. Deviation from this reference condition can be expressed as follows in terms of the base distance $\bar{r}_{ss}$, the striking distance to the shield wire :

(Toutes les valeurs de $\bar{r}_s$ sont estimées pour le courant critique)

$$\bar{r}_{sg} = K_{sg}\,\bar{r}_{ss} \qquad (10)$$

$$\bar{r}_{sw} = K_{sw}\,\bar{r}_{ss} \qquad (11)$$

(All $\bar{r}_s$ values estimated for critical current)

La figure 12 illustre trois écarts défavorables par rapport au modèle de référence, à savoir :

Figure 12 illustrates three unfavorable deviations from the reference model, namely:

$$K_{sg} < 1.0$$

$$K_{sw} > 1.0$$

θ_g est négatif/*is negative*

Si le sol était réellement une surface plane, on devrait s'attendre à ce que K_{sg} ait une valeur un peu inférieure à l'unité .Dans la réalité, si toutefois cette condition est approchée, ce n'est que rarement à cause des irrégularités de surface réparties au hasard telles que l'herbe, les buissons, les arbres ou d'autres perturbations du profil du terrain. On n'a obtenu aucun résultat expérimental qui fasse penser que K_{sg} doive être inférieur à l'unité dans le modèle analytique pratique. Au contraire, la présence d'épaisses forêts le long du tracé de la ligne augmente effectivement la distance d'amorçage à la terre de sorte que K_{sg} peut être supérieur à l'unité à moins que ce ne soit la hauteur effective des conducteurs qui ne se trouve réduite. Pour citer un exemple extrême, il est arrivé *que l'on n'observe aucune défaillance d'effet d'écran* au cours

If the earth were actually a plane surface, one would expect K_{sg} to have a value somewhat less than unity. This condition is rarely, if ever, approached in the field because of randomly-distributed surface irregularities such as grass, brush, trees or other perturbations of the profile. No experimental results have been obtained which suggest that K_{sg} should be less than unity in the practical analytical model. On the contrary, however, the presence of dense forest along the line route effectively increases the striking distance to earth so that K_{sg} can be greater than unity or, alternatively, the effective height of the conductors is reduced. As an extreme example, no shielding failures were observed *on one line, over a period of six years, which had a shielding angle of 63°. The explanation lies in the 70 % forest with tree heights equal to*

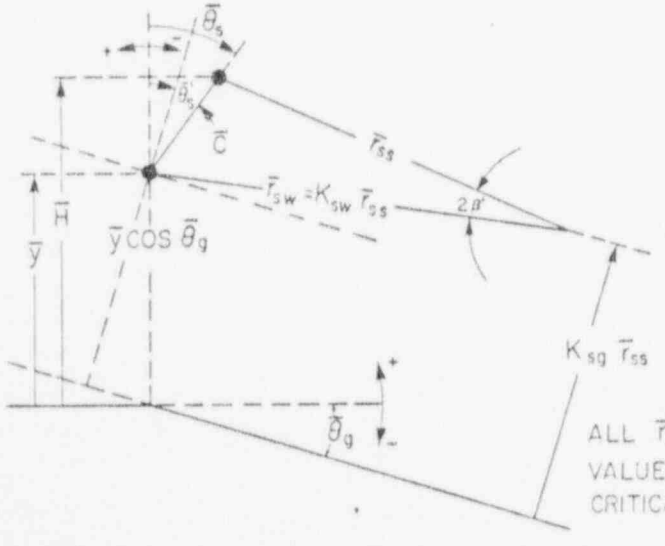

FIG. 12

Ecarts défavorables par rapport au modèle analytique de référence

Unfavorable deviations from the reference analytical model

All $\bar{r}_s$ values critical = Toutes les valeurs de $\bar{r}_s$ critiques

d'une période de six années sur une ligne ayant un angle de protection de 63°. L'explication réside dans la présence de forêts à 70 % avec des arbres dont les hauteurs étaient égales ou supérieures à celles des conducteurs de la ligne. Il semble très improbable, du moins dans un avenir envisageable, qu'une recherche statistique ou expérimentale permette de faire la distinction entre les distances d'amorçage. Dans la suite de la discussion, on a supposé que ces distances correspondaient au courant de foudre critique nécessaire pour provoquer le contournement des isolateurs et qu'elles étaient grossièrement comparables à la hauteur du pylône. Etant données les incertitudes existant dans la répartition géométrique des charges au cours des derniers stades de développement de l'éclair il ne semble pas intéressant d'essayer de déterminer avec davantage de précision les distances d'amorçage d'après des calculs de champ électrique. Néanmoins, il faut reconnaître que le fait de considérer les valeurs de K_{sg} et K_{sw} comme des constantes est une approximation utile pour l'estimation de l'influence de distances d'amorçage inégales et pour donner au facteur d'écart K des valeurs appropriées lorsqu'on se sert de la figure 7.

or greater than the phase conductor heights. It appears highly improbable that any statistical or experimental research can, at least for the forseeable future, distinguish between the striking distances. In the foregoing discussion it has been assumed that these distances corresponded to the critical lightning current required to cause insulator sparkover and were roughly comparable to the height of the tower. Because of the uncertainties involved in the geometrical distribution of charge in the last stages of leader development, it does not seem profitable to attempt more accurate determination of the striking distances from electric field calculations. Nevertheless, it should be recognized that the treatment of the K_{sg} and K_{sw} values as constants is an approximation useful for estimating the effect of unequal striking distances and the assignment of appropriate values to the deviation factor K when Figure 7 is used.

Si l'on donne à K_{sg} et K_{sw} des valeurs définies, l'équation (1) prend la forme plus compliquée suivante :

If definite values are assigned to K_{sg} and K_{sw}, equation (1) takes on the more complicated form

$$\bar{\theta}_{sc} = \bar{\theta}_g + \text{arc sin}\left[(K_{sg}/K_{sw}) - \frac{(\bar{S}/\bar{r}_{sc})}{K_{sw}} \cos\bar{\theta}_g\right] - \text{arc cos}\frac{(\sin 2\beta')}{(\bar{C}/\bar{r}_{sc})} \tag{12}$$

où

where

$$2\beta' = \text{arc cos}\left[\frac{1 + K_{sw}^2 - (\bar{C}/\bar{r}_{sc})^2}{2K_{sw}}\right] \tag{13}$$

Les équations (12) et (13) se réduisent aux équations (1) et (2) si les valeurs de K sont prises égales à l'unité. On a souligné plus haut que les courbes d'estimation de la figure 7 sont basées sur le modèle de référence avec des distances d'amorçage égales et un angle de sol nul pour lequel les équations sont

Equations (12) and (13) reduce to equations (1) and (2) if the K values are taken as unity. It has been pointed out earlier that the estimating curves of Figure 7 are based on the reference model for equal striking distances and zero ground angle for which the equations are

$$\bar{\theta}_{sc} = \text{arc sin}\left[1 - \frac{K\bar{S}}{\bar{r}_{sc}}\right] - \beta \tag{14}$$

$$\beta = \text{arc sin}\frac{\bar{C}}{2\bar{r}_{sc}} \tag{15}$$

où l'on peut donner au facteur d'écart K des valeurs permettant d'obtenir une variation raisonnable des facteurs de troisième ordre. La figure 13 est un diagramme de correction permettant de modifier l'entrée dans la figure 7 pour tenir compte de l'influence d'une valeur supposée de K_{sg}. On peut également déterminer l'influence d'un K_{sw} donné d'après ce diagramme en donnant à K la valeur préliminaire de $1/K_{sw}$ et en faisant la lecture sur une droite correspondant à un K_{sg} modifié, $K'_{sg} = K_{sg}/K_{sw}$.

where the deviation factor K can be assigned values to provide for reasonable variation in third-order factors. Figure 13 is a correction chart for modifying the entry to Figure 7 to include the effect of an assumed value of K_{sg}. The effect of an assumed K_{sw} can also be obtained from this chart by assigning K the preliminary value of $1/K_{sw}$ and reading up to a modified K_{sg} line of $K'_{sg} = K_{sg}/K_{sw}$. Errors are associated with the spacing angle 2 β' of equation (12). The angle $\beta = \beta'$ only for $K_{sw} = 1.0$. These matters are more easily understood through the following examples :

Des erreurs se trouvent associées à l'angle d'espacement 2 β' de l'équation (12). L'angle β est égal à β' seulement pour $K_{sw} = 1,0$. Cela se comprend plus facilement dans les exemples suivants :

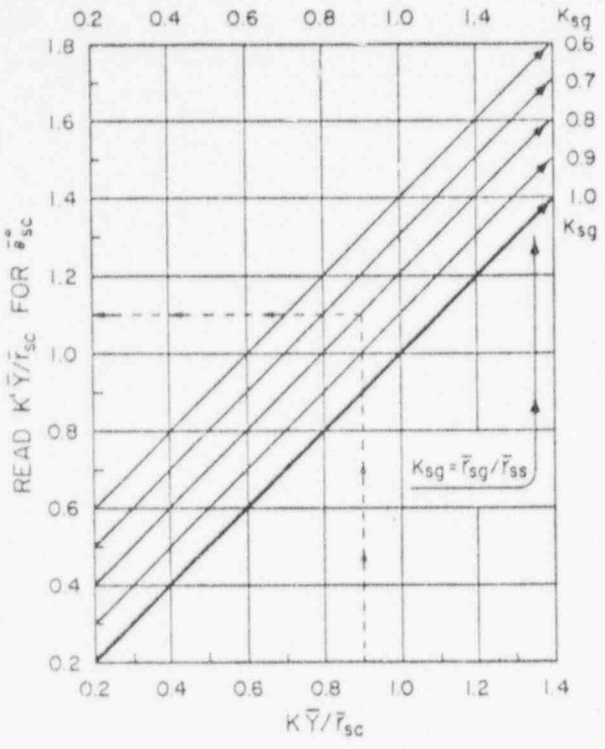

FIG. 13
Courbes de correction pour $K'\,y/r_{sc}$ en fonction de K_{sg}
Correction curves for $K'\,\bar{y}/\bar{r}_{sc}$ as a function of K_{sg}
Read $K'Y'/r_{sc}$ for $\bar{\theta}'_{sc}$ = Lecture de $K'Y'/r_{sc}$ pour $\bar{\theta}'_{sc}$

5.21. *Exemples.*

5.211. — Prenons

$$\bar{\theta}_{sg} = 0 \qquad \bar{y}/\bar{r}_{sc} = 1.00 \qquad \bar{C}/\bar{r}_{sc} = 0.40$$

$$K_{sg} = 0.95 \qquad K_{sw} = 1.05$$

alors

$$2\,\beta' = \text{arc cos}\left[\frac{1.00 + 1.10 - 0.16}{2.10}\right] = 22.5°$$

$$\frac{\sin 2\beta'}{0.40} = \frac{0.3827}{0.40} = 0.957$$

$$\text{arc cos. } 957 = 16.9° \qquad \text{arc sin}\left[\frac{0.95}{1.05} - \frac{1.00}{1.05}\right] = \underline{-3.0°}$$

Puis $\bar{\theta}_{sc} = -3{,}0° - 16{,}9° \cong \underline{-20°}$

par un calcul exact en se servant des équations (12) et (13).

5.212. — En utilisant les mêmes données que ci-dessus sauf que l'on prend K_{su} et K_{sw} égaux à l'unité comme dans le modèle de référence et en appliquant les équations (14) et (15) en donnant à K la valeur 1,15, on obtient :

$$\beta = \text{arc sin } 0.2 = 11.5°$$

$$\bar{\theta}_{sc} = \text{arc sin } (1 - 1.15) - 11.5°$$

$$\bar{\theta}_{sc} = -8.6° - 11.5° \cong \underline{-20°}$$

Dans cet exemple, K a été choisi de façon à ce qu'on obtienne un résultat correspondant à la solution exacte. On peut lire le même angle sur la figure 7.

5.213. — Si l'on donne à K la valeur préliminaire de $1/K_{sw} = 0.95$ et une valeur ajustée de

$$K'_{su} = K_{su}/K_{sw} = 0.95/1.05 = 0.90$$

5.21. *Examples*

5.211. — *Let*

$$\bar{\theta}_{sg} = 0 \qquad \bar{y}/\bar{r}_{sc} = 1.00 \qquad \bar{C}/\bar{r}_{sc} = 0.40$$

$$K_{sg} = 0.95 \qquad K_{sw} = 1.05$$

Then

$$2\,\beta' = \text{arc cos}\left[\frac{1.00 + 1.10 - 0.16}{2.10}\right] = 22.5°$$

$$\frac{\sin 2\beta'}{0.40} = \frac{0.3827}{0.40} = 0.957$$

$$\text{arc cos. } 957 = 16.9° \qquad \text{arc sin}\left[\frac{0.95}{1.05} - \frac{1.00}{1.05}\right] = \underline{-3.0°}$$

Then $\bar{\theta}_{sc} = -3.0° - 16.9° \cong \underline{-20°}$

by exact calculation using equations (12) and (13).

5.212. — *Using the same data as above except that K_{su} and K_{sw} are taken as unity as in the reference model and applying equations (14) and (15) with K assigned the value 1.15 there results :*

$$\beta = \text{arc sin } 0.2 = 11.5°$$

$$\bar{\theta}_{sc} = \text{arc sin } (1 - 1.15) - 11.5°$$

$$\bar{\theta}_{sc} = -8.6° - 11.5° \cong \underline{-20°}$$

In this example K has been selected to result in agreement with the exact solution. The same angle can be read from Figure 7.

5.215. — *If K is assigned the preliminary value of $1/K_{sw} = 0.95$ and an adjusted value of*

$$K'_{su} = K_{su}/K_{sw} = 0.95/1.05 = 0.90$$

le diagramme de correction de la figure 13 donne $K' = 1{,}05$ et il en résulte :

$$\bar{\theta}_{sc} = \text{arc sin}\,(1 - 1.05) - 11.5^\circ$$

$$\bar{\theta}_{sc} = -2.8^\circ - 11.5^\circ = -14.3^\circ$$

On trouve également ce résultat d'après la figure 7.

5.214. — Si l'on compare les exemples 5.211 et 5.213, on trouve que l'erreur se situe dans l'utilisation d'un angle β à la place de l'angle correct donné par

$$\delta = \text{arc cos}\,\frac{(\sin 2\beta')}{(\bar{C}/\bar{r}_{sc})} = 16.9^\circ$$

Si on utilise l'angle δ, les calculs de l'exemple 5.213 permettent d'obtenir

$$\bar{\theta}_{sc} = -2.8^\circ - 16.9^\circ = -19.7^\circ$$

ce qui se situe à l'intérieur des erreurs de lecture du diagramme de correction de la figure 13.

Ces exemples ont été donnés pour illustrer le rôle du facteur d'écart K appliqué au modèle analytique de référence tel qu'il est défini à la figure 7 et dans les équations (14) et (15). Il semble que l'on doive réserver ce facteur pour les incertitudes provenant des facteurs de troisième ordre et que sa valeur puisse bien se situer dans la zone

$$1.1 \leqslant K < 1.2 \qquad (16)$$

Pour sauvegarder la correspondance entre les figures et les équations, ces exemples ont été déterminés en se servant des distances *moyennes* d'amorçage et en partant de l'angle de protection critique *moyen* $\bar{\theta}_{sc}$. Dans les études, on pense qu'il est souhaitable de se servir des distances d'amorçage « effectives » comme cela est défini plus haut. Il n'est pas nécessaire d'apporter de changement aux équations mis à part l'utilisation de valeurs effectives où cela est indiqué et la désignation de l'angle de protection par la valeur « effective » $\bar{\theta}_{sc}$.

5.3. Variations des facteurs de premier ordre.

Les hauteurs de référence $\bar{y}$ pour le conducteur de phase et $\bar{H}$ pour le câble de garde S correspondent en fait aux hauteurs *moyennes* pour la ligne toute entière en tenant compte de toutes les influences des variations de profil. Pour faire des estimations, il est commode de définir trois catégories de profils, en les précisant autant qu'il le faut lorsqu'on dispose de données précises.

5.31. Profil plat ..... $y' = y_t - 2\,S_c/3$ (17)

5.32. Profil ondulé ..... $y' = y_t$ (18)

5.33. Profil montagneux .... $y' \geqslant 2\,y_t$ (19)

La hauteur moyenne du câble de garde S au-dessus du conducteur W est prise égale à

5.34.

$$\bar{b} = (H_t - y_t) + 2\,(S_c - S_g)/3 = b_t + 2\,(S_c - S_g)/3 \qquad (20)$$

et

$$\bar{H} = \bar{y} + \bar{b} \qquad (21)$$

the correction chart of Figure 13 yields $K' = 1.05$ and there results :

This result is also found from Figure 7.

5.214. — Comparing examples 5.211 and 5.213, one finds that the error lies in the use of the angle β instead of the correct angle given by

If the angle δ is used, the procedure of example 5.213 yields

within the reading errors of the correction chart of Figure 13.

These examples have been given to illustrate the role of the deviation factor K applied in the reference analytical model as depicted in Figure 7 and in equations (14) and (15). It is felt that this factor should be reserved for the uncertainties arising from third order factors and that its value may well lie in the range

To preserve the association of figures and equations, these examples have been worked out using the mean striking distances and deriving the mean critical shielding angle $\bar{\theta}_{sc}$. For design purposes it is believed desirable to use « effective » striking distances as defined earlier. No changes need be made in the equations except the use of effective values where indicated and the designation of the shielding angle as the « effective » value $\bar{\theta}_{sc}$.

5.3. Deviations in first-order factors.

The reference heights $\bar{y}$ for the phase conductor and $\bar{H}$ for the ground wire S are their mean heights for the entire line including all effects of varying profile. For estimating purposes it is convenient to define three profile classes, refining them as needed where detailed data are available.

5.31 *Flat Profile* ..... $y' = y_t - 2\,S_c/3$ (17)

5.32 *Rolling Profile* ..... $y' = y_t$ (18)

5.33 *Mountainous Profile* . $y' \geqslant 2\,y_t$ (19)

The mean height of the shield wire S above the conductor W is taken to be

5.34

$$\bar{b} = b_t + 2\,(S_c - S_g)/3 \qquad (20)$$

and

$$\bar{H} = \bar{y} + \bar{b} \qquad (21)$$

où

S_c = flèche du conducteur de phase W
S_g = flèche du câble de garde S
y_t = hauteur du conducteur au droit du pylône
H_t = hauteur du câble de garde au droit du pylône
$b_t = H_t - y_t$
$\bar{b}$ = espacement vertical moyen entre le conducteur et le câble de garde.

Comme de tels calculs représentent un point de départ essentiel, il est clair qu'une prise en considération attentive des variations de la hauteur du conducteur est nécessaire si l'on veut obtenir un dispositif de protection efficace.

Citons, parmi de telles considérations :

5.35. — Pour des portées très longues avec des flèches importantes du conducteur, une partie importante du conducteur dépasse nettement la hauteur moyenne pour un profil plat. Dans ce cas, une façon convenable d'apprécier les choses serait de suggérer de baser la protection sur la hauteur du conducteur au quart de la portée ou même au droit du pylône comme dans le cas du profil ondulé.

5.36. — Si la ligne traverse des terrains montagneux dans une grande partie de son tracé, on peut fractionner en conséquence l'étude de la protection de la ligne ou bien la baser sur les hauteurs de conducteur dans les parties montagneuses. Les traversées de rivières importantes nécessitent en général une étude particulière. Dans certains cas extrêmes, l'existence d'un troisième câble de garde central peut se justifier.

6. — Exemple de disposition.

Ce chapitre précise un procédé méthodique pour la détermination d'un système efficace de protection en se servant des concepts déterminés précédemment. Alors que les étapes indiquées sont spécifiques, l'exemple est hypothétique.

6.1. Le profil d'un tracé de ligne donné impose les structures de pylône nécessaires pour obtenir des distances au sol minimales pour une ligne à 500 kV. Le profil est défini comme étant à 40 % plat, 40 % ondulé et 20 % montagneux.

Les autres données nécessaires sont les suivantes :

Hauteur du conducteur au droit du pylône	$y_t = 22$ m
Flèche du conducteur	$S_c = 12$ m
Hauteur du câble de garde au droit du pylône (préliminaire)	$H_t = 31$ m
Flèche du câble de garde	$S_g = 6$ m
Tension critique d'amorçage au choc (ICFO)	(—) = 2 000 kV
Impédance caractéristique du conducteur	Z = 360 Ω

6.2. Les hauteurs moyennes des conducteurs et du câble de garde deviennent, en se basant sur les hypothèses préliminaires :

Zone à profil plat :

$$\bar{y}_F = y_t - 2S_c/3 = 14 \text{ m}$$

where

S_c = *sag of phase conductor W*
S_g = *sag of ground wire S*
y_t = *height of conductor at tower*
H_t = *height of ground wire at tower*
$b_t = H_t - y_t$
$\bar{b}$ = *mean vertical spacing between conductor and ground wire*

While such calculations provide an essential starting point, it is clear that careful consideration of deviations in conductor height are required if efficient shielding design is to be achieved.

Among such considerations are the following :

5.35. — *For very long spans with large conductor sag, an important fraction of the conductor substantially exceeds the mean height for flat profile. In this case good judgement might suggest that shielding be based on the conductor height at quarter span or even at the tower as in the case of rolling profile.*

5.36. — *If a large fraction of the line route traverses mountainous terrain, the shielding design may be sectioned accordingly or be based on the conductor heights for the mountainous portion. Long river crossings will, in general, require individual treatment. In extreme cases, a third centrally-located ground wire may be justified.*

6. — Design example.

This section outlines an orderly procedure for the design of an effective shielding system using the concepts developed earlier. While the steps indicated are specific, the example is hypothetical.

6.1. — *The profile of a proposed line route will have dictated the required tower structures to meet minimum clearances to ground for a 500 kV line. The profile is classified as 40 % flat, 40 % rolling and 20 % mountainous. Other pertinent data are :*

Conductor height at tower	$y_t = 22$ *m*
Conductor sag	$S_c = 12$ *m*
Ground wire height at tower (preliminary)	$H_t = 31$ *m*
Ground wire sag	$S_g = 6$ *m*
Impulse critical flashover voltage (ICFO)	(—) = 2000 *kV*
Conductor surge impedance	Z = 360 *ohms*

6.2. — *The mean heights of phase conductors and ground wire become, based on preliminary assumptions :*

Flat profile portion :

$$\bar{y}_F = y_t - 2S_c/3 = 14 \text{ m}$$

Zone à profil ondulé :

$$\bar{y}_R = y_t = 22 \text{ m}$$

Zone à profil montagneux :

$$\bar{y}_M = 2\, y_t = 44 \text{ m}$$

Hauteur moyenne pour la ligne :

$$\bar{y} = 0{,}4 \times 14 + 0{,}4 \times 22 + 0{,}2 \times 44$$
$$\bar{y} = 23{,}2 \text{ m}$$

Espacement vertical moyen :

$$\bar{b} = 9 + 8 - 4 = 13 \text{ m}$$

Hauteur moyenne du câble de garde :

$$\bar{H} = \bar{y} + \bar{b} = 36{,}2 \text{ m}$$

Arrivé à ce point, on peut recalculer si on le désire l'impédance caractéristique. Nous supposerons ici que la valeur de 360 Ω est confirmée.

6.3. — Le courant de foudre critique dans le conducteur de phase est

Rolling profile portion :

$$\bar{y}_R = y_t = 22 \text{ m}$$

Mountainous profile portion :

$$\bar{y}_M = 2\, y_t = 44 \text{ m}$$

Mean height for line :

$$\bar{y} = 0.4 \times 14 + 0.4 \times 22 + 0.2 \times 44$$
$$\bar{y} = 23.2 \text{ m}$$

Mean vertical spacing :

$$\bar{b} = 9 + 8 - 4 = 13 \text{ m}$$

Mean ground wire height :

$$\bar{H} = \bar{y} + \bar{b} = 36.2 \text{ m}$$

At this point the surge impedance may be recalculated if desired. It will be assumed here that the value of 360 ohms is confirmed.

6.3. — *The critical lightning current to the phase conductor is*

$$I_c = 2E/Z = 2 \times 2000/360 = 11.1 \text{ kA}$$

$$I_{oc} = 1.1 \times 11.1 = 12.2 \text{ kA}$$

On attire ici l'attention sur l'utilisation au cours de l'étude de la distance d'amorçage « efficace » telle que l'on a

Here attention is drawn to the use of the « effective » striking distance for design purposes so that

$$\hat{r}_{sc} = 6.0 \times 12.2^{0.8} = 44.4 \text{ m}$$

6.4. — La hauteur relative (normalisée) du conducteur est

6.4. — *The per unit (normalized) conductor height is*

$$\bar{y}/\hat{r}_{sc} = 23.2/44.4 = 0.52$$

Supposons au départ que C soit légèrement supérieur à b ou que l'on ait $C = 14$ m. L'espacement relatif devient alors

As a preliminary figure, assume C slightly larger than b or C = 14 m. Then the per unit spacing becomes

$$\bar{C}/\hat{r}_{sc} \cong 14/44.4 \cong 0.32$$

Pour les conditions de référence, $K = 1{,}0$ et l'on fait une lecture sur la figure 7, pour les valeurs relatives ci-dessus de sorte qu'on a

For reference conditions K = 1.0 and Figure 7 is read, for the per unit values above, as

$$\hat{\theta}_{sc} \cong 20°$$

6.5. — Considérons maintenant l'écart du conducteur au-dessus de la valeur de référence et l'effet de champ du dispositif de protection sur l'ensemble. Etant donné que seule la zone montagneuse du tracé de la ligne a une hauteur moyenne supérieure à la valeur de référence, cette hauteur relative devient

6.5. — *Consider now the deviation of the conductor above the reference value and the potential effect on the design of the shielding system. Since only the mountainous portion of the line route has a mean height above the reference value, this per unit height becomes*

$$\bar{y}_M/\hat{r}_{sc} = 44.0/44.4 = 0.99$$

L'estimation de $\bar{C}$ peut maintenant être contrôlée

The estimate of $\bar{C}$ may now be checked.

$$\bar{C} = \bar{b}/\cos\hat{\theta}_{sc} = 13.0/\cos 20° = 13.8$$

$$\bar{C}/\hat{r}_{sc} = 0.31$$

Si l'on se sert de ces valeurs relatives, la figure 7 donne une estimation de

If these per unit values are used, Figure 7 gives an estimate of

$$\hat{\theta}_{sc} = -8° \ (K = 1.0)$$

et les équations (14) et (15) donnent une valeur calculée de

and equations (14) and (15) give a calculated value of

$$\hat{\theta}_{sc} = -8.3°$$

6.6. — Etant donné que la ligne se trouve bien protégée sur 80 % de son tracé si l'on se sert des paramètre correspondant à la zone montagneuse, il est raisonnable d'appliquer la limite inférieure de

6.6. — *Since the line is conservatively shielded for 80 % of the route if the parameters for the mountainous portion are used, it is reasonable to apply the lower limit of K = 1.1 as a precaution*

$K = 1{,}1$ à titre de précaution contre les écarts de troisième ordre et il faut se servir de la figure 7 avec la valeur relative corrigée de

against third-order deviations and Figure 7 should be entered with the revised per unit value of

$$K\,\bar{y}/\bar{r}_{sc} = 1.1 \times 0.99 = 1.09$$

et

and

$$\bar{C}/\bar{r}_{sc} = 0.31$$

pour obtenir

to obtain

$$\hat{\theta}_{sc} = -13°$$

Le décalage horizontal a du conducteur de phase W est donné par

The horizontal offset a of the phase conductor W is given by

$$a = \bar{C} \sin \hat{\theta}_{sc} = 13.8\ (-0.225)$$

$$a = -3.1\ m$$

où le signe négatif indique que le câble de garde se trouve « à l'extérieur » du conducteur de phase.

where the negative sign indicates that the ground wire is " outboard " of the phase conductor.

6.7. — On peut maintenant se servir de l'équation (21) pour déterminer l'écart vertical entre le conducteur et le câble de garde au droit du pylône.

6.7. — *Equation (21) may now be used to determine the vertical separation between conductor and ground wire at the tower.*

$$b_t = \bar{b} - 2\,(S_c - S_g)/3$$

$$b_t = 13.0 - 2\,(12 - 6)/3$$

$$b_t = 9.0\ \text{m}$$

L'angle de protection au droit du pylône est alors

The shielding angle at the tower is then

$$\theta_t = \text{arc tg}(-3{,}1/9{,}0) = \text{arc tg}(-0{,}344)$$
$$\theta_t = -19°$$

θ_t = arc tan(— 3.1/9.0) = arc tan(— 0.344)
θ_t = — 19°

La conception réelle du sommet du pylône se trouvera bien entendu influencée par les marges nécessaires compte tenu des problèmes mécaniques associés aux décharges de glace ou aux oscillations du conducteur si le tracé de la ligne se trouve dans des régions où l'on rencontre ces problèmes.

The actual design of the tower top will, of course, be affected by the clearances required for mechanical problems associated with unloading ice or conductor oscillations if the line route is located in areas where these problems are encountered.

7. — Estimation des déclenchements correspondant à des défauts de l'effet d'écran.

Les figures 14 à 18 représentent des courbes d'estimation correspondant à des déclenchements dus à des défaillances de l'effet d'écran pour des lignes inefficacement protégées. Elles sont tirées de la référence [2] sans modification. Bien qu'elles soient similaires aux courbes de la référence [7], elle en diffèrent en ce que le facteur K_{sg} est pris égal à l'unité au lieu de 0,9 à la référence [7]. Pour déterminer de telles courbes, il est nécessaire de faire l'hypothèse d'espacements moyens entre conducteurs et câble de garde correspondant au niveau d'isolement des lignes typiques équipées de pylônes métalliques.

Lorsqu'on se sert de ces courbes, il est essentiel de savoir que l'ordonnée n_{10} donne le taux de déclenchement sous la forme

n_{10} = *nombre de déclenchements annuels* (22)
pour 100 miles pour une densité de coups de foudre de

D_s = *10 coups de foudre par mile carré* (23)
et par an

7. — Estimation of shielding failure trip-outs.

Figures 14 to 18 are estimating curves for shielding failure tripouts for ineffectively-shielded lines. They are taken from reference [2] without change. Although similar to the curves of references [7], they differ in that the K_{sg} factor is taken as unity instead of 0.9 as in reference [7]. For the development of such curves it is necessary to assume average conductor-to-ground wire spacing corresponding to the insulation levels of typical steel-tower lines.

In using these curves, it is essential to know that the ordinate n_{10} gives the trip-out rate in

n_{10} = trip-outs per 100 miles per year (22)
for a stroke density of

D_s = 10 strokes per square mile per year (23)

La référence [7] donne une estimation de la densité de coups de foudre applicable aux figures 14-18 à savoir

D_s = 0,4 (T.D.) coups de foudre par mile carré/année (24)

ou

D_s = 0,154 (T.D.) coups de foudre par kilomètre carré/année. (25)

Ainsi n_{10} correspond environ à 25 T.D. (journées d'orage par an). Etant donné que ces approximations numériques ont été tirées de niveaux T.D. dans la zone 25-55 avec les valeurs les plus précises (voir tableau 5) pour le niveau 40 T.D. il semble prudent de s'interroger sur l'extrapolation linéaire pour des niveaux T.D. extérieurs à cette zone. La référence (8) a adopté la relation d'extrapolation

$$D_s = k\,(T.D.)^{1.5} \qquad (26)$$

dans ce but. A l'intérieur de la zone 25-55 T.D., une simple proportion linéaire des taux de déclenchement semble cependant se justifier.

On recommande de lire d'abord directement les courbes d'estimation pour trouver n_{10} (une interpolation peut être nécessaire).

Puis

$n'_{10} = n_{10}/1{,}61$ = nombre de déclenchements pour 100 km pour une année pour une densité de coups de foudre de 3,86 par km carré et par an. (27)

On peut ensuite obtenir des estimations correspondant à d'autres hypothèses d'exposition grâce à l'utilisation des équations (24) - (27). Il faut remarquer en passant que les distances d'amorçage *moyennes* telles quelles sont données par l'équation (5) sont applicables à ces courbes d'estimation, l'équation (7) étant réservée aux dispositifs de protection.

Reference [7] estimates the stroke density applicable to Figures 14-18 to be

D_s = *0.4 (T.D.) strokes per square mile/year (24)*

or

D_s = *0.154 (T.D.) strokes per square km/year (25)*

Thus n_{10} corresponds to approximately 25 T.D. (thunderstorm days per year). Since these numerical approximations have been derived from T.D. levels in the range from 25-55 with the most accurate data (See Table 5) at the 40 T.D. level, it appears prudent to question linear extrapolation for T.D. levels outside this range. Reference [8] has adopted the extrapolation relation

for this purpose. Within the range 25-55 T.D., however, simple linear proportion of the trip-out rates seems to be justified.

It is recommended that the estimating curves first be read directly to find n_{10} (interpolation may be required).

Then

$n'_{10} = n_{10}/1.61$ = *trip-outs per 100 kilometers per year for a stroke density of 3.86 per square kilometer per year (27).*

Estimates for other exposure assumptions can then be obtained through the use of equations (24) - (27). It should be noted in passing that the mean *striking distances as given by equation (5) are applicable to these estimation curves, equation (7) being reserved for shielding design.*

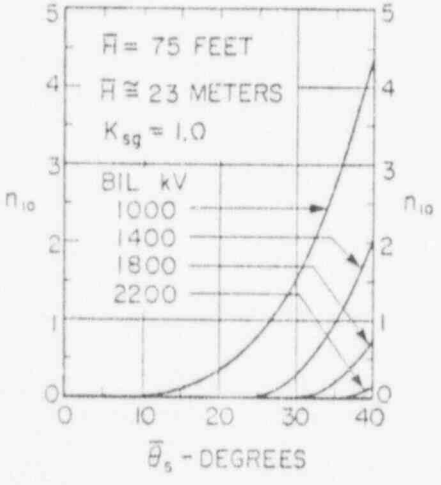

FIG. 14

Courbes d'estimation correspondant aux déclenchements dus à une défaillance de l'effet d'écran pour des lignes ayant une protection inefficace

Estimating curves for shielding-failure trip-outs for lines with ineffective shielding

Feet = Pieds
Meters = Mètres
Degrees = Degrés

8. — Le mécanisme d'amorçage secondaire.

Aucun modèle analytique du mécanisme d'amorçage secondaire n'est considéré dans ce rapport étant donné qu'ils ont été traités d'une manière

8. — The backflash mechanism.

Analytical models of the backflash mechanism are not considered in this report because they have been exhaustively treated in the literature for many years.

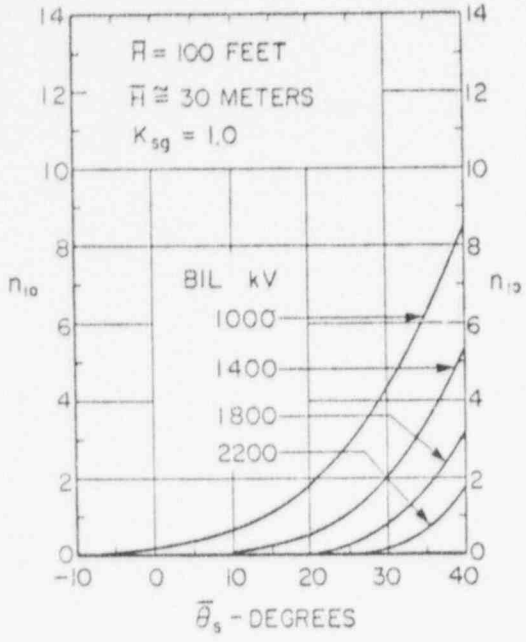

FIG. 15

Courbes d'estimation correspondant aux déclenchements dus à une défaillance de l'effet d'écran pour des lignes ayant une protection inefficace

Estimating curves for shielding-failure trip-outs for lines with ineffective shielding

Feet = Pieds
Meters = Mètres
Degrees = Degrés

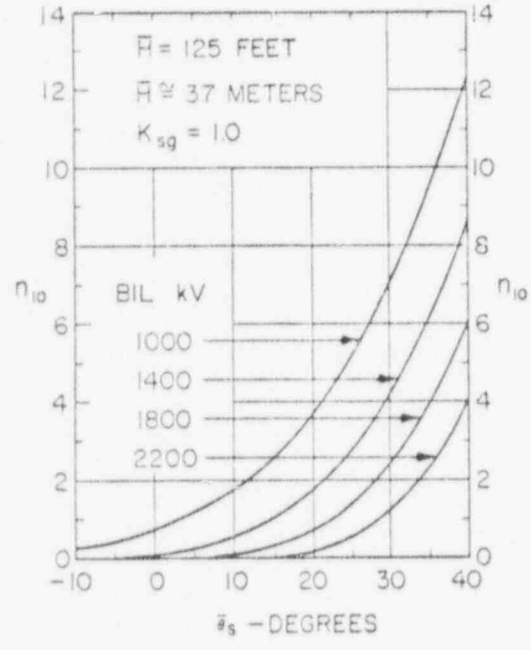

FIG. 16

Courbes d'estimation correspondant aux déclenchements dus à une défaillance de l'effet d'écran pour des lignes ayant une protection inefficace

Estimating curves for shielding-failure trip-outs for lines with ineffective shielding

Feet = Pieds
Meters = Mètres
Degrees = Degrés

exhaustive pendant de nombreuses années dans la littérature technique.

Il a cependant été considéré comme essentiel que l'appareil détecteur de cheminement soit également capable de réagir aux défaillances d'effet d'écran et aux phénomènes d'amorçages secondaires. Le tableau 2 montre que cet objectif a été atteint. Les différentes sortes de phénomènes d'amorçage secondaire enregistrés vont des phénomènes correspondant à un circuit simple à simple conducteur à des phénomènes correspondant à un circuit double multiconducteur. De plus, les conditions de mise à la terre vont de moins de 5 Ω pour un défaut à deux ternes sur une ligne à fort isolement et equipée de pylônes très élevés, à la mise à la terre de contrepoids dans des sols à forte résisti-

It was considered essential, however, that the Pathfinder instrument be equally capable of responding to shielding failure and backflash events. Table 2 shows that this objective has been met. The kinds of backflash events recorded range from single-circuit, single-conductor events to double-circuit, multiconductor events. Moreover, grounding conditions range from under five ohms for a double-circuit fault on a highly insulated line with very high towers to counterpoise grounding in very high resistivity soil for double-circuit, multiconductor faults on a moderately insulated line with very low towers. Thus, virtually the whole range of possible backflash events has been recorded, and these events are fully con-

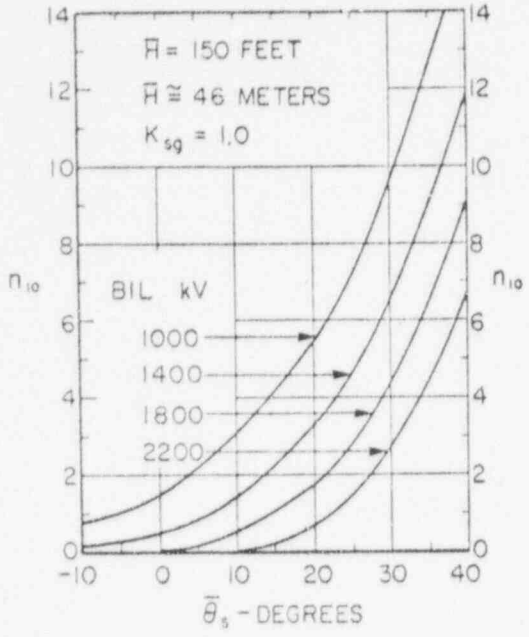

FIG. 17

Courbes d'estimation correspondant aux déclenchements dus à une défaillance de l'effet d'écran pour des lignes ayant une protection inefficace

Estimating curves for shielding-failure trip-outs for lines with ineffective shielding

Feet = Pieds
Meters = Mètres
Degrees = Degrés

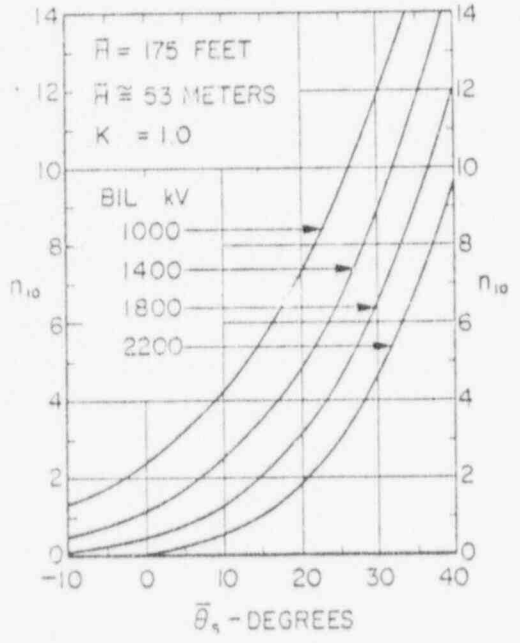

FIG. 18

Courbes d'estimation correspondant aux déclenchements dus à une défaillance de l'effet d'écran pour des lignes ayant une protection inefficace

Estimating curves for shielding-failure trip-outs for lines with ineffective shielding

Feet = Pieds
Meters = Mètres
Degrees = Degrés

vité pour des défauts sur des lignes deux ternes à plusieurs conducteurs faiblement isolées et équipées de pylônes très bas. Ainsi, la totalité du domaine des phénomènes possibles d'amorçage secondaires a été virtuellement enregistrée et ces phénomènes sont tout à fait compatibles avec la théorie existant déjà et couramment admise. Les variables sont même plus nombreuses que celles de la théorie de la protection, et ce n'est que récemment qu'un progrès appréciable a été fait pour la détermination des répartitions en fréquence et en amplitude des courants de foudre des formes d'onde et des vitesses maximales d'accroissement du courant [10]. Cette étude ainsi que celle de [8] montre l'importance que l'on continue à attacher à la recherche dirigée vers une meilleure connaissance des dispositifs de

sistent with past and currently-accepted theory. The variables are even more numerous than those of shielding theory, and it is only recently that substantial progress is being made in defining lightning current amplitude frequency distributions, wave shapes and maximum rates of current rise [10]. Both this study and that of [8] indicate the continuing importance of research directed toward better knowledge of grounding systems for high-resistivity soils and of the fundamental properties of soil as a frequency-sensitive lossy dielectric.

mise à la terre pour les terrains à forte résistivité et des propriétés fondamentales du terrain en tant que diélectrique affaiblissant et sensible à la fréquence.

9. — Conclusions.

9.1. — Dépendant des conditions géométriques du pylône, du profil de la ligne et du terrain, du niveau d'isolement et de l'impédance du pylône par rapport à la terre lointaine, les mécanismes de défaillance de l'effet d'écran et d'amorçage secondaire peuvent contribuer tous les deux d'une façon significative au taux de déclenchement par coup de foudre.

9.2. — Les défauts dus à une défaillance de l'effet d'écran prédominent dans le taux de déclenchement par coup de foudre lorsque des angles de protection importants se trouvent associés à des conducteurs élevés et à des résistances de pied de pylônes faibles.

9.3. — Les défauts dus à des phénomènes d'amorçage secondaire prédominent dans le taux de déclenchement par coup de foudre lorsque des impédances de pylône élevées se trouvent associées à des niveaux d'isolement faibles et à de faibles hauteurs de conducteurs.

9.4. — Les défaillances de l'effet d'écran peuvent être réduites à des phénomènes rares lorsque les angles de protection des câbles de garde sont convenablement associés avec les hauteurs et les espacements des conducteurs de phase et des câbles de garde. Etant donné que cette association est d'une nature statistique, il faut prévoir une marge convenable dans le dispositif de protection pour permettre des écarts géométriques et électriques par rapport au modèle analytique de référence.

9.5. — Les phénomènes d'amorçage secondaire peuvent être réduits à des phénomènes rares grâce à des techniques bien connues de protection mises au point pendant une période d'environ 40 ans. Alors que la ligne « garantie contre la foudre » reste un but illusoire, des taux de déclenchement spécifiques de 0,25 et moins ont été obtenus dans des régions ayant en moyenne 40 journées d'orage par an. De tels taux de déclenchement sont associés à une protection efficace et à une impédance faible du pylône par rapport à la terre.

9.6. — La mise au point d'une protection efficace devrait être basée sur un terrain nu, un profil de ligne donné et des angles de sol moyens, en considérant les influences des forêts et des autres perturbations de la surface du sol comme des différences favorables.

9.7. — Des recherches supplémentaires concernant la distance d'amorçage sont nécessaires pour les courants critiques élevés résultant des niveaux d'isolement accrus et des impédances caractéristiques de conducteur réduites dans les lignes à ultra-haute tension proposées. Pour éliminer les incertitu-

9. — Conclusions.

9.1. — Depending on conditions of tower geometry, line profile and terrain, insulation level and tower indicial impedance to remote ground, both the shielding failure and backflash mechanisms can contribute significantly to the lightning trip-out rate.

9.2. — Shielding failure faults dominate the lightning trip-out rate when large shielding angles are associated with high conductors and low tower footing resistances.

9.3. — Backflash event faults dominate the lightning trip-out rate when high tower impedances are associated with low insulation levels and low conductor heights.

9.4. — Shielding failures can be reduced to rare events when the shielding angles of the ground (shield) wires are properly co-ordinated with the heights and spacings of phase conductors and ground wires. Because this co-ordination is statistical in nature, a suitable margin should be provided in the shielding design to allow for geometrical and electrical deviations from the reference analytical.

9.5. — Backflash events can be reduced to rare events through well-known techniques of protection developed over a period of approximately 40 years. While the « lightning-proof » line remains an elusive goal, specific trip-out rates of 0.25 and lower have been achieved in areas having mean incidence of 40 thunderstorm days per year. Such trip-out rates are associated with effective shielding and low tower indicial impedance to earth.

9.6. — Design for effective shielding should be based on nominally bare earth, the line profile and mean ground angles, leaving the effects of forestation or other surface perturbations as favorable deviations.

9.7. — Additional investigation of striking distance is required for the high critical currents resulting from the increased insulation levels and reduced conductor surge impedances of proposed UHV lines. To eliminate the uncertainties associated with the extrapolation of present analytical models to the

des correspondant à l'extrapolation des modèles analytiques actuels au domaine ultra-haute tension, il est fortement recommandé d'utiliser des *angles de protection négatifs* tels que ceux qui conviennent pour des lignes à très haute tension.

9.8. — Des recherches supplémentaires sont recommandées pour améliorer la connaissance des propriétés fondamentales de la terre en tant que diélectrique affaiblissant et sensible à la fréquence et pour appliquer cette connaissance à la mise au point de dispositifs améliorés de mise à la terre des pylônes.

UHV domain, it is highly recommended that negative shielding angles, *such as those adequate for EHV lines, should be used.*

9.8. — Additional research is recommended to improve knowledge of the fundamental properties of the earth as a frequency-sensitive lossy dielectric and to apply this knowledge to the design of improved tower grounding systems.

10. — Remerciements.

L'Institut Electrique Edison et les compagnies qui en font partie ont fourni une participation directe aux recherches expérimentales et statistiques. Nous remercions chaleureusement la Bonneville Power Administration et la Tennessee Valley Authority pour leur coopération et pour les données statistiques très importantes qu'elles nous ont fournies. La coopération de nombreuses personnes, particulièrement des membres des Comités de la CIGRE et de l'IEEE ainsi que de sociétaires de l'Institut de Recherche IIT a été particulièrement appréciée.

Les compagnies membres de l'EEI ayant participé directement à l'étude expérimentale réelle ont été :

American Electric Power Corporation
Atlantic City Electric Company
Carolina Power and Light Company
Commonwealth Edison Company
The Detroit Edison Company
Florida Power Corporation
New England Electric System
Ohio Valley Electric Corporation
Public Service Company of Colorado
Texas Electric Service Company
Union Electric Company
Virginia Electric and Power Company

Nous remercions sincèrement les responsables de projets dans ces compagnies et toutes les personnes qui ont contribué à la recherche, l'enregistrement et la vérification de valeurs réelles.

10. — Acknowledgements.

The Edison Electric Institute and its member companies have furnished direct participation in the experimental and statistical investigations. The cooperation of the Bonneville Power Administration and of the Tennessee Valley Authority in furnishing very extensive statistical data is gratefully acknowledged. The co-operation of many individuals, particularly members of CIGRÉ and IEEE committees and associates at the IIT Research Institute is especially appreciated.

EEI member companies participating directly in the field experimental study were :

American Electric Power Corporation
Atlantic City Electric Company
Carolina Power and Light Company
Commonwealth Edison Company
The Detroit Edison Company
Florida Power Corporation
New England Electric System
Ohio Valley Electric Corporation
Public Service Company of Colorado
Texas Electric Service Company
Union Electric Company
Virginia Electric and Power Company.

We sincely thank the project representatives for these companies and all the persons who worked at patrolling, reporting and verifying field data.

BIBLIOGRAPHIE — REFERENCES

[1] AIEE Committee Report, "A Method of Estimating the Lightning Performance of Transmission Lines", (*AIEE Trans., Power Apparatus and Systems*, vol. PAS-69 Part II, 1950, pp. 1187-1196).

[2] WHITEHEAD, E. R. — "Final Report of Edison Electric Institute Research Project RP 50-Mechanism of Lightning Flashover", (Edison Electric Institute, 90 Park Avenue, New York, N.Y. 10016. EEI Publication No. 72-900.

[3] Ohio Brass Company, Mansfield, Ohio, *Lightning Performance of Typical Transmission Lines*, Second Edition, 1955.

[4] CHAMBERS, F. and ALMON, Jr., C. P. — "Performance of 161 kV and 115 kV Transmission Lines", (*AIEE Trans. Power Apparatus and Systems*, vol. 81, 1962 (pp. 431-459). (Supplementary data furnished by private correspondence).

[5] LEVITOV, V. I., et *al.*, — "Operational Experience on the 500 kV Networks in the USSR.". (Report No. 416, *CIGRE Proceedings*, Paris, France, 1966).

[6] ARMSTRONG, H. R. and WHITEHEAD, E. R. — "Field and Analytical Studies of Transmission Line Shielding", (*IEEE Trans. Power Apparatus and Systems*, vol. PAS-87, 1968, pp. 270-281).

[7] BROWN, G. W. and WHITEHEAD, E. R. — "Field and Analytical Studies of Transmission Line Shielding-Part II", (*IEEE Trans. Power Apparatus and Systems*, vol. 88, 1969, pp. 617-626).

[8] WHITEHEAD, E. R. — "Progress Report on CIGRE Working Group 33-01 Survey of the Lightning Performance of EHV Lines". (Presented as an Internal Working Document to the Working Group Meeting at Barbizon, France, 24-26 August, 1972).

[9] WITEHEAD, E. R. — "Supplementary Report of Edison Electric Institute Research Project RP 50-Mechanism of Lightning Flashover", (Edison Electric Institute, 90 Park Avenue, New York, N. Y. 10016).

[10] POPOLANSKY, F. — "Frequency Distribution of Amplitudes of Lightning Currents", (*Electra*, No. 22 May 1972, pp. 139-147).

REF. 26

TOUR D'HORIZON DE LA CIGRÉ CONCERNANT LES PERFORMANCES DES LIGNES DE TRANSPORT A TRES HAUTE TENSION VIS-A-VIS DES COUPS DE FOUDRE

rédigé par E.R. WHITEHEAD

pour le Groupe de Travail 33.01
du Comité d'Etudes n° 33
(Surtensions et coordination de l'isolement),
et publié à la demande du Président du Comité

M. V. PALVA

1. Introduction.

Au cours de l'année 1968, un Groupe de Travail présidé par le Dr. R.H. Golde a établi un questionnaire conçu pour permettre l'analyse des performances des lignes de transport à très haute tension vis-à-vis des coups de foudre avec une précision nettement plus grande que celle des tours d'horizon analogues pour les lignes de transport à haute tension.

Le questionnaire fut envoyé en avril 1968 aux représentants de 27 pays. Vers le milieu de 1969, on avait reçu de 15 pays des signes d'intérêt et de volonté de coopération. A cause de son départ en retraite imminent, le Dr. Golde demanda à être relevé de ses fonctions et le Dr. E.R. Whitehead fut d'accord pour continuer cette tâche étant donné sa proximité avec le projet de recherche RP 50 de l'Institut Electrique Edison. L'organisation des mesures et les méthodes analytiques propres à cette recherche ont été avantageusement combinées avec celles de ce tour d'horizon.

Ce rapport résume et analyse la quantité très importante de données rassemblées par ce tour d'horizon et présente les conclusions tirées des résultats par l'auteur. L'auteur s'est cependant efforcé de présenter ces résultats sous des formes qui facilitent leur étude dans le cadre des progressions possibles concernant la théorie et la pratique de la protection contre les coups de foudre.

2. Les pays participants et la taille des échantillons.

Les représentants des pays participants ont fourni leurs renseignements sous des formes qui s'adaptaient le mieux à leurs systèmes d'enregistrement. Dans certains cas, les données furent indiquées pour des lignes de transport individuelles tandis que dans d'autres cas, elles furent fournies pour un ensemble de lignes d'une tension donnée. Pour cette

CIGRE SURVEY OF THE LIGHTNING PERFORMANCE OF EXTRA-HIGH-VOLTAGE TRANSMISSION LINES

prepared by E. R. WHITEHEAD

for Working Group 33.01 of Study Committee No. 33
(Overvoltages and Insulation Coordination)
and published at the request of the Chairman
of the Committee

Mr. V. PALVA

1. Introduction.

During the year 1968 a Task Force chaired by Dr. R.H. Golde developed a questionnaire designed to permit the analysis of the lightning performance of EHV transmission lines with substantially greater refinement than that of similar surveys of HV transmission lines.

In April 1968, the questionnaire was sent to representatives of 27 countries. By mid-1969 indications of interest and cooperation were received from 15 countries. Because of impending retirement, Dr. Golde asked to be relieved of this assignment, and Dr. E.R. Whitehead agreed to continue the work because of its close relationship to the Edison Electric Institute Research Project RP 50. The data organization and analytical methods of that research have been combined with those of the survey advantageously.

This report summarizes and analyzes the very large amount of data developed by the survey, and presents the author's conclusions from the results. The author has, however, endeavoured to present the data in forms which facilitate their study in connection with possible advances in lightning protection theory and practice.

2. Participating countries and sample size.

The representatives of participating countries have submitted their data in forms most compatible with their record-keeping systems. In some cases data were submitted for individual transmission lines, while in others data were furnished for all lines at a given voltage. For this reason, all data are grouped under Reporting Units *as received. Table I*

TABLEAU I — TABLE I

Tableau des pays participants et de leurs rapports élémentaires

Participating countries and their tabulated reporting units

Pays – *Countries*		Rapports élémentaires *Reporting Units*
AUS	Australie – *Australia*	41 - 47, 63 - 82
CAN	Canada	85 - 89
CZ	Tchécoslovaquie – *Czechoslovakia*	84
DEN	Danemark – *Denmark*	90 - 91
FIN	Finlande – *Finland*	110 - 121
I	Italie – *Italy*	48 - 50
JAP	Japon – *Japan*	105 - 108
N	Norvège – *Norway*	10
POL	Pologne – *Poland*	83
RSA	Afrique du Sud – *South Africa*	1 - 9, 11 - 23
RHO	Rhodésie – *Rhodesia*	57 - 62
SWE	Suède – *Sweden*	92 - 104
UK	Royaume Uni – *United Kindom*	109
USA	Etats-Unis – *United States*	24 - 40
ZAM	Zambie – *Zambia*	51 - 55

TABLEAU II — TABLE II

Dimension des échantillons

Sample size

Pays *Countries*	15
Rapports élémentaires *Reporting units*	121
Kilomètres de lignes aériennes *Kilometres of tower line*	22.409
Années - kilomètres *Kilometre - years*	171.112
Nombre moyen d'années *Mean years*	7.636
Rapports élémentaires ayant fait l'objet d'une analyse quantitative *Units quantitatively analyzed*	41
Années - kilomètres analysées *Kilometre - years analyzed*	120.065
Période maximale d'observation en années *Longest observation period - years*	25
Tensions des lignes en kilovolts *Line voltages, kilovolts*	220-735

raison, toutes les valeurs sont groupées telles qu'elles furent reçues en *rapports élémentaires*. Le tableau I donne la liste des pays participants et indique les rapports élémentaires correspondants.

Dans quelques cas, le détail des résultats ne fut pas présenté sous forme de tableau correspondant

lists participating countries and the corresponding reporting units.

In a few cases, the detailed data were not tabulated for numbered reporting units either because

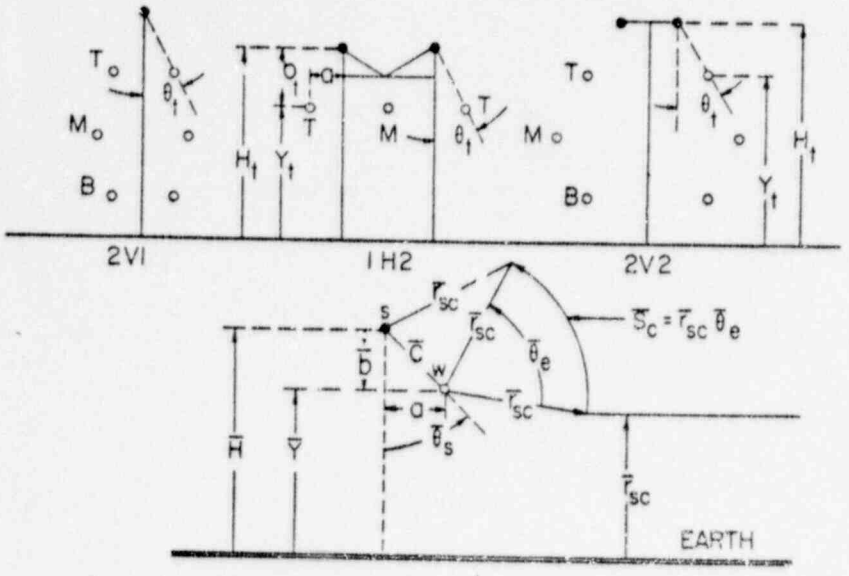

FIG. 1
Principales dispositions de conducteurs
Principal conductor configurations.

à des rapports élémentaires numérotés soit à cause de la faible dimension de l'échantillon soit par suite du manque d'informations suffisantes. Ces cas sont convenablement signalés.

2.1. *Principales configurations de conducteurs.*

La figure 1 représente les principales configurations de conducteurs pour les lignes de transport ayant fait l'objet de ce tour d'horizon. Elles couvrent 95 % des rapports élémentaires et 97 % des années-kilomètres. Cette figure montre aussi la géométrie unissant les paramètres moyens utilisés dans l'analyse de l'effet d'écran.

3. Discussion.

3.1. *Les limites des valeurs et des analyses.*

Bien que l'on pense que le questionnaire soit dans sa conception probablement le plus complet dans son genre qui ait jamais été mis en circulation, il possède des limitations propres concernant l'efficacité avec laquelle les valeurs peuvent être obtenues et analysées. Pour des lignes construites dans un passé récent, il n'est pas possible de disposer de la période minimale d'observation désirée de cinq ans. Même pendant une telle période, il est tout à fait possible que les taux moyens de déclenchement sur coups de foudre observés varient dans le rapport 2 par rapport à la moyenne « vraie » à long terme lorsque cette valeur est très faible. Plus on souhaite que l'analyse soit quantitative, plus il est nécessaire que les données utilisées soient stables. Pour quelques rapports élémentaires, il est simplement impossible de recueillir les données avec le détail requis pour une analyse efficace.

Les considérations développées dans le paragraphe suivant conduisent naturellement aux concepts de :

of small sample size or lack of sufficient information. These are suitably noted.

2.1. Principal conductor configurations.

Figure 1 shows the principal conductor configurations for the transmission lines of the survey. These cover 95 per cent of the reporting units and 97 per cent of the kilometer-years. This figure also shows the geometry relating the mean parameters used in the analysis of shielding.

3. Discussion.

3.1. Limitations on data and analyses.

Although it is thought that the design of the questionnaire is probably the most complete for its purpose that has ever been circulated, there are inherent limitations on the effectiveness with which the data can be obtained and analyzed. For lines built in the recent past, a desired minimum of a five-year observation period may not be available. Even for this period it is quite possible for the observed mean lightning outage rates to vary by a factor of two from the "true" long-time mean when this value is very low. The more quantitative one wishes the analysis to be, the more stable must be the data used. For a few reporting units the data are simply not available in the detail required for effective analysis.

The considerations of the foregoing paragraph lead naturally to the concepts of

3.1.1. Analyse quantitative.

3.1.2. Analyse qualitative.

Ces concepts sont utiles pour maintenir une façon convenable de prendre les choses en considération lorsqu'on évalue les nombreuses données entrant dans le tour d'horizon. Il est clair que les taux de déclenchement sont quantitatifs, mais on ne peut pas toujours les regrouper d'une façon telle qu'il soit possible de déduire avec certitude l'influence des paramètres de structure ou d'environnement. D'autre part, des considérations qualitatives déduites des études théoriques ou expérimentales peuvent aider à déterminer des paramètres de ligne appropriés pour une évaluation quantitative et faire entrevoir des processus permettant d'effectuer des recherches sur les anomalies apparentes.

3.1.1. *Quantitative analysis.*

3.1.2. *Qualitative analysis.*

These concepts are useful in maintaining a proper perspective when evaluating the many data of the survey. Clearly the tripout rates are quantitative, but it is not always possible to group them in such a manner that the influence of structural or environmental factors can be reliably deduced. On the other hand, qualitative considerations derived from theoretical or experimental studies can assist in the development of appropriate line parameters for quantitative evaluation and suggest ways in which apparent discrepancies can be investigated.

3.2. *Déclenchements par défaillance de l'effet d'écran.*

Les résultats du présent tour d'horizon viennent étayer les conclusions d'autres études d'ensemble [8.1, 8.2] selon lesquelles des performances exceptionnelles de lignes haute tension et très haute tension vis-à-vis de la foudre nécessitent que ces lignes soient « efficacement protégées ». Indépendamment du modèle analytique particulier employé, la théorie « électro-géométrique » de l'effet d'écran sur les lignes de transport requiert, pour un effet d'écran efficace, une diminution des angles moyens de protection proportionnelle à l'augmentation de la hauteur moyenne du conducteur. Réciproquement, pour un angle moyen de protection donné, le taux de déclenchement correspondant aux défaillances de l'effet d'écran augmente rapidement avec la hauteur moyenne des conducteurs. Ce taux de défaillance de l'effet d'écran est très sensible à l'influence du *profil* de la ligne, du *terrain* avoisinant et, dans les études analytiques, de la *distance d'amorçage* correspondant à la valeur prévue du courant de foudre à la terre.

3.2. Shielding failure tripouts.

The results of the present survey support the conclusion of other extensive studies [8.1] [8.2] that exceptional lightning performance of HV and EHV lines requires that the line be " effectively shielded ". Regardless of the particular analytical model employed, the " electro-geometric " theory of transmission line shielding requires that mean shielding angles decrease as mean conductor heights increase for effective protection. Conversely, for a fixed mean shielding angle the tripout rate associated with shielding failure increases sharply with mean conductor height. This shielding failure rate is substantially affected by the influence of the line profile, *the contiguous* terrain *and, in analytical studies, by the* striking distance *associated with the prospective lightning current to earth.*

3.2.1. *Influence du profil.*

Pour les besoins de ce rapport, le terme *profil* correspond à la hauteur variable des conducteurs le long d'un tracé suivant l'axe de la ligne. On suppose que la surface du sol est nue et unie. Pour certains rapports élémentaires (30 - 31 - 32), le profil de la ligne et les hauteurs correspondantes des conducteurs sont connus avec beaucoup de précision tandis que pour d'autres on ne dispose que de peu de renseignements. Dans le cadre de ce rapport, trois catégories générales de profil furent définies de la façon suivante :

Plat : Hauteur moyenne des conducteurs égale à la hauteur au droit du pylône diminuée des deux tiers de la flèche des conducteurs.

Ondulé : Hauteur moyenne des conducteurs égale à leur hauteur au droit du pylône.

Montagneux : Hauteur moyenne des conducteurs égale au double de la hauteur des conducteurs au droit du pylône.

3.2.1. The profile effect.

For the purpose of this report, the term profile *refers to the variable elevation of the conductors along a path centered on the line route. The earth surface is assumed to be bare and smooth. For some of the reporting units (30-31-32) the line profile and the derived conductor heights are known very accurately while for others little information is available. For reporting purposes, three general classes of profile were defined as*

Flat : *Mean conductor height equal to height at the tower minus two thirds the conductor sag.*

Rolling : *Mean conductor height equal to that at the tower.*

Mountainous : *Mean conductor height equal to double the conductor height at the tower.*

La répartition des profils selon ces catégories, exprimée en pourcentages approximatifs, est l'un des ensembles de données demandées dans le questionnaire. L'application de ce renseignement est illustrée dans un exemple de calcul traité à l'annexe 7.1. On peut estimer d'après la répartition des profils et d'après un pylône ayant des dimensions représentatives, les hauteurs moyennes des conducteurs et des câbles de garde.

3.2.2. *Influence du terrain.*

Le terme *terrain* utilisé dans ce rapport correspond à des éléments tels que des *forêts* entourant la ligne, un paysage *ouvert* caractérisé par des pâturages ou de la broussaille basse, un paysage *boisé* caractérisé par des bosquets d'arbres épars ne répondant pas au terme plus fort de forêt. Il est évident qu'il devient impossible d'affecter un indice numérique significatif aux caractéristiques du terrain bien que leurs influences puissent se refléter dans les chiffres de performances. Il est clair qu'au cours de l'analyse de ces paramètres on doit aussi inclure dans le terme *terrain* des particularités telles que le parallélisme de deux lignes et l'existence de constructions le long du tracé de la ligne. Il faut dire à cette occasion qu'il est possible de simuler les caractéristiques du terrain dans les études sur calculateur des performances des lignes [8.4]. Etant donné l'impossibilité d'exprimer numériquement les influences du terrain dans la présente étude, ces influences seront identifiées qualitativement lorsqu'elles apparaîtront afin d'en tenir compte dans les performances apparemment anormales.

3.2.3. *Influence de la distance d'amorçage.*

Il est évident que l'influence de la distance d'amorçage ne se reflète qu'indirectement dans les valeurs de performances de ce tour d'horizon et ce en correspondance seulement implicite avec l'influence de la hauteur et de l'angle de protection. Les études de [8.1] sont basées sur les distances d'amorçage.

$$\bar{r}_{ac} = 6{,}7\ I_{oc}^{4/5} \quad \text{distance moyenne d'amorçage}$$
$$r_{ac} = 6{,}0\ I_{oc}^{4/5} \quad \text{distance d'amorçage effective} \qquad (1)$$
et $I_{oc} \cong 1{,}1\ I_c$ courant à terre possible

Des études récentes menées par l'auteur et ses assistants ont conduit à affiner comme suit les relations concernant la distance d'amorçage [8.3]

$$\bar{r}_{ac} = 9{,}4\ I_{oc}^{2/3} \quad \text{distance moyenne d'amorçage}$$
$$r_{ac} = 8{,}5\ I_{oc}^{2/3} \quad \text{distance d'amorçage effective} \qquad (2)$$

Les équations (2) ne sont elles-mêmes que de bonnes approximations des relations plus précises suivantes :

$$\bar{r}_{ac} = 21 + 30\ [1 - \exp(I_{oc}/6)]$$
$$r_{ac} = 1{,}81 + 27\ [1 - \exp(I_{oc}/6)] \qquad (3)$$

The distribution of the profile among these classes, in estimated percentages, is one of the sets of data requested in the questionnaire. The application of this information will be illustrated in a sample calculation in Appendix 7.1. From the profile distribution and a representative dimensioned tower, the mean heights of the conductors and ground wires can be estimated.

3.2.2. The terrain effect.

The term terrain, *as used in this report, refers to such features as* forests *contiguous to the line, open countryside characterized by grassland or low bush,* wooded, *characterized by occasional groves of trees not requiring the stronger term,* forest. *It is evident that it becomes impossible to assign a meaningful numerical index to terrain features, though their effects may be reflected in the performance data. During the analysis of these data it became clear that such features as parallel lines and buildings along the line route must also be included in the term* terrain. *It should be mentioned in passing that terrain features can be simulated in computer studies of line performance [8.4]. Because of the impossibility of quantifying the effects of terrain in the present study, these effects will be qualitatively identified where they appear to account for apparently anomalous performance.*

3.2.3. Striking distance effect.

Obviously, the striking distance effect is reflected only indirectly in the performance data of the survey and this only implicitly in relation to the effects of height and shielding angle. The studies of [8.1] are based on striking distances

$$\bar{r}_{ac} = 6{,}7\ I_{oc}^{4/5} \quad \textit{mean striking distance}$$
$$r_{ac} = 6{,}0\ I_{oc}^{4/5} \quad \textit{effective striking distance} \qquad (1)$$
and $I_{oc} \cong 1{,}1\ I_c$ *prospective current to earth*

Recent studies by the author and his students have led to refinement in the striking distance relation as follows [8.3]

$$\bar{r}_{ac} = 9{,}4\ I_{oc}^{2/3} \quad \textit{mean striking distance}$$
$$r_{ac} = 8{,}5\ I_{oc}^{2/3} \quad \textit{effective striking distance} \qquad (2)$$

Equations (2) are themselves close approximations to the more accurate relations

$$\bar{r}_{ac} = 21 + 30\ [1 - \exp(I_{oc}/6)]$$
$$r_{ac} = 1{,}81 + 27\ [1 - \exp(I_{oc}/6)] \qquad (3)$$

Tableau III — Table III

Performances et paramètres correspondant à 41 rapports élémentaires représentatifs

Performance and parameters for 41 representative reporting units

N° *Data Unit*	Années km Km Years	TTR (10)	U kV	U_c(50 %) kV	$\bar{R}$ Ohms	$\bar{Z}_c$ Ohms	H_s m	Y_s m	S_g m	S_c m	a m	θ_s deg	% F	Profile K	M	$\bar{H}$ m	$\bar{\epsilon}$ m	$\bar{C}$ m	$\bar{\theta}_e$ deg	$\bar{\theta}_e$ rad	$Y\theta_e$ m	I_c kA	r_{ac} m	$\bar{r}_{ac}$ m	$\bar{Y}/\bar{r}_{ac}$	$\bar{Y}/\bar{r}_{ac}$	$\bar{C}/\bar{r}_{ac}$	$\bar{C}/\bar{r}_{ac}$	$\bar{\theta}_{ac}$ deg	$\hat{\theta}_{ac}$ deg	$\hat{\theta}_{ac}$ rad	$\hat{S}_c$ rad	$\bar{S}_c$ m	$\hat{S}_c$ m
30	5 900	0.24	230	1 500	5	400	29	20	7.0	10.4	3.2	19	50	50	0	28.0	16.0	12.4	15	0.262	4.19	7.5	38.5	34.7	0.41	0.46	0.32	0.37	27.0	23.0	− 0.21	− 0.14	− 8.1	− 4.8
31	1 570	3.44	345	1 600	5	400	43	35	5.0	9.0	7.3	29	50	50	0	43.0	*25.0	19.4	*22	*0.384	9.60	8.0	10.0	36.0	0.62	0.70	0.48	0.53	8.4	2.1	0.24	0.35	9.6	12.6
32	1 760	5.70	345	1 600	5	400	49	41	11.0	15.0	5.3	34	75	16	9	43.4	34.4	10.5	31	0.541	18.69	8.0	10.0	36.0	0.86	0.96	0.26	0.29	0.6	− 6.0	0.53	0.65	21.2	23.4
33	790	0.25	500	2 130	25	360	33	25	9.0	12.5	2.9	20	35	40	25	38.4	20.4	10.4	16	0.279	7.92	11.8	52.2	47.0	0.55	0.60	0.20	0.22	21.0	17.2	− 0.09	− 0.02	− 4.7	− 0.9
34	660	0.38	500	2 130	25	360	33	25	9.0	12.5	2.9	20	20	35	45	41.6	34.0	10.4	16	0.279	9.65	11.8	52.2	47.0	0.66	0.74	0.20	0.22	12.1	8.6	0.07	0.13	3.6	6.1
35	590	0.60	500	2 130	25	360	33	25	9.0	12.5	2.9	20	86	14	0	28.0	18.0	10.4	16	0.279	5.02	11.8	52.2	47.0	0.34	0.38	0.20	0.22	35.5	32.6	− 0.34	− 0.29	− 17.7	− 13.6
36	660	0.76	500	2 130	25	360	33	25	9.0	12.5	2.9	20	30	40	30	40.0	39.0	10.4	16	0.279	8.37	11.8	52.2	47.0	0.58	0.64	0.20	0.22	19.1	15.3	− 0.05	− 0.16	− 2.8	− 8.6
39	3 340	0.19	345	1 600	5	360	34	27	7.0	17.3	− 3.5	− 19	100	0	0	29.3	15.5	14.4	− 15	− 0.262	− 4.06	8.9	33.0	38.7	0.36	0.40	0.34	0.38	30.0	26.0	− 0.78	− 0.72	− 33.8	− 27.7
40	4 360	0.09	220	1 580	12	400	37	19	7.0	10.0	2.0	18	0	100	0	27.0	19.0	8.3	14	0.244	4.67	7.9	29.8	35.8	0.16	0.53	0.21	0.23	25.3	21.3	− 0.29	− 0.13	− 7.9	− 4.6
43	960	0.00	330	1 585	20	360	27	22	13.0	17.0	2.9	30	20	70	10	31.5	23.9	8.2	21	0.366	8.75	8.8	42.7	38.4	0.56	0.62	0.19	0.21	20.7	16.3	0.00	0.03	0.0	3.1
41	960	0.00	330	1 585	16	360	27	22	13.0	17.0	2.9	30	20	70	10	31.5	23.9	8.2	21	0.366	8.75	8.8	42.7	38.4	0.56	0.62	0.19	0.21	20.7	16.3	0.00	0.03	0.0	3.1
45	724	0.00	500	2 025	3	320	36	27	7.9	13.8	3.8	29	20	75	5	41.4	26.5	15.4	14	0.244	6.67	12.6	54.5	49.0	0.49	0.54	0.28	0.31	22.6	18.4	− 0.15	− 0.08	− 8.2	− 3.3
51	1 476	0.47	330	1 470	13cc	360	35	26	14.0	17.5	4.1	23	59	19	22	36.2	24.8	12.1	20	0.349	8.65	8.2	30.8	36.7	0.61	0.68	0.30	0.33	14.4	9.7	0.19	0.18	4.0	6.6
52	1 320	0.04	330	1 470	20cc	360	35	26	14.0	17.5	4.1	23	77	10	13	31.8	20.4	12.1	20	0.349	7.12	8.2	30.8	36.7	0.50	0.56	0.30	0.33	21.4	16.5	− 0.02	0.06	− 1.0	2.2
56	3 676	0.31	330	1 470	16cc	360	35	26	14.0	17.5	4.1	23	100	0	0	25.7	14.3	12.1	20	0.349	4.99	8.2	30.8	36.7	0.35	0.39	0.30	0.33	32.0	28.0	− 0.21	− 0.14	− 8.5	− 5.1
57	3 108	0.29	330	1 470	21cc	360	35	26	14.1	17.5	4.1	23	80	13	7	30.0	18.3	12.1	20	0.349	6.46	8.2	30.8	36.7	0.45	0.50	0.30	0.33	24.8	20.4	− 0.08	− 0.01	− 3.9	− 0.2
58	3 876	0.33	330	1 470	22cc	360	35	26	14.1	17.5	4.1	23	83	11	6	29.3	17.5	12.1	20	0.349	6.25	8.2	30.8	36.7	0.44	0.49	0.30	0.33	25.4	21.0	− 0.09	− 0.02	− 3.8	− 0.6
64	1 260	0.50	330	1 570	30dc	360	28	21	12.0	15.0	2.9	23	10	40	50	39.5	30.5	9.5	18	0.314	9.58	8.7	32.4	38.2	0.72	0.80	0.22	0.24	10.0	4.5	0.14	0.23	5.9	10.0
65	1 337	0.40	330	1 570	12dc	360	28	21	12.0	15.0	2.9	23	10	80	10	41.1	22.1	9.5	18	0.314	6.91	8.7	32.4	38.2	0.52	0.58	0.22	0.24	22.4	18.0	− 0.08	0.00	− 3.2	0.0
66	1 464	0.19	330	1 570	26dc	360	28	21	12.0	15.0	2.9	23	10	90	0	29.0	20.0	9.5	18	0.314	6.28	8.7	32.4	38.2	0.47	0.52	0.22	0.24	25.7	21.7	− 0.13	− 0.07	− 5.7	− 2.5
67	1 504	0.36	330	1 570	20dc	360	28	21	12.0	15.0	2.9	23	10	90	0	29.0	20.0	9.5	18	0.314	6.28	8.7	32.4	38.2	0.47	0.52	0.22	0.24	25.7	21.7	− 0.13	− 0.07	− 5.7	− 2.5
80	1 600	0.21	330	1 570	12dc	360	28	21	12.0	15.0	2.9	23	30	30	40	35.4	26.4	9.5	18	0.314	6.29	8.7	32.4	38.2	0.62	0.69	0.22	0.24	16.1	11.0	0.03	0.12	1.4	4.7
81	3 060	0.51	300	1 610	10cc	360	30	18	7.5	9.4	5.6	25	60	30	10	29.0	16.0	14.5	21	0.302	6.43	8.9	33.0	38.7	0.37	0.41	0.34	0.38	29.2	24.4	− 0.11	0.02	− 4.6	− 0.9
85	5 200	1.04	315	1 300	30cc	400	43	34	7.0	11.0	2.2	14	0	100	0	17.6	34.0	13.8	9	0.157	5.34	6.5	31.8	31.4	0.98	1.10	0.40	0.44	− 10.4	− 19.1	0.34	0.49	11.8	15.0
86	3 256	1.60	315	1 300	30cc	400	43	34	7.0	11.0	2.2	14	0	100	0	17.6	34.6	13.8	9	0.157	5.34	6.5	31.8	31.4	0.98	1.10	0.40	0.44	− 10.4	− 19.1	0.34	0.49	11.8	15.0
87	8 600	0.00	735	2 880	30cc	320	30	27	7.0	14.0	4.8	20	0	100	0	34.7	27.0	17.3	15	0.262	7.07	18.0	68.6	61.8	0.39	0.44	0.27	0.30	29.8	25.4	− 0.26	− 0.19	− 17.7	− 11.0
88	2 570	0.20	500	1 800	110cc	360	34	24	15.3	16.8	3.9	20	50	50	0	29.6	18.4	11.8	19	0.332	6.11	10.0	46.5	41.8	0.40	0.44	0.26	0.31	29.0	23.7	− 0.18	− 0.08	− 8.0	− 3.4
89	2 345	0.31	500	1 800	110cc	360	34	24	15.3	16.8	3.9	20	50	50	0	29.6	18.4	11.8	19	0.332	6.11	10.0	46.5	41.8	0.40	0.44	0.26	0.31	29.0	23.7	− 0.18	− 0.08	− 8.0	− 3.4
92	1 357	0.21	300	1 750	− cc	360	25	17	10.2	12.9	4.7	31	89	20	0	18.0	10.0	9.3	30	0.524	5.24	9.7	45.7	41.2	0.22	0.24	0.20	0.22	45.3	43.1	− 0.27	− 0.23	− 12.6	− 9.4
93	1 568	0.42	300	1 750	− cc	360	25	17	8.3	10.6	4.7	31	70	20	10	19.3	20.0	10.4	27	0.471	4.71	9.7	45.7	41.2	0.22	0.24	0.23	0.25	41.4	41.7	− 0.53	− 0.26	− 14.0	− 10.6
94	1 557	0.45	300	1 750	− cc	360	28	18	8.3	10.3	5.5	29	75	20	5	25.4	14.0	12.7	26	0.454	6.36	9.7	45.7	41.2	0.30	0.34	0.28	0.31	36.4	32.4	− 0.18	− 0.11	− 8.3	− 4.7
95	1 401	0.19	300	1 750	− cc	360	28	18	8.3	10.3	5.5	29	70	20	10	26.7	15.3	12.7	26	0.454	6.95	9.7	45.7	41.2	0.34	0.37	0.28	0.31	33.4	30.0	− 0.13	− 0.07	− 5.9	− 2.9
96	1 458	0.00	300	1 750	− cc	360	26	18	8.3	10.3	4.7	31	60	30	10	25.3	16.0	10.4	27	0.471	7.54	9.7	45.7	41.2	0.35	0.39	0.23	0.25	33.9	30.2	− 0.12	− 0.06	− 5.5	− 2.4
97	1 701	0.38	300	1 750	− cc	360	26	18	8.3	10.3	4.7	31	60	30	10	25.3	16.0	10.4	27	0.471	7.54	9.7	45.7	41.2	0.35	0.39	0.23	0.25	33.9	30.2	− 0.12	− 0.06	− 5.5	− 2.4
98	1 872	0.64	300	1 750	− cc	360	28	18	8.3	10.3	6.0	31	80	20	0	24.2	12.8	12.9	28	0.489	6.26	9.7	45.7	41.2	0.28	0.31	0.28	0.31	38.0	34.5	− 0.18	− 0.11	− 8.0	− 4.7
99	1 862	0.10	300	1 750	− cc	360	28	18	8.3	10.3	6.0	31	80	20	0	24.2	12.8	12.9	28	0.489	6.26	9.7	45.7	41.2	0.28	0.31	0.28	0.31	38.0	34.5	− 0.18	− 0.11	− 8.0	− 4.7
105	3 828	2.47	275	1 220	24	400	30	26	9.0	12.0	3.3	14	24	15	63	36.5	*30.5	16.4	*12	*0.210	8.05	6.1	33.4	30.0	1.20	1.35	0.49	0.54	− 25.3	− 36.2	0.65	0.84	21.7	25.2
106	3 726	1.48	275	1 220	8	400	30	26	9.0	12.0	3.3	14	35	22	43	50.4	*34.4	16.4	*12	*0.210	7.22	6.1	33.4	30.0	1.04	1.15	0.49	0.54	− 16.5	− 24.4	0.50	0.63	16.6	19.0
107	6 926	2.57	275	1 220	25	400	30	26	9.0	12.0	3.3	14	24	14	62	36.2	*30.2	16.4	*12	*0.210	8.44	5.8	32.4	29.2	1.21	1.38	0.50	0.55	− 28.5	− 38.0	0.71	0.87	22.9	25.5
108	8 037	2.88	275	1 220	13	400	30	26	9.0	12.0	3.3	14	20	8	72	59.1	*33.1	16.4	*12	*0.210	9.05	6.1	33.4	30.0	1.30	1.44	0.49	0.54	− 31.5	− 41.7	0.76	0.94	25.3	28.1
109	17 844	3.55	400	1 690	4	340	50	29	11.0	11.0	10.3	26	8	92	0	30.0	*28.7	23.7	*26	*0.454	12.90	10.0	46.5	41.8	0.62	0.69	0.51	0.57	7.3	1.6	0.32	0.42	15.0	17.5

* Phase milieu pour une disposition verticale à circuit double

* *Middle phase of double circuit vertical arrangement*

$I_{ac} = 1.1\, I_c$

$\bar{r}_{ac} = 9.4\, I_{ac}^{2/3}$

$\hat{r}_{ac} = 8.5\, I_{ac}^{2/3}$

$\bar{S}_c = \bar{r}_{ac}\, \bar{\theta}_e$

$\hat{S}_c = \hat{r}_{ac}\, \hat{\theta}_e$

$I_c = \dfrac{2U(50\,\%)}{\bar{Z}}$

$\bar{\theta}_e = \bar{\theta}_s - \bar{\theta}_{ac}$

$\hat{\theta}_e = \hat{\theta}_s - \hat{\theta}_{ac}$

S_g (Portée de fil de terre)

S_g *(Sag of ground wire)*

S_c (Portée de conducteurs)

S_c *(Sag of conductor)*

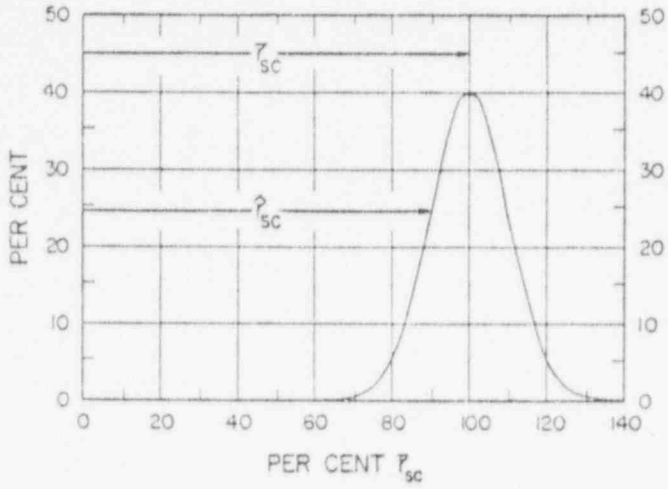

Fig. 2
Définition de $\bar{r}_{sc}$ et $\hat{r}_{sc}$.
Definition of $\bar{r}_{sc}$ and $\hat{r}_{sc}$.

Dans les équations (1) à (3) le courant est exprimé en kiloampères et la distance d'amorçage en mètres.

Les approximations (1) et (2) diffèrent d'une façon insignifiante pour les lignes à haute tension et les lignes à très haute tension. Pour la conception des lignes à ultra haute tension les équations (2) sont plus précises.

La figure 2 définit la relation entre r_{sc} et r_{sc} dans laquelle l'écart type de la répartition des distances d'amorçage est pris égal à 10 %. L'influence de ces quantités fait l'objet de la discussion du chapitre suivant.

3.2.4. *La mise en évidence des défaillances d'effet d'écran.*

Le tableau III présente les valeurs de performances et les paramètres pour 41 rapports élémentaires représentatifs. Le caractère représentatif de ces rapports est mis en évidence par leur répartition géographique étendue et leur amplitude de 120 065 années-kilomètres.

Si l'on représente les valeurs de S.T.R. (40) en fonction de la hauteur des pylônes, de la hauteur moyenne du câble de terre (câble écran), de la hauteur des conducteurs ou de l'angle de protection, aucune corrélation significative n'apparaît. Si l'on n'a aucune base analytique pour se guider, on pourra encore essayer d'obtenir un facteur de classement en partant de combinaisons arbitraires de certains paramètres. Un tel facteur est représenté par le produit de la hauteur moyenne des conducteurs par l'angle moyen de protection $Y\theta_s$. Ce facteur a les dimensions d'un arc d'exposition en mètres mais est dépourvu de toute base théorique. La figure 3 montre le résultat du relevé des S.T.R. (40) en fonction de $Y\theta_s$. Il est possible de déterminer brutalement, en-dehors d'une petite région de dispersion résiduelle, une tendance marquée et bien définie. Les deux points les plus hauts correspondent à des lignes connues d'après leur équipement pour avoir des taux de déclenchement à la foudre par défaillance de l'effet d'écran extrêmes [8.1]. On

In equations (1) through (3) current is in kiloamperes and striking distance is in meters.

The approximations (1) and (2) differ insignificantly for HV and EHV lines. For the design of UHV lines, equations (2) are more accurate.

Figure 2 defines the relation between $\bar{r}_{sc}$ and $\hat{r}_{sc}$, where the standard deviation of the striking distance distribution is taken as 10 per cent. The influence of these quantities is discussed in the next section.

3.2.4. The evidence for shielding failures.

Table III presents the performance and parameters for 41 representative reporting units. The representative character of these units is evidenced by their broad geographical distribution and their exposure of 120,065 kilometer-years.

If the S.T.R. (40) values are plotted against tower height, mean ground wire (shield wire) height, conductor height, or shielding angle, no significant correlations become apparent. If one had no analytical basis for guidance, he might seek arbitrary parameter combinations as his next effort to obtain an ordering factor. Such a factor is the product of mean conductor height and mean shielding angle, $Y\theta_s$. This factor has the dimensions of an exposure arc in meters but without theoretical foundation. Figure 3 shows the result of plotting the S.T.R. (40) against $Y\theta_s$. A definite and striking trend is abruptly established out of a small region of residual scatter. The two highest points are for lines known from instrumentation to have extreme shielding-failure lightning tripout rates. [8.1] A similar though somewhat more scattered correlation is obtained if the product of the mean ground wire height and mean shielding angle, $H\theta_s$, is used. Either of these arbitrary products suffers from the lack of an analytical base. Another deficiency lies in the fact that no

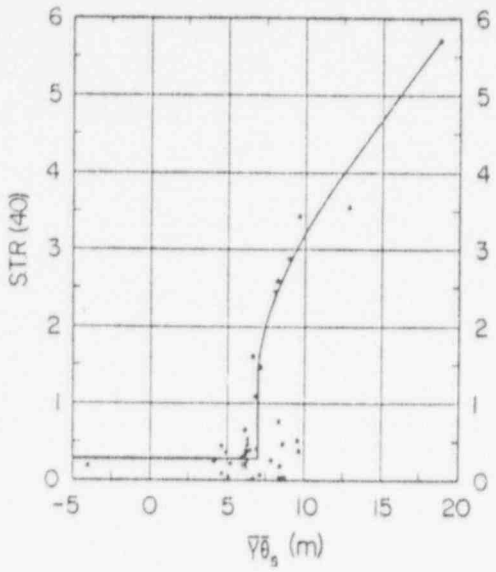

FIG. 3
Relation entre Yθ, et le S.T.R. (40).
Relation between Yθ, and S.T.R. (40).

obtient une relation analogue si l'on utilise le produit de la hauteur moyenne du fil de terre et de l'angle de protection moyen $H\theta_s$. Aussi bien l'un que l'autre de ces deux produits arbitraires souffrent du manque de base analytique. Un autre inconvénient réside dans le fait qu'il n'est tenu aucun compte du courant de seuil théorique qui peut être admis dans le conducteur et qui est donné par :

$$I_c = 2\, U_{50\,\%}/Z_c \qquad (4)$$

où I_c représente le courant critique dans le conducteur en kiloampères,
$U_{50\,\%}$ représente la rigidité diélectrique au choc critique de l'isolement de la ligne en kilovolts,
et Z_c représente l'impédance caractéristique des conducteurs en ohms.

La définition des « arcs d'exposition » est donnée à la référence [8.1]

$$\begin{aligned} \overline{S}_c &= \overline{r}_{sc}\,(\overline{\theta}_s - \overline{\theta}_{sc}) = \overline{r}_{sc}\,\overline{\theta}_e \\ \overline{\theta}_e &= (\overline{\theta}_s - \overline{\theta}_{sc}) \end{aligned} \qquad (5)$$

où S_c est un arc de référence associé à la distance moyenne d'amorçage r_{sc} et à l'angle « excédentaire » θ_e. D'une façon analogue,

$$\hat{S}_c = \hat{r}_{sc}\,(\hat{\theta}_s - \hat{\theta}_{sc}) = \hat{r}_{sc}\,\hat{\theta}_e \qquad (6)$$

est défini d'après la distance effective d'amorçage et l'angle excédentaire correspondant.

La figure 4 indique la relation entre S_c en mètres et la valeur de S.T.R. (40). Si la distance d'amorçage et l'angle de protection étaient des quantités précises, il ne pourrait pas y avoir de défaillance de l'effet d'écran pour des arcs de référence négatifs. Etant donnée la distribution des distances d'amorçage suggérée par la figure 2, il est logique de s'attendre à quelques défaillances de l'effet d'écran pour de faibles valeurs négatives de S_c et pour un terrain dégagé. La figure 4 semble confirmer ce point de vue.

La figure 5 montre la relation entre S_c et la valeur correspondante de S.T.R. (40), et les défaillances

account is taken of the theoretical threshold current which can be accepted by the conductor given by

$$I_c = 2\, U_{50\,\%}/Z_c \qquad (4)$$

where I_c is the critical current into the conductor in kiloamperes,
$U_{50\,\%}$ is the critical impulse strength of the line insulation in kilovolts,
and Z_c is the surge impedance of the conductor in ohms.

Reference [8.1] defines " exposure arcs "

$$\begin{aligned} \overline{S}_c &= \overline{r}_{sc}\,(\overline{\theta}_s - \overline{\theta}_{sc}) = \overline{r}_{sc}\,\overline{\theta}_e \\ \overline{\theta}_e &= (\overline{\theta}_s - \overline{\theta}_{sc}) \end{aligned} \qquad (5)$$

where S_c is a reference arc associated with the mean striking distance r_{sc} and the " excess " angle θ_e. In a similar manner

$$\hat{S}_c = \hat{r}_{sc}\,(\hat{\theta}_s - \hat{\theta}_{sc}) = \hat{r}_{sc}\,\hat{\theta}_e \qquad (6)$$

is defined for the effective striking distance and its corresponding excess angle.

Figure 4 shows the relation between S_c in meters and the S.T.R. (40). If the striking distance and shielding failures for small negative values of S_c be no shielding failures for negative reference arcs. Because of the distribution of striking distances suggested by Figure 2, it is logical to expect some shielding failures for smalle negative values of S_c and open terrain. Figure 4 appears to support this view.

Figure 5 shows the relation between S_c and the corresponding S.T.R. (40), and shielding failures

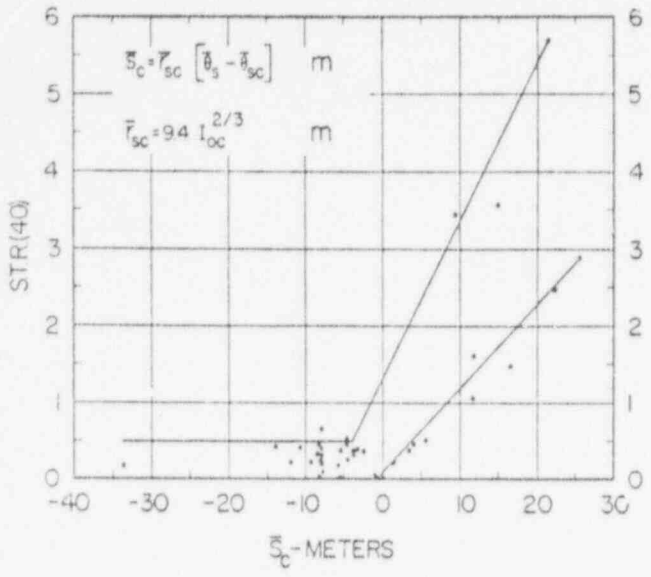

Fig. 4
Relations entre S_c et le S.T.R. (40).
Relation between S_c and S.T.R. (40).

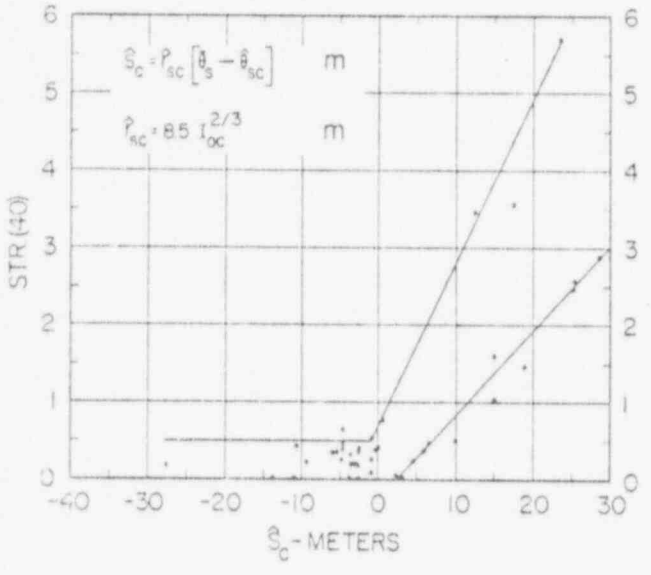

Fig. 5
Relation entre S_c et le S.T.R. (40).
Relation between S_c and S.T.R. (40).

de l'effet d'écran se trouvent virtuellement éliminées des valeurs négatives de S_c.

Le taux de déclenchement spécifique pour 40 jours d'orage par an [S.T.R. (40)] a été estimé par prorata linéaire comme étant :

$$S.T.R.(40) = S.T.R.(T.D.) \times 40/T.D.$$

Dans les deux figures 4 et 5, les valeurs de S.T.R. (40) pour des arcs d'exposition de référence positifs sont rassemblées entre des limites supérieure et inférieure, la limite supérieure s'appliquant à un terrain 100 % dégagé tandis que la limite inférieure est caractérisée par un certain nombre de particularités du terrain qui compensent nettement les effets du profil sur la hauteur moyenne des conducteurs. Etant donné qu'il n'est possible ni de chiffrer effectivement de telles caractéristiques ni de compter sur leur caractère permanent, il faut baser la conception des systèmes de protection sur un terrain nu. Le tableau III présente les renseignements disponibles correspondant à certaines caractéristiques du terrain pour les points situés à la limite inférieure.

are virtually eliminated for negative values of S_c.

The specific tripout rate for forty (40) thunder days per year, S.T.R. (40), has been estimated by linear proration as

$$S.T.R.(40) = S.T.R.(T.D.) \times 40/T.D.$$

In both Figures 4 and 5, the S.T.R. (40) values for positive reference exposure arcs are grouped into upper and lower bounds for which the upper is known to apply to 100 per cent open terrain, while the lower is characterized by a number of terrain features which substantially offset the effects of profile on the mean conductor height. Since it is neither possible to quantify such features effectively nor to rely on their permanence, the design of shielding systems should be based on bare earth. Table III presents the available information relating to certain terrain features for the points on the lower bound.

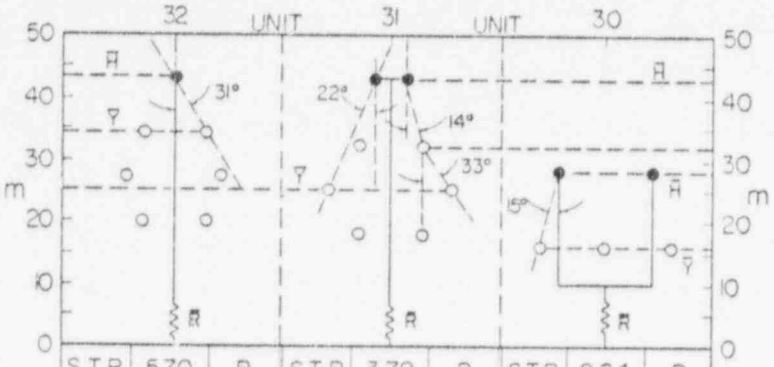

S.T.R.	5.70	P	S.T.R.	3.70	P	S.T.R.	0.24	P
Km-Yr	1265	%	Km-Yr	1573	%	Km-Yr	5900	%
$U_{50\%}$	1600	F 75	$U_{50\%}$	1600	F 50	$U_{50\%}$	1500	F 50
U-kV	345	R16	U-kV	345	R 50	U-kV	230	R 50
T.D.	40	M9	T.D.	43	M 0	T.D.	40	M 0
R	5 OHMS		R	5 OHMS		R	5 OHMS	

FIG. 6

Paramètres et performances correspondant aux rapports élémentaires 30, 31, et 32.

Parameters and performance for reporting units 30, 31 and 32.

Yr. = an

Pour différentes raisons, il ne faut pas considérer les « arcs d'exposition » comme des mesures réelles de la susceptibilité aux défauts par défaillance d'effet d'écran mais seulement comme des variables utiles associées au modèle analytique de référence [8.1]. Il est important d'éclaircir la question de l'utilisation des deux distances d'amorçage. Pour la conception des systèmes de protection, c'est la distance « effective » d'amorçage qui doit être utilisée. Pour des études comportant des estimations des taux de déclenchements par défaillance de l'effet d'écran, c'est la distance « moyenne » d'amorçage qui doit être utilisée.

Pour conclure la discussion portant sur les déclenchements par défaillance de l'effet d'écran, il faut se reporter à la figure 6. Cette figure est importante car les trois lignes sont toutes situées dans des régions ayant des niveaux de journées d'orage strictement comparables, les résistances de terre étant les mêmes, et les niveaux d'isolement étant virtuellement les mêmes. Les seules différences entre elles concernent les hauteurs moyennes et les angles de protection. Cette figure illustre, comme peu d'autres données peuvent le faire, la façon dont le taux de déclenchements par défaillance de l'effet d'écran dépend de ces variables.

For various reasons the " exposure arcs " are not to be taken as actual measures of shielding failure susceptibility but only as useful variables associated with the analytical model of reference [8.1]. It is important to be clear with respect to the use of the two striking distances. For the design of shielding systems, the " effective " striking distance should be used. For studies involving estimates of shielding failure rates, the " mean " striking distance should be used.

In concluding the discussion of shielding failure tripouts reference should be made to Figure 6. This figure is important because all there lines are located in areas having strictly comparable T.D. levels, the ground resistances are the same, and the insulation levels are virtually equal. The only differences among them are those of mean heights and shielding angles. This figure illustrates, as few other data can, the dependence of shielding failure tripout rate on these variables.

3.3. *Déclenchements par amorçage secondaire.*

Il doit maintenant être évident que la grande majorité des lignes incluses dans ce tour d'horizon sont en fait efficacement protégées soit de par leur conception propre soit peut-être avec l'aide des caractéristiques favorables du terrain. La figure 7 montre la répartition de tous les S.T.R. (40) inférieurs à 1,0 pour l'ensemble des rapports élémentaires. La valeur moyenne de 0,26 représente une performance excellente. 86 % des valeurs sont infé-

3.3. Backflash tripouts.

It should now be evident that the great majority of the lines included in the survey are in fact effectively shielded, either inherently or perhaps with the aid of favourable terrain features. Figure 7 shows the distribution of all S.T.R. (50) less than 1.0 for all reporting units. The median value of 0.26 represents excellent performance. Eighty six (86) per cent of the values are equal to or less than 0.50. While these data are of considerable interest

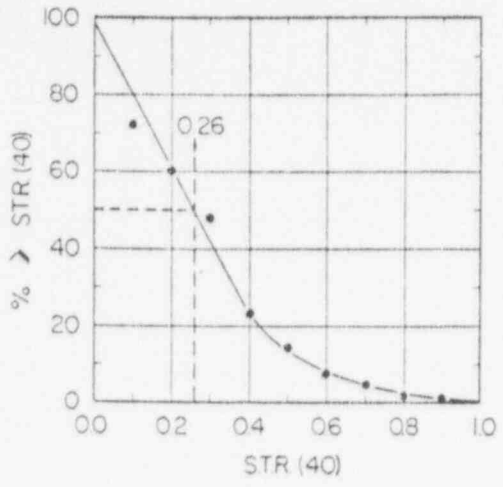

Fig. 7
Répartition des valeurs de S.T.R. (40) inférieures à 1,0
Distribution of S.T.R. (40) values less than 1.0.

rieures ou égales à 0,50. Outre que ces chiffres présentent un intérêt considérable en ce sens qu'ils représentent un ensemble de performances que l'on peut atteindre, ils signifient également que les incertitudes statistiques qui les accompagnent excluent virtuellement la détection de différences dans les performances attribuables théoriquement à des variables telles que :

in that they demonstrate a range of performance that can be achieved, they also mean that their accompanying statistical uncertainties virtually preclude detection of differences in performance theoretically attributable to such variables as

3.3.1. La hauteur moyenne du câble de garde (câble écran).

3.3.1. Mean height of ground (shield) wire.

3.3.2. La hauteur moyenne des pylônes.

3.3.2. Mean height of towers.

3.3.3. Les influences du terrain.

3.3.3. Terrain effects.

3.3.4. Les influences du dispositif de mise à la terre.

3.3.4. Grounding system effects.

3.3.5. Les niveaux d'isolement - $U_{50\ \%}$.

3.3.5. Insulation levels-$U_{50\ \%}$.

Ces difficultés de détection n'impliquent en aucune façon qu'il n'existe pas de dépendance des performances par rapport à ces variables. Ce qui semble être vrai est que la probabilité de déclenchement par la foudre est si faible qu'il est impossible de déterminer des dépendances distinctes. Un autre facteur est simplement le fait que les lignes de transport dans le monde sont, avec des exceptions importantes, conçues et construites d'une façon beaucoup plus uniforme qu'on ne les réalise habituellement. Pour mettre un accent particulier sur les remarques de ce paragraphe, on a préparé deux tableaux.

These difficulties of detection by no means imply that performance dependencies on these variables do not exist. What seems to be true is that the probability of lightning tripout is so low that it is impossible to identify separate dependencies. Another factor is simply that the transmission lines of the world are, with important exceptions, much more uniformly designed and constructed than commonly realized. In an effort to stress the remarks of this section, two tables have been prepared.

3.3.6. Le tableau IV présente les « moyennes courantes » calculées pour le rapport élémentaire n° 30 pour une période continue d'observation de 25 années, la plus longue du tour d'horizon. Le taux de déclenchements spécifiques indiqué l'est pour le niveau réel de journées d'orage de 40 et n'est pas une valeur extrapolée. On insiste ici sur la variabilité des performances pour une seule ligne.

3.3.6. Table IV presents the "running means" calculated for reporting unit No. 30 for a continuous observation period of 25 years, the longest of the survey. The specific tripout rate given is for the actual T.D. level of 40 and is not an extrapolated value. Here the emphasis is on the variability of performance for a single line.

3.3.7. Le tableau V présente les S.T.R. (40) pour 10 rapports élémentaires portant en moyenne sur

3.3.7. Table V presents the S.T.R. (40) for 10 reporting units averaging 401 kilometers length, 10.3

Tableau IV — Table IV

Répartition des S.T.R. (40) pour le rapport élémentaire n° 30 et une période d'observation de 25 années. Le niveau de T.D. de 40 est celui de la ligne et les valeurs ne sont pas des valeurs ajustées.

Distribution of S.T.R. (40) for reporting unit No. 30 for the observation period of 25 years. The T.D. level of 40 is that of the line and values are not adjusted values.

Nombre d'années sur lequel porte la moyenne
Number of Years Averaged

1	2	3	4	5	6	7	8	9	10	11	12	13	14	15	16	17	18	19	20	21	22	23	24	25
.850	.635	.565	.530	.590	.494	.484	.424	.424	.424	.386	.388	.358	.364	.339	.318	.324	.306	.290	.276	.282	.270	.258	.248	.238
.850	.635	.565	.530	.424	.494	.424	.424	.376	.381	.386	.353	.358	.334	.339	.318	.300	.306	.290	.276	.262	.270	.258	.248	
.425	.425	.424	.424	.424	.424	.424	.424	.376	.381	.348	.353	.358	.334	.339	.318	.300	.282	.290	.276	.262	.250	.240		
.425	.425	.424	.424	.424	.354	.364	.371	.376	.339	.348	.353	.326	.334	.310	.318	.300	.282	.268	.276	.262	.250			
.425	.425	.424	.424	.340	.354	.364	.371	.376	.339	.348	.318	.326	.334	.310	.291	.300	.282	.268	.254	.242				
.425	.425	.424	.318	.340	.354	.364	.371	.376	.339	.348	.318	.326	.303	.310	.291	.274	.282	.268	.254					
.425	.212	.282	.318	.340	.354	.364	.318	.329	.339	.309	.318	.294	.303	.282	.291	.274	.259	.246						
.425	.212	.282	.318	.340	.354	.303	.318	.329	.339	.309	.318	.294	.303	.282	.291	.249	.235							
.425	.212	.282	.318	.254	.282	.303	.318	.282	.296	.309	.318	.294	.272	.282	.265	.249								
.425	.212	.282	.318	.254	.282	.242	.265	.282	.296	.309	.282	.294	.272	.254	.265									
.425	.212	.282	.212	.254	.282	.242	.212	.235	.254	.280	.282	.294	.272	.254										
.425	.212	.282	.212	.254	.212	.242	.212	.235	.254	.280	.247	.228	.212											
.000	.212	.141	.212	.254	.212	.242	.212	.235	.212	.232	.212	.196												
.000	.212	.141	.212	.254	.212	.242	.212	.236	.212	.193	.176													
.000	.212	.141	.212	.170	.212	.182	.212	.188	.169	.154														
.000	.212	.141	.106	.170	.141	.121	.106	.094	.085															
.000	.212	.141	.106	.170	.141	.121	.106	.094																
.000	.212	.141	.106	.085	.070	.121	.106																	
.000	.212	.141	.106	.085	.070	.060																		
.000	.000	.141	.106	.085	.070																			
.000	.000	.141	.106	.085																				
.000	.000	.000	.106																					
.000	.000	.000																						
.000	.000																							
.000																								

Années considérées *Years Averaged*	Années-kilomètres pour chaque valeur *Kilometer-Years for Each Value*
1	236
5	1180
10	2360
15	3540
20	4720
25	5900

Tableau V — Table V

Performances et paramètres pour 10 rapports élémentaires correspondant à une moyenne portant sur une longueur de 401 km, une période d'observation de 10 années, et une exposition de 4 119 années-kilomètres.
Performances and parameters for 10 reporting units averaging 401 km in length, 10 years observation period and 4 119 kilometer-years exposure.

N° *Data Unit*	Longueur *Length km*	Période années *Period Years*	Années-kilomètres *Kilometer Years*	S.T.R. (40)	*U*(50 %) kV	*H* mètres *H meters*	*R ohms*	Renseignements concernant le terrain *Terrain information*
30	236	25	5900	0.24	1500	28.0	5	Dégagé *Open*
39	963	3	3140	0.19	1600	29.3	5	Dégagé *Open*
40	223	20	4460	0.09	1580	27.0	12	Dégagé à légèrement boisé *Open to lightly wooded*
56	308	12	3676	0.34	1470	25.7	40	Dégagé *Open*
57	259	12	3108	0.39	1470	30.0	21cc	Dégagé *Open*
58	323	12	3876	0.33	1470	29.3	22cc	Dégagé *Open*
84	NA*	NA*	(3000)*	0.51	1610	29.0	10cc	Dégagé *Open*
87	1000	8	8000	0.00	2080	44.7	30cc	Dégagé *Open*
88	367	7	2569	0.20	1800	29.6	110cc	Dégagé *Open* 75 % Forestier *Forested 75 %*
89	335	7	2345	0.31	1800	29.6	110cc	25 % Dégagé *Open 25 %* 75 % Forestier *Forested 75 %*
Valeurs moyennes *Mean values*	401	10.3	4119	0.26	1560	30.0	37	Dégagé *Open*

* Non compris dans les valeurs moyennes car la longueur et la durée ne sont pas spécifiées
* *Not included in mean values because length and time not specified.*

TABLEAU VI — TABLE VI

Performances, paramètres et renseignements concernant le terrain pour 12 rapports élémentaires correspondant à la courbe limite inférieure pour des arcs d'exposition positifs

Performances, parameters and terrain information for 12 reporting units on lower bound curve for positive exposure arcs

N° *Data Unit*	Longueur *length km*	Période années *Period Years*	Années-kilomètres *Kilometer Years*	S.T.R. (40)	Arcs de référence *Reference Arcs* $\hat{S}_c$	m $\hat{S}_c$	Renseignements concernant le terrain *Terrain information*	
34	160	5	800	0.38	3.6	6.1	Dégagé à boisé	*Open to wooded*
43	225	4	900	0.00	0.0	3.1	39 % Forestier	*39 % Forested*
44	225	4	900	0.00	0.0	3.1	39 % Forestier	*39 % Forested*
51	123	12	1476	0.47	4.0	6.6	100 % Dégagé parallèle à la ligne 52 construite à 45,7 km à l'ouest en 1966.	*100 % Open Parallel line 52 erected 45.7 meters West in 1966*
52	220	6	1320	0.04	−1,0	2.2	" " "	" " "
80	225	8	1800	0.23	1.4	4.7	Pas disponible d'après les renseignements reçus	*Not available from data submitted*
85	400	13	5200	1.04	11.8	15.0	" "	" "
86	250	13	3250	1.60	11.8	15.0	" "	" "
105	348	11	3828	2.47	21.7	25.2	48 % Forestier	*48 % Forested*
106	318	12*	3736	1.48	16.6	19.0	44 % couvert de buissons	*44 % Bush*
107	632	11*	6920	2.57	22.9	25.5	46 % Forestier	*46 % Forested*
108	738	11*	8037	2.88	25.3	29.1	12 % Forestier	*12 % Forested*

* Jusqu'à l'année dernière

* *To nearest year*

une longueur de 401 km, 10,3 années d'observation, et pour 4 119 années-kilomètres. La répartition géographique couvre le monde entier. Ce tableau donne également la liste des niveaux d'isolement au choc, des hauteurs moyennes de câbles de garde, des valeurs relevées concernant le dispositif de mise à la terre et de certains renseignements concernant le terrain. Ce qui ressort ici est la variabilité des performances pour des lignes très éloignées ayant une exposition comparable. Mis à part l'exception possible du rapport n° 87, il est impossible de déduire une relation quelconque entre les paramètres portés sur cette liste et les taux de déclenchements. Pour le rapport n° 87 la valeur élevée du niveau d'isolement pourrait compenser une certaine augmentation de l'exposition due à la valeur plus élevée de la hauteur moyenne du câble de garde. Il est intéressant de remarquer que le domaine des valeurs du tableau IV en faisant porter la moyenne sur une période de 10 ans correspond d'une façon très proche à celui du tableau V pour une période analogue.

years of observation, for 4,119 kilometer-years. Geographical distribution is world-wide. This table also lists impulse insulation levels, mean ground wire heights, reported grounding system data and terrain information. Here the emphasis is on the variability of performance for widely-separated lines having comparable exposure. With the possible exception of unit No. 87, it is impossible to derive any relationship between the parameters listed and the tripout rates. For unit No. 87, the high value of the insulation level could offset any increase in exposure caused by the higher value of mean ground wire height. It is interesting to note that the range of values in Table IV for an averaging period of ten (10) years corresponds closely to that of Table V for a similar period.

3.4. *Répartition des déclenchements par la foudre en fonction des phases et des conducteurs pour les rapports élémentaires* 105, 106, 107 *et* 108.

Le tableau VII montre la répartition de 356 déclenchements par la foudre selon les phases et les circuits pour les lignes à circuit double des rapports élémentaires 105, 106, 107, 108 qui couvrent 22 521 années-kilomètres sur 2 036 km de ligne pour une période moyenne d'observation de 11 ans. Le

3.4. Distribution of lightning tripouts among phases and circuits for reporting units 105, 106, 107 and 108.

Table VII shows the distribution of 356 lightning tripouts among phases and circuits for the double circuit lines of reporting units 105, 106, 107, 108 which cover 22,521 kilometer-years on 2036 kilometers of line for a mean observation period of 11 years. The mean annual thunderstorm days are

TABLEAU VII — TABLE VII

Répartition des déclenchements dus à la foudre par rapport aux phases et aux circuits pour les rapports élémentaires 105-108

Distribution of lightning tripouts among phases and circuit for reporting units 105-108.

n° *Data Unit*	105		106		107		108					
Phases *Phases*	Circuit seul *Single Circuit*	Circuit double *Double Circuit*	Circuit seul *Single Circuit*	Circuit double *Double Circuit*	Circuit seul *Single Circuit*	Circuit double *Double Circuit*	Circuit seul *Single Circuit*	Circuit double *Double Circuit*	Totaux *Totals* SC	DC	Pourcentage *Per Cent* SC	DC
Supérieure *Top*	12	1	6	0	29	4	22	6	69	11	18.4	3.1
Moyenne *Middle*	22	2	8	0	29	14	52	9	111	25	31.2	7.0
Inférieure *Bottom*	0	2	3	2	3	4	5	1	11	9	3.1	2.5
Supérieure et moyenne *Top and middle*	1	3	0	3	1	11	2	1	4	18	1.1	5.1
Supérieure et inférieure *Top and bottom*	1	2	1	2	2	0	1	1	5	5	1.4	1.4
Moyenne et inférieure *Middle and bottom*	0	1	1	1	2	5	3	0	6	7	1.7	2.0
Les 3 phases *Three phases*	0	2	0	0	1	6	1	0	2	8	0.6	2.2
Autres *Others*	0	0	0	0	0	0	0	9	0	9	0.0	2.5
Indéterminés *Unknown*	9	3	4	3	12	3	17	5	42	14	12.0	3.9
Total	45	16	23	11	79	47	103	32	250	106	70.0	30.0
									Grand Total	356		100

nombre moyen annuel de journées d'orage est 25.45. La valeur moyenne correspondante de S.T.R. (40) est alors 2.48. La recherche de la référence [8.1] indique que les défaillances de l'effet d'écran sont presque entièrement limitées aux phases supérieures ou moyennes d'un circuit sur une ligne à circuit double. Occasionnellement, une défaillance d'effet d'écran peut intéresser à la fois les phases supérieure et intermédiaire, mais une défaillance de l'effet d'écran intéressant un circuit double est virtuellement impossible. Une défaillance d'effet d'écran intéressant le conducteur inférieur est théoriquement possible pour des pylônes extrêmement élevés, un profil extrêmement montagneux, ou bien des traversées de rivière élevées. Dans des conditions normales cependant, un tel phénomène est extrêmement improbable. En se servant de ces considérations comme base pour l'étude du tableau VII qui va

25.45. The corresponding mean S.T.R. (40) is then 2.48. The research of reference [8.1] indicates that shielding failures are almost wholly confined to top or middle phases of one circuit on a double circuit line. Occasionally, a shielding failure can involve both the top and middle phases, but a double-circuit shielding failure is virtually impossible. Shielding failure involving the bottom conductor is theoretically possible for extremely high towers, extremely mountainous profile, or high river crossings. For normal conditions, however, such an event is very improbable. Using these facts as a basis for further study of Table VII, it is possible to derive the following estimates :

suivre, il est possible d'en déduire les estimations suivantes :

Composant	S.T.R. (40)
Déclenchements d'un circuit simple	1,74
Déclenchements d'un circuit double	0,74
	2,48
Déclenchements par défaillance de l'effet d'écran	1,59
Déclenchements par amorçage secondaire	0,89
	2,48

Dans le partage entre les défaillances de l'effet d'écran et les phénomènes d'amorçage secondaire, la catégorie « indéterminée » pour les déclenchements de circuit simple, 12 %, fut attribuée d'une façon égale à ces deux causes. Le taux de déclenchements par amorçage secondaire résultant obtenu de cette façon est apparemment incompatible avec les valeurs de la figure 7. Il y a 4 possibilités d'explications.

1) La hauteur moyenne H correspondant à toutes les valeurs élémentaires numérotées en-dessous de 100 dans le tableau III est 32,2 m tandis que celle correspondant aux valeurs élémentaires 105 à 108 est 55,55 m.

2) La hauteur moyenne H_t des pylônes pour les valeurs élémentaires numérotées en-dessous de 100 est 32 m tandis que celle correspondant aux valeurs élémentaires 105 à 108 est 40 m.

3) Il est possible que toute la catégorie « indéterminée » pour des déclenchements de circuit simple doive être attribuée à des défaillances de l'effet d'écran. Dans ce cas, le partage devient alors :

Déclenchements par défaillance de l'effet d'écran, S.T.R. (40) = 1,74.

Déclenchements par amorçage secondaire, S.T.R. (40) = 0,74.

4) La tension critique d'amorçage au choc est $U_{50\,\%}$ = 1 220 kV pour les rapports élémentaires 105 à 108 tandis que celle correspondant aux rapports numérotés en-dessous de 100 dans le tableau III a une valeur moyenne de 1 680 kV.

L'influence de ces facteurs ne peut pas être évaluée statistiquement mais il paraît probable que leurs effets combinés puissent se répercuter sur le S.T.R. (40) correspondant à des amorçages secondaires comme cela a été dit ci-dessus.

3.5. *Indicateur binaire des performances vis-à-vis des coups de foudre.*

Les niveaux extrêmement bas de S.T.R. (40) que l'on peut obtenir avec des lignes bien conçues, les niveaux très élevés relevés sur des lignes médiocrement protégées et la forte dispersion de ces niveaux de performances pour des valeurs raisonnables d'exposition exprimées en années-kilomètres font penser à l'utilité d'un indice de performances simple. Un tel indice est défini par

$$\text{S.T.R. (40)} = 2^M$$

Component	*S.T.R. (40)*
Single circuit tripouts	*1.74*
Double circuit tripouts	*0.74*
	2.48
Shielding failure tripouts	*1.59*
Backflash tripouts	*0.89*
	2.48

In the division into shielding failures and backflash events, the " unknown location " category for single-circuit tripouts, 12 per cent, was allocated equally between these causes. The resulting backflash tripout rate so obtained is apparently inconsistent with the data of Figure 7. There are four possible avenues of explanation :

1) The mean height H of all data units numbered less than 100 in Table III is 32.2 meters while that of data units 105 through 108 is 55.55 meters.

2) The mean height H_t of the towers for data units numbered less than 100 is 32 meters while that of data units 105 through 108 is 40 meters.

3) It is possible that all the " unknown location " category for single-circuit tripouts should be allocated to shielding failures. In this case the division then becomes :

Shielding failure tripouts, S.T.R. (40) = 1.74.

Backflash tripouts, S.T.R. (40) = 0.74.

4) The impulse critical impulse flashover voltage $U_{50\,\%}$ = 1220 kV for reporting units 105 through 108 while that of those numbered less than 100 in Table III averages 1680 kV.

The influence of these factors cannot be evaluated statistically, but it seems probable that their combined effect could result in backflash S.T.R. (40) as deduced above.

3.5. A binary order index of lightning performance.

The very low levels of S.T.R. (40) obtainable with well-designed lines, the very high levels experienced on poorly-shielded lines and the high dispersion of these performance levels for reasonable values of exposure in terms of kilometer years suggest the usefulness of a simple performance index. Such an index is defined by

$$\text{S.T.R. (40)} = 2^M$$

où M est « l'ordre binaire » des performances. La correspondance entre l'ordre M et les niveaux de performances est indiquée dans le tableau suivant grâce à des commentaires qualitatifs indiquant les types possibles de conditions pouvant conduire à ces niveaux de performances.

Ordre de performances M	S.T.R. (40) (1000 an.-km.)	Commentaires qualitatifs
− 4	0,0 - 0,0625	Anti-foudre ?
− 3	0,125	Mise à la terre et protection supérieures
− 2	0,250	Mise à la terre et protection excellentes
− 1	0,500	Mise à la terre et protection bonnes
0	1.000	bonne (assez bonne) mise à la terre Assez bonne (bonne) protection
1	2,000	Bonne mise à la terre Assez bonne protection
2	4,000	Bonne mise à la terre Protection médiocre
3	8,000	Mise à la terre médiocre Protection médiocre
4 - 5	16 - 32	Mise à la terre et protection médiocres et faible niveau d'isolement ou lignes *non protégées*.

D'un point de vue statistique, il est fortement improbable que les niveaux de performances prévus pour les lignes considérées classées dans la catégorie $M = -2$ ou moins se vérifient au cours de périodes pratiques d'observation.

where M is the " binary order " of the performance. The correspondence between the order M and performance levels is indicated in the following table along with qualitative comments giving the possible ranges of conditions which could result in these performance levels.

Performance Order M	*S.T.R. (40) (1 000 km-yr)*	*Qualitative Comments*
− 4	0.0 - 0.0625	*Lightning proof ?*
− 3	0.125	*Superior grounding and shielding*
− 2	0.250	*Excellent grounding and shielding*
− 1	0.500	*Good grounding and shielding*
0	1.000	*Good (fair) grounding* *Fair (good) shielding*
1	2.000	*Good grounding* *Fair shielding*
2	4.000	*Good grounding* *Poor shielding*
3	8.000	*Poor grounding* *Poor shielding*
4 - 5	16 - 32	*Poor grounding and shielding and low insulation level or unshielded lines*

From a statistical point of view, it is highly unlikely that predicted performance levels for proposed lines estimated at $M = -2$ or lower will be verified in practical observation periods.

4. Conclusions.

4.1. Un échantillon à l'échelle du monde entier concernant les performances vis-à-vis de la foudre des lignes de transport à très haute tension a été constitué à partir de 15 pays en réponse à un questionnaire soigneusement préparé. Les valeurs de performances ainsi que les caractéristiques physiques et électriques des lignes ont été disposées selon un format commun présenté au tableau IX par 121 rapports élémentaires. Ce tableau représente une dimension d'ensemble de l'échantillon de 171 112 *années-kilomètres*, 22 409 *km de ligne et* 7 636 *années moyennes* d'observation.

4.2. Une part considérable de l'échantillon, 120 065 années-kilomètres, était accompagnée de renseignements suffisamment détaillés pour permettre un traitement analytique utile. Les résultats de cette analyse sont présentés au tableau III pour 41 rapports élémentaires représentatifs. Les paramètres électriques, physiques et ceux qui s'en déduisent furent alors étudiés du point de vue de leurs in-

4. Conclusions.

4.1. A world-wide sample of the lightning performance of EHV transmission lines has been collected from 15 countries in response to a carefully-prepared questionnaire. The data on performance as well as the electrical and physical characteristics of these lines have been organized in a common format presented in Table IX by 121 reporting units. This table represents a total sample size of 171,112 kilometer-years, 22,409 kilometers of line, *and* 7,636 mean years *of observation.*

4.2. A substantial portion of the sample, 120,065 kilometer-years, included information in sufficient detail to permit useful analytical treatment. The results of this analysis are presented in Table III for 41 representative reporting units. The electrical, physical, and derived parameters were then studied for their effects on the specific lightning tripout rate referred to the base value of 50 thunder days.

fluences sur le taux spécifique de déclenchement à la foudre en prenant une valeur de base de 40 journées d'orage.

4.3. Etant donné le domaine très vaste des dimensions d'échantillons pour les rapports élémentaires individuels en années-kilomètres et les incertitudes correspondantes dans la valeur de S.T.R. (40), le rapport élémentaire correspondant à la plus longue période d'observation de 25 années fut analysé pour déterminer ce taux pour des périodes moyennes allant de 1 à 25 ans. Ces « moyennes courantes » sont présentées au tableau IV. Les valeurs de ce tableau sont utiles pour évaluer l'incertitude des autres valeurs au moins d'une façon qualitative.

4.4. On n'a trouvé aucune relation significative et donc les valeurs de S.T.R. (40) ont été relevées en fonction de la hauteur du pylône, de la hauteur moyenne du câble de garde, de la hauteur des conducteurs ou de l'angle de protection *lorsqu'on prend ces paramètres séparément.* Une corrélation significative apparaît lorsque l'on utilise le paramètre $Y\theta_4$ déduit arbitrairement ou le paramètre S_c déduit d'une façon analytique. Les figures 3 et 4 montrent ces relations. Les défaillances d'effet d'écran constituent le composant principal de la valeur de S.T.R. (40) pour les arcs d'exposition S_c positifs de la figure 4.

4.5. Il est regrettable, mais cela était prévisible, qu'il n'ait pas été possible de déceler une relation significative entre la valeur de S.T.R. (40) et l'un des paramètres suivants :

Hauteur moyenne du câble de terre.
Hauteur moyenne des pylônes.
Influences du terrain.
Résistance du système de mise à la terre.
Niveau d'isolement au choc.

Ces difficultés de détection ne veulent pas dire que de telles relations n'existent pas. Si elles existent, leur domaine d'influence doit se trouver à l'intérieur des incertitudes du tableau IV et du faible niveau des taux moyens de déclenchements par amorçage secondaire de la figure 7.

4.6. La figure 7 montre la répartition des valeurs de S.T.R. (40) entre 0 et l'unité pour tous les rapports élémentaires corrects. La distribution est pondérée en années-kilomètres. La valeur moyenne est 0,26 et 86 % des valeurs sont inférieures à 0,50.

4.7. Il n'a pas été possible de chiffrer pratiquement les caractéristiques du terrain le long du tracé de la ligne compte tenu de leur influence sur le taux de déclenchements à la foudre. On a mis en évidence expérimentalement (8.1 - 8.2) et analytiquement (8.4) des effets bénéfiques des arbres d'une hauteur convenable. Ces effets apparaissent cependant quantitativement sur les figures 4 et 5 où l'on peut voir pour des arcs d'exposition positifs des limites distinctes supérieure et inférieure. Le tableau VI présente les renseignements qualitatifs correspondant à certaines caractéristiques du terrain pour des points situés à la limite inférieure. On sait que les points situés à la limite supérieure correspondent à un terrain virtuellement 100 % dégagé. Etant donné qu'il n'est pas possible de chiffrer effec-

4.3. *Because of the wide range of sample size for individual reporting units in kilometer-years and the corresponding uncertainties in the S.T.R. (40), the reporting unit having the longest observation period of 25 years was analyzed to determine this rate for averaging periods from one to 25 years. These "running means" are presented in Table IV. The data of this table are useful in evaluating the uncertainty in other data — at least in a qualitative manner.*

4.4. *No significant relationships are found when the values of S.T.R. (40) are plotted against tower height, mean ground wire height, conductor height or shielding angle* when these parameters are taken separately. *Significant correlation appears, when the arbitrary derived parameter $Y\theta_4$ or the analytically-derived parameter S_c is used. Figures 3 and 4 show these correlations. Shielding failures are the main component of the S.T.R. (40) for the positive exposure arcs S_c of Figure 4.*

4.5. *Regrettably, but predictably, it has not been possible to detect any significant relation between the S.T.R. (40) and any of the following parameters :*

Mean height of the ground wire.
Mean height of the towers.
Terrain effects.
Grounding system resistance.
Impulse insulation level.

These difficulties of detection do not imply that such relations do not exist. If they exist, their range of influence must be within the uncertainty implied in Table IV and the low level of median backflash tripout rates of Figure 7.

4.6. *Figure 7 shows the distribution of S.T.R. (40) values between zero and unity for all pertinent reporting units. The distribution is weighted by kilometer-years. The median value is 0.26, and 86 per cent of the values are less than 0.50.*

4.7. *It has not been possible to quantify usefully the terrain features along the line route with respect to their effect on the lightning tripout rate. Beneficial effects from trees of substantial height have been found experimentally [8.1 - 8.2] and analytically [8.4]. These effects appear quantitatively, however, in Figures 4 and 5 where distinct upper and lower bounds appear for positive exposure arcs. Table VI presents the qualitative information relating to certain terrain features for points on the lower bound. The points on the upper bound are known to apply to virtually 100 per cent open terrain. Since it is neither possible to quantify favourable terrain features effectively nor to rely on their permanence, the design of shielding systems should be based on bare earth.*

tivement des caractéristiques favorables du terrain ni de compter sur leur caractère permanent, il faut baser la conception des systèmes de protection sur un terrain nu.

4.8. L'utilisation d'une distance moyenne d'amorçage pour la conception des systèmes de protection implique l'existence de défaillances d'effet d'écran résiduelles pour les petits arcs moyens d'exposition négatifs. La figure 4 semble confirmer cette déduction. L'utilisation d'une distance d'amorçage « effective » inférieure d'un écart-type à la valeur moyenne devrait réduire ces défaillances résiduelles de l'effet d'écran. La figure 5 montre qu'une distance d'amorçage effective inférieure de 10 % à la distance moyenne élimine virtuellement les phénomènes résiduels. La valeur moyenne doit être utilisée pour les projets prévisionnels et la valeur effective doit être utilisée pour la conception des systèmes de protection. On ne peut considérer que comme fortuite la précision apparente de ces résultats.

4.8. The use of a mean striking distance for the design of the shielding system implies residual shielding failures for small negative mean exposure arcs. Figure 4 seems to support this deduction. The use of an "effective" striking distance one standard deviation less than the mean value would reduce these residual shielding failures. Figure 5 shows that an effective striking distance 10 per cent below the mean virtually eliminates the residuals. The mean value should be used for prediction purposes and the effective value should be used for design of shielding systems. The apparently accurate results here can only be considered fortuitous.

4.9. Une étude des figures 4 et 7 suggère que, pour des lignes ayant de faibles résistances de mise à la terre de 30 ohms ou moins, les interprétations approximatives suivantes peuvent être utiles :

4.9. A study of Figures 4 and 7 suggests that, for lines with low voltage ground resistances of 30 ohms or less, the following approximate interpretations may be useful :

4.9.1. Les valeurs de S.T.R. (40) inférieures à environ 0,5 correspondent à un composant de défaillances d'effet d'écran négligeable.

4.9.1. S.T.R. (40) values under about 0.5 have a negligible shielding-failure component.

4.9.2. Les valeurs de S.T.R. (40) dépassant 1,0 correspondent probablement à un composant de défaillances d'effet d'écran considérable.

4.9.2. S.T.R. (40) values in excess of 1.0 probably have a substantial shielding-failure component.

4.9.3. L'utilisation d'angles de protection *négatifs* conduit à des arcs d'exposition négatifs importants qui procurent une grande marge de protection contre les écarts de profil défavorables par rapport à la moyenne.

4.9.3. The use of negative shielding angles results in large negative exposure arcs which provide a wide protective margin against unfavourable profile deviations from the mean.

4.10. Il ne semble pas y avoir de différence d'approximation dans la conception des systèmes de protection pour les lignes à haute tension et les lignes à très haute tension. Il n'est pas encore clair, cependant, que cela soit vrai pour la conception des lignes à ultra haute tension principalement à cause des tensions de ligne plus élevées et des hauteurs moyennes plus importantes des conducteurs. Pour cette raison, l'auteur conseille fortement de prendre en considération des angles de protection *négatifs* comme moyen pour se constituer une marge prudente contre les incertitudes et les variations normales du profil de la ligne (8.5).

4.10. There do not appear to be any differences of approach to the design of shielding systems for HV and EHV lines. It is not yet clear, however, that this is true for the the design of UHV lines, principally because of the higher line voltages and the higher mean heights of the conductors. For this reason, the author strongly suggests consideration of negative shielding angles as a means of providing a prudent margin against these uncertainties and normal variations in line profile (8.5).

5. Tableaux d'analyse.

Les tableaux III à VII présentent les résultats d'analyses et des valeurs particulières concernant les différentes parties. Les résultats sont discutés en détail dans le texte.

5. Analysis tables.

Tables III through VII present the results of analysis or breakdown of data into component parts. The results are discussed in detail in the text.

6. Tableaux de valeurs.

Le tableau IX présente les valeurs originales correspondant à 121 rapports élémentaires telles qu'elles ont été recueillies dans les réponses au questionnaire. Les remarques numérotées sont incluses dans les définitions des symboles et des abréviations du tableau VIII.

6. Data tables.

Table IX presents the original data for 121 reporting units as taken from the replies to the questionnaire. The numbered notes are included with the definitions of symbols and abbreviations of Table VIII.

TABLEAU VIII — TABLE VIII

Définitions et remarques

Definitions and notes

Abréviation, Symbole ou Remarque *Abbreviation, Symbol or Note*	Définition ou Explication	*Definition or Explanation*
T.D.	Journées d'orage (normalement annuelles)	*Thunder Days (Normally annual)*
N.A.	Non disponible (ou non fourni)	*Not Available (or not furnished)*
F	Profil plat	*Flat profile*
R	Profil ondulé	*Rolling profile*
M	Profil montagneux (utilisé parfois pour la description du terrain)	*Mountainous profile (sometimes used as terrain description)*
(HM)	Terrain entre collines et montagnes	*Hilly to mountainous terrain*
(F)	Terrain forestier (donné habituellement en pourcent.)	*Forested terrain (usually given as per cent)*
(O)	Terrain dégagé (prés, végétation basse, etc.)	*Open terrain (grassland, low vegetation, etc.)*
(O-W)	Terrain variable de dégagé à légèrement boisé	*Variable terrain, open to lightly wooded*
D-C	Ligne à circuit double	*Double-circuit line*
BF	Amorçage secondaire	*Back flashover*
SF	Défaillance de l'effet d'écran	*Shielding failure*
cc	Contrepoids continu	*Continuous counterpoise*
rc	Contrepoids radial	*Radial counterpoise*
de	Electrode profonde (tige ou tube)	*Deep electrode (rod or pipe)*
S_c	Arc d'exposition utilisant $\bar{r}_{sc}$	*Exposure arc using* $\bar{r}_{sc}$
S_c	Arc d'exposition utilisant r_{sc}	*Exposure arc using* r_{sc}
O_{sc}	Angle de protection critique utilisant $\bar{r}_{sc}$	*Critical shielding angle using* $\bar{r}_{sc}$
O_{sc}	Angle de protection effectif utilisant r_{sc}	*Effective shielding angle using* r_{sc}
U	Tension de service d'un rapport élémentaire	*Operating voltage of a reporting unit*
$U_{50\%}$	Tension critique d'amorçage au choc	*Critical impulse flashover voltage*
S.T.R.	Déclenchements sur coup de foudre par 100 km et par an	*Lightning tripouts per 100 km per year*
S.T.R.(40)	S.T.R. pour 40 T.D.	*S.T.R. for 40 T.D.*
H	Hauteur du câble de garde. H_t (au droit du pylône) $\bar{H}$ (moyenne)	*Ground wire height. H_t (at tower), $\bar{H}$ (mean)*
Y	Hauteur du conducteur. Y_t (au droit du pylône), $\bar{Y}$ (moyenne)	*Conductor height. Y_t (at tower), $\bar{Y}$ (mean)*
$\bar{C}$	Espacement moyen entre les conducteurs et le câble de garde	*Mean spacing between conductor and ground wire*
a	Décalage horizontal entre les conducteurs et le câble de garde	*Horizontal offset between conductor and ground wire*

Remarques

(1) Longueur cumulée correspondant aux rapports élémentaires - km
(2) Période moyenne en années correspondant au tableau
(3) Années-kilomètres cumulées pour le tableau
(4) En se basant sur une proportion linéaire
(5) Ensemble de toutes les lignes pour une tension donnée
(6) ou NA Valeur correspondante non fournie
(7) D'après le projet de recherche RP 50 de l'EEI (8.1 - 8.2)
(8) Non reporté sur la table à cause de l'insuffisance des valeurs ou de la durée d'exposition
(9) Déclenchements omis sur une traversée de rivière non protégée.

Notes

(1) Cumulative length of reporting units - km
(2) Mean period for table in years
(3) Cumulative kilometer-years for table
(4) Based on linear proration
(5) All lines at given voltage summarized
(6) or NA Indicated data not furnished
(7) From EEI Research Project RP 50 (8.1-8.2)
(8) Untabulated because of insufficient data or exposure
(9) Omitting tripouts on unshielded river crossing.

Tableau IX — Table IX

Liste des principales données fournies par les rapports élémentaires

Summary of principal data by reporting units

N° du rapport élémentaire *Reporting Unit Number*		1	2	3	4-9	10	11-16	17-18 14-C	20	21-23	24	25	26-29
Lettres code du pays *Country code letters*		RSA	RSA	RSA	RSA (8)	N	A (9) RSA	RSA	RSA	RSA	USA	USA	USA
U (ligne) *U (line)*	kV	400	400	400	275	275	275	275	275	275	287	345	345
Longueur *Length*	(1) km	198	198	198	(8)	1 366	(8)	159	242	(8)	170	282	(8)
Période *Period*	(2) années *years*	2	2	2		3		2	2		16	13	
Années-kilomètres *Kilometer-years*	(3) an. km *km-yr*	396	396	396		4 098		318	484		5 920	1 666	
T.D. moyen/an *Mean TD/year*	TD	NA	NA	NA		NA		NA	NA		7.5	7.5	
N° de câbles de garde *No. of ground wires*		2	2	2		(5)		1	2		None	None	
Angle de protection *Shield angle*	deg	15	15	15		"		30	30		–	–	
Résistance de terre *Ground resistance*	ohms	30	30	30		"		7	15		–	–	
U (50 %)	kV	2 050	2 050	2 050		"		1 425	1 425		1 425	1 700	
Profil plat *Flat profile*	%	90	90	90		"		90	90		–	–	
Profil ondulé *Rolling profile*	%	5	5	5		"		5	5		50	50	
Profil montagneux *Mountainous profile*	%	5	5	5		"		5	5		50	50	
Classement nominal du terrain *Nominal terrain class*	%	100 % 0	100 % 0	100 % 0		"		100 % 0	100 % 0		(6)	(6)	
(pour la valeur réelle de TD) *STR (at actual TD rate)*		0.25	0.00	0.58		0.32		1.08	0.62		1.1	0.7	
(pour 10 TD/an) *STR (at 10 TD/year*	*(4)	NA	NA	NA		NA		NA	NA		7.5	3.7	

*Voir tableau 8 pour des remarques supplémentaires concernant les valeurs indiquées dans ce tableau.
(1) 3 013 km
(2) 5.20 années moyennes
(3) 15,671 an.-km

*See Table 8 for supplementary notes relating to data given in this table.
(1) 3 013 km
(2) 5.20 mean years
(3) 15,671 km-yr.

N° du rapport élémentaire *Reporting Unit Number*		30	D[31]C	D[32]C	33	34	35	36	37/38	39	40
Lettres code du pays *Country code letters*		USA (7)	USA (7)	USA (7)	USA (7)	USA (7)	USA (7)	USA (7)	USA (7)	USA (7)	USA (7)
U (ligne) *U (line)*	kV	230	345	345	500	500	500	500	500	345	220
Longueur *Length*	(1) km	236	143	115	132	160	132	132	(8)	963	223
Période *Period*	(2) années *years*	25	11	11	6.0	3.0	4.5	3.0		3.25	20
Années-kilomètres *Kilometer-years*	(3) an. km *km-yr*	5 900	1 570	1 760	790	480	590	360		3 130	4 460
T.D. moyen/an *Mean TD/year*	TD	40	43	40	40	40	40	40		40	32
N° de câbles de garde *No. of ground wires*		2	2	1	2	2	2	2		2	2
Angle de protection *Shield angle*	deg	19	20	34	20	20	20	20		19	18
Résistance de terre *Ground resistance*	ohms	5	5	5	< 25	< 25	< 25	< 25		5	12
U (50 %)	kV	1 500	1 600	1 600	2 130	2 130	2 130	2 130		1 600	1 500
Profil plat *Flat profile*	%	50	50	75	45	20	90	30		100	–
Profil ondulé *Rolling profile*	%	50	50	10	40	35	10	40		–	100
Profil montagneux *Mountainous profile*	%	–	–	9	25	45	–	40		–	–
Classement nominal du terrain *Nominal terrain class*	%	0	0–W	0–W	0–W	0–W	45 % F	0		0	0–W
(pour la valeur réelle de TD) *STR (at actual TD rate)*		0.24	3.70	5.70	0.25	0.38	0.09	0.76		0.19	0.07
(pour 10 TD/an) *STR (at 10 TD/year)*	*(4)	0.24	3.44	5.70	0.25	0.38	0.00	0.76		0.19	0.09

*Voir tableau 8 pour des remarques supplémentaires concernant les valeurs indiquées dans ce tableau.
(1) 2 236 km
(2) 8,84 km
(3) 19 760 an.-km

*See Table 8 for supplementary notes relating to data given in this table.
(1) 2 236 km
(2) 8,84 mean years
(3) 19,760 km-yr.

Tableau IX (suite) — Table IX (continued)

N° du rapport élémentaire *Reporting Unit Number*			41	42	43	44	45	46	47	48	49	50	51	52
Lettres code du pays *Country code letters*			AUS	AUS	AUS	AUS	AUS	AUS	AUS	ITALY	ITALY	ITALY	ZAM	ZAM
U (ligne) *U (line)*		kV	330	330	330	330	500	330	330	380	380	380	330	330
Longueur *Length*	(1)	km	115	115	225	225	181	45	71.5	141	60	(8)	123	220
Période *Period*	(2)	années *years*	4	4	4	4	4	13	5	2	2		12	6
Années-kilomètres *Kilometer-years*	(3)	an.-km *km-yr*	460	469	900	900	724	585	358	282	136		1 476	1 320
T.D moyen/an *Mean TD/year*		TD	30	30	30	30	15	23	23	24	21		85	91
N° de câbles de garde *No. of ground wires*			2	2	2	2	2	2	2	2	2		2	2
Angle de protection *Shield angle*		deg	30	30	30	30	20	27	27	25	25		23	23
Résistance de terre *Ground resistance*		ohms	14	20	20	16	3	Nacc	54	5	4		13cc	20cc
U(50 %)		kV	1 585	1 585	1 585	1 585	2 045	1 430	1 430	1 430	1 430		1 470	1 470
Profil plat *Flat profile*		%	35(0)	45(0)	20	20	20(0)	52	74	69 54 % (0)	100		59	77
Profil ondulé *Rolling profile*		%	30(0)	30(0)	70	70(30F)	50(0) 25(F)	29	16	17	–		19	10
Profil montagneux *Mountainous profile*		%	35(F)	35(F)	10	10	5(F)	19	10	14	–		22	13
Classement nominal du terrain *Nominal terrain class*		%	65 % (0)	65 % (0)	30 % (F)	10 % (F)	70 % (0)	100 % (F)	100 % (F)	54 % (0)	100 % (0)		100 % (0)	100 % (0)
(pour la valeur réelle de TD) *STR (at actual TD rate)*			0.00	0.43	0.00	0.00	0.00	0.34	0.00	0.35	0.00		0.01	0.00
(pour 30 TD/an) *STR (at 30 TD/year)*		*(4)	0.00	0.57	0.00	0.00	0.00	0.00	0.00	0.58	0.00		0.37	0.035

*Voir tableau 8 pour des remarques supplémentaires concernant les valeurs indiquées dans ce tableau.
(1) 1 530 km
(2) 4,97 années moyennes
(3) 7,610 an.-km

*See *Table 8 for supplementary notes relating to data given in this table.*
(1) 1 530 km
(2) 4,97 *mean years*
(3) 7,610 km-yr.

N° du rapport élémentaire *Reporting Unit Number*			53	54	55	56	57	58	59	60	61	62
Lettres code du pays *Country code letters*			ZAM	ZAM	ZAM	ZAM	RHO	RHO	RHO	RHO	RHO	RHO
U (ligne) *U (line)*		kV	330	330	330	330	330	330	330	330	330	330
Longueur *Length*	(1)	km	(8)	211	211	308	259	123	(8)	(8)	141	205
Période *Period*	(2)	années *years*		3	3	12	12	12			3	3
Années-kilomètres *Kilometer-years*	(3)	an.-km *km-yr*		633	633	3 678	3 108	1 476			423	615
Mean TD/year		TD		109	109	98	78	78			71	50
N° de câbles de garde *No. of ground wires*				2	2	2	2	2			2	2
Angle de protection *Shield angle*		deg		23	23	23	23	23			23	23
Résistance de terre *Ground resistance*		ohms		32 cc	18 cc	10 cc	21 cc	22 cc			8	15
U(50 %)		kV		1 470	1 470	1 470	1 470	1 470			1 470	1 470
Profil plat *Flat profile*		%		100	100	100	90	83			100	99
Profil ondulé *Rolling profile*		%		–	–	–	13	11			–	1
Profil montagneux *Mountainous profile*		%		–	–	–	7	6			–	–
Classement nominal du terrain *Nominal terrain class*		%		100 % (0)	100 % (0)	100 % (0)	100 % (0)	100 % (0)			100 (0)	100 % (0)
(pour la valeur réelle de TD) *STR (at actual TD rate)*				0.63	1.10	0.84	0.77	0.64			0.00	0.47
(pour 30 TD/an) *STR (at 30 TD/year)*		*(3)		0.23	0.40	0.31	0.30	0.33			0.00	0.32

*Voir tableau 8 pour des remarques supplémentaires concernant les valeurs indiquées dans ce tableau.
(1) 1 658 km
(2) 7,82 années moyennes
(3) 12,963 an.-km

*See *Table 8 for supplementary notes relating to data given in this table.*
(1) 1 658 km
(2) 7,82 *mean years*
(3) 12,963 km-yr.

Tableau IX (suite) — Table IX (continued)

N° du rapport élémentaire *Reporting Unit Number*		63	64	65	66	67	68	69	70	71	72	73	74
Lettres code du pays *Country code letters*		AUS	AUS	AUS	AUS	AUS	AUS	AUS	AUS	AUS	AUS	AUS	AUS
U (ligne) *U (line)*	kV	330	330	330	330	330	330	330	330	330	330	330	330
Longueur *Length* (1)	km	100	150	191	183	188	42	84	68	34	69	34	77
Période *Period* (2)	années *years*	8	8	7	8	8	5	8	8	8	8	8	8
Années-kilomètres (3) *Kilometer-years*	an. km *km-yr*	800	1 200	1337	1 464	1 504	210	672	544	272	552	272	616
T.D. moyen/an *Mean TD/year*	TD	20	20	20	30	30	30	30	30	30	30	30	30
N° de câbles de garde *No. of ground wires*		2	2	2	2	2	2	2	2	2	2	2	2
Angle de protection *Shield angle*	deg	23.5	23.5	23.5	23.5	23.5	23.5	23.5	23.5	23.5	23.5	23.5	23.5
Résistance de terre *Ground resistance*	ohms	30 de	30 de	12 de	20 de	20 de	30 de	17 de	25 de	17 de	17 de	17 de	30 de
U (50 %)	kV	1 570	1 570	1 570	1 570	1 570	1 570	1 570	1 515	1 515	1 425	1 470	1 570
Profil plat *Flat profile*	%	10	10	10	10	10	10	30	10	30	20	20	20
Profil ondulé *Rolling profile*	%	10	10	20	90	90	90	70	90	70	80	80	40
Profil montagneux *Mountainous profile*	%	50	50	10	–	–	–	–	–	–	–	–	40
Classement nominal du terrain *Nominal terrain class*	%	M	M	R	R	R	R	R	R	R	R	R	M
(Pour la valeur réelle de TD) *STF (at actual TD rate)*		1.37	0.25	0.20	0.14	0.27	0.00	0.15	0.73	0.00	0.54	0.00	0.32
(Pour 40 TD/an) *STR (at 40 TD/year)*	*(4)	2.74	0.50	0.40	0.19	0.36	0.00	0.20	0.97	0.00	0.72	0.00	0.43

*Voir tableau 8 pour des remarques supplémentaires concernant les valeurs indiquées dans ce tableau.
(1) 1220 km
(2) 7.166 années moyennes
(3) 8.743 an.km

*See Table 8 for supplementary notes relating to data given in this table.
(1) 1220 km
(2) 7.166 mean years
(3) 8.743 km-yr.

N° du rapport élémentaire *Reporting Unit Number*		75	76	77	D[2]C	D[3]C	80	81	82	83	84	D[4]C	D[5]C
Lettres code du pays *Country code letters*		AUS	AUS	AUS	AUS	AUS	AUS	AUS	AUS	POL(5)	CZEC(5)	CAN	CAN
U (ligne) *U (line)*	kV	330	330	330	330	330	330	330	330	400	400	315	315
Longueur *Length* (1)	km	85	(8)	15	117	124	225	(8)	(8)	317	NA	400	250
Période *Period* (2)	années *years*	8	–	8	8	8	8	–	–	1	NA	13	13
Années-kilomètres (3) *Kilometer-years*	an. km *km-yr*	680	–	360	936	992	1800	–	–	317	3 000	5 200	3 250
T.D. moyen/an *Mean TD/year*	TD	30	–	30	30	30	30	–	–	31	31	5	10
N° de câbles de garde *No. of ground wires*		2	–	2	2	2	2	–	–	2	2	2	2
Angle de protection *Shield angle*	deg	23.5	–	23.5	23.5	23.5	23.5	–	–	20	25	14	14
Résistance de terre *Ground resistance*	ohms	17 de	–	10 de	12 de	12 de	12 de	–	–	5ee	10ee	30ee	30ee
U (50 %)	kV	1 570	–	1 570	1 665	1 695	1 570	–	–	1 695	1 610	1 300	1 300
Profil plat *Flat profile*	%	20	–	100	20	20	30	–	–	8	50	–	–
Profil ondulé *Rolling profile*	%	40	–	–	40	40	30	–	–	46	40	100	100
Profil montagneux *Mountainous profile*	%	40	–	–	40	40	40	–	–	46	10	–	–
Classement nominal du terrain *Nominal terrain class*	%	H	–	F	H	H	RM	–	–	RM	Dégagé *Open*	Dégagé *Open*	Dégagé *Open*
(Pour la valeur réelle de TD) *STR (at actual TD rate)*		0.59	–	0.00	0.11	0.00	0.17	–	–	0.00	0.10	0.13	0.1
(Pour 40 TD/an) *STR (at 40 TD/year)*	*(4)	0.79	–	0.00	0.15	0.00	0.23	–	–	0.00	0.51	1.04	1.6

*Voir tableau 8 pour des remarques supplémentaires concernant les valeurs indiquées dans ce tableau.
(1) 1563 km
(2) 10.6 années moyennes
(3) 16.535 an.km

*See Table 8 for supplementary notes relating to data given in this table.
(1) 1563 km
(2) 10.6 mean years
(3) 16.535 km-yr.

TABLEAU IX (suite) — TABLE IX (continued)

N° du rapport élémentaire *Reporting Unit Number*		87	88	89	90	91	92	93	94	95	96	97	98
Lettres code du pays *Country code letters*		CAN	CAN	CAN	DEN	DEN	SWE	SWE	SWE	SWE	SWE	SWE	SWE
U (ligne) *U (line)*	kV	735	500	500	400	400	400	400	400	400	400	400	400
Longueur *Length*	km	1 000	367	335	222	48	419	392	173	156	193	243	208
Période *Period* (1)	années *years*	8	7	7	3	4	3	4	9	9	6	7	9
Années-kilomètres *Kilometer-years* (2)	an. km *km-yr*	8 000	2 570	2 345	666	192	1 257	1 568	1 557	1 404	1 158	1 701	1 872
T.D. moyen/an *Mean TD/year* (3)	TD	5	16	22	20	15	15.0	12.5	17.0	14.7	12.0	12.6	16.9
N° de câbles de garde *No. of ground wires*		2	2	2	2	2	2	2	2	2	2	2	2
Angle de protection *Shield angle*	deg	20	20	20	33	33	31	31	29	29	31	31	31
Résistance de terre *Ground resistance*	ohms	30cc	110cc	110cc	9	9	NAcc	NAcc	NAcc	NAcc	NAcc	NAcc	NAcc
U (50 %)	kV	2 880	1 800	1 800	1 750	1 750	1 750	1 750	1 750	1 750	1 750	1 750	1 750
Profil plat *Flat profile*	%	–	50	50	100	100	80	70	75	70	60	60	80
Profil ondulé *Rolling profile*	%	100	50	50	–	–	20	20	20	20	30	30	20
Profil montagneux *Mountainous profile*	%	–	–	–	–	–	–	10	5	10	10	10	–
Classement nominal du terrain *Nominal terrain class*	%	Dégagé *Open*	25 %(O) 75 %(F)	25 %(O) 75 %(F)	Dégagé *Open*	Dégagé *Open*	40 %(O) 60 %(F)	20 %(O) 80 %(F)	15 %(O) 85 %(F)	100 %(F)	10 %(O) 90 %(F)	100 %(F)	40 %(O) 60 %(F)
(Pour la valeur réelle de TD) *STR (at actual TD rate)*	(9)	0.00	0.00	0.17	0.45	0.00	0.08	0.13	0.19	0.07	0.00	0.12	0.27
(Pour 40 TD/year) *(STR for 40 TD/year)*	*(4)	0.00	0.20	0.31	0.90	0.00	0.21	0.42	0.45	0.19	0.00	0.38	0.64

*Voir tableau 8 pour des remarques supplémentaires concernant les valeurs indiquées dans ce tableau.
(1) 3 756 km
(2) 6.47 années moyennes
(3) 24.290 an. km

*See Table 8 for supplementary notes relating to data given in this table.
(1) 3 756 km
(2) 6.47 mean years
(3) 24.290 km-yr

N° du rapport élémentaire *Reporting Unit Number*		99	100	101	102	103	104	105	106	107	108	109(5)	110
Lettres code du pays *Country code letters*		SWE	SWE	SWE	SWE	SWE	SWE	JAP D–C	JAP D–C	JAP D–C	JAP D–C	UK D–C	FIN
U (ligne) *U (line)*	kV	400	220	220	220	220	220	275	275	275	275	400	400
Longueur *Length*	km	207	(8)	265	66	67	84	348	318	632	738	2 974	122
Période *Period* (1)	années *years*	9	–	9	9	9	9	11.00	11.75	10.95	10.89	6	5
Années-kilomètres *Kilometer-years* (2)	an. km *km-yr*	1 863	–	2 385	594	603	756	3 828	3 736	6 920	8 037	17 844	610
T.D. moyen/an *Mean TD/year* (3)	TD	16	–	13	11	12	11	25.7	24.5	28.3	23.3	9	10
N° de câbles de garde *No. of ground wires*		2	–	2	2	2	2	2	2	2	2	1	2
Angle de protection *Shield angle*	deg	31	–	55/31	55/31	55/31	55/31	13.5	13.5	13.5	13.5	39	30
Angle de protection *Ground resistance*	ohms	NA cc	–	NA cc	NA cc	NA cc	NA cc	23.0	8.0	25.0	13.0	4.0	15^{cc}_{cc}
U (50 %)	kV	1 750	–	1 500	1 500	1 500	1 500	1 220	1 220	1 160	1 220	1 690	1 300
Profil plat *Flat profile*	%	80	–	70	70	70	70	24	35	24	20	8	75
Profil ondulé *Rolling profile*	%	20	–	20	20	20	20	13	22	14	8	92	25
Profil montagneux *Mountainous profile*	%	–	–	10	10	10	10	63	43	62	72	–	–
Classement nominal du terrain *Nominal terrain class*	%	30 % (O) 70 % (F)	–	10 % (O) 90 % (F)	100 % (F)	100 % (F)	100 % (F)	29 % (O) 40 % (F)	13 % (O) 44 % (F)	26 % (O) 46 % (F)	20 % (O) 12 % (F)	95 % (O)	44 % (O) 56 % (F)
(pour la valeur réelle de TD) *STR (at actual TD rate)*		0.16	–	0.17	1.35	0.66	1.45	1.59	0.91	1.82	1.68	0.80	0.16
(pour 40 TD/an) *STR (at 40 TD/year)*	*(4)	0.40	–	0.52	4.90	2.20	5.27	2.47	1.48	2.57	2.88	3.55	0.64

*Voir tableau 8 pour des remarques supplémentaires concernant les valeurs indiquées dans ce tableau.
(1) 5021 km
(2) 8.1 années moyennes
(3) 47.177 an. km

*See Table 8 for supplementary notes relating to data given in this table.
(1) 5021 km
(2) 8.1 mean years
(3) 47.177 km-yr

TABLEAU IX (suite) — TABLE IX (continued)

N° du rapport élémentaire *Reporting Unit Number*			111	112	113	114	115	116	117	118	119	120	121
Lettres code du pays *Country code letters*			FIN	FIN	FIN	FIN	FIN	FIN	FIN	FIN	FIN	FIN	FIN
U (ligne) *U (line)*		kV	400	400	400	220	220	220	220	220	220	220	220
Longueur *Length*	(1)	km	398	155	83	71	39	17	100	80	298	298	83
Période *Period*	(2)	années *years*	5	12	12	9	13	13	5	5	18	17	12
Années-kilomètres *Kilometer-years*		an. km *km-yr*	1 990	1 860	996	639	507	221	500	400	5 184	5 066	996
TD moyen/an *Mean TD/year*	(3)	TD	10	8	8	14	11	13	11	11	10	10	10
N° de câbles de garde *No. of ground wires*			2	2	2	2	2	2	2	2	2	2	NONE
Angle de protection *Shield angle*		deg	30	30	30	30	28	28	28	29	29	28	–
Résistance de mise *Ground resistance*		ohms	23 re ec	32 re ec	28 re ec	45 re ec	15 re ec	30 re ec	30 re ec	25 re ec	50 re ec	30 re ec	40 re ec
U (50 %)		kV	1 350	1 400	1 450	800	900	850	900	900	1 000	900	750
Profil plat *Flat profile*		%	75	70	70	60	90	70	70	90	70	70	60
Profil ondulé *Rolling profile*		%	25	30	30	40	10	30	30	10	30	30	40
Profil montagneux *Mountainous profile*		%	–	–	–	–	–	–	–	–	–	–	–
Classement nominal du terrain *Nominal terrain class*		%	37 % (O) 63 % (F)	10 % (O) 90 % (F)	18 % (O) 82 % (F)	36 % (O) 64 % (F)	44 % (O) 56 % (F)	57 % (O) 43 % (F)	47 % (O) 53 % (F)	84 % (O) 16 % (F)	10 % (O) 90 % (F)	17 % (O) 83 % (F)	16 % (O) 84 % (F)
(pour la valeur reelle de TD) *SFR (at actual TD rate)*			0.70	0.16	0.10	0.78	0.90	0.91	1.60	0.00	0.35	0.15	4.80
(pour 10 TD/an) *SFR (at 10 TD/year)*		*(4)	2.80	0.80	0.50	2.21	0.99	2.89	5.82	0.00	1.40	1.80	19.20

*Voir tableau 8 pour des remarques supplémentaires concernant les valeurs indiquées dans ce tableau.
(1) 1 612 km
(2) 11,4 années moyennes
(3) 18 359 an.-km

*See Table 8 for supplementary notes relating to data given in this table.
(1) 1 612 km
(2) 11.4 mean years
(3) 18 359 km-yr.

7. Appendices.

7.1. *Exemple de calcul des paramètres moyens d'une ligne à partir des caractéristiques des pylônes et du profil.*

Rapport élémentaire n° 84		Grandeur	Mètres
Répartition du profil		H_t	30,0
Plat	60 %	Y_t	18,0
Ondulé	30 %	S_c	9,4
Montagneux	10 %	S_g	7,5
		a	5,6

$$\bar{Y}_F = Y_t - \frac{2}{3} S_c = 18.0 - 6.3 = 11.7 \text{ m}$$

$$\underline{\bar{Y}_F \cong 12 \text{ m}}$$

$$\bar{H}_F = H_t - \frac{2}{3} S_g = 30 - 5 = 25 \text{ m}$$

$$\bar{H}_F - \bar{Y}_F = \bar{H} - \bar{Y} = 25 - 12 = 13 \text{ m}$$

$$\bar{Y} = 0.6 \times 12 + 0.3 \times 18 + 0.1 \times 36 \cong 16 \text{ m}$$

$$\bar{H} = \bar{Y} + \bar{H}_F - \bar{Y}_F = 16 + 13 = 29 \text{ m}$$

$$\bar{\theta}_t = \text{arc tan } a/(\bar{H} - \bar{Y}) = \text{arc tan } 5.4/13$$

$$\bar{\theta}_t = 22.6^\circ = 23^\circ = 0.4 \text{ radians}$$

7. Appendices.

7.1. Sample calculation of mean line parameters from tower and profile data.

Reporting unit No. 84		*Item*	*Meters*
Profile Distribution		H_t	30.0
Flat	60 %	Y_t	18.0
Rolling	30 %	S_c	9.4
Mountainous	10 %	S_g	7.5
		a	5.6

$$\bar{Y}_F = Y_t - \frac{2}{3} S_c = 18.0 - 6.3 = 11.7 \text{ m}$$

$$\underline{\bar{Y}_F \cong 12 \text{ m}}$$

$$\bar{H}_F = H_t - \frac{2}{3} S_g = 30 - 5 = 25 \text{ m}$$

$$\bar{H}_F - \bar{Y}_F = \bar{H} - \bar{Y} = 25 - 12 = 13 \text{ m}$$

$$\bar{Y} = 0.6 \times 12 + 0.3 \times 18 + 0.1 \times 36 \cong 16 \text{ m}$$

$$\bar{H} = \bar{Y} + \bar{H}_F - \bar{Y}_F = 16 + 13 = 29 \text{ m}$$

$$\bar{\theta}_t = \text{arc tan } a/(\bar{H} - \bar{Y}) = \text{arc tan } 5.4/13$$

$$\bar{\theta}_t = 22.6^\circ = 23^\circ = 0.4 \text{ radians}$$

7.2. *Questionnaire.*

Cette annexe décrit le questionnaire mis en circulation dans les pays participants dans lequel on a omis volontairement les chapitres ou les remarques qui furent si rarement repris dans les rapports qu'on peut les laisser de côté. On y trouve de brèves remarques attirant l'attention sur ces chapitres. Les chapitres que l'on a dû incorporer pour réduire le travail d'analyse sont indiqués également.

TABLEAU I

Valeurs caractéristiques

Chapitre	Description
1.	(a) Pays ..... (b) Organisme ou représentant rapporteur ....
2.	Désignation de la ligne (nom ou nombre) ....
3.	Tension nominale, kV .....
4.	Longueur de la ligne, km .....
5.	Nombre de circuits (accrochés aux pylônes)
6.	Nombre de câbles de garde (câbles écran) (*voir remarque 1*) .....
7.	Longueur moyenne des cantons de pose, m
8.	Flèche moyenne des conducteurs, m .....
9.	Flèche moyenne des câbles de garde, m .....
10.	Nombre de pylônes d'alignement (si rapidement disponible) .....
11.	Nombre de pylônes d'angle (si rapidement disponible) .....
12.	Type de mise à la terre des pylônes (Remarque 2) .....
13.	Résistance en continu du système de mise à la terre des pylônes, le câble de garde étant déconnecté. Valeur ohmique minimale ..... Valeur ohmique moyenne ..... Valeur ohmique maximale .....
14.	Matériau constituant les pylônes (fer, bois)
15.	Matériau constituant les bras (fer, bois) .....
16.	Type de terrain traversé (Remarque 3) .....
17.	Répartition des profils (Remarque 4) .....
18.	Nombre et disposition des chaines d'isolateurs
19.	Réglage éventuel des éclateurs sur les chaines ..... m
20.	Tension d'amorçage 50 % au choc, à sec ..... kV Longueur hors tout des chaines ..... m

Remarque 1. Fournir des croquis cotés des pylônes d'alignement et d'angle indiquant la disposition des conducteurs et des câbles de garde, les dimensions et les hauteurs correspondantes, et les angles de protection.

Remarque 2. Lorsqu'on utilise pour la mise à la terre des contrepoids continus, il faut indiquer les sections de ligne correspondantes sur le croquis de la remarque 3. La disposition des conducteurs pour des contrepoids continus ou radiaux doit être indiquée.

7.2. Questionnaire.

This appendix describes the questionnaire circulated to participating countries, amended to omit items or notes which were reported so infrequently as to be disregarded. Brief notes are included here to call attention to such items. Items which should have been included to reduce the labour of analysis are indicated.

TABLE I

Design Data

Item	*Description*
1.	*(a) Country* ..... *(b) Organization or reporting representative*
2.	*Designation of line (name or number)* ———
3.	*Rated voltage, kV* .....
4.	*Route length of line, km* .....
5.	*Number of circuits (carried on tower)* ....
6.	*Number of overhead ground (shield) wires* (See Note 1) .....
7.	*Average span length, m* .....
8.	*Average sag of phase conductor, m* .....
9.	*Average sag of ground wire, m* .....
10.	*Number of straight line towers* ..... *(If readily available)*
11.	*Number of angle towers* ..... *(If readily available)*
12.	*Type of tower grounding (Note 2)* .....
13.	*D-C resistance of tower grounding system with ground (shield) wire disconnected. Minimum ohms* ..... *Average ohms* ..... *Maximum ohms* .....
14.	*Tower material (steel, wood)* .....
15.	*Crossarm material (steel, wood)* .....
16.	*Type of terrain traversed (Note 3)* .....
17.	*Profile distribution (Note 4)* .....
18.	*Number and arrangement of suspension insulators* .....
19.	*Setting of arc gaps, if any, across insulators* ..... *m*
20.	*50 % impulse flashover voltage, dry* ..... *kV* *Taut string length* ..... *m*

Note 1. Furnish dimensioned sketches of suspension and angle towers showing arrangement of phase conductors and ground (shield) wires, relevant dimensions and heights, and shielding angles.

Note 2. Where continuous counterpoises are used for grounding, the appropriate sections of line should be indicated on the sketch of Note 3. The arrangement of conductors for continuous or radial counterpoises should be shown.

Remarque 3. On fournira un croquis ou une carte indiquant le tracé de la ligne en notant le type du terrain, les portions forestières où des arbres dépassent environ la moitié de la hauteur des pylônes, la largeur du « droit de passage », et les conditions de sol. Lorsque deux ou plusieurs lignes sont parallèles sur des distances importantes, il faut indiquer la distance séparant les centres des pylônes. La direction des orages doit aussi être indiquée si on la connaît.

Remarque 4. En se basant sur les définitions ci-dessous, fournir s.v.p. une estimation de la répartition des profils comme suit :

% Plat % Ondulé % Montagneux

Plat, hauteur au-dessus du sol du conducteur inférieur en milieu de portée *inférieure* à sa hauteur au-dessus du sol au droit du pylône.

Ondulé, hauteur au-dessus du sol du conducteur inférieur en milieu de portée *égale* à sa hauteur au-dessus du sol au droit du pylône.

Montagneux, hauteur au-dessus du sol du conducteur inférieur en milieu de portée *considérablement plus importante* que sa hauteur au-dessus du sol au droit du pylône.

Note 3. *A sketch or map should be furnished showing the route of the line with indication of the type of terrain, forested sections where trees exceed in height about half that of the towers, width of "rights-of-way", and soil conditions. Where two or more lines run parallel for substantial distances, the separation between tower centers should be indicated. Direction of storm should also be indicated, if known.*

Note 4. *Based on the definitions below, please furnish an estimate of the profile distribution as :*

% Flat % Rolling % Mountainous

Flat, *midspan ground clearance of bottom conductor* less than *that at the tower.*

Rolling, *midspan ground clearance of bottom conductor* equal to *that at the tower.*

Mountainous, *midspan ground clearance of bottom conductor* substantially greater than *that at the tower.*

Tableau II

Réponses statistiques annuelles

Chapitre — Description

1. Pays .....
2. Désignation de la ligne (nom ou nombre) .....
3. Année ou ensemble d'années .....
4. Défauts dus à la foudre (compter tous les déclenchements automatiques du circuit comme un défaut, indépendamment de la durée de l'interruption).
   - 4.1. Nombre de défauts sur des lignes à circuit simple .....
   - 4.2. Nombre de défauts sur des lignes à circuit double :
     Circuit 1 .....
     Circuit 2 .....
     Circuits 1 et 2 .....
   - 4.3. Répartition des défauts entre les conducteurs :

Phase	Ligne à Circuit simple	Ligne à circuit double		
		Circuit 1	Circuit 2	Circuits 1 et 2
Supérieure				
Intermédiaire				
Inférieure				
Supérieure et moyenne				
Supérieure et inférieure				
Moyenne et inférieure				
Les trois phases				

Table II

Annual Statistical Returns

Item — *Description*

1. *Country* .....
2. *Designation of line (name or number)* .....
3. *Year or accumulated years* .....
4. *Lightning faults (count every automatic disconnection of the circuit as a fault independent of the duration of the service interruption).*
   - 4.1. *Number of faults on single-circuit lines* .....
   - 4.2. *Number of faults on double-circuit lines:*
     Circuit 1 .....
     Circuit 2 .....
     Circuits 1 and 2 .....
   - 4.3. *Distribution of faults among phase conductors :*

Phase	*Single-circuit Line*	*Double-circuit line*		
		Circuit 1	*Circuit 2*	*Circuits 1 & 2*
Top				
Middle				
Bottom				
Top and middle				
Top and bottom				
Middle and bottom				
All three phases				

Pour des dispositions horizontales ou en double delta (triangulaires) des conducteurs, utiliser s.v.p. le repérage de la figure jointe (voir Fig. 1) ou fournir un repérage et un croquis analogues.

5. Activité orageuse

5.1. Nombre de journées d'orage .....
S'il existe des différences appréciables le long de la ligne, prière de les indiquer et de fournir une valeur moyenne estimée pour la ligne .....

5.2. Méthode par laquelle est établi le renseignement de 5.1. .....

5.3. Durée annuelle des orages en heures d'orage, si ce chiffre est disponible .....

5.4. Méthode par laquelle est établi le renseignement de 5.3. .....

Commentaires : Les renseignements demandés dans les remarques 2 et 3 furent si rarement fournis que l'on peut dire qu'il n'est pas réaliste de compter dessus. D'autre part, les estimations demandées dans les remarques 1 et 4 furent presque toujours données. L'analyse des valeurs aurait été facilitée si l'impédance caractéristique du conducteur utilisé pour l'évaluation de la protection avait été donnée ou bien si le diamètre *extérieur* du conducteur avait été donné ainsi que les dimensions du faisceau.

Remerciements

Au nom du Groupe de Travail 33.01 de la CIGRÉ, l'auteur exprime sa reconnaissance la plus profonde aux représentants des pays ayant participé à ce tour d'horizon pour leur excellente coopération pendant une période de temps importante. On espère cependant que les résultats obtenus seront une expression encore plus concrète de nos remerciements.

For horizontal or double-delta (triangular) conductor configurations, please use the coding of the accompanying figure (see Figure 1) or furnish a similar coding and sketch.

5. *Thunderstorm activity*

5.1. *Number of thunderstorm days* .....
If there are notable differences along the length of the line, please so indicate and furnish an estimated mean value for the line .....

5.2. *Method by which the information of 5.1. is established* .....

5.3. *Annual duration of thunderstorms in thunderstorm hours, if this figure is available* .....

5.4. *Method by which the information of 5.3 is established* .....

Comments : *The information requested in Notes 2 and 3 was so rarely furnished as to suggest that it was unrealistic to expect it. On the other hand, the estimates requested in Notes 1 and 4 were nearly always furnished. Analysis of the data would have been facilitated if either the surge impedance of the conductor used for shielding evaluation had been available or if the outside diameter of the conductor had been supplied along with the bundle dimensions.*

In Appreciation

On behalf of CIGRÉ Working Group 33.01 the author wishes to express most sincere appreciation to the representatives of the countries participating in this survey for their excellent co-operation over an extended period. It is hoped, however, that the results will convey our thanks in more tangible fashion.

Bibliographie — References

[1] D.W. Gilman and E.R. Whitehead. — Le mécanisme des amorçages dus à la foudre sur les lignes de transport à haute et à très haute tension. — The Mechanism of Lightning Flashover on High-Voltage and Extra-High-Voltage Transmission Lines, Electra, No. 27, mars/March, 1973, pp. 65-96.

[2] E.R. Whitehead. — Final Report of Edison Electric Institute Mechanism of Lightning Flashover Research Project RP 50, EEI Publication No. 72-900, Edison Electric Institute, 90 Park Avenue, New York, N.Y., U.S.A. 10016.

[3] E.R. Love. — Improvements in Lightning Stroke Modeling and Applications to the Design of HV and EHV Transmission Lines, Thesis submitted in partial fulfillment of the requirements for the Master of Science degree, University of Colorado, Boulder, Colorado, U.S.A.

[4] J.R. Gobbe, Ah Choy Liew and M. Darveniza. — Monte Carlo Determination of the Frequency of Lightning Strokes to and Shielding Failures on Transmission Lines, IEEE Trans., PA & S, Vol. PAS 90, September/October, 1971, pp. 2305-2312.

[5] E.R. Whitehead, M. Darveniza and F. Popolansky. — Protection contre la foudre des lignes de transport à ultra-haute tension, Rapport 33-73 (CE) 04 présenté au Colloque du Comité d'Etudes n° 33, Cracovie, Pologne, du 17 au 22 septembre 1973. — Lightning Protection of UHV Lines, report 33-73 (SC) 04 presented at the Colloquium of CIGRÉ Study Committee No. 33, Cracow, Poland, 17-22 September, 1973.

THE FREQUENCY DISTRIBUTION OF CURRENT MAGNITUDES OF LIGHTNING STROKES TO TALL STRUCTURES

Michael A. Sargent

Ontario Hydro, Toronto, Canada (On leave from the Cairns Regional Electricity Board, Cairns, Australia)

Abstract – The frequency distribution of stroke current magnitudes proposed in the literature are examined to evaluate the influences that the height and type of structure have on the distribution of current magnitudes observed in the structures. These analyses have been performed using a three-dimensional electro-geometric model[1]. Results indicate that both the height and the type of the structure on which current measurements are made significantly influence the observed frequency distribution. It is suggested that these effects contribute to the differences existing between alternative distributions found in the literature.

INTRODUCTION

The amplitudes of lightning stroke currents injected into various structures have been the subject of investigation for many years. Many alternative frequency distributions of amplitudes have been proposed – for example[2-5] – with marked deviations between them. These differences have been primarily ascribed to measurement errors[3] in older records. However, differences exist even between the more modern records, suggesting another undefined influence. The work reported here indicates that a possible source of the differences is the variation of the height and type (tower or line) of the structure on which the measurements are made.

In this report, the influence of the structure type and height on the distribution of stroke current amplitudes measured in it, is investigated using a three-dimensional electrogeometric analysis[1]. While it is recognized that the electrogeometric technique is still being calibrated against field data[6,7] no attempt has been made to validate the technique further. Rather the approach has been to use earlier calibrations[6,7] in the model to provide the preliminary results reported here. Quantitative results of greater accuracy must await the final validation of the electromagnetic technique.

It is hoped that the analyses reported here will assist in defining the sources of differences between observed distributions, and contribute to the development of an acceptable distribution of stroke current magnitudes for lightning performance calculations. As demonstrated in recent analysis[8,10] this parameter is of great significance in these calculations.

ELECTROGEOMETRIC TECHNIQUE

The electrogeometric technique has been developed and expanded by several investigators[6-9,1] as a method of determining the effectiveness of transmission shielding. The basis of the technique is that the termination point of a lightning stroke is determined when the tip of the downward leader stroke reaches a point where the distance to the most likely target first equals the strike distance (r_s). The three-dimensional model used in the present work is described in[1] and only the assumptions of the model will be stated, as follows:

(i) The location of the leader stroke is independent of any components of the model until within the striking distance of that component.

(ii) The frequency distribution of the stroke current amplitudes *to ground* – $P_g(I)$ – is known.

(iii) The strike distance (r_s) is directly related to the prospective stroke current magnitude as

$$r_s = K_I (I)^b \tag{1}$$

where K_I, b are constants

(iv) The probability distribution of the approach angle (ψ) of the leader stroke in *any* vertical plane is described by

$$g(\psi) = K_m \cos^m \psi \qquad -\pi/2 \leq \pi/2 \tag{2}$$

where ψ is measured from the vertical.

Brown and Whitehead[6] have calibrated a two-dimensional electrogeometric model against field data from transmission line shielding, and proposed the following relationships

$$r_s = 7.1\ I^{0.75} \quad \text{metres} \tag{3a}$$

$$r_{sg} = K_{sg} r_s \quad \text{(strike distance to ground)} = r_s \tag{3b}$$

$$g(\psi) = 2/\pi\ \cos^2 \psi \tag{3c}$$

$$P_g(I) = \text{AIEE distribution (2)} \tag{3d}$$

In the present work, equations (3a), (3b) and (3c) are used exclusively, while alternative analyses were performed using various relationships for $P_g(I)$. Throughout the analyses it has been assumed that the number of strokes per year, dN, to a ground area dA depends only on the element area – that is, the ground flash density N_o is constant over the area modelled, and

$$dN = N_o\, dA \tag{4}$$

EFFECT OF STRUCTURE HEIGHT AND TYPE

Simple Analytic Model

The simple analytic model illustrated in Figure 1 will be used to identify the reasons for the influence of structure height and type on the frequency distribution of stroke current amplitudes observed in the structure.

Consider a point T located at height h above a flat horizontal ground plane (where T could correspond to the top of a tower or chimney or be a point on a horizontal wire), and a vertical leader stroke of prospective return current amplitude I_o. The strike distances to ground, (r_{sg}), and to point T, (r_s), may then be evaluated. The area effectively protected against the stroke by the component T is proportional to the chord AB of half length X where

$$X = \left[r_s^2 - (r_{sg} - h)^2 \right]^{1/2} \qquad r_{sg} > h \tag{5}$$

$$= r_s \qquad r_{sg} \leq h$$

It should be noted that in general

Paper T72 216-5, recommended and approved by the Transmission & Distribution Committee of the IEEE Power Engineering Society for presentation at the IEEE Winter Meeting, New York, N.Y., January 30-February 4, 1972. Manuscript submitted June 18, 1971; made available for printing December 3, 1971.

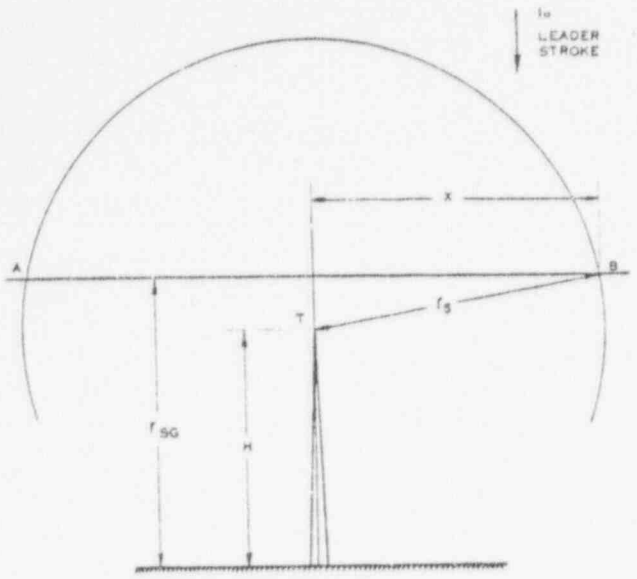

Fig. 1. Simple analytic model for calculation of protective zones

$$X = fn\ (r_s,\ h) \tag{6}$$

$$= fn\ (I_o,\ h) \tag{6}$$

as the strike distances are related to prospective stroke current. It is also seen that as the prospective stroke current magnitude increases, or as the height of the structure increases, the value of X increases. The area protected by the point T is of the general form.

$$A = K_2 X^n \tag{7}$$

where K_2, n are constants depending on the type of structure being considered.

If the probability $P_g(I_o)$ that a stroke current of magnitude I_o will occur in the model is evaluated from the assumed distribution of current amplitudes to ground, then the number of strokes of amplitude I_o expected to be incident on point T can be calculated as

$$P_T(I_o) = P_g(I_o) \cdot N_o \cdot dA$$

$$= P_g(I_o) \cdot N_o \cdot K_2 X^n \tag{8}$$

Note that X is a function of I_o and h, and therefore it is not possible to simplify the relationship to the form

$$P_T(I_o) = \text{constant} \cdot P_g(I_o) \tag{9}$$

Rather the proportion of stroke currents of magnitude I_o observed in the structure is determined by the amplitude-dependent weighting factor K_2X^n as well as the assumed current distribution to ground. Since X increases with the current amplitude and structure height, the distribution $P_T(I)$ will be biased towards the higher current amplitude values, the extent of the bias being dependent on the structure height, h.

It should also be noted that the type of structure will have an effect on the distribution of current values observed. The area protected by the point T, as expressed in (7) is

$$dA = K_2 X^n$$

For a single vertical structure (tower or chimney), $K_2 = \pi$ & n = 2. For a horizontal wire, approximating a transmission line earthwire, $K_2 = 2L$ (where L is the line length), and n=1.

The extent to which the distribution $P_T(I)$ is biased towards high current amplitudes and by the height of the structure is dependent on the power of n in equation (7) and thus is more pronounced for the case of single towers than for transmission lines.

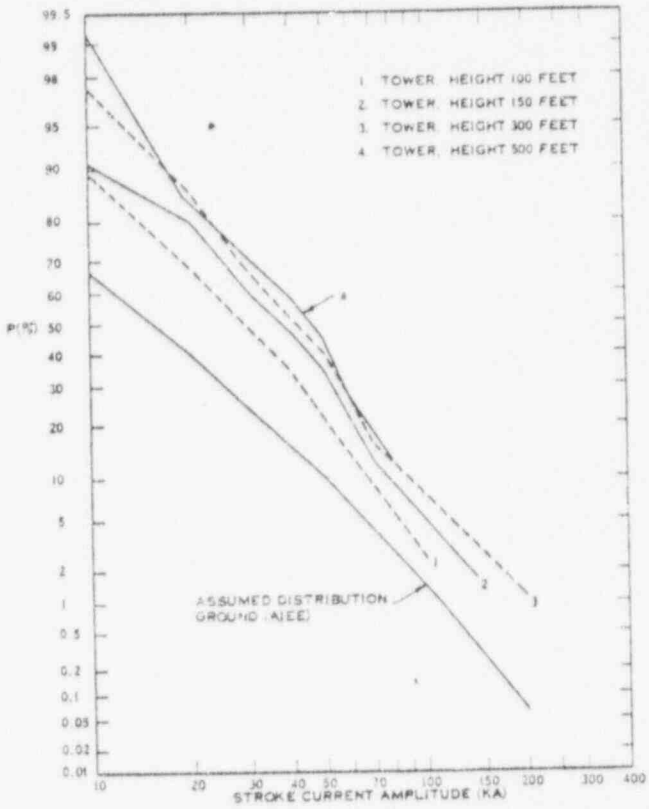

Fig. 2. Effect of structure height on frequency distribution (I_{min} = 2KA)

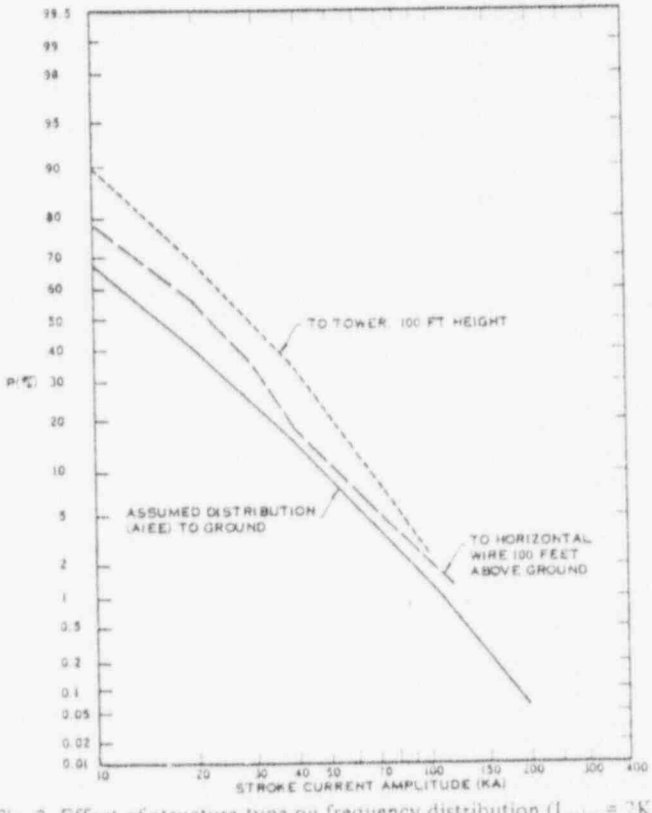

Fig. 3. Effect of structure type on frequency distribution (I_{min} = 2KA)

EFFECT OF STRUCTURE HEIGHT

The distribution of stroke current amplitudes in isolated towers has been simulated using the Monte Carlo electrogeometric technique[1]. The model adopted for the analyses was a single vertical tower located in the centre of a horizontal plane one mile square. The stroke parameters used were those proposed by Brown and Whitehead[6]. Analyses were performed for tower heights in the range 100 – 500 feet. The results of these analyses are shown in Figure 2. It is seen that the height of the tower has a marked influence on the distribution of stroke current amplitudes observed in the structure, with the distributions being biased increasingly towards the high amplitude current values as the tower height increases.

EFFECT OF STRUCTURE TYPE

The distribution of stroke current amplitudes incident on a horizontal wire 100 feet above the ground has been simulated by the same electrogeometric technique. This wire approximates the configuration of a transmission line, in that the line provides an essentially horizontal electrode system compared with the vertical electrode of an isolated tower. The distribution of currents incident on this wire is compared, in Figure 3, with the distribution calculated for a vertical tower of 100 feet height. It is noted that:

(a) The structure type has significant influence on the observed distribution.

(b) The distribution of stroke currents to tower is biased further towards higher amplitude values than the distribution to the wire, exactly the effect predicted by the previous simple analytic model.

PROTECTIVE ZONE OF STRUCTURES

The earliest methods of designing shielding networks for protection against lightning strokes were normally based on the concept of protective zones or angles. Though this approach does not account for the variation of protective zone with prospective current amplitude of the stroke (as a result of the strike distance concept) it still provides a convenient and useful technique for preliminary design. Analysis of the results of the investigations reported in the previous sections yielded estimates of the average protected zones of the various structures, which are summarized in Table I. It is noted that in the range of structure heights investigated (50 – 500 feet) the protective angle, θ, of a structure of height h (ie. a tower of height h or an earth-wire h feet above the ground) can be calculated as

$$\tan \theta = \frac{50.8}{h^{0.707}} \qquad (10)$$

where h is in feet. A comparison between the protected swathe calculated per (10) and that obtained from the Monte Carlo simulation is made in Table I showing the excellent agreement. It is interesting to note that the protective angle is a function of tower height.

It should be noted that equation (10) has been derived using specific input data as summarized in equation (3), and that the use of other data for distribution of stroke current magnitude and for strike distance will provide different results. It should also be noted that the protective zone referred to is an average zone – the estimated zone will be optimistic for low amplitude current and pessimistic for high amplitude currents.

TABLE I
PROTECTIVE ZONES OF TALL STRUCTURES

Structure Type	Height Above Ground Plane (feet)	Protective Zone at Ground Plane* (feet)	
		Monte Carlo Simulation	Calculation Equation (10)
Tower	50	140	159
	100	184	196
	150	221	220
	300	270	271
	500	320	315
Horizontal Wire	100	195	196

*Protective zones for towers is radius at ground level. Protective zone for wire is zone width on each side of wire.

SIMULATION OF OBSERVED DISTRIBUTIONS

The analyses of the previous section have been based on the assumption that the frequency distribution of stroke current amplitudes to ground is identical with the AIEE distribution[2]. This assumption must now be re-examined. The AIEE distribution has been defined as a result of current measurements on transmission lines and towers. As shown in previous sections, the heights of these structures will cause the distribution to be biased towards higher current amplitudes with respect to the true distribution of current amplitudes to level ground. Therefore, the use of a distribution obtained from measurements on tall structures in the electrogeometric model is not accurate – the true distribution of stroke currents to level ground is required.

In this section a distribution of current amplitudes to level ground will be proposed. This distribution will be used in the electrogeometric model to demonstrate that several of the current distributions proposed in the literature[2,4,5] can be approximately simulated accounting for the average heights of structures on which these measurements were made. It should be noted that the exact simulation of these distributions is not possible as current measurements used in each observed distribution have been obtained from structures of various heights.

A synthetic distribution of stroke current magnitudes to level ground has been developed during these analyses, from consideration of the relationships expressed in equations (5), (7) and (8). The synthetic distribution was obtained by assuming that any observed dis-

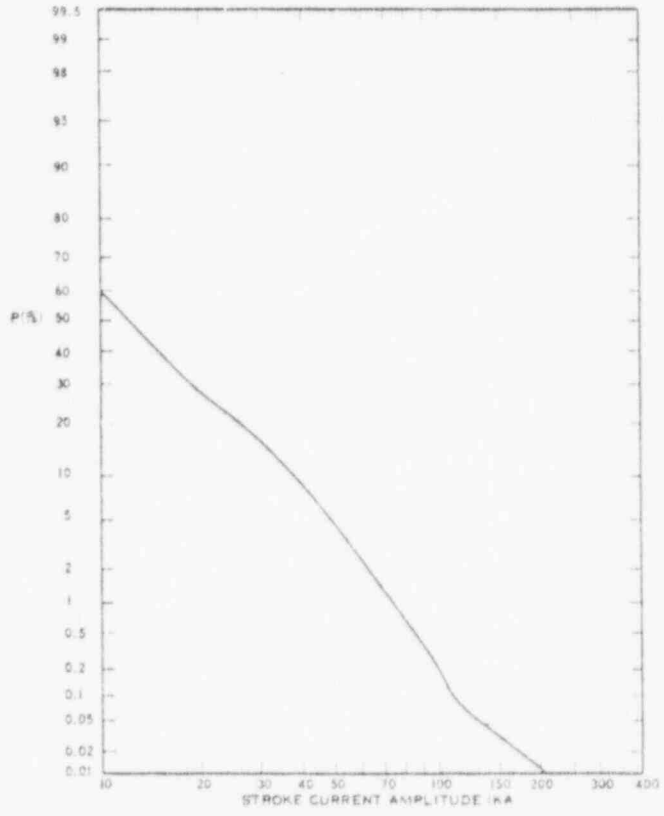

Fig. 4. Synthetic distribution of stroke current amplitudes to level ground (I_{min} = 2KA)

tribution would correspond to $P_T(I)$ in equation (8). The effects of structure height and types were then evaluated according to equations (5) and (7) to provide an estimate of the true distribution of stroke current magnitudes to level ground, $P_g(I)$. This distribution, called synthetic to differentiate between it and the various observed distributions, has been used in the analyses of this section.

The synthetic distribution developed is shown in Figure 4. The distribution assumes a minimum significant current of 2KA and a maximum current (.001% probability) of 350KA.

This distribution has been used, together with the Brown-Whitehead data for strike distances and approach angle (equations 3a, 3b, and 3c) in the simulation of the observed distributions proposed by the AIEE[2], Popolansky[4] and Berger[5]. For each distribution the average heights of the structures on which measurements were made have been used, except for the Popolansky distribution where two heights were analyzed (50m and 75m) because of the large range of tower heights involved.

The results of these simulations are compared with the observed distributions in Figure 5 (for the Popolansky distribution), Figure 6 (for Berger's distribution), and Figure 7 (for the AIEE distribution). In general it is noted that the correlation between observed and calculated distributions is good. Some discrepancy is noted at higher current amplitudes in the comparison for the AIEE distribution, possibly due to the fact that this is a composite distribution, derived from many sources – both transmission line measurements and tall tower measurements – while the simulation considered only a horizontal wire 20m above the ground.

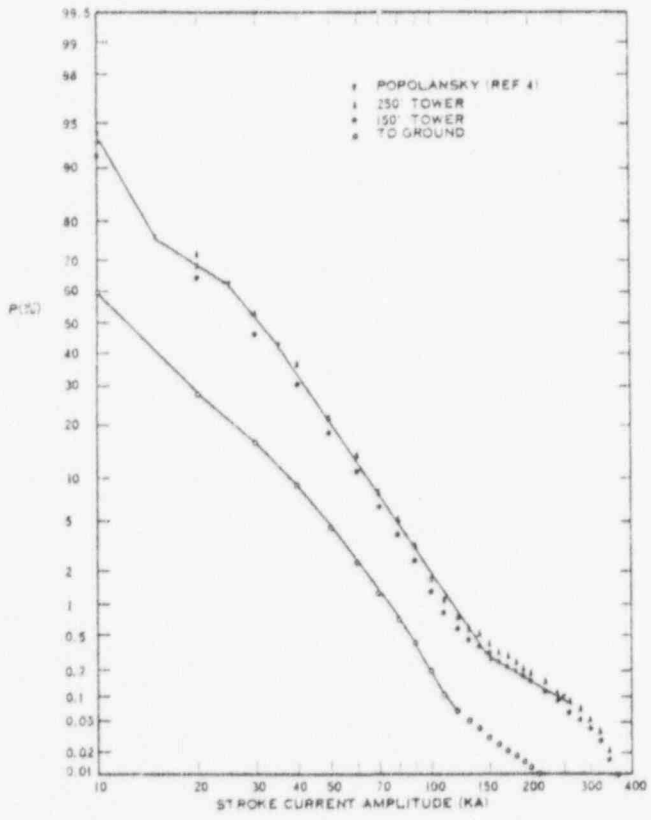

Fig. 5. Simulation of Popolansky's distribution of strokes to tall objects (I_{min} = 2KA).

The close simulation of these three observed distributions indicates the importance of considering structure height and type when establishing distributions of stroke current magnitude for lightning performance calculations. The effect of the structure dimensions is seen to be a major contributor to the discrepancies between observed distributions, and the correlation indicated in Figs 5-7 has not required arbitrarily assumed correction factors to adjust the current magnitudes of the various distributions.

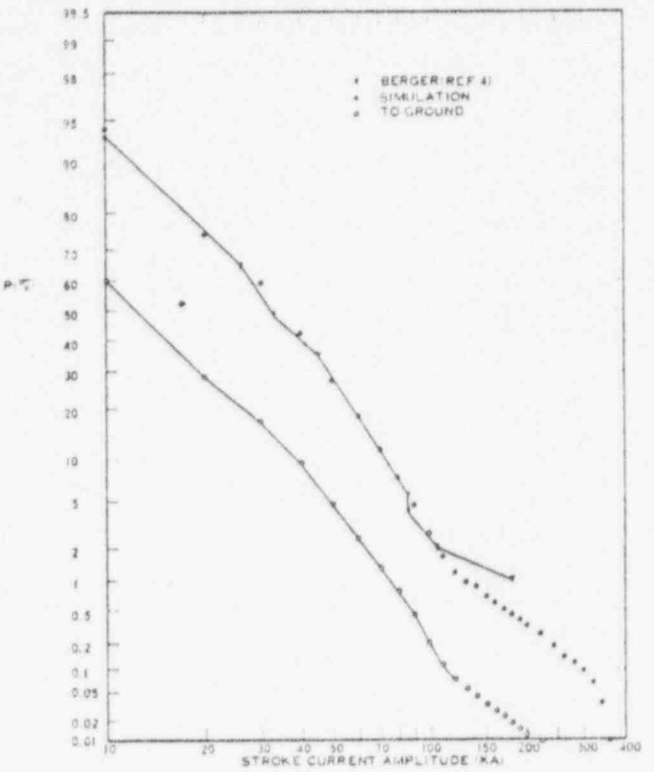

Fig. 6. Simulation of Berger's distribution of downward strokes on Mt. San Salvatore

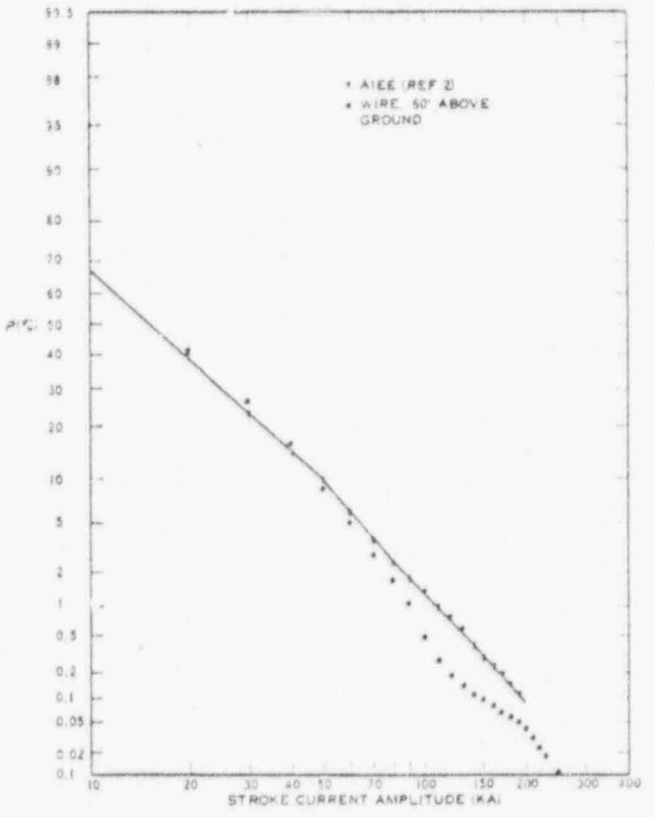

Fig. 7. Simulation of AIEE distribution of current amplitudes of lightning strokes

CONCLUSIONS

As noted previously the numerical results of these analyses cannot be considered definitive, while data concerning strike distances and leader characteristics are imprecisely known. However, it is considered that the results identify an important factor causing differences between observed distributions of stroke current magnitude. As the relevant data involved in the analyses becomes more precise, the techniques used in these investigations could be utilized to provide a realistic distribution of stroke current magnitude for lightning performance calculations. With this limitation in mind, the following conclusions can be drawn.

1. A three dimensional electrogeometric analysis has been used to investigate the effect of structure height and type on the distribution of stroke current amplitudes observed in the structure.

2. These analyses indicate that the structure height and type do have significant influences on the observed distribution, and contribute to the differences noted between these distributions.

3. A synthetic distribution of current amplitudes to level ground has been developed.

4. Using this synthetic distribution, several observed distributions have been simulated, with good agreement, using the electrogeometric technique and accounting for the differences in height and type of structures from which the observed distributions were obtained.

5. A simple expression for estimating the protective-zone of a tall structure has been developed.

ACKNOWLEDGEMENTS

The investigations reported were undertaken at the W. P. Dobson Research Laboratory of Ontario Hydro, Toronto, Canada. The author wishes to acknowledge the award of the E. S. Cornwall Memorial Scholarship by the University of Queensland, Australia.

REFERENCES

[1] M. A. Sargent. "Monte Carlo Simulation of the Lightning Performance of Overhead Shielding Networks of High Voltage Stations", Paper submitted for the IEEE Winter Power Meeting, 1972.

[2] AIEE Committee Report. "A Method of Estimating Lightning Performance of Transmission Lines", AIEE Trans, Vol. 69, 1950, pp 1187-96.

[3] S. Szpor. "Comparison of Polish Versus American Lightning Records", Trans IEEE, Vol PAS-88, May, 1969, pp 646-52.

[4] F. Popolansky. "Measurement of Lightning Currents in Czechoslovakia and the Application of Obtained Parameters in the Prediction of Lightning Outages of EHV Transmission Lines", CIGRE 1970, Report 33-03.

[5] K. Berger, E. Vogelsanger. "Messungen und Resultate der Blitzforshung der Jahre 1965 – 1963 auf dem Monte San Salvatore", Bulletin des Schwizerischen Elecktrotechnischen Vereins, Bd 56, 1965, pp 2-22.

[6] G. W. Brown, E. R. Whitehead. "Field and Analytic Studies of Transmission Line Shielding, Part II", Trans IEEE, Vol PAS-88, May 1969, pp 617-26.

[7] E. R. Whitehead. "Lightning Performance of EHV Lines", Report to CIGRE Working Group 33.01 (Lightning), Stuttgart, Germany, August, 1970.

[8] J. R. Currie, Liew Ah Choy, M. Darveniza. "Monte Carlo Determination of the Frequency of Lightning Strokes and Shielding Failures on Transmission Lines", IEEE Paper 71-TP-174-PWR, 1971 Winter Power Meeting, New York, N.Y.

[9] F. S. Young, J. M. Clayton, A. R. Hileman. "Shielding of Transmission Lines", Trans IEEE, Vol 82S, Feb, 1963, pp 132-54.

[10] Liew Ah Choy, M. Darveniza. "A Sensitivity Analysis of Lightning Performance Calculations for Transmission Lines", IEEE Transactions Paper 70-TP-615-PWR, 1970 Summer Power Meeting and EHV Conference, Los Angeles, California.

Discussion

Hans Linck (Ontario Hydro, Toronto, Ont., Canada): The author is to be commended for his valuable contribution to the analysis of lightning current magnitudes. He has shed new light on the question of apparent discrepancies between current measurements by different investigators. It appears quite feasible now to explain the variations of individual magnitude-frequency distributions in terms of physical dimensions of the structures on which the measurements were made. The author demonstrates how object geometry can be incorporated in the analytical treatment of lightning exposure of tall structures.

Having shown that the percentages of stroke current magnitudes may be computed with confidence, the author's comments would be appreciated on the question of predicting the actual number of strokes to an object. Expression (10) of the paper suggests a way of calculating the ground area protected by a tall structure. For a single vertical tower of height H, placed on a horizontal ground plane, the protected area A may be expressed as

$$A = \pi x (50.8 \times H^{.293})^2 \quad (1)$$

It is interesting to compare equation (1) with the following one which was derived from lightning observations on communications systems[1]:

$$A = \pi x (4 \times H)^2 \quad (2)$$

It is immediately apparent that for large height H, equation (2) gives a larger protected area, and consequently a greater number of strokes to a tall object, compared with equation (1). In Figure 1 of this discussion the calculated annual number of strokes to a single tower, for a ground flash density of 10 per square mile and year, is plotted as a function of tower height, using both equation (1) and equation (2). Also plotted is a point indicating the average number of negative downward strokes per tower as recorded by K. Berger in Switzerland[2]. It is seen that the number of strokes predicted by the author's expression is very much lower than that obtained from equation (2) as well as that recorded by Berger.

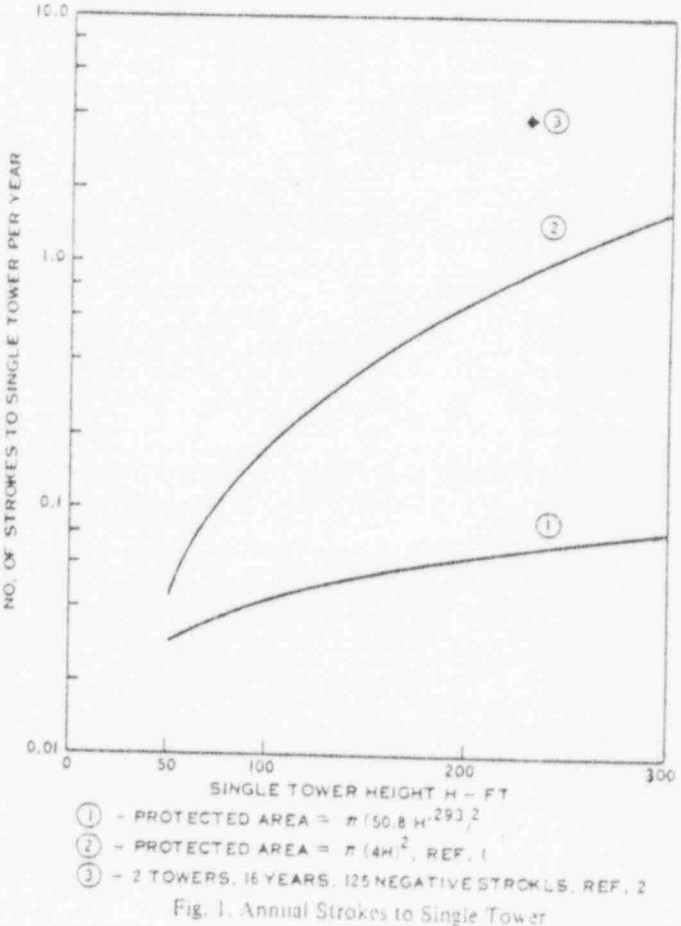

Fig. 1. Annual Strokes to Single Tower

Manuscript received February 22, 1972.

It is also of interest to relate Popolansky's data[3] to equations (1) and (2). Popolansky recorded 208 strokes to tall chimneys during an 8-year period. The number of chimneys surveyed is not known to this discusser, but estimates can be made using equations (1) and (2). For an average height of 200 ft, equation (1) leads to 0.064 strokes to one chimney per year. In order to record 208 strokes in 8 years, or 26 strokes per year, the average number of chimneys surveyed would have had to be about 400. On the other hand, if we apply equation (2), the number of chimneys is calculated as 36. If we take Berger's value of 3.9 negative downward strokes per year to a single tower, then the calculated number of chimneys is 7. Even if we take into account differences in ground flash density and annual variations in lightning severity, it seems that an excessive number of chimneys is required by the electrogeometric model to account for the number of strokes recorded by Popolansky.

The computer program developed by the author was employed to obtain an estimate of the number of strokes to a single 200-ft tower over a 2000-year period. The ground flash density was 10 and the ground stroke distribution was the author's synthetic distribution. The computed total number of strokes to the tower was 100. If we divide the data covering 2000 tower-years into 10-year exposure periods for 200 towers, we find that 5 towers were struck three times in 10 years, 22 towers were struck twice, 41 towers were struck once, and 132 towers were not hit during a 10-year period. If these exposure figures are realistic at all, it must be concluded that the relatively larger numbers of strokes recorded by Berger and Popolansky must have been due to some factor not accounted for in the electrogeometric model. As expected, the current magnitude distribution curve for the 100 strokes to the 200-ft single tower closely followed that of Figure 5 in the paper.

Recognizing the fact that the electrogeometric method has proven its capability to predict transmission line outage rates[4] and substation lightning exposure[5], the question must be raised why the computed number of strokes to individual tall objects is so much lower than that reported by several investigators. Perhaps, it is necessary to study further such factors as strike distance and leader angle distributions when object geometry is not of the transmission line type. Some slight doubt also remains about the validity of the concept of uniform ground flash density.

REFERENCES

[1] W. F. Gordon. "Development Report – Lightning Environments", Sandia Laboratories, Livermore, California, April 1969. Distributed by: Clearinghouse for Federal Scientific and Technical Information, U.S. Department of Commerce/National Bureau of Standards.

[2] R. B. Anderson. "A Comparison between some Lightning Parameters Measured in Switzerland with those in Southern Africa", Report to CIGRE Study Committee 33, Working Group 01, June 1971.

[3] F. Popolansky. "Frequency Distribution of Amplitudes of Lightning Currents", Report to CIGRE Study Committee 33, Working Group 01, June 1971.

[4] Reference 8 of the paper.

[5] M. A. Sargent. "Monte Carlo Simulation of the Lightning Performance of Overhead Shielding Networks of High Voltage Stations", IEEE Paper T72 055-7, 1972 Winter Power Meeting, New York, N.Y.

Michael A. Sargent: I would like to thank Mr. Linck for his comments and for his continued interest in the work reported in the paper.

Mr. Linck raises the question of correlation between the number of strokes to an object predicted by the reported technique and that observed in field investigations. The relationship between strokes to individual towers, the ground flash density and the thunderday level is ill defined even after many years of intensive field studies. In the discussion it was stated that lightning observations on communications systems indicated that the protected area A of a single vertical tower of height H can be express as –

$$A = \pi (4H)^2. \tag{1}$$

This expression is in contrast to that suggested by Golde[A1] wherein

$$A = \pi (2H)^2. \tag{2}$$

Similar expressions of the form

$$A = \pi (KH)^2 \tag{3}$$

appear in many national standards on lightning protection where the value of K specified varies from standard to standard, in the range $1 \leqslant K \leqslant 2$. It is of interest to note that the value of K developed by Golde from considerations of towers of up to 100 feet in height – namely 2 – yields a base radius of 200 feet for the protective cone of a tower one hundred feet high. This compares favourably with the value of 196 feet calculated by the formula proposed in this paper, and tabulated in Table I of the paper.

Further support for the parameters used in the electrogeometric model can be derived from an analysis of the results of the field investigations of Hylten-Cavallius and Stromberg[A2]. In a nine year study of lightning currents to tall structures in Sweden, 28 negative strokes of magnitudes greater than 2kA were recorded, yielding a stroke incidence figure of 0.025 strokes per structure per year in a region where the ground flash density averaged 4 strokes per square mile per year. The average height of the structures involved in the investigation was approximately 200 feet. If this observed stroke incidence is adjusted to a ground flash density of 10 per square mile per year, then the stroke incidence for structures of an average height of 200 feet is 0.0625. This figure is again remarkably close to the incidence figure of 0.064 calculated according to the formula proposed in the paper.

The foregoing indicates that the parameters used in the electrogeometric model of the paper are not unrealistic. However, as noted in the conclusions to the paper, the numerical results of the analyses cannot be considered definitive while data relating to the parameters are imprecisely known.

REFERENCES

A1. R. H. Golde "The Frequency of Occurrence and the Distribution of Lightning Flashes to Transmission Lines", Trans. A.I.E.E., Vol. 64, Pt. III, pp. 902 – 10, 1945.

A2. N. Hylten-Cavallius, A. Stromberg "Field Measurements of Lightning Currents", A.S.E.A. Research, Number 8, 1964.

Manuscript received April 25, 1972.

MONTE CARLO SIMULATION OF THE LIGHTNING PERFORMANCE OF OVERHEAD SHIELDING NETWORKS OF HIGH VOLTAGE STATIONS

REF. 29

by

Michael A. Sargent
The Hydro-Electric Power Commission of Ontario, Toronto, Canada
(On leave from the Cairns Regional Electricity Board, Cairns, Australia)

Abstract—An electrogeometric model is utilized to evaluate the effectiveness of overhead skywire and tower networks in shielding substation equipment from direct lightning strokes. Monte Carlo techniques are used to simulate the service performance of shielding designs. An evaluation of the sensitivity of the technique to uncertainties in the design parameters is made.

INTRODUCTION

The coordination of insulation in transmission substations requires consideration of the magnitude, frequency of occurence, and type of overvoltages impressed on the insulation. An important overvoltage is that produced by lightning surges incident at the substation, either by transference from incoming transmission lines or by direct strokes to the substation equipment due to penetration of the overhead shielding of the station by a stroke.

Direct strokes to substation equipment produce onerous conditions for station insulation, and it is the practice to protect the equipment from these direct strokes by provision of overhead shielding such as masts and/or groundwires. The design of such shielding systems in normally on the basis of protective angles or zones. In recent years it has been recognized that the protective zone of shielding systems is a function of the prospective stroke current magnitude [1],[2],[3],[4]. The electrogeometric model has been developed as an improved technique for calculating the effectiveness of transmission line shielding. This technique is here applied to the problem of designing the overhead shielding of high voltage stations.

A Monte Carlo method of manipulating the probabilistic input data has been used in preference to alternative analytic techniques. Monte Carlo techniques, with the use of fast digital computers, provide a facile method of simulating the performance of a system. In particular, when uncertainties exist in a study data, the Monte Carlo method enables alternative data to be evaluated rapidly.

ELECTROGEOMETRIC MODEL

The electrogeometric model used in this work is similar to that used by previous investigators [1],[2],[3],[4] and only the assumptions inherent in the model will be enumerated. These assumptions are

(i) The strike distance to a system component (r_{sc}) is related to the prospective stroke current magnitude (I) as

$$r_{sc} = K_{sc} \cdot K_I \cdot (I)^b \qquad (1)$$

where K_I, b are constants dependent on the form of the relationship between strike distance and stroke current magnitude, and K_{sc} is a constant dependent on the type of component assumed to be the target point of the stroke.

(ii) The frequency distribution (h(I)) of stroke current magnitudes is known.

(iii) The statistical distribution of the leader approach angle in *any* vertical plane is given as

$$g(\psi) = \begin{cases} 0 & \psi < -\pi/2 \\ K_m \cos^m \psi & -\pi/2 < \psi < \pi/2 \\ 0 & \pi/2 < \psi \end{cases} \qquad (2)$$

where Km and M are constants and ψ is the approach angle measured from the vertical.

(iv) The location of the leader stroke is not influenced by any system component until within the strike distance from that component.

It should be noted that previous analyses using the electrogeometric model [1],[4] have been concerned primarily with the performance of transmission line shielding, and have restricted the model to a two dimensional approach, in a vertical plane at right angles to the line. In reference 4, the influence of dimensional variations of the line in the third dimension has been considered, but still restricts the model of the leader stroke to a two dimensional system.

When the problem of substation shielding is considered it is evident that a generalized three-dimensional approach is required, as the substation has dimensional limits in all three co-ordinates of the rectangular Cartesian system. This extension of the model to three dimensions requires that the leader approach angle be considered as a 'solid' angle, rather than the two-dimensional angle specified in previous work. This solid angle can be established by specifying the projected angles in two vertical planes, assumed at right angles for mathematical convenience.

It is assumed in this work that the statistical distribution of the leader approach angle in both of these planes is identical (as is embodied in assumption (iii)), as there appears to be no physical or experimental reason for specifying a difference.

SYSTEM MODEL

The system modelled in this technique consists of the substation and surrounding terrain. The substation is assumed located at the middle of a flat horizontal plane one mile square. Forestation can be represented if desired.

The substation model consists of the following:

(i) Substation busbars and equipment (represented by a horizontal plane of the appropriate height and dimensions).

(ii) Substation strung buses.

(iii) Substation shielding masts and skywires.

(iv) Incoming transmission line towers and groundwires.

In the following discussions the term 'system' will be used to denote the complete physical model of the substation and surrounding terrain. The term 'component' will be used to denote specific items of the system – e.g., towers, ground, forestation or buses. Rectangular Cartesian coordinates are used throughout, with the Z-axis assumed vertical (Fig. 1).

MONTE CARLO TECHNIQUE

The application of Monte Carlo methods to lightning performance calculations has been described by Anderson [8]. In this technique the required parameters for each stroke incident are selected at random from the appropriate probabilistic distributions. The desired calculation is

Paper T 72 055-7, recommended and approved by the Substations Committee of the IEEE Power Engineering Society for presentation at the IEEE Winter Meeting New York, N.Y., January 30-February 4, 1972. Manuscript submitted June 18, 1971; made available for printing November 11, 1971.

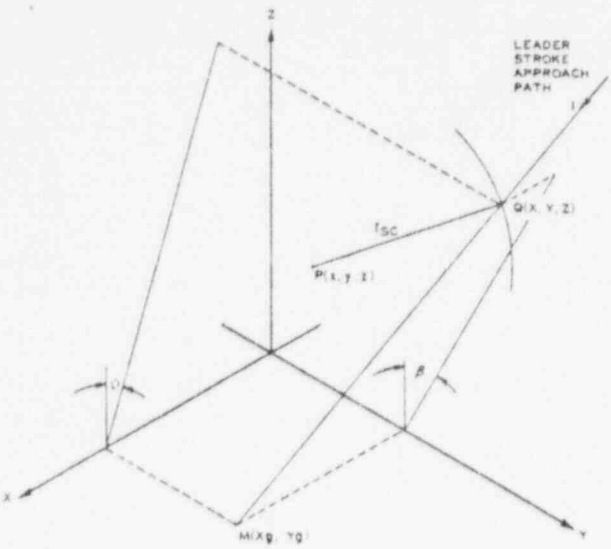

Fig. 1. Cartesian co-ordinate system for three-dimensional electrogeometric analysis

then performed with these parameters and other relevant data to provide a result. The whole procedure is then repeated many times until a statistically meaningful analysis of the results can be made. In effect, the Monte Carlo technique simulates the performance of the system, subject to the assumptions of the calculations and accuracy of the input data.

In the simulation of the performance of substation shielding networks, the following parameters are required for computation of each stroke incident, and are selected at random from the appropriate distributions:

(i) stroke current magnitude (I)

(ii) projected leader approach angle in the X-Z vertical plane (ψ) and in the Y-Z vertical plane (β)

(iii) prospective ground termination point (X_g, Y_g) of the stroke, independent of the components of the system model.

Other parameters involved in the calculations are dimensions and locations of system components (heights, location of towers, groundwires, substation and forestation).

Electrogeometric Analysis

The method of analysis used in the three-dimensional electrogeometric model is illustrated with reference to Figure 1. The parameters relating to a specific stroke incident – prospective ground point M (X_g, Y_g), leader approach angle (ψ, β) and prospective current magnitude (I) – are known. The strike distance, r_{sc}, to a system component can then be calculated.

Referring to Figure 1, let P (x, y, z) be a point on a system component and Q (X, Y, Z) be a point on the leader stroke approach path such that the distance PQ, (d_{PQ}) is given by

$$d_{PQ} = r_{sc} \tag{3}$$

Thus Q is a point of interception of the sphere, centre P and radius r_{sc}, (defining the attractive region for component point P) and the leader stroke path QM. The intercept height (Z-coordinate of point Q) then defines the height above the reference plane (X-Y) at which the leader will be attracted to point P.

The criterion to be applied to determine if the leader will terminate at P is that this intercept height will be greater than the intercept heights for all other points of the system modelled – that is, the leader stroke enters the attractive zone of point P before it enters the attractive zone of other component points. Thus to determine the termination point of the leader stroke it is necessary to calculate the intercept heights for all possible points on the system model. The stroke is then assumed to terminate at that point giving the maximum intercept height.

It should be noted that once the parameters of the stroke incident (X_g, Y_g, ψ, β, I) are specified then the three coordinates of the point Q are no longer independent and may be written in the form

$$\left.\begin{aligned} X &= f_1(z) \\ Y &= f_2(z) \\ Z &= z \end{aligned}\right\} \tag{4}$$

Also, if a particular system component is considered then the co-ordinates of point P on such a component are similarly inter-related and may be written as

$$\left.\begin{aligned} x &= f_3(z) \\ y &= f_4(z) \\ z &= z \end{aligned}\right\} \tag{5}$$

The distance PQ may be calculated as

$$\begin{aligned} d_{PQ} &= \sqrt{(X-x)^2 + (Y-y)^2 + (Z-z)^2} \\ &= F(Z,z) \\ &= r_{sc} \end{aligned} \tag{6}$$

where r_{sc} is a constant for a particular component. In the majority of cases involved in the analysis, equation (6) can be rearranged to express Z as an explicit function of z

$$Z = G(z) \tag{7}$$

For a particular component it is desired to find the point P (and hence value of z) which makes Z a maximum. This may be obtained from the solution of the equation

$$\frac{dZ}{dz} = G^1(z) = 0 \tag{8}$$

Once the values of z satisfying equation (8) are determined, the maximum intercept height for the component can be obtained by substitution in equation (7).

This analysis can then be applied to each system component to determine the eventual target of the stroke.

VALIDITY OF TECHNIQUE

Before the developed technique can be confidently applied to the design of shielding networks it is necessary to demonstrate the validity of the method by correlating calculated results with field data. However, the field data available for the performance of substation shielding is meager and insufficient to completely calibrate the model. Therefore, the approach has been to use the theoretical values determined by Brown and Whitehead [2] for the initial calculations, as the satisfactory correlation between analytic results and field data for transmission line shielding provides some confidence in the values used. The influence of variations in these parameters were then examined to evaluate the sensitivity of the technique to uncertainties in the input data.

Comparisons with Field Data

Data relating to the incidence of lightning strokes to substation shielding networks was available for two substations of the Ontario Hydro system [9]. Physical details of these substations are given in Table I, together with the observed occurences of strokes to the substations. Analyses were performed for the shielding network of these stations using the Brown-Whitehead model, viz

TABLE I

CORRELATION OF CALCULATED AND OBSERVED OCCURENCE
OF LIGHTNING STROKES TO SUBSTATIONS

Substation	Burlington TS	Leaside TS
Area	23 acres	12 acres
Size (feet)	1015 x 1015	735 x 735
Thunderday Level	20 - 25	25
Main Busbar Height	40 feet	40 feet
Shielding	Masts/Skywires	Masts/Skywires
Shielding Tower Height	100 feet	100 feet
Observed Strokes to Station per Year	0.5 - 1.0	0.4
Calculated Strokes to Station per Year*	0.71	0.42

*Calculations for 1000 years of service

$$r_s = 7.1I^{.75} \text{ metres (I in KA)}$$

$$r_{sg} = r_s$$

$$g(\psi) = 2/\pi \cos^2 \psi \qquad (9)$$

$$N_o = 0.4 \text{ TD strokes/sq.mi/yr}$$

$$h(I) = \text{AIEE distribution}^{12}$$

The calculated performance of the shielding networks is shown in Table I. The correlation between observed and calculated incidence of strokes to the stations is seen to be satisfactory.

SENSITIVITY OF RESULTS TO MODEL PARAMETERS

The correlations achieved between calculated results and field data using the Brown-Whitehead electrogeometric model have been satisfactory, for analyses of the performance of both transmission line shielding [2] and of substation shielding. However, it is recognized that there are conflicting view concerning the values of, and the relationships between, model parameters. To determine those parameters which have the most significant influence on the calculated performance of shielding networks, a sensitivity analysis has been made of the effects of variations in these parameters.

The substation model adopted for these studies is shown in Figure 2, the dimensions being typical of EHV switchyards.

The stroke parameters involved in the calculations are:

(a) ground-flash density, N_o
(b) strike distance, r_s
(c) leader approach angle, ψ
(d) distribution of stroke current magnitude, h(I)

Variations of these parameters have been investigated and are discussed in subsequent sections. In general the frequency of occurence of strokes to the substation will be expressed as a percentage of the strokes incident on an area of one square mile surrounding the station, rather than as strokes per year. This format has the advantage that it does not require the ground flash density of thunderday level to be specified for the comparative analyses of this section.

Ground Flash Density

The influence of ground flash density on the incidence of strokes to substations is significant, as variations in the assumed value produce proportional variations in the number of strokes to the substation per year. The value proposed by Brown and Whitehead (12 strokes per square mile per year for a thunderday level of 30) agrees well with current American practice. However, some investigators are proposing that this value may be too high [10]. To accommodate significant variations in this parameter compensating variations in other parameters would be required if the electrogeometric model is to remain valid.

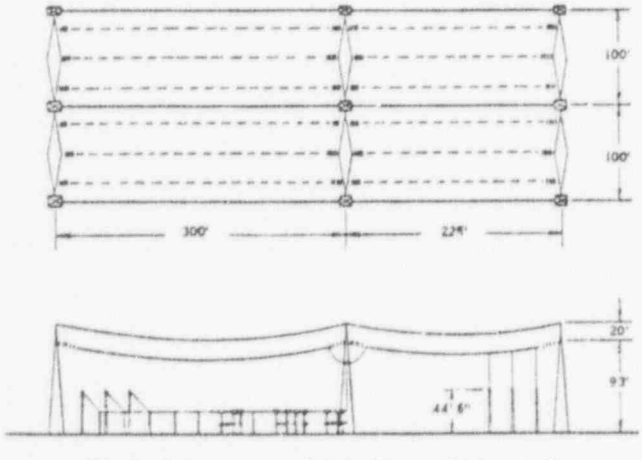

Fig. 2. Substation model used in sensitivity studies

Strike Distance

Several investigators [2],[4],[6],[7] have proposed relationships between the strike distance and prospective stroke current. The effect of varying the assumed functional relationship is shown in Table II, for several proposed distributions of stroke current magnitude. It is noted that the frequency of occurrence of strokes to the substation and the

TABLE II

INFLUENCE OF STRIKE DISTANCE AND OF DISTRIBUTION OF STROKE CURRENT MAGNITUDE ON THE FREQUENCY OF STROKES TO SUBSTATION MODEL

Strike Distance Data	Distribution of Stroke Current Magnitude					
	AIEE[12]		Popolansky[10]		Szpor[11]	
	*Strokes to Shielding	Strokes to Busbar	Strokes to Shielding	Strokes to Busbar	Strokes to Shielding	Strokes to Busbar
Brown-Whitehead[2]	23	0	19	0	22	0
Armstrong-Whitehead[4]	24	0				
Golde[7]	14	3	17	0	11	0
Wagner[6]	13	0	16	0	13	0

*Strokes per 1000 strokes to one square mile surrounding station
$K_{sg} = K_{sc} = 1.0$
$g(\psi) = 2/\pi \cos^2\psi$

frequency of penetration of the shielding network, are significantly influenced by the data adopted for striking distance. The results presented in Table II are for the condition where $K_{sc} = 1.0$ – that is, the strike distance to shielding, busbars and ground are assumed equal. The leader approach angle distribution used was the Brown-Whitehead $\cos^2\psi$ relationship.

The effect of varying the value of K_{sc} was investigated, and results are shown in Figure 3. It is seen that the magnitude of the resultant effect is dependent on the relationship assumed between strike distance and prospective stroke current, being most significant for the data according to Wagner [6].

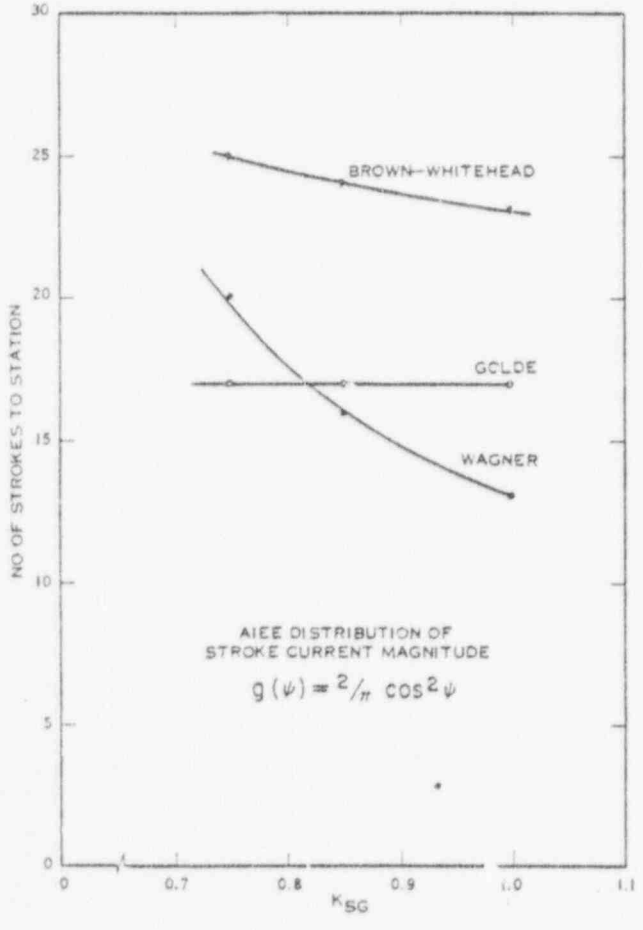

Fig. 3. Effect of variation of K_{sg} on frequency of strokes to station ($r_{sg} = K_{sg} \cdot r_s$ = strike distance to ground)

Distribution of Stroke Current Magnitude

Analyses have been performed for three alternative distributions of stroke current magnitude – AIEE [12], Popolansky [10], Szpor [11]. The influence of variations in this parameter is shown in Table II, related to the alternative data for strike distance. The effect is seen to be minor, except for the strike distance data according to Golde [7].

Leader Approach Angle Distribution

The functional relationship for leader approach angle probability has been assumed to be

$$g(\psi) = K_m \cos^m(\psi) \qquad -\pi/2 \leq \psi \leq \pi/2$$

Analyses have been performed for the cases of m = 1, m = 2, and m = ∞

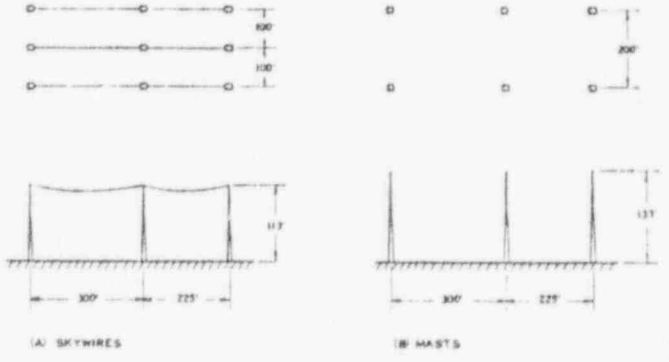

Fig. 4. Alternative shielding systems, Ontario Hydro 500 kv switchyards

TABLE III

INFLUENCE OF ASSUMED DISTRIBUTION OF LEADER APPROACH ANGLE ON FREQUENCY OF STROKES TO SUBSTATION MODEL

Distribution of Stroke Current Magnitude	Strike Distance Data	Total Strokes to Station*		
		m = 1 Km = 1/2	m = 2 Km = 2/π	m = ∞
AIEE	Brown-Whitehead	21	23	15
	Armstrong-Whitehead		24	
	Golde	16	17	18
	Wagner	12	13	8
Popolansky	Brown-Whitehead	28	19	28
Szpor	Brown-Whitehead	25	22	27

*Strokes per 1000 strokes to one square mile surrounding station
$g(\psi) = K_{ni} \cos^m \psi$
$K_{sg} = K_{sc} = 1.0$

TABLE IV

COMPARISON OF THE PERFORMANCE OF ALTERNATIVE SHIELDING SYSTEMS FOR 500 KV SWITCHYARDS

Overhead Shielding System	Strokes to Station per Year		
	To Shielding	To Busbar	Total
Skywires	0.135	0.005	0.140
Masts	0.155	0.015	0.170

N_O = 10 Strokes/square mile/year
200 years of service analysed

(all strokes vertical), for $K_{sc} = 1.0$. The results of these analyses are summarized in Table III. Variations in the assumed distribution have some influence on the calculated frequency of strokes to the substation, but the effects are obscured by influences of other parameters such as strike distance and distribution of stroke current magnitude.

Application of Technique

Analyses have been performed to compare the effectiveness of existing skywire shielding of typical Ontario Hydro 500 KV switchyards with an alternative shielding system using masts, as shown in Figure 4. The Brown-Whitehead model calibrations (equations 9) have been used for these analyses.

The results of these calculations are summarized in Table IV, indicating a slightly better performance from the skywire shielding system.

CONCLUSIONS

1. An electrogeometric model has been developed to estimate the performance of overhead shielding networks of high voltage stations. The electrogeometric analysis has been extended to the general three-dimensional case for this purpose.
2. Monte Carlo techniques have been utilized to simulate the service performance of the shielding networks.
3. Good correlation between calculated and observed performance has been achieved for the limited field data available, using the model calibration proposed by Brown-Whitehead.
4. The sensitivity of the technique to variations of input data has been examined. These analyses indicate that the parameters having most influence on the calculated results are ground flash density and strike distance.
5. The analyses for alternative shielding systems of Ontario Hydro stations indicate that similar performance can be obtained for systems using masts to that of the present skywire system.

ACKNOWLEDGEMENTS

The investigations reported were undertaken at the W. P. Dobson Research Laboratory of Ontario-Hydro, Toronto, Canada. The author wishes to acknowledge the award of the E. S. Cornwall Memorial Scholarship by the University of Queensland, Brisbane, Australia.

REFERENCES

[1] F. S. Young, J. M. Clayton, A. R. Hileman. "Shielding of Transmission Lines", Trans IEEE, Vol. 82S, pp. 132-54, Feb. 1963.

[2] G. W. Brown, E. R. Whitehead. "Field and Analytic Studies of Transmission Line Shielding, Part II", Ibid, Vol. 88, pp. 617-26, May 1969.

[3] J. R. Currie, Liew Ah Choy, M. Darveniza. "Monte Carlo Determination of the Frequency of Lightning Strokes and Shielding Failures on Transmission Lines", IEEE Paper 71-TP 174-PWR, Winter Power Meeting, New York, N.Y. 1971.

[4] H. R. Armstrong, E. R. Whitehead. "Field and Analytic Studies of Transmission Line Shielding". Trans IEEE, Vol. PAS-87, pp, 270-81, Jan. 1968.

[5] A. Braunstein. "Lightning Strokes to Transmission Lines and Shielding Effects of Ground Wires", IEEE Paper 70-TP 102-PWR, Winter Power Meeting, New York, N.Y. 1970.

[6] C. F. Wagner. "The Lightning Stroke as Related to Transmission Line Performance", Elec. Engrg., Vol. 82, pp. 388-394, June 1963.

[7] R. H. Golde. "The Lightning Conductor", J. Franklin Inst., Vol. 283, p. 451-477, June 1967.
[8] J. G. Anderson. "Monte Carlo Computer Calculation of Transmission Line Lightning Performance", AIEE Trans., Vol. 80, pp. 414-20, Aug. 1961.
[9] H. Linck. Ontario Hydro Technical Report.
[10] F. Popolansky. "Measurement of Lightning Currents in Czechoslovakia and the Application of Obtained Parameters in the Prediction of Lightning Outages of EHV Transmission Lines", CIGRE Report 33-03, 1970.
[11] S. Szpor. "Comparison of Polish Versus American Lightning Records", Trans IEEE, Vol. PAS-88, pp. 646-52, May 1969.
[12] AIEE Committee Report, "A Method of Estimating the Lightning Performance of Transmission Lines", AIEE Trans, Vol. 69, pp. 1187-96, 1950.

Discussion

Ian Grant (General Electric Company, Pittsfield, Mass. 01201): This is another excellent paper by Dr. Sargent. The results derived are evidently in excellent agreement with field performance, and are interesting in that the stroke incidence to the substation considered in Table I is slightly over double that to the same area of flat land in each case. The technique should be very useful in optimising the shielding design of substations.

A major problem with the Monte Carlo technique is the large number of samples which must be considered for reliable results. For complex problems the computer costs can be prohibitive.

Would the author comment on the reliability of the results obtained for the 200 or 1000 years of service considered, and also indicate the number of nodes considered in the substations and the approximate computer time used. Was the alternative approach to this problem of deriving the relationship between stroke magnitude and the area within which it would strike the substation, and then obtaining the final result of strokes to the substation by calculating in the probability of these magnitudes, explored in any depth?

Also, how were the field results listed in Table I obtained? With the experience of these calculations, can the author suggest a simple criterion for the complete protection of substations against shielding failures.

Manuscript received February 22, 1971.

Hans Linck (Ontario Hydro, Toronto, Ont., Canada): The author deserves credit for presenting an up-to-date approach to the study of station shielding requirements by suggesting a three-dimensional electrogeometric model and combining it with a statistical shielding failure evaluation. In the past, substation shielding principles were based on the results of laboratory experiments [1], and a shielding angle of about 45°, using either masts or overhead groundwires, has been adopted widely as good practice.

When new station designs are under evaluation, certain considerations indicate the need for a more refined tool to determine shielding effectiveness; strokes to existing stations and shielding failures are known to occur but from service records it is very difficult to establish a realistic risk factor. Furthermore, as a consequence of the continuing increase in electric power demand, the number of large stations is rising steadily; at the same time, compacting of stations for reasons of real estate costs as well as appearance is becoming more predominant. With new structures and lay-outs, conventional shielding arrangements may be difficult to incorporate. On the other hand, with low-profit construction, there is less danger of a severe lightning stroke terminating on station equipment. The question then arises whether any, or how much, shielding is actually required to achieve a certain degree of protection for vulnerable equipment.

Manuscript received February 22, 1972.

Using the author's method, shielding failure calculations were performed for several existing stations with different shielding arrangements. Depending upon station area and geometry, one shielding failure every 50 to 150 years was computed. Then, various mast and skywire combinations for a new, large transformer station were investigated and their performance compared with that of existing station shielding. Generally speaking, skywires were more effective than masts, when heights were varied from 75 to 125 ft. Omission of shielding for station entrance spans was found acceptable. From computed data on stroke termination points and current magnitudes, it was possible to place shielding masts and wires so that more vulnerable apparatus, for instance transformers, would receive the highest degree of protection.

In Table I of the paper, the author compares calculated and observed strokes to two transformer stations. The field data were obtained during a five-year period when klydonographs and magnetic links were installed on skywires and live buses of both stations, to record frequency and magnitude of station surges [2]. This kind of information is necessary to validate any new method and to calibrate the model before extrapolation to new applications can be considered. Since 1953, when the AIEE Lightning Protective Devices Subcommittee published an industry survey on station shielding practices [3], very little information has come forth dealing with this subject. In his paper, the author shows an elegant way for the complete evaluation of station shielding when past experience cannot be called upon to provide the answer.

REFERENCES

[1] C. F. Wagner, G. D. McCann, C. M. Lear. "Shielding of Substations", AIEE Transactions, Vol. 61, pp. 96-100, February 1942.
[2] H. Linck. "Surge Measurements in High Voltage Stations", Trans IEEE, Vol. PAS 87, pp. 1718-1723, August 1968.
[3] AIEE Subcommittee on Lightning Protective Devices. "Present Practice Regarding Direct Stroke Shielding in the Lightning Protection of Stations and Substations", AIEE Conference Paper, January 1953.

Michael A. Sargent: The author would like to thank the discussers for their comments. As stated by Mr. Linck the incentive to develop the technique reported in this paper was the need to evaluate the performance of shielding arrangements for novel substation designs, and the recently evolved electrogeometric model provided an analytic method of sufficient power to evaluate the critical differences between alternative shielding networks.

Mr. Grant notes that the Monte Carlo technique utilised requires a large number of samples to be considered. This is indeed so. However, with the availability of modern high speed digital computer systems, the cost of this process is not prohibitive. For example the simulation of 2000 years of service for a substation model comprising main busbars, strung busbars, 15 lightning masts, two earthwires and surrounding terrain was achieved for a cost of approximately 300 dollars. As with any statistical sampling technique sufficient samples must be taken to ensure the reliability of the obtained results. In the case of the reported technique the results of significance are those in which a lightning stroke is calculated as terminating on the substation. Sufficient samples must therefore be considered to obtain a spectrum of these significant results. In this context the number of samples required for a "bad" design will be much less than that required for a "good" design. Typically the simulation of 1000 years of service is sufficient.

The alternative approach suggested by Mr. Grant was considered but abandoned as unsuited for the complex geometries required in the substation model. Such an approach was found to be more applicable to the simpler transmission line geometries.

The field results listed in Table I were obtained in a five year investigation, as detailed in reference 2 of Mr. Linck's discussion. At the present time it would be premature to define a realistic, simple criterion for "complete" or "essentially perfect" protection of substations against shielding failures; this will require definition of the maximum stroke current amplitude which could be tolerated as a shielding failure, in comparison with induced surge currents.

Manuscript received April 17, 1972.

IEEE Transactions on Power Apparatus and Systems, vol. PAS-94, no. 5, September/October 1975

SHIELDING OF MODERN SUBSTATIONS AGAINST DIRECT LIGHTNING STROKES

H. Linck
Ontario Hydro
Toronto, Ont., Canada

ABSTRACT

Lightning protection studies of transmission lines have revealed the limitations of conventional shielding practice for both high-voltage lines and stations. A new technique for station shielding design was developed replacing the former approach of relying on an ill-defined relationship between shielding angle and station exposure. This new technique is particularly suited to assessment of overhead shielding systems for large stations with high reliability requirements; it also permits evaluation of the effectiveness of shielding structures meeting aesthetic considersations.

INTRODUCTION

The effectiveness of lightning protection schemes for high-voltage and extra-high-voltage stations depends upon the degree of overhead shielding against direct strokes to the station area.[1] Quantitive information on shielding efficiency in terms of shielding failure exposure as a function of shielding angle, had been obtained previously from laboratory experiments on both station and transmission line miniature models.[2,3] Application of this information to ehv-line design resulted in excessive shielding failure outages; consequently, a new method has been proposed recently to determine transmission line shielding requirements.[4]

As far as station shielding is concerned, discrepancies between predicted and actual shielding failure rates do not seem to have occured. This apparent agreement may be explained by the fact that the number of strokes to a station of medium size is at least one order of magnitude smaller than the number of strokes to a transmission line of average length. Therefore, the observation period for the former would have to be considerably longer before reliable data on station shielding failures are accumulated. For example, if a shielded station is struck by lightning once every year, and if one out of a hundred strokes causes a shielding failure, the exposure being one percent, then one shielding failure would occur in a hundred years. On the other hand, if each mile of transmission line intercepts one stroke every year, and if the exposure again is one percent, then a 100-mile line would experience one shielding failure every year.

The problem of the accuracy of shielding failure predictions becomes prominent in two situations of modern station design. Because of the increasing power capacity of generating and transmission facilities, the physical size of high-voltage and extra high-voltage stations is growing steadily. The question then arises whether the conventional approach shielding design is still applicable for these large stations considering that the actual number of strokes to an area proportional to its size and therefore the shielding failure also increases in proportion. The other question concerns shielding design for aesthetically appealing low-profile stations. In this case, complete omission of overhead shielding structures would be most desirable. But the associated shielding failure risk may not be acceptable. Therefore, the problem remains how to obtain a realistic estimate of the efficiency of shielding arrangements not conforming to conventional practice.

In summary, the need exists for a method permitting a reasonably accurate estimate of the true shielding failure risk for stations where an overly conservative protection scheme would seriously interfere with station design; on the other hand, it is mandatory that the shielding requirements for high-security stations be determined with a sufficient degree of confidence.

ANALYTICAL MODEL OF STATION SHIELDING

In an earlier paper,[5] an electro-geometric model technique was described for a station shielding study, incorporating latest knowledge concerning the shielding effect of overhead lightning conductors. A comparison with field data demonstrated the validity of the basic assumptions underlying this new method. Further elaborations led to the conclusion that the complex computer analysis employed in the original work could be used for a simplified design procedure applicable to a large variety of station shielding problems, and providing a shielding failure estimate of greatly improved accuracy, compared with the conventional approach of using the shielding angle as the sole criterion.

The following parameters form the framework for the new technique of shielding design.

1. The groundflash density (GFD).
   The frequency of strokes to a station is determined by the number of lightning discharges leaving the cloud area directly above and descending vertically towards the station. In addition, some strokes originating in a fringe area near but outside this cloud area may also be attracted to the station once they have progressed far enough downwards. The annual number of strokes to a station is directly proportional to the groundflash density which for a thunderday level of 25 has been adopted as 10 strokes per square mile per year, or 3.9 strokes per km^2-years.
2. Current amplitudes of strokes to ground.
   In the electro-geometric model,[5] the termination point of a downward stroke approaching the vicinity of objects on the ground is influenced by the charge in the leader channel and hence, by the prospective current amplitude of the return stroke. Therefore, the chance of a shielding failure also depends upon the stroke current amplitude. The probability of a certain amplitude to occur, can be expressed in the form of a statistical distribution. For the purpose of this study, the current amplitude distribution of strokes to the ground was that derived from strokes to tall structures,[6] see Fig. 1.

Paper T 75 060-9, recommended and approved by the IEEE Substations Committee of the IEEE Power Engineering Society for presentation at the IEEE PES Winter Meeting, New York, N.Y., January 26-31, 1975. Manuscript submitted Aug. 19, 1974, made available for printing Nov. 20, 1974.

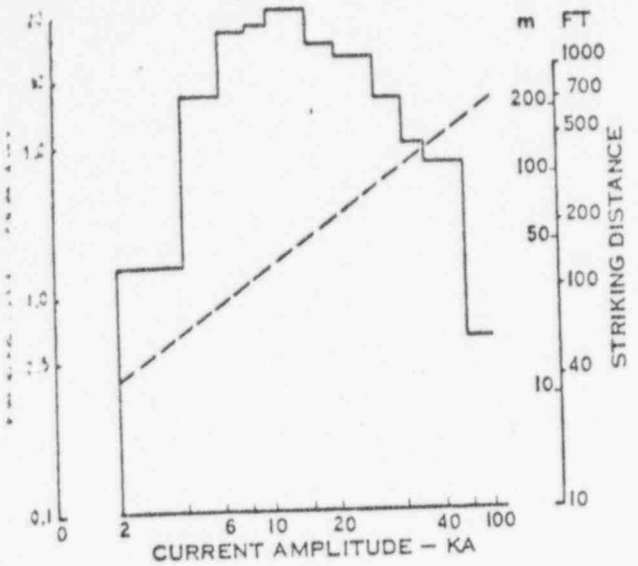

FIGURE 1

GROUND STROKE CURRENT CHARACTERISTICS
—— AMPLITUDE PROBABILITY
--- STRIKING DISTANCE

Striking distance to elevated objects.

The critical distance at which the leader head is attracted to an object placed on the ground, is related to the charge in the leader channel and therefore also is a function of the prospective current amplitude. The striking distance-current amplitude relationship is the subject of continuing research.[4] As far as station shielding is concerned, the parameter values for the striking-distance function employed in Ref. 5 and 6 have been found to produce results agreeing with service experience (Fig. 1.). Minor deviations from these values have no significant influence on the validity of the shielding failure prediction.

4. The leader approach angle.

Observations show that many lightning strokes approaching the ground do not follow a straight downward path. This characteristic was represented in the original electro-geometric model by assuming a three-dimensional leader angle distribution.[5] Subsequent studies indicate that for station shielding design the long-term average effect of the angle distribution is of a secondary nature; therefore, in the simplified shielding design method the leader approach is assumed to be vertical only.

5. Stroke termination point.

When the lightning stroke leader discharge approaches a station equipped with overhead lightning conductors for direct-stroke shielding, it will terminate on that part of the station structure first coming within striking distance. Whether the stroke is intercepted by the lightning conductor or whether it continues on until it terminates on another object in the station, depends upon the position of the lightning conductor relative to that of the station bus, transformers, and other equipment. The difference in height between the lightning conductors and equipment, the so-called effective height of the former, and also the horizontal distance between them, determine the risk of a shielding failure. Conventionally, this distance and the effective height define the shielding angle. With the new method, the protected distance, and hence the corresponding shielding angle, is a function of stroke current amplitude and its statistical distribution.

6. The shielding failure risk.

The chance of a stroke causing a shielding failure may be stated in different ways. According to past practice, the so-called exposure is defined as that percentage of strokes to the station not intercepted by the shielding system.[3] If shielding design is based on a constant value of exposure, say 0.1% or 1.0%, then the actual number of shielding failures is proportional to station area. In this method, a constant shielding angle corresponding to the exposure specified, is selected regardless of station size.

A more practical and meaningful measure of shielding effectiveness is the shielding failure risk, defined as the number of years in which one shielding failure event is predicted. If a constant value, for instance 100 years, is adopted for all stations, the designer has to be aware of the fact that in order to meet this requirement, large stations need more effective shielding than small ones. In other words, the shielding angle must be reduced as station area increases (assuming that other factors do not change significantly).

Using these parameters, the basic method of shielding failure calculation is outlined in Appendix A. Results are plotted in Fig. 2 for a single 100-ft. length of horizontal skywire, and in Fig. 3 for a single vertical mast. In both cases the assumed groundflash density was 10 strokes per sq. mile and year.

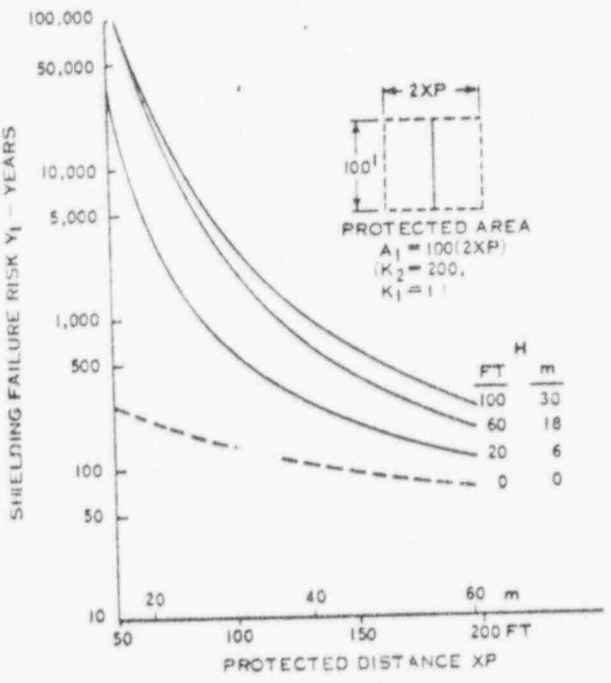

FIGURE 2

SHIELDING FAILURE RISK FOR SKYWIRE OF 100 FT LENGTH
H = EFFECTIVE HEIGHT
(GFD = 10)

90005039

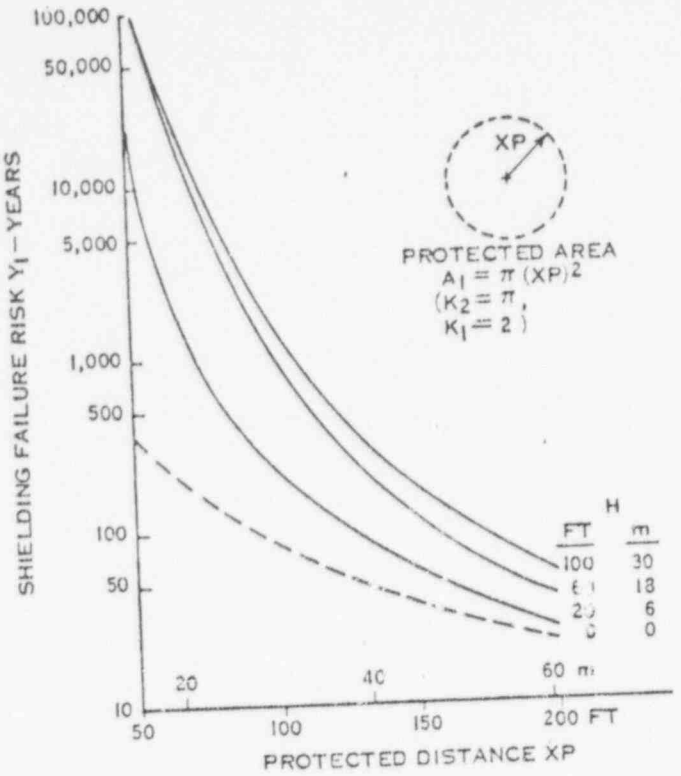

FIGURE 3

SHIELDING FAILURE RISK FOR SINGLE VERTICAL MAST

H = EFFECTIVE HEIGHT

(GFD = 10)

SHIELDING SYSTEM DESIGN

Shielding performance must be related to the overall reliability of the power system, taking into account the economic balance between cost of the lightning protection scheme and the probable loss resulting from shielding failure events.

Once a shielding failure risk has been specified, a tentative decision will be made concerning the shielding method and its overall dimensions most suitable for a particular station. The following factors influence this decision:

1. Choice of vertical or horizontal lightning conductors; electrical, mechanical, aesthetic requirements.
2. Lightning conductor height above ground, and effective height above equipment.
3. Number and preferred locations of lightning conductors including supports.

These factors are interrelated; therefore, a new station design may require several solutions before the optimum shielding system is determined.

In order to find these solutions, the following step-by-step procedure is suggested:

1. Specify total protected area A, approximated by a rectangle of length L and width W, and shielding failure risk Y.
2. Divide A into n equal areas A1.
3. Determine the shielding failure risk for area A1 as $Y1 = (A/A1)Y = nY$, years.
4. Assume each area A1 to be protected by one lightning conductor as per Fig. 2 for skywires and Fig. 3 for masts.
5. Determine protected distance XP for area A1 according to Fig. 2 or 3;

   for skywires: $XP = A1/200$, ft.

   for masts: $XP = \sqrt{A1/\Pi}$, ft.
6. Knowing Y1 and XP, the effective lightning conductor height H is now obtained from Fig. 2 or 3.
7. a) Horizontal lightning conductors: for a skywire unit-length of 100 ft. (Fig. 2) the total number of parallel skywires with length L (or W) is 100n/L (or 100n/W). Distance between skywires is 2XP, and between outer skywires and the station boundary the protected distance is XP.

   b) Vertical lightning conductors: The total number of masts is n. Because of the circular shape of the area protected by a vertical mast, the total area protected depends on the shape selected for unit-areas A1.

Example: For a total protected area A = 1000x1000 m² (305x305 m²), a shielding failure risk Y = 100 years, and a groundflash density No = 10 p.sq.m.-yrs. (3.84 p.km²-yrs.), the number n of unit-areas A1 was varied, and the following parameters determined and tabulated below:

Shielding failure risk for unit-area A1 - Y1
Protected distance for single 100-ft skywire - XPS
Protected distance for single mast - XPM
Effective height of skywires - HS
Effective height of masts - HM
Total number of parallel skywires - S
Total number of masts - M

n	Y1 yrs.	A1 ft²/m²	XPS ft/m	HS ft/m	S	XPM ft/m	HM ft/m	M
100	10,000	10,000/930	50/15	<20/6	10	56/17	20/6	[illegible]
80	8,000	12,500/1163	62.5/19	22/6.7	8	63/19	30/9	[illegible]
50	5,000	20,000/1860	100/30.5	>100/30.5	5	79/24	60/18	[illegible]

In this example no consideration was given to strokes originating in the earlier mentioned fringe area outside area A. When skywires or masts are placed at a distance XPS or XPM from the station boundary, equipment at the boundary of the protected area remains exposed to strokes from the fringe area. Fig. 4 shows the risk of such an event to occur when the equipment height Ho varies from 20 to 100 ft. It is noted that for practical purposes the width of the fringe area does not exceed 150 ft. when Ho is 100 ft. or less. Very often this additional exposure is only a minor factor at stations connected to overhead transmission lines because of the shielding effect of the lines themselves. But when vulnerable equipment is located near the station boundary and not shielded by other objects in the vicinity, it is advisable to locate lightning conductors on the boundary line; in this way exposure to strokes from the fringe area is avoided.

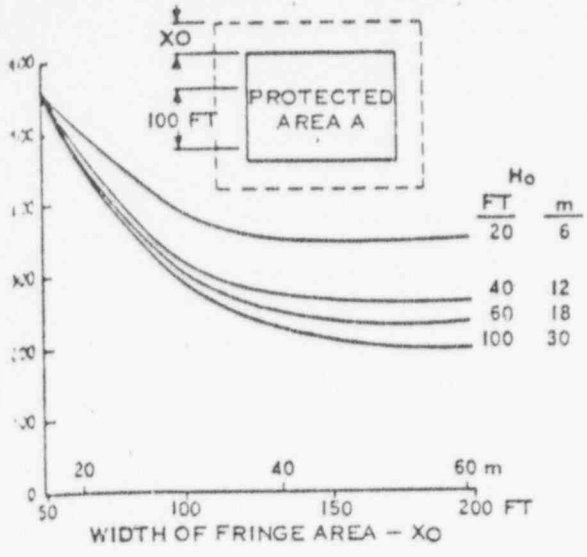

FIGURE 4

RISK OF STROKE TO 100 FT (30 m) OF UNSHIELDED STATION BOUNDARY

H_o = EQUIPMENT HEIGHT AT BOUNDARY OF AREA A (GFD = 10)

The data used for plotting Figs. 2, 3, and 4 were based on a groundflash density of 10 strokes per sq.mile-year, being typical of a thunderday level T = 25. For other thunderday levels T', in the range from 25 to 55, linear extrapolation of the groundflash density is recommended.[4] With the number of shielding failures directly proportional to the groundflash density, the shielding failure risk is inversely proportional to the thunderday level. In order to apply Figs. 2, 3, and 4 for values T'>25, the shielding failure risk must be adjusted by the ratio 25/T'.

When different degrees of shielding are considered for different areas A1, A2, . . . An, the shielding failure risks are determined individually. The total shielding failure risk Y for

$$A = A1 + A2 + \ldots + An \text{ is obtained from}$$
$$Y = 1/(1/Y1 + 1/Y2 + \ldots + 1/Yn).$$

COMPARISON WITH CONVENTIONAL METHOD

For shielding design purposes the 0.1% exposure criterion has been employed frequently in the past; the corresponding shielding angle is approximately $\alpha = 60°$ between lightning conductors, and $\beta = 45°$ to equipment at the station boundary.[3] Because of the shielding problems with extra-high-voltage lines referred to earlier, smaller shielding angles of $\alpha = 45°$ and $\beta = 30°$ have been suggested for station shielding. Also, instead of 0.1% exposure, a 1.0% value has been considered as a more realistic estimate.

A comparison was made between these different assumptions for station shielding design, using both the earlier method and that reported in this paper. Station size was varied from 2 acres (9020 m^2) to 200 acres (902,000 m^2); the degree of shielding was expressed in terms of shielding failure risk as a function of station area. The groundflash density was 10 strokes per sq.m.-yr. (3.84 strokes p. km^2-yr.) and the effect of strokes from the fringe area was ignored. Protected areas A were assumed as squares, with skywires of equal length arranged in parallel and at an effective height of H = 60-ft (18 m) above equipment height of Ho = 40 ft (12 m).

Results of this comparison are plotted in Fig. 5. It is noted that for shielding angles $\alpha = 60°$ and $\beta = 45°$ the shielding failure risk for the 0.1% exposure estimate is much too optimistic compared with that of the electro-geometric technique; but it is shown also that for stations with protected areas up to about 20 acres the actual shielding failure risk is so small that the effect of the prediction error may not be serious as far as service performance is concerned. On the other hand, for station areas of the order of 100 acres, the frequency of shielding failures is so much higher that a large prediction error cannot be tolerated.

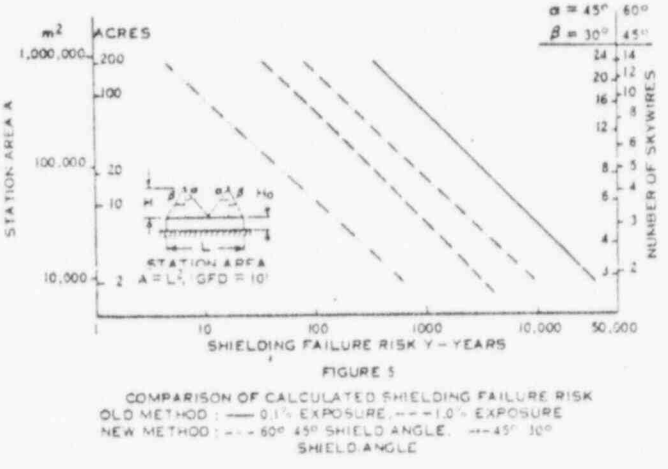

FIGURE 5

COMPARISON OF CALCULATED SHIELDING FAILURE RISK
OLD METHOD: —— 0.1% EXPOSURE, – – – 1.0% EXPOSURE
NEW METHOD: – – – 60° 45° SHIELD ANGLE, ——45° 30° SHIELD ANGLE

For a shielding design with $\alpha = 45°$ and $\beta = 30°$, an assumed exposure of 1.0% would result in a conservative estimate of the shielding effectiveness, predicting one shielding failure in 65 years for a 100-acre station, whereas the electro-geometric technique predicts one such event in 150 years.

Fig. 5 also shows the number of skywires for the two shielding angle combinations. For the 45°/30° scheme about 60% more skywires are needed compared with the 60°/45° scheme, indicating the significant benefit to be derived from application of the new shielding design method, enabling the designer to determine the exact extent of shielding required to meet a specified shielding failure risk.

CONCLUSIONS

A new technique has been employed to develop a simplified method for determining direct-stroke shielding requirements for high-voltage and extra-high-voltage stations. Major errors inherent in the convential approach to shielding design are eliminated.

Improved accuracy in predicting the occurrence of shielding failures for a large variety of shielding structures is an important asset in achieving adequate shielding performance for large stations where high service security must be ascertained, and also at stations where a minimum degree of shielding is desirable for aesthetic reasons.

The new technique is recommended as the basis for an up-to-date industry-wide station shielding guide.

APPENDIX A

Calculation of Shielding Failure Risk

Assume an area A on a horizontal plane, with a lightning conductor of height H placed at its centre. Distance between the lightning conductor projection on the plane and the area boundary is X.

If a stroke with current amplitude IP and striking distance RP descends on area A, it will be attracted to the lightning conductor if it approaches within the distance [6]

$$XP = \left[RP^2 - (RP - H)^2\right]^{1/2}, \text{ for } RP > H$$

and $XP = RP$, for $RP \leq H$.

The area shielded against strokes IP is [6]

$$AP = k2(XP)^{k1},$$

where k1 and k2 are constants determined by the shape of area AP (Fig. 2, 3). If XP<X, and therefore AP<A, then strokes IP descending on area A-AP will not be attracted to the lightning conductor; they will constitute shielding failures in area A.

Stroke current amplitudes vary over a large range (Fig. 1). For currents with amplitudes I1, I2 . . . Im, striking distances R1, R2, . . . Rm, and probabilities of occurrence P1, P2, . . . Pm, maximun distances from the lightning conductor X1, X2, . . . Xm exist beyond which the strokes will bypass the lightning conductor. The sum of these strokes to the plane within A and not intercepted by the lightning conductor, is the number of shielding failures in area A.

The number of shielding failures per year, or the shielding failure rate, is a function of the total annual number of strokes to area A, and of the frequency distribution of current amplitudes. For a groundflash density No in unit-area Ao, annual number of strokes to area A is

$$NA = No(A/Ao).$$

The annual number of shielding failures Ns in area A, as a function of current amplitude is

$$Ns = No/Ao \left[(A - k2(X1)^{k1}P1) + (A - k2(X2)^{k1}P2 + \ldots + (A - k2(Xm)^{k1}Pm\right]$$

$$= No/Ao \left[A - \sum_{n=1}^{n=m}(AnPn)\right], \text{ shielding failures per year.}$$

The corresponding shielding failure risk is

$$YA = 1/Ns, \text{ years per shielding failure.}$$

The exposure of area A to shielding failures is

$$EA = (Ns/NA)100, \text{ percent}$$

REFERENCES

(1) USA Standard USAS C.62.2-1969. Guide for applicati... valve-type lightning arresters for alternating-current syst...

(2) C. F. Wagner, C. D. McCann, G. L. MacLane, Jr. Shie... of transmission lines. AIEE Trans., 1941, vol.60 pp. 313-...

(3) C. F. Wagner, G. D. McCann, C. M Lear. Shieldin... substations. AIEE Trans., February 1942, vol.61, pp. 96-...

(4) D. W. Gilman, E. R. Whitehead. The mechanism... lightning flashover on high-voltage and extra-high-vo... transmission lines. Electra, no.27, March 1973, pp. 65-9...

(5) M. A. Sargent. Monte Carlo simulation of the lightn... performance of overhead shielding networks of high-vo... stations. IEEE Trans., vol. Pas-91, no.4, July/Aug. 197... 1651-1656.

(6) M. A. Sargent. The frequency distribution of curr... magnitudes of lightning strokes to tall structures. IE... Trans. Pas-91, no.5, Sept./Oct. 1972, pp. 2224-2229.

Discussion

E. Whitehead (Professor -Adjoint, University of Colorado): The late C. F. Wagner was fond of saying that "The lightning specialist should have his head in the clouds and his feet on the ground." His own interpretation of this remark was that, while the specialist must strive to learn more about the theoretical aspects of lightning phenomena, he should also provide the designer with simple guides to provide effective shielding. In this paper, Mr. Linck has indeed provided a useful engineering guide to the rapid determination of effective shielding systems for transmission substations, based upon the theoretical and experimental work referenced.

A key word in the above comment is the word "effective". How effective? Mr. Linck provides the design engineer and system planning engineer with the easily-understood concept of *shielding failure risk* as a mean years per shielding failure. This is really what is needed for the rigorous evaluation of shielding systems. In the process of this evaluation, the system planning engineer and system operator must accept responsibility for the assignment of a "satisfactory" risk. It seems safe to say that no one has ever analyzed a physical system. One analyzes his best "model" of the physical system. That model which explains or predicts the behaviour of the system with least discrepancies from the actual behaviour is "best" at any point in time. Given a few successes, we sometimes invest our models with greater correspondence with "reality" than is warranted. The writer has used the term "electrogeometric" to indicate any theory that related the electrical properties of the lightning stroke to its own geometry and that of the transmission line or other system structure which constituted a prospective target. A key feature of such theories is the concept that the leader tip must be relatively close to such structures before it to earth before the exact point to be struck is determined. In some cases a simple voltage-distance relation has been used, while in others an equivalent result is obtained by employing electric field intensity for streamer development over the shortest prospective path. A point I have attempted to stress is that, while these concepts have validity in an average sense, there seems to be a very small probability of significant deviation from our assumptions. If the pre-cursor corona (ahead of the leader tip) consists of a family of discrete corona filaments, or electron avalanches, then such an avalanche could penetrate an "effective" shielding system. By analogy with an electron which penetrates a "forbidden" potential hill in quantum mechanics, I have termed this penetration "tunnelling". Happily, such events may occur without causing insulator flashover since they appear to be associated with low prospective currents. One cannot, however, rule out the occasional penetration of a filament associated with a stronger stroke.

Again, I should like to congratulate Mr. Linck on an extremely useful paper which I am glad to have available for practical design recommendations.

Manuscript received February 18, 1975.

H. Linck: Professor Whitehead's discussion forms a valuable contribution to the paper. His appreciation of the usefulness as well as the limitations of the recommended technique of station shielding design is well expressed in his arguments concerning simulation of physical phenomena.

One of the main points in the paper, as emphasized by professor Whitehead, is recognition of the fact that, like in other branches of engineering, shielding design should be based on a sound estimate of the failure risk. Previous methods had been found inadequate when applied to transmission line design. Therefore, it was a logical step to take advantage of most recent knowledge of the shielding phenomena as reported in reference 4 of the paper.

The question has been asked whether in assessment of the station shielding failure risk a distinction should be made between shielding failures and shielding failure flashovers. In stations, such a distinction is not recommended because

a) station electrical clearances are more complex and usually smaller than transmission line clearances; therefore, the consequences of a stroke penetrating the shielding system at stations are more difficult to foresee,
b) lightning inside a station area can cause severe voltage and current surges, with resulting interference problems in low-voltage control and protection circuits.

When it becomes desirable to determine whether or not individual shielding failure events will result in insulation flashover, the computation method of reference 5 of the paper can be employed to produce detailed information on flashover probability.

Manuscript received April 10, 1975.

IEEE Transactions on Power Apparatus and Systems, Vol. PAS-95, no. 4, July/August 1976

SHIELDING OF HIGH-VOLTAGE AND EXTRA-HIGH-VOLTAGE SUBSTATIONS

REF. 3,

Abdul M. Mousa
Teshmont Consultants Ltd.
Winnipeg, Manitoba, Canada

ABSTRACT

This paper provides an application procedure and graphs for the design of the shielding of high-voltage and extra-high voltage substations, where negative shielding angle configurations are usually encountered. It covers the shielding by both ground wires and masts. The method employed is an extension of Gilman-Whitehead electrogeometric model.

INTRODUCTION

In 1942, Wagner[1] published application curves covering the negative shielding angle configuration which is usually encountered in substations. Those curves were based on laboratory model tests, and were superseded by the introduction of the electrogeometric model of the lightning stroke by Young[2] et al who published shielding application curves for positive shielding angles based on a tentative calibration of the electrogeometric model. Recently, Gilman-Whitehead[3] perfected the calibration of the electrogeometric model, as given by equations (1) to (6) in this paper. M. Sargent [4] proposed extension of the electorgeometric model into a three-dimensional model and Braunstein[5] developed a sophisticated more accurate criterion for determination of the termination point of the lightning stroke. This paper adopts Gilman-Whitehead electrogeometric model, presents the equations which result when this model is applied to negative shielding angles for both shield wires and masts, and provides application curves for the design of the shielding of substations.

It is to be noted that backflash does not occur in substations because of the low-resistance grounding, and thus the provision of effective shielding would result in a substation design, which is practically flashover-free.

THE ELECTROGEOMETRIC MODEL

For the purpose of designing effectively shielded HV and EHV transmission lines, Gilman-Whitehead[3] based their electrogeometric model on the following:

1. 90% to 95% of the lightning strokes to earth lower negative charge. This is a basic assumption in the lightning stroke pathfinder project upon which Ref. (3) is based.

2. The critical lightning current to the phase conductor, I_c, is given by,

$$I_c = ICFO/(Z/2) \quad \ldots\ (1)$$

where ICFO = the negative polarity impulse critical flashover voltage of the porcelain and air gaps of the line.

Z = the surge impedance of phase conductor with ground return.

Equation (1) is oversimplified, because the potential at the point struck is materially affected by reflections from adjacent towers (and from equipment in case of substations), but Brown-Whitehead[6] state that the alternatives are not justified in the presence of other basic uncertainties.

The surge impedance, Z, is given by,

$$Z = 60 \ln (2h_{av.}/r) \quad \ldots\ (2)$$

where $h_{av.}$ = average height of the phase conductor.
= height at the tower minus two-thirds of the sag of the conductor.

r = the outside radius of the phase conductor, if single, or the geometric mean radius of the phase in case of bundled conductors.

3. The critical prospective lightning current to zero resistance earth, I_{oc}, is given by,

$$I_{oc} = 1.1\ I_c \quad \ldots\ (3)$$

4. The effective striking distance, r_{sc}, in meters, is related to I_{oc}, in kA, by the equation,[7]

$$r_{sc} = 8.5\ I_{oc}^{2/3} \quad \ldots\ (4)$$

Equation (4) is based on a previous equation for the mean striking distance, and an assumption that the standard deviation of the striking distance σ', is 10%. Any variability in the critical flashover strength of the tower is assumed to be included in σ'.

5. The effective striking distance to ground, r_{sg}, is equal to the effective striking distance to conductors and ground wires, r_{sc},

$$r_{sg} = K_{sg}\ r_{sc} = r_{sc} \quad \ldots\ (5)$$

Gilman-Whitehead state that the randomly distributed surface irregularities make K_{sg} close to unity, and that there is no experimental data to show otherwise.

6. A deviation factor, K, is applied to the actual height of the phase conductors, h, to obtain an effective conductors height to be used in the model. The deviation factor K provides for the uncertainties arising from the third-order factors[3],

$$1.1 \leq K < 1.2 \quad \ldots\ (6)$$

The third-order factors include the effect of power-frequency voltage on the striking distance, the effect of stroke corona on ICFO, and the effect of struck object on the striking distance.

SHIELDING OF SUBSTATIONS BY GROUNDWIRES

The layout of substations constitutes either a two-level bus arrangement, as in the case of double-

Paper F 76 007-6, recommended and approved by the IEEE Substations Committee of the IEEE Power Engineering Society for presentation at the IEEE PES Winter Meeting & Tesh Symposium, New York, N.Y., January 25-30, 1976. Manuscript submitted August 28, 1975, made available for printing November 3, 1975.

breaker scheme, or a three-level bus arrangement, as in the cases of main-and-transfer bus scheme, one-and-third breaker scheme, and one-and-half breaker scheme. In all cases, the shielding system is designed to provide effective shielding for the highest-level bus, and this will automatically provide effective shielding for the buses at the lower levels. Thus, the shielded system under consideration is mostly reduced to a 3-phase flat configuration with two ground wires located at the border of the bay as shown in Fig. 1.

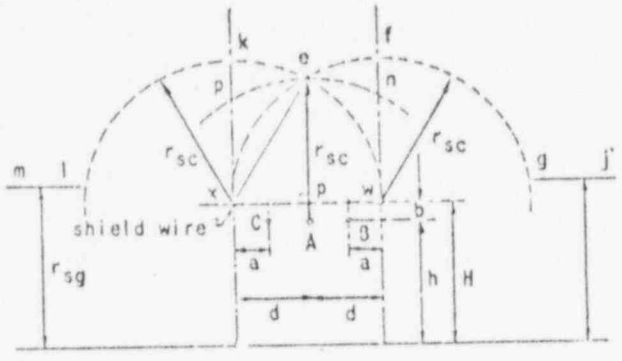

Fig. 1. Shielding of the center phase

In the electrogeometric model of transmission lines, the center phase is assumed to be effectively shielded by the two closely-located ground wires, and accordingly, exposure arcs are considered for the outer phases only. This does not apply to the electrogeometric model of substations shown in Fig. 1, and thus the shielding requirements are subdivided into:

1. Shielding the system against lightning strokes approaching between the 2 ground wires. From the geometry of shielding, it can be shown that, if the 2 ground wires are designed to provide effective shielding for the center phase, then the outer phases will automatically have better shielding. Since the shielding requirements of the center phase are governing for this group of strokes, we are going to refer to this item as "shielding of the center phase".

2. Shielding the system against strokes approaching outside the 2 ground wires. For this group of strokes, the shielding requirements of the outer phase are governing and accordingly, we are going to refer to this item as "shielding of the outer phases". Since the station usually consists of several bays, then this item is relevant only to the right hand side (R.H.S.) phase in the outermost R.H.S. bay and the L.H.S. phase in the outermost L.H.S. bay.

For both shielding requirements mentioned above, if the shielding is designed for a given critical lightning current I_c, then shielding is automatically provided against higher stroke currents, but some of the lower stroke currents may penetrate the shielding system, depending on their location.

Gilman-Whitehead[3] base the shielding of transmission lines on the average conductor height along the span. Because of the importance of substations, the shielding here is based on the parameters both at the supporting structure and at mid-span.

Shielding of the Center Phase

From the geometry of Fig. 1, it can be shown that the minimum superelevation of the ground wires (height above the phase conductors) necessary for effective shielding is given by,

$$\frac{b_{min.}}{d} = \frac{r_{sc}}{d} - \sqrt{\left(\frac{r_{sc}}{d}\right)^2 - 1} \qquad \ldots\ (7)$$

where 2d = the spacing between the ground wires.

Equation (7) shows that the shielding requirements of the center phase are independent of the heights of the conductors above ground. Equation (7) is plotted in Fig. 2, from which it can be seen that the superelevation, b, becomes excessively high when the ratio r_{sc}/d approaches unity, thus resulting in an uneconomical design. It is therefore proposed that the ground wires spacing be selected such that,

$$(r_{sc}/d) \quad > 1.5 \qquad \ldots\ (8)$$

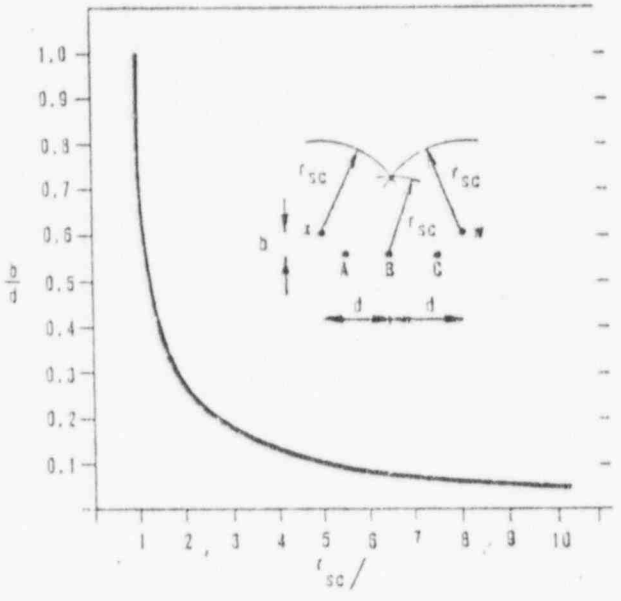

Fig. 2. Ground wires superelevation versus effective striking distance (in normalized form)

Shielding of the Outer Phases

Fig. 3 shows the electrogeometric model when the

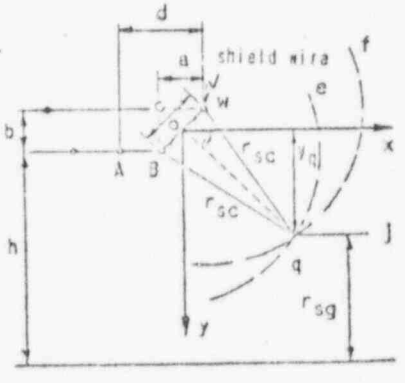

Fig. 3. The electrogeometric model for the outer phase

horizontal distance, a, between the outer phase and the ground wire is so that the exposure arc of the

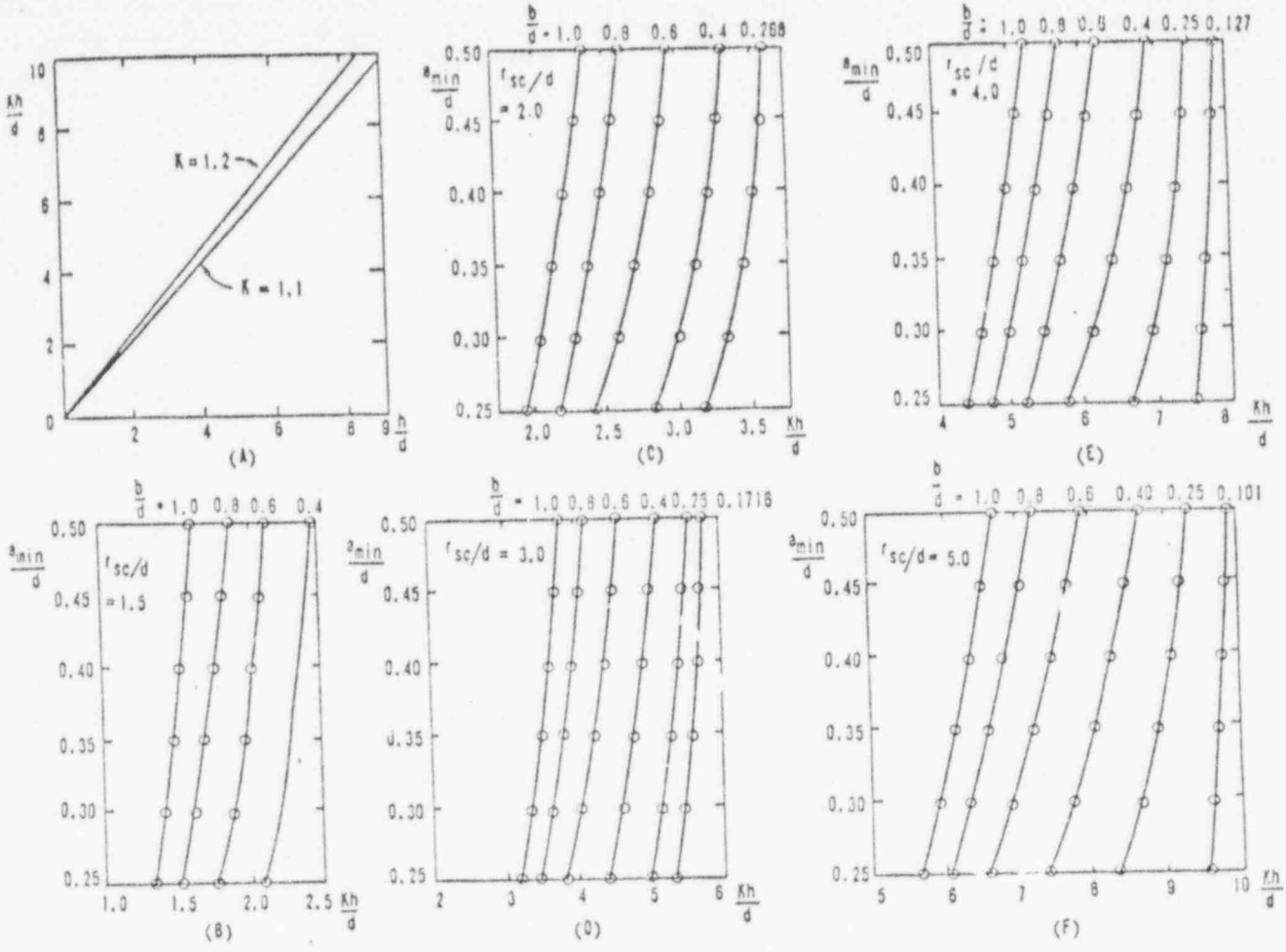

Fig. 4. Minimum horizontal distance between conductors and ground wires for effective shielding of the outer phase (K_{sg} = 1.0)

outer phase is eliminated. From Fig. 3, we get,

$$Y_q + r_{sg} = h + (b/2) \quad .... (9)$$

If h is replaced by Kh in equation (9) to account for the third-order factors, we get,

$$Y_q + r_{sg} = Kh + (b/2) \quad .... (10)$$

Equation (10) relates the 4 variables a, h, b and r_{sc} and can be written in 3 different forms:

1. To give the maximum permissible conductors height in terms of a, b, and r_{sc},

$$Kh_{max.} = K_{sg}\, r_{sc} - \frac{b}{2} + \frac{a}{2}\sqrt{\frac{4r_{sc}^2 - a^2 - b^2}{a^2 + b^2}} \quad .... (11)$$

Equation (11) applies both when all variables are in meters (feet) and when all variables are expressed in per unit of d (normalized form). The normalized form of equation (11) is plotted in Fig. 4 for K_{sg} = 1.0.

Fig. 4 shows that for constant conductors height, h, and constant horizontal spacing between ground wire and conductor, a, an increase in the superelevation, b, results in an increase in r_{sc} and hence an increase in the critical lightning current against which the ground wire can provide shielding. Thus, although increasing the superelevation of the ground wires improves the shielding of the center phase, it reduces the shielding of the outer phases.

2. To give the minimum permissible horizontal distance between the ground wire and the outer phase in terms of h, b and r_{sc},

$$a_{min}^4 + 4\left[(Kh + \frac{b}{2} - K_{sg} r_{sc})^2 - r_{sc}^2 + \frac{b^2}{4}\right] a_{min}^2 + 4b^2 (Kh + \frac{b}{2} - K_{sg} r_{sc})^2 = 0 \quad .... (12)$$

which is a second degree equation in a_{min}^2

3. To give the effective striking distance of the critical stroke current determined by the geometry of the system in terms of a, b and h,

$$r_{sc}^2 \left[K_{sg}^2 - \frac{a^2}{a^2+b^2}\right] - 2K_{sg}(Kh + \frac{b}{2}) r_{sc} + \left[(Kh + \frac{b}{2})^2 + \frac{a^2}{4}\right] = 0 \quad .... (13)$$

If we substitute K_{sg} = 1.0 in equation (13), we get,

$$r_{sc}^2 - 2(Kh + \frac{b}{2})(1 + \frac{a^2}{b^2}) r_{sc} + (1 + \frac{a^2}{b^2})\left[(Kh + \frac{b}{2})^2 + \frac{a^2}{4}\right] = 0 \quad .... (14)$$

PROCEDURE FOR THE DESIGN OF SUBSTATION SHIELDING

1. Calculate the surge impedance of the phase conductor of the highest level bus with ground return, using equation (2).

2. Calculate I_c using equation (1).

3. From Fig. 5, find the ratio r_{sc}/d corresponding to I_c and the bay width, 2d. Fig. 5 is based on equations 3 and 4.

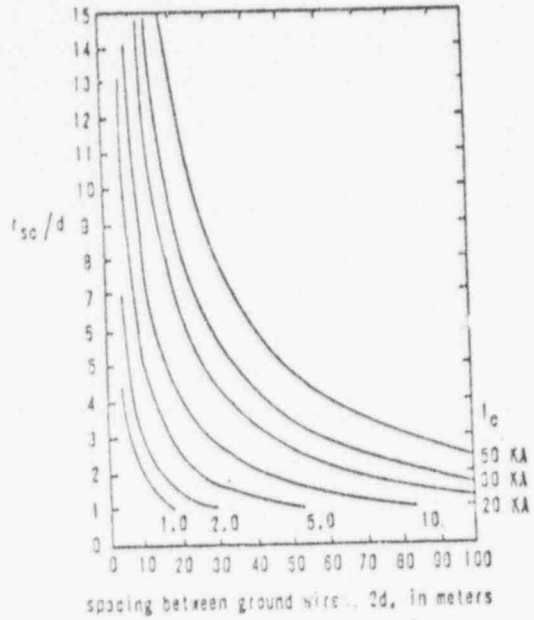

Fig. 5. Ratio r_{sc}/d in terms of 2d and I_c

4. From Fig. 2 find the ground wires superelevation at the supporting structure, b_c.

5. Repeat steps 3 and 4 using the spacing between ground wires (2d') at mid-span with allowance for conductor swing,

$$2d' = 2d + 2(\text{sag of ground wire}) \times \sin\alpha \quad \ldots\ldots (15)$$

where α = swing angle of shielding wire.

This step gives the minimum ground wires superelevation required at mid-span, b_{mid}.

6. From steps 4 and 5 find the necessary differential sag between conductors and ground wires.

7. Calculate the minimum ground wires superelevation based on mechanical and electrical clearance requirements, b'_{min}. The mechanical requirements include provision for problems of iceunloading and conductor oscillation where applicable. The spacing, c, between ground wires and conductors is usually of the order of the phase-to-phase spacing.

$$b'_{min} = \sqrt{c^2 - a^2} \quad \ldots\ldots (16)$$

8. From steps 4 to 7 select the ground wires superelevation at both the structure and mid-span.

Usually the ground wires spacing is equal to one bay width. However, it is sometimes attractive to select a ground wires spacing equal to twice the bay-width, thus reducing the quantity of ground wires used in the station, for either of the following reasons:

i) Sometimes the minimum ground wires superelevation necessary for electrical clearance purposes far exceeds the minimum ground wires superelevation necessary for adequate shielding. This especially happens in some EHV substations where the high critical lightning current results in moderate shielding requirements, i.e. low b_{min} as can be seen from Figure 2 while the large electrical clearance requirement results in large b'_{min}. In such case selecting (b) a little bit higher than b'_{min} would satisfy the shielding requirement based on a ground wire spacing equal to twice the bay-width.

ii) Sometimes there are conductors crossing from one bay to another. In such case it is convenient to design for a ground wires spacing equal to twice the bay-width to avoid the use of ground wires which are crossing over the phase conductors, and which may cause a 3-phase fault in case of failure of the ground wire.

Based on the above discussion and according to the results of Steps 4 to 7, it may be worthwhile investigating an alternative shielding system based on a ground wires spacing equal to twice the bay width.

9. Check the shielding of the outer phases at the tower using Fig. 4 as follows: Enter Fig. 4-A with the ratio h/d to determine the ratio Kh/d (K = 1.15 or 1.2). Select the applicable graph from Fig. 4-B to 4-F based on the ratio r_{sc}/d. Then select the applicable curve from the family of curves of that graph according to the ratio b/d, then find the ratio a_{min}/d corresponding to Kh/d. If this value exceeds the actual a/d, then the design has to be revised to accommodate this requirement.

10. Repeat step 9 to check the shielding of outer phases at mid-span, with allowance for conductors swing.

11. If the shielding requirements of the outer phase impose serious limitations on the design of the shield wires or on the bay width, then it may be convenient to design the main ground wires to provide shielding for the center phase only, and provide an auxiliary ground wire on every side of the station to provide shielding for the outer phase, as shown in Fig. 6. Fig. 6 also shows the use of ground wires spacing equal to twice the bay width.

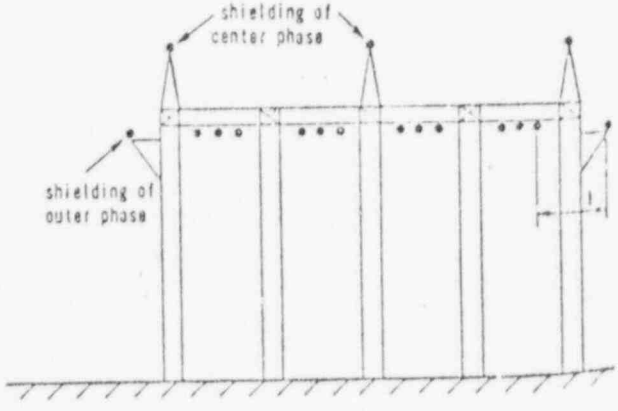

Fig. 6. Auxiliary shielding wires

Special Applications

1. Shielding of substations lower than 110 kV: The pathfinder project on which Gilman-Whitehead based their paper investigated lines of voltages of 110 kV and higher. For those lines, it is estimated that 90 to 95% of the significant lightning strokes lower negative charge and hence the "negative" polarity impulse critical flashover voltage is used in equation (1) to calculate the critical lightning current. According to Ref. (8), the percentage of strokes having positive polarity is relatively high for strokes of lower current amplitudes. Thus, for effective shielding of substations lower than 110 kV, it is proposed to calculate the critical lightning current based on the "positive" polarity impulse critical flashover voltage.

2. Shielding of HVdc substations: Anderson[9] ignores the power-frequency voltage across the insulator string of ac lines because its average is zero, while Gilman-Whitehead[3] treat it as a third-order factor, which is accounted for, together with other third-order factors, by the deviation factor K. This cannot be accepted for HVdc Systems, and accordingly it is proposed to calculate the critical lightning current using the following equation,

$$I_c = \frac{\text{ICFO} - \text{Nominal dc voltage}}{2/2} \quad \ldots\ (17)$$

The deviation factor K (= 1.15) is still to be retained to account for the other third-order factors.

3. Shielding of UHV substations: Ref. (3) on which this paper is based does not cover UHV lines, and accordingly the procedures given here are not valid for UHV substations. J.G. Anderson[9] proposes shielding UHV lines based on K_{sg} = 0.67, K = 1.0 and surge impedance based on the assumption that the bundle is a single conductor having a radius equal to 1.5 times the bundle radius. A somewhat different relation between r_{sc} and Ic is also proposed.

SHIELDING BY MASTS

Shielding by a Single Mast

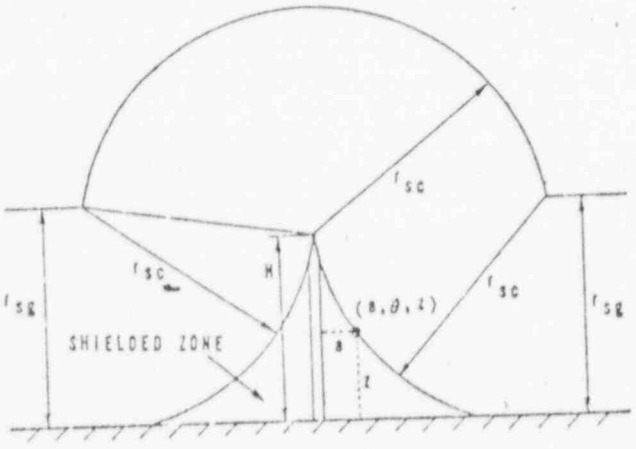

Fig. 7. Shielding by a single mast

Fig. 7 shows the zone shielded by a single mast for a critical lightning current whose striking distance is r_{sc}. The equation of the boundary surface of the shielded zone, in cylindrical co-ordinates (a, θ, Z), is given by,

$$(r_{sg}-KZ)^2 + \left[\sqrt{r_{sc}^2 - (r_{sg}-H)^2} - a\right]^2 = r_{sc}^2 \quad \ldots\ (18)$$

From equation (18), the height of the mast necessary to shield a point of height h and radial distance a from the mast, is given by,

$$\frac{H}{r_{sc}} = K_{sg} - \sqrt{1-\left[\frac{a}{r_{sc}} + \sqrt{1-(K_{sg}-\frac{Kh}{r_{sc}})^2}\right]^2} \quad \ldots\ (19)$$

If we substitute K_{sg} = 1.0 in equation (19), we get,

$$\frac{H}{r_{sc}} = 1 - \sqrt{1-\left[\frac{a}{r_{sc}} + \sqrt{\frac{Kh}{r_{sc}}\left(2-\frac{Kh}{r_{sc}}\right)}\right]^2} \quad \ldots\ (20)$$

Equation (20) is graphically represented in Fig. 8.

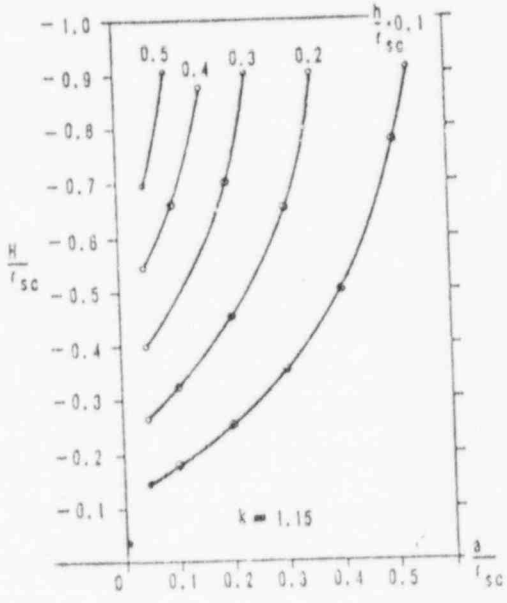

Fig. 8. Shielding curves of a single mast

Shielding of a Rectangular Area by 4 Masts Located at the Corners

1. Assume that a group of parallel conductors is located in a bay of width $2d_1$ and that the section of the bus of length $2d_2$ is to be shielded by 4 masts located at the corners of the rectangle as shown in Fig. 9. The effective striking distance surface of the 4 masts consists of 4 segments of 4 spheres, centers at the tops of the 4 masts and radii r_{sc}. The lowest point on this surface is at the center of the 4 masts. For shielding against strokes approaching within the area bounded by the 4 masts, the shielding requirements of the sections of the bus at the center of the bay are governing. For effective shielding of a point p on this center bus of height h and at a distance x along the axis of the bay, the minimum superelevation b of the masts above point p should be such that,

$$\frac{b}{d} = \frac{r_{sc}}{d} - \sqrt{\left(\frac{r_{sc}}{d}\right)^2 - 1} \quad \ldots\ (21)$$

where $d = \sqrt{d_1^2 + x^2}$ $\ldots\ (22)$

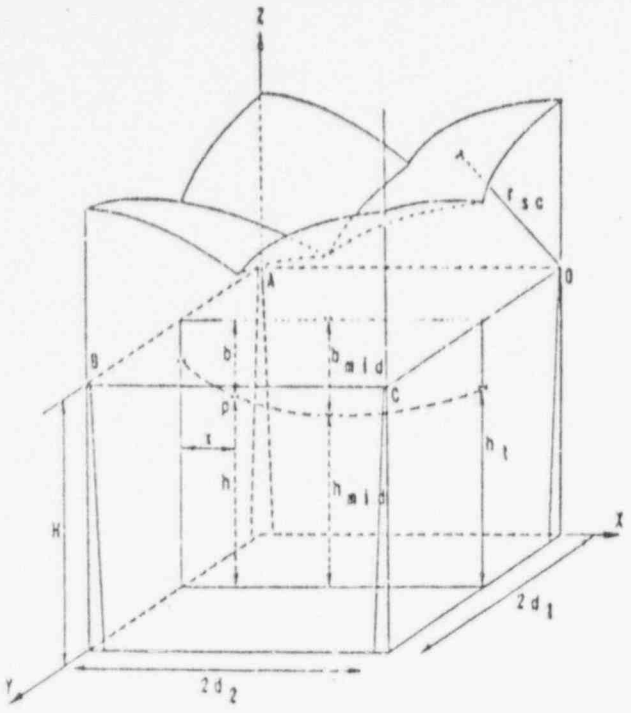

Fig. 9. Shielding of an area bounded by 4 masts

Shielding of the different points along the bus is to be checked using equations (21) and (22). If it is required to shield equipment within a uniform height h, then it is sufficient to design for effective shielding of the point at the center of the 4 masts, i.e.,

$$d = \sqrt{d_1^2 + d_2^2} \qquad \ldots\ (23)$$

2. For shielding against strokes approaching outside the area enclosed by the 4 masts, the following limitations apply to the horizontal distance a between the outer phase and the plane of 2 masts next to it,

$$a = \sqrt{r_{sc}^2 - (K_{sg} r_{sc} - Kh)^2} - \sqrt{r_{sc}^2 - X^2 - (K_{sg} r_{sc} - H)^2} \qquad \ldots\ (24)$$

Equation (24) is based on the geometrical relations of Fig. 10, and can be written in the form,

$$\frac{H}{r_{sc}} = K_{sg} - \sqrt{1 - \frac{X^2}{r_{sc}^2} - \left[\frac{a}{r_{sc}} - \sqrt{1-(K_{sg} - \frac{Kh}{r_{sc}})^2}\right]^2} \qquad \ldots\ (25)$$

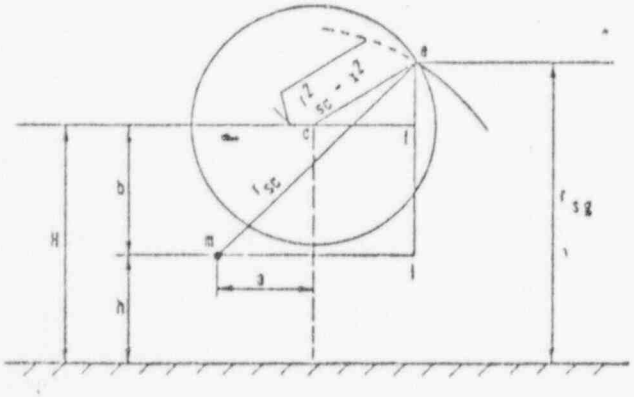

Fig. 10. Shielding of outer phase by masts

If we substitute $K_{sg} = 1.0$ in equation (25), we get,

$$\frac{H}{r_{sc}} = 1 - \sqrt{1 - \frac{X^2}{r_{sc}^2} - \left[\frac{a}{r_{sc}} - \sqrt{\frac{Kh}{r_{sc}}\left(2 - \frac{Kh}{r_{sc}}\right)}\right]^2} \qquad \ldots\ (26)$$

If the distance a is practically constant along the bay, then it is sufficient to determine a from equation (26) based on $X = d_2$ (at mid-bay).

CONCLUSIONS

1. The equations and procedure for the design of the shielding of substations by ground wires and masts are presented.

2. The ratio of the effective critical striking distance to half the spacing between the ground wires should be not less than 1.5 if an economical design is to be achieved.

3. Sometimes it is convenient and/or economical to employ a ground wires spacing equal to twice the bay-width, thus eliminating about half the quantity of ground wires and their supporting spikes.

4. The horizontal distance between the outer phase and the ground wire, which is usually based on the required conductor-to-structure clearance and the structure width, may have sometimes to be increased to satisfy the shielding requirements of the outer phases.

5. Where economically justified, the main ground wires may be designed to provide shielding against strokes approaching directly above the station, and an auxiliary ground wire is added on every side of the station to provide shielding against strokes occuring on the sides of the station.

ACKNOWLEDGMENT

The work reported was undertaken at Teshmont Consultants Ltd., Winnipeg, Canada. The author wishes to thank Messrs. R. E. Harrison, R. K. Shemie and V. Burtnyk for valuable discussions.

REFERENCES

(1) C.F. Wagner, G.D. McCann, and C.M. Lear, "Shielding of Substations", AIEE Trans., Vol. 61, pp 96-100, February 1942.

(2) F. S. Young, J. M. Clayton, and A. R. Hileman, "Shielding of Transmission Lines", IEEE Trans. (Power Apparatus and Systems, Special Supplement), Vol. 82S, pp 132-154, 1963.

(3) D.W. Gilman and E.R. Whitehead, "The Mechanism of Lightning Flashover on High-Voltage and Extra-High-Voltage Transmission Lines", Electra No. 27, March 1973, pp 65 - 96.

(4) M. A. Sargent, "Monte Carlo Simulation of the Lightning Performance of Overhead Shielding Networks of High Voltage Stations", IEEE Trans. (Power Apparatus and Systems), Vol. 91, pp 1651-1656, July/August 1972.

(5) A. Braunstein, "Lightning Strokes to Power Transmission Lines and the Shielding Effect of Ground Wires", IEEE Trans. (Power Apparatus and Systems), Vol. 89, pp 1900-1910, November/December 1970.

(6) G.W. Brown and E. R. Whitehead, "Field and Analytical Studies of Transmission Line Shielding: Part II" IEEE Trans. (Power Apparatus and Systems) Vol. 88, pp 617-626, May 1969.

(7) E. R. Whitehead, "CIGRE Survey of the Lightning Performance of Extra-High-Voltage Transmission Lines", Electra No. 33, March 1974, pp 63-89.

(8) Electrical Transmission and Distribution Reference Book. East Pittsburgh: Westinghouse Electric Corporation, 1950, Chapter 15, Section 4 and Chapter 16, Section 27.

(9) Transmission Line Reference Book 345 kV and Above Palo Alto, CA: Electric Power Research Institute, 1975, Chapter 12.

Discussion

William H. Dainwood (Tennessee Valley Authority, Knoxville, TN): The paper is very interesting from a substation or switchyard designer's position. There are several questions and comments that could be raised concerning the author's approach to overhead shielding. First, a definition and discussion of negative shielding angle configurations, which the author refers to in his "INTRODUCTION," would be helpful. Also, in the "INTRODUCTION" the term "backflash" is used. This may have different meanings for different people. I would like to know what Mr. Mousa means in his statement. In equation (2), $Z = 60 \ln (2h_{av}/r)$, the author does not mention any units. I'm wondering if h_{av} and r may be expressed in any units as long as they are the same. Also, in relation to equation (2), why are there two definitions for h_{av}? I notice also that the author has used the term critical lightning current I_c. Is this term the same as the stroke current? Under the heading "SHIELDING OF SUBSTATIONS BY GROUNDWIRES," the author states that ". . ., but some of the lower stroke currents may penetrate the shielding system, depending on their location". I would suggest that this may be true, but there is no way of knowing this without checking. This statement is in agreement with A. Braunstein's paper, reference (5). There appears to be an error concerning figure 4(c). On the left hand side at the top there needs to be a line separating the numerator and denominator a_{min}/d. Under step 5 of the "PROCEDURE FOR THE DESIGN OF SUBSTATION SHIELDING," what is meant by α, swing angle of shielding wire? I would also like to know if the paper is strictly theoretical or has the procedure been used for practical substation shielding problems?

Mr. Mousa also states that, for overhead shielding, it is sometimes attractive to select ground wire spacing equal to twice the bay width, thus reducing the quantity of ground wires used in the station. His electrogeometric model may show this can be done but using the analytical equations developed by A. Braunstein, reference (5) in the author's paper, we have not found this to be good design practice, especially in large EHV switchyards at generating plants.

I would also like to know if Mr. Mousa's equations and procedure can be used for skewed or nonparallel shield wires. It appears that his method is valid only for two-dimensional systems and good for parallel conductors only.

There is one area that might be worth some future investigation and that would be to computerize the design procedure for overhead shielding. The procedure as it now stands seems to be quite laborious and time consuming.

Manuscript received February 17, 1976.

J. Chiloyan (Northeast Utilities Service Co., Hartford, CT): The author is to be commended for his efforts in expanding the application of Gilman-Whitehead's electrogeometric model to that of substation shielding.

The discussor would like to offer the following comments which the author may wish to consider:

1) To insure satisfactory shielding of substations we have based our design on L. V. Bewley's [1] formula, where the height above ground of approaching thunder clouds is set at 1500 ft. The formula may be stated as: $x = (3000h-h^2)^{1/2} - (3000y-y^2)^{1/2}$
where: x = horizontal distance between mast and protected structure, in ft.

h = height of mast above ground, in ft.

y = height of protected structure above ground, in ft.

When the height of the mast is 100 ft. and the height of the protected structure is 25 ft., the calculated value of the horizontal distance between mast and protected structure is 266 ft. Applying the author's method of shielding by a single mast to this 345kV station, with a surge impedance of 300 ohms and a negative polarity impulse critical flashover voltage of 1650kV, results in a horizontal distance of 52 ft. Many utility companies throughout the country use the Bewley formula for shielding design and apparently with satisfactory success. The author's approach is obviously more conservative and would be more costly. We would ask the author if he could provide justification for the use of this more conservative and costly type of substation shielding.

2) In our rigid bus design arrangements, overhead ground conductors are not brought into the substation proper but are brought to line dead-end towers in the substation where they are terminated. The proximity of line take-off towers to underlying rigid buses is such that economical shielding is obtained by installing lightning rods on these towers. Only when the height of these lightning rods becomes excessive have we resorted to ground supported mast to shield areas remote from the line take-off towers.

3) Has the author considered the application of the electrogeometric model to shielding of non-live structures such as control houses metalclad switchgear? These structures may be remotely positioned from effectively shielded buses.

4) In large substations where shielding is provided by several masts, should not each mast be designed on the basis of its specific shielding area structures? This approach would be more economical than that of designing all masts on the basis of the highest bus level.

5) Should not Equation (10) on page 3 of the paper correctly read $Y_q + r_{sg} = Kh + (b)/2$?

REFERENCES

[1] L. V. Bewley "Traveling Waves on Transmission Systems" Chapter 14, Section 10, published 1963.

Abdul M. Mousa: The author is grateful for the interest shown by Mr. J. Chiloyan and Mr. W. H. Dainwood. I would like to mention that it took many years and great efforts to establish, calibrate and verify the electrogeometric model for the shielding of transmission lines. The work reported in this paper is no more than a mathematical application of the currently accepted theory to new geometries. The latter sections of the paper establish what is needed for effective shielding by masts and the degree of conservatism in the results, if any, is that inherent in Professor Whitehead's empirical relationship between the stroke current and the striking distance. The earlier shielding theories developed in the pre-electrogeometric model era had little evidence from physics, statistical field data or representative laboratory work to substantiate them. The equation used by Mr. Chiloyan was first published by Peek in 1931 [10]. It is interesting to note that the application of another one of those earlier theories, namely Wagner's (1), to the case described by Mr. Chiloyan results in a shielded radius of 100 ft. as compared to the 266 ft. given by the Peek-Bewley formula.

The shielding technique described in this paper has been applied to the design of a 500/220 kV ac substation and to ±500 kV dc converter stations. The converter stations consisted of several areas of different voltages (±500 kV dc, ±250 kV dc and 230 kV ac), different bus types (rigid and strain) and/or different bus geometries (heights and diameters). The shielding of each individual area was based on the specific conditions in that area.

It is important to note that the design of the two wire shielding system described herein provides effective shielding against all lightning strokes whose current exceeds the critical lightning current, I_c, for every point within the volume $CC_1 C'_1 C' BB_1 B'_1 B$ shown in Fig. 11. Thus the same procedure can be applied to the shielding of equipment, e.g. a transformer bank, by replacing it by an equivalent 3 – conductor system which prescribes a shielded volume which contains the equipment. This would be done by selecting the height and sag of the three conductors such that the surface BACCAB touches the uppermost point(s) of the equipment (conductors may be chosen to be of zero sag and constant height equal to the height of the equipment), and by locating the outer conductors such that they are directly above the outermost points of the equipment. Thus, shielding of the outermost points of the equipment would correspond to shielding of the outer

Manuscript received February 17, 1976.

phase as described in this paper, and shielding of the main body of the equipment would correspond to shielding of the center phase.

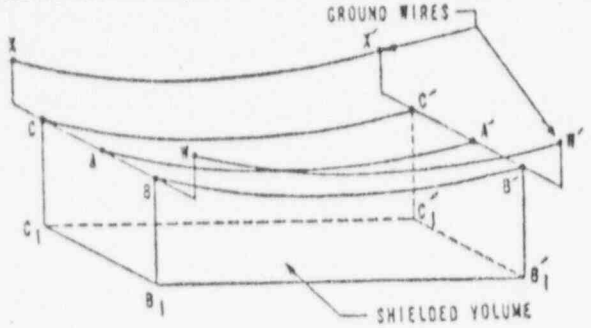

Fig. 11. Volume shielded by 2 ground wires

The object of shielding is to divert direct lightning strokes away from live conductors, and as such, there is no shielding problem for metalclad switchgear or isolated phase bus systems. This paper may be applied to the protection of station buildings against lightning, if the maximum innocuous stroke current can be estimated.

Based on experience gained from many applications, the author suggests that the use of masts should be discontinued, except for isolated areas in the stations. If a ground wire shielding system was compared to an equivalent mast shielding system, the ground wire shielding system will be found to be of considerably lower heights, its cost will be comparable or lower than that of the mast system (this also applies to the shielding of most rigid bus systems where ground wires would require independent poles to support them), and its backflash rates will be much lower than that of the mast system. As an example, Fig. 12 shows the ground wire shielding system for a bay of a 345 kV station having the parameters mentioned by Mr. Chiloyan. The required superelevation is 5 ft., and based on an assumed 5 ft. sag for a 300-400 ft. span, the height of the wire-supporting structures would be 35 ft. as compared to the 100 ft. high masts mentioned by Mr. Chiloyan. This shows that the ground wire system is more aesthetic and is relatively inexpensive.

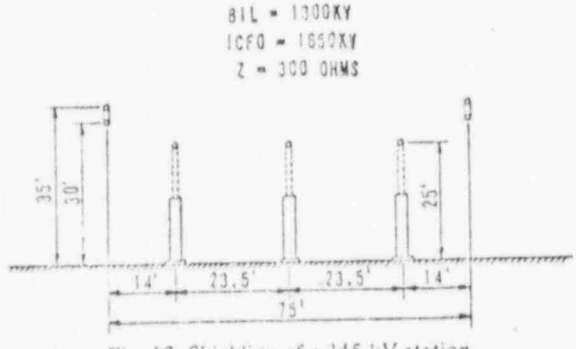

Fig. 12. Shielding of a 345 kV station

Following the successful interception of a stroke by the shielding system, the stroke will be diverted to ground through the mast or through the structures supporting the ground wire(s), and the potential of these grounded bodies will transiently drop (for a negative stroke) below the potential of true ground. The probability of a backflash (a flashover from grounded structures to live conductors) will be higher for a mast system than for a ground wire system, because mast currents are much higher for the following reasons,

i. For the same height, the average stroke current collected by a mast is higher than that of a ground wire [11].

ii. Masts of comparable shielding performance are usually higher and hence the distribution of stroke current amplitudes collected by them is more biased towards the high amplitude current values [11].

iii. Each mast carries the full stroke current, while two or more structures share the current of a stroke collected by a ground wire (this factor indicates the importance of continuity in the overhead ground wire scheme in stations).

Thus, while the probability of a backflash in a station shielded by ground wires is small, that probability for a station shielded by masts is fairly high (the previous sentence qualifies the statement in the INTRODUCTION).

While assessing the shielding performance of masts applied to some existing low voltage stations, the author noted that some of them are not only ineffective, but also wasteful. As shown in Fig. 13, the area shielded by a mast increases as the mast height is increased, up to a mast height equal to the striking distance. Any additional mast height beyond that does not contribute any shielding effect, a limitation which the "shielded cone" old theories did not recognize.

The cylindrical equation of the boundary of the maximum shieldable zone is given by,

$$\frac{a}{r_{sc}} = 1 - \sqrt{\frac{Kh}{r_{sc}}\left(2 - \frac{Kh}{r_{sc}}\right)} \qquad \ldots\ldots(27)$$

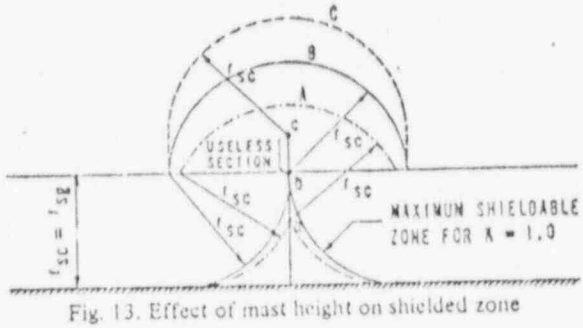

Fig. 13. Effect of mast height on shielded zone

The necessary superelevation of a system of two nonparallel ground wires having spacings of $2d_1$ & $2d_2$ at the supporting structures, where d_1 is larger than d_2, may be established based on a system of two parallel ground wires having a spacing equal to $2d_1$. In investigating the shielding at mid-span for this case, the swing angle, α, should be neglected.

Referring to Mr. Dainwood's comment, I would like to qualify my statement about the use of ground wires spacing equal to twice the bay width. This concept was successfully applied to a 220 kV switchyard where the bay width was 15 meters (about 50 ft.). Applicability to other cases can be checked using the inequality no. (8). The statement in the paper should not be construed as suggesting the universal applicability of this concept.

"Negative shielding angle configuration" is the arrangement whereby the entire live conductor system to be shielded is located between two ground wires, as shown in Fig. 1. The "critical lightning current" is the maximum stroke current that would not cause flashover if it hits the live conductors. "α" is the swing angle of the ground wires due to wind action.

Mr. Dainwood's guess about the units of h_{av} and r is correct. The resulting value of the surge impedance, Z, will be in ohms. The paper gives a definition of h_{av} and the applicable equation for calculating it for the flat terrain usually encountered in substations. Different equations are used for the calculation of h_{av} for the sections of transmission lines where the terrain is rolling or mountainous, as shown in Section 5.3 of Ref. (3).

The design procedure described in this paper is too simple to warrant computerization, and the equations herein are written in a format suitable for manual and graphical use. This design procedure becomes even simpler in many applications if we note that the minimum permissible horizontal clearance, a_{min}, between the ground wire and the outer phase would be zero, if,

$$r_{sc} \geq \left(Kh + \frac{b}{2}\right) \qquad \ldots\ldots(28)$$

The inequality no. (28) results from equation (12) by substituting $a_{min} = o$ & $K_{sc} = 1.0$, and serves as a quick check on the shielding of the outer phase for low-level bus systems.

The discussors are right about the typing errors they noted. Few other typing errors appeared in the preprint copies and they have been corrected in the transactions copy.

Subsequent to the presentation of this paper, it came to the author's attention that the shielding of the center phase of transmission lines of flat configuration has been studied by E.T.B. Gross et al [12].

REFERENCES

[10] W. W. Lewis, The Protection of Transmission Systems Against Lightning, New York: Dover Publications, Inc., Second Edition, 1965, Chapter VI.

[11] M. Sargent, "The Frequency Distribution of Current Magnitudes of Lightning Strokes to Tall Structures", *IEEE Trans. (Power Apparatus and Systems)*, Vol. 91, pp. 2224-2229, September/October 1972.

[12] P. Chowdhuri, E.T.B. Gross and S. P. Negreira, "Shielding of Transmission Lines Against Lightning", Journal of Franklin Institute, Vol. 286, No. 4, pp. 269-279, October 1968.

IEEE TRANSACTIONS ON

INDUSTRY APPLICATIONS

NOVEMBER/DECEMBER 1978 VOLUME IA-14 NUMBER 6

A PUBLICATION OF THE IEEE INDUSTRY APPLICATIONS SOCI

Protection Zone for Buildings Against Lightning Strokes Using Transmission Line Protection Practice

RALPH H. LEE, FELLOW, IEEE

Abstract—The nature of the zone of protection of structures from an elevated rod or wire, inadequately defined in the past, can be determined with high reliability using data developed by E. R. Whitehead of the Illinois Institute of Technology under contract from the Edison Electric Institute for the protection of high-voltage electric transmission lines. The vertical boundary of this zone of protection is not linear, as has been believed in the past, but is a circular arc, tangent to the ground, of 150-ft radius for 99.5 percent protection and 125-ft radius for 99.9 percent protection.

HISTORICAL PRACTICE

EVER SINCE the time of Benjamin Franklin [1], we have been aware that elevated "air terminals" provided protection to lower objects from direct lightning strokes. The shape and extent of the zone of protection have, however, been variously defined over the intervening 200 years. As documented in a technical paper by B. Wilson [2] in 1778, Franklin believed that a conical zone below and around the air terminal with an angle of 58° from vertical was suitable, although no record remains of experimental or theoretical development of this figure. Later workers in the field recommended different zones, as shown in Table I.

The decrease in angle or zone of protection with progressing time may be due to recognition of failure of earlier criteria. This and the possible failures may also have occurred as a result of progressively higher structures. The only departure from a linear-sided zone is that of Preece [4], whose cone has sides of circular form, with radius of 100 m, tangent to the ground. Thus a 100-m high rod would have a very small angle of protection for objects near 100 m, but nearly 45° maximum angle of protection for objects close to ground level. Likewise, a rod of, say, 50 m in height would have a protection angle of 30° near its top and a protection angle of about 60° for low objects 100 ft from its base. Preece's hypothesis does not appear to have attracted much following, possibly because of complexity of application.

RECENT PRACTICE

In the early 1920's, F. W. Peek [5] conducted scale model tests which yeilded conical protection angles of 64-76°, or protective ratios (width to height) of 2:4. These values were adopted in the U.S.A. "Lightning Protection Code," National Fire Protection Association (NFPA) 78, in 1932, being reduced to 45° and 64° (ratios 1 and 2) in 1945, at which point they remain to date. The 1:1 ratio is recommended for important structures, the 1:2 ratio for less important ones.

TABLE I
ZONES OF PROTECTION FROM VERTICAL LIGHTNING ROD (3)

Date	Source	Zone	
		Shape	Angle
1823	Gay Lussac	Cylinder	64°
1874	de Fonvielle	Cone	64°
1875	Paris Commission	Cone	60°
1875	Chapman	Cylinder	45°
1881	Adams	Cone	45°
--	Hypothesis	Cylinder	30°
1881	Preece	100 m rad. circ. cone	var.
--	Melsens	Cone	30°

In NFPA 78, there are no criteria for protection zones between two or more high terminals. However, the generalized recommendations for conventional lightning rod installations on roofs employ vertical terminals not less than 2 ft high, spaced not more than 25 ft apart around the periphery of a flat roof, and not more than 50 ft apart within that periphery. It appears to be recognized that areas between high points receive a much flatter zone of protection than areas surrounding a single high point or wire.

In addition to this recognized flat protection zone between or among multiple air terminals or rods, there are the reports of failures of very high structures to provide protection within even the sharpest of conical zones. This was documented by Lodge [2] and Anderson [6] and has been noted more recently around such structures as the Empire State Building and the Eiffel Tower. In these cases, lower structures, well within even the 30° angle of protection from their tops, have sustained direct strokes. Also, there are some reports of lightning strokes terminating on such high structures *below* their tops. Such reports have reduced the credibility of the protection capability of higher objects against lightning in terms of the linear cone principle.

LIGHTNING STROKE PHENONENA

A knowledge of lightning stroke formation is helpful in understanding how diverter elements (rods, wires, etc.) provide protection. The step leader, originating in a cloud charge center, progresses in discrete elements of from 10-80 m in length at intervals averaging 50 μs between steps. The predominant length of step is 50 m, or just over 150 ft. Each step is

Paper IPSD 77-9, approved by the Power Systems Support Committee of the IEEE Industry Applications Society for presentation at the 1977 Industrial and Commerical Power Systems Conference, Pittsburgh, PA, May 9-12. Manuscript released for publication March 6, 1978.

The author is with Lee Electrical Engineering, Inc., Wilmington, DE 19807.

0093-9994/78/1100-0465$00.75

random in direction, accounting for the jagged appearance of the overall lightning stroke. Only when the leader tip comes within a distance of about 100 m (330 ft) of an object of opposite polarity, does it tend to progress in the direction of that object. At about this instant, a short streamer, or electric discharge, is likely to develop from that and other nearby objects on earth toward the oncoming stepped leader.

Evidence recently published by Golde [7] shows that at a point in the vicinity of 100 m, the direction and character of the downward leader are positively diverted toward the point to be "struck" and that the downward leader and an upward streamer meet somewhere in this terminal length. On completion of the ionizing path, the actual "stroke" occurs over this path with heavy current flowing from earth to cloud to neutralize the originating charge center. Restrokes frequently follow the same ionized path without the slow stepping character of the leader. These are believed to be due to recharging of the original charged center from other centers within the cloud by "strokes" within the cloud. The current magnitude of the stepped leader is only about 100 A, that of the return stroke averages about 20 000 A.

From this analysis, it follows that unless the stepped leader nears the earth within about 100 m of a high object, it is unlikely to be attracted to that object and may strike the earth's surface or some other object beyond the 100-m distance. This bears out the earlier observation that very high objects, say above 100-m high, frequently do not protect much lower nearby objects which are well within the conventional cone of theoretical protection.

ELECTRIC TRANSMISSION LINE RESEARCH

In the electric power transmission line field, a 30° protection angle from the vertical had long been used to provide satisfactory performance. With the inception of systems operating above 230 kV with greater tower heights, the 30° standard angle was found too great, yielding a much poorer lightning outage performance [8]. Subsequently, the Edison Electric Institute (EEI) initiated Research Project RP-50 with the Illinois Institute of Technology (IIT) Research Institute. This project was directed by ITT's E. R. Whitehead, culminating in a report [9]. See Appendix for a summary of this method.

The project entailed both theoretical and practical analysis, including performance measurements over a nine-year period, at 4600 locations on 433 mi of overhead lines ranging from 110-345kV on systems of 12 EEI member companies. A statistical analysis of the performance of the lines and their conductor configurations was the real basis of the conclusion of the project.

The results showed inverse interrelation between protection angle and height above ground. The suitable protection angles for the range of heights normally used are shown in Table II for systems having a basic impulse insulation level (BIL) of 1400 kV. Higher BIL's would operate as well with flatter protection angles. The 1400 kV BIL is used here because the clearances associated with it are typical of those generally used in building lightning protection. Fig. 1 shows the range of protection for this BIL and various heights. The 99.5 percent protection could be increased to 99.9 percent by a 10° decrease in the protection angle. The 25- and 50-ft height values were obtained by extrapolation of the data for heights of 75 and 100 ft. Heights are for the overhead ground (static) wire.

TABLE II
PROTECTION ANGLES FOR 99.5 PERCENT PROTECTION

Height above ground	Protection Angle
(25 ft.)	(60°)
(50 ft.) Extrapolated.	(47°)
75 ft.	33°
100 ft.	20°
125 ft.	10°
150 ft.	0°
175 ft.	-10°
200 ft.	-20°

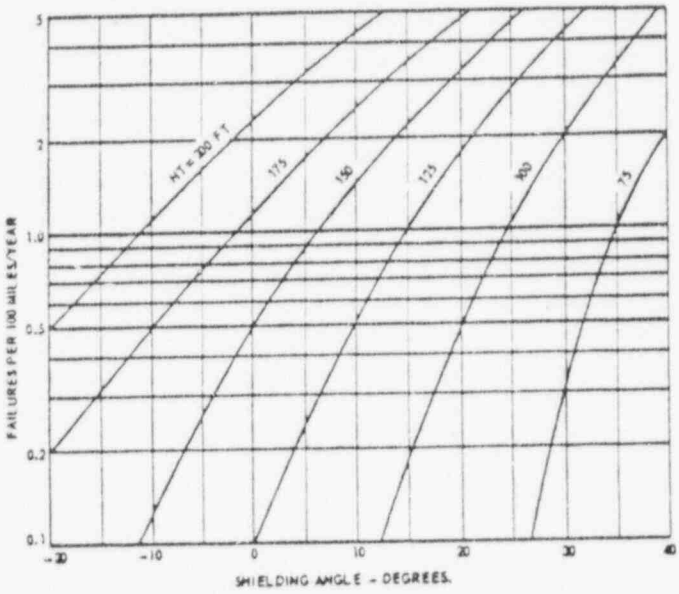

Fig. 1. Shielding failure rate reheight and shielding angle for 1400 kV BIL (9).

Outage rate per year per 100 mi of line equates closely to the complement of percent efficiency, since at this (30)-isokeraunic level, the probable outage rate per 100 mi of line per year is 100.

Note that at 150 ft above ground, a zero angle of protection is provided by the higher conductor. At 175 ft, height and above, the negative angle indicates that a protecting conductor needs to extend beyond the position of the object to be protected. This requirement is illustrated in many of the more recently built EHV transmission lines, in which the overhead ground wire is carried outboard of the outer phase conductors.

STRUCTURE PROTECTION CRITERIA

Plotting the data of Table II on linear scales in Fig. 2, it is seen that the connection of the lengths centering on the 25 ft multiples of height forms almost exactly an arc of a circle of radius 150 ft, tangent to the earth surface at a point 150 ft away from the 150-ft high (zero protection angle) point.

This 150-ft radius criterion matches up very well with the 50-m predominant step length noted earlier and provides a factor of safety of just over two for the point of influence of the path of the leader toward the ultimate strike point.

Its use provides us with a tool for reliable design of diverter elements for lightning protection by a single elevated rod or wire. This is illustrated in Fig. 3. An object above ground level

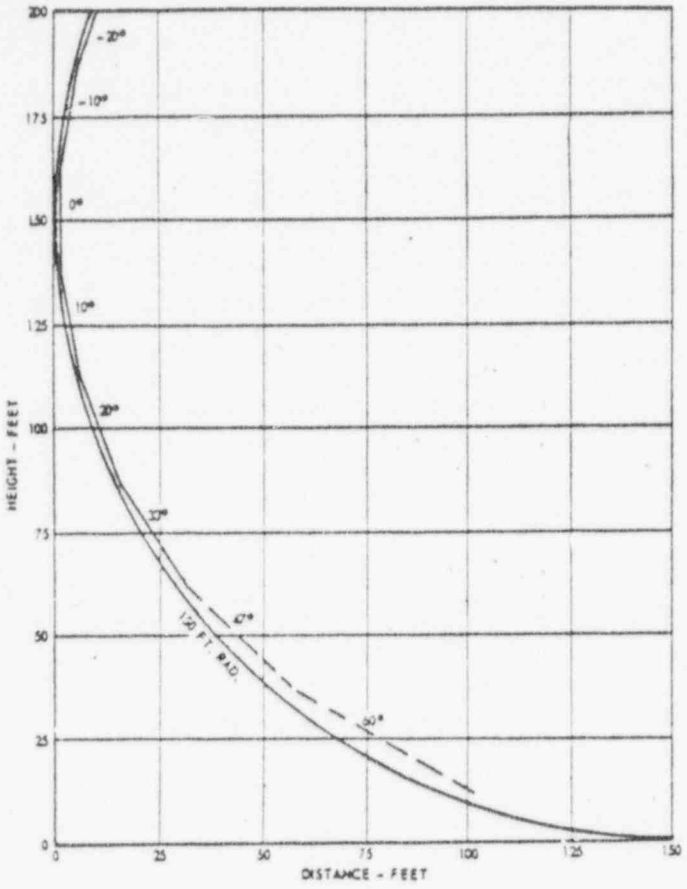

Fig. 2. Plot of data from Table II with 150 ft radius circle inscribed (9).

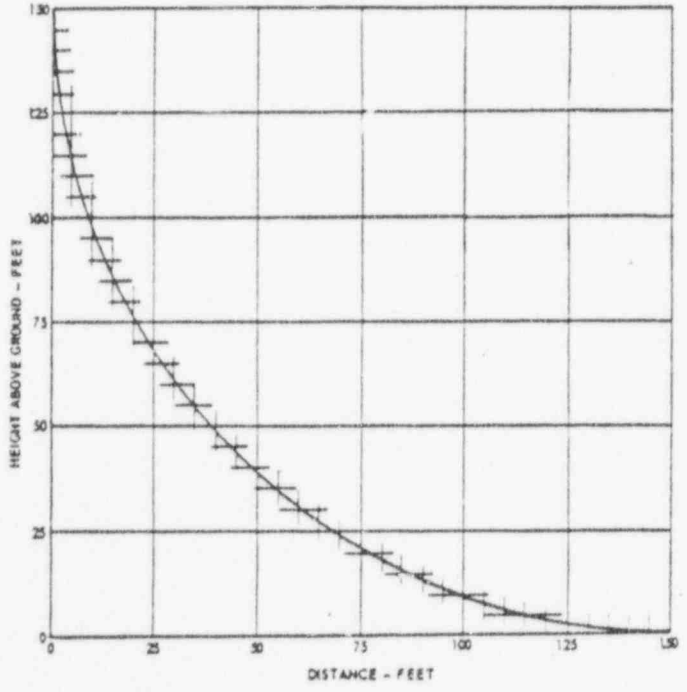

Fig. 3. Lightning protection from single mast or wire. Mast–cone, 150 ft radius. Wire–tent 150 ft radius. Sides, conical ends. Protecting point lies along line. All points below line are protected.

TABLE III
PROTECTION FOR 37.5 FT HIGH OBJECT BY SINGLE ROD OF WIRE

Distance from Point to be Protected	Total Height of Protecting Terminal	Super-elevation of protecting Terminal
5 ft.	42.5 ft.	5 ft.
12.5 ft.	50 ft.	12.5 ft.
25 ft.	67 ft.	30 ft.
37.5 ft.	88.5 ft.	51 ft.
50 ft.	150 ft.	112.5 ft.

will be protected against direct lightning strokes if it does not protrude above the surface of an inverse circular-sided cone of 150-ft radius, tangent to the ground and touching the protecting object. The 150-ft radius for 99.5 percent protection could, as with the transmission lines, be reduced to 125 ft to provide 99.9 percent protection.

Another way to visualize this is to imagine a sphere (ball) of 150- ft radius (300- ft diameter) rolling over the surface of the earth and up and over all projections above the earth's surface. All objects touched by the ball are susceptible to direct stroke, while those not touched by the ball, because of its being lifted over them by higher (protecting) objects, are not susceptible to direct stroke. It is readily seen then that objects more than 150 ft away from even a very high structure will receive little or no protection from that structure.

Fig. 4 illustrates this concept; points below the 150-ft radius curve, tangent to the ground and touching the mast such as structure B, are protected. Those which project through this radius such as structure A, similar in size to but farther from the mast, are subject to direct stroke. The new protection curve left of the mast is a combination of two 150-ft radius curves intersecting on structure A, or the locus of a 150-ft radius sphere rolling up and over structure A and then from the roof of A until it touches the mast at point C. The height of the mast above the shaded curve tangents is a "useless height," providing no additional protection, although NFPA 78 considers it useful. The "useless height" term is also used by Mousa in [10, Fig. 13], similar to Fig. 4 of this paper.

The use of Fig. 3 is illustrated below. An object 37.5-ft high is to be protected (see Table III). In solution, the 37.5-ft high object will be 100 ft from the point of tangency with ground. It can be protected by any of the higher air terminals of the following heights and distances horizontally from the point to be protected, taken from the arc of Fig. 3.

Similarly, a 125-ft high stack could just barely be protected by a 150-ft terminal just 2 ft horizontally offset and practically would have to be protected by terminals directed upward from the stack top.

PROTECTION FROM TWO OR MORE ELEMENTS

The concept of a 300-ft diameter sphere rolling over all protective objects also yields data supportive of protection between two or more elevated elements, similar to the two overhead ground wires of electric transmission lines. Where the 300-ft diameter sphere rolls over two elevated objects, the surface tends to penetrate between them only to the extent that its diameter and the separation of the objects will permit. Then, any object which remains below the sphere's surface re-

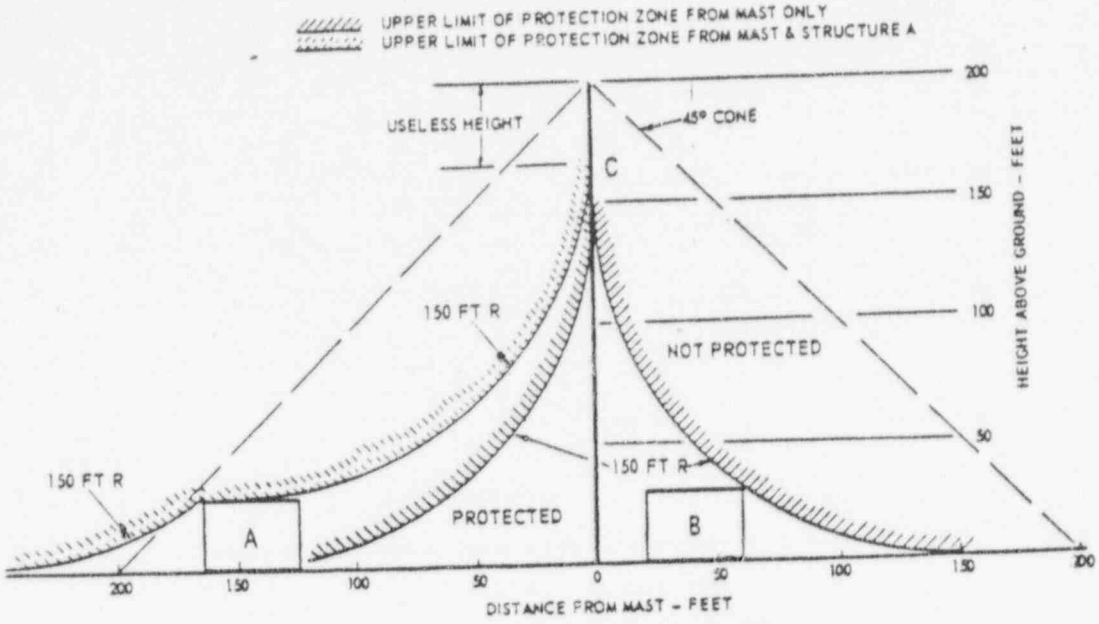

Fig. 4. 300 ft diameter rolling sphere principle.

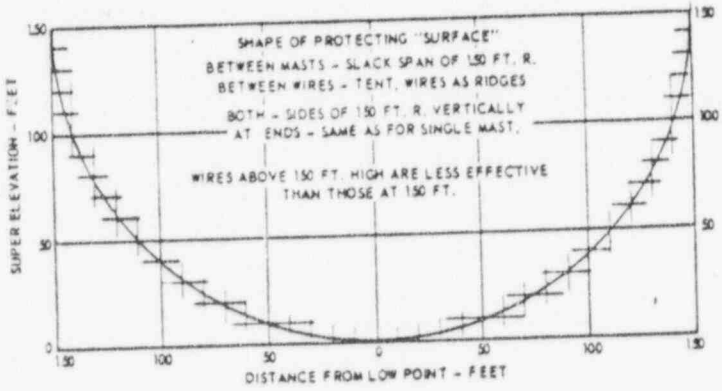

Fig. 5. Lightning protection between masts or wires. Protecting points lie along curve. All points below curve are protected.

mains protected. This zone of protection in the area between elevated points or conductors is useful, additionally, in substations or anywhere else where relatively large areas require protection. Fig. 5 shows that elevated points 150 ft apart will provide protection for a point midway between them only 20 ft lower than the elevated points, for example.

Fig. 6(a) illustrates the degree of protection of a 60-ft high 100-ft diameter tank using a single overhead grounded wire (point A) and the 45° protection angle of NFPA 78. To provide this angle, the wire height would have to be 110 ft. Shown also are arcs of 150-ft radius, tangent to the earth, showing that the 45° cone would not be effective.

Fig. 6(b) shows that two overhead grounded wires (points B and C) 20 ft above the tank and 10 ft inboard from the outer edges in the plane of the sketch would provide effective protection using the rolling 300-ft diameter sphere illustration of principles outlined in this paper.

EFFECT OF SLOPING GROUND SURFACE

The effect of sloping ground surface near the point requiring protection will affect the required protective elements. The only practical method for determination is the graphical one with development of the profile of the earth surface out to a distance approaching 150 ft, particularly on the downhill side of the point of interest. The 150-ft radius circle tangent to the earth's surface and just clearing the point to be protected will indicate the locus of the top of positions of the protecting element. It will be found that this element will need to be higher when the structure to be protected is downhill from it rather than on level ground. Likewise, a structure uphill from the protecting element permits this element to be lower.

DISCUSSION OF PROPOSED METHOD

Protection systems utilizing the principles of the EEI study and the rolling 300-ft diameter sphere show the suitability of the conventional multiterminal lightning rod NFPA system for large relatively flat areas. They would deviate substantially from the fixed angle linear cone recommendations of NFPA 78, however, for structures outside the height range of 37.5-62.5 ft, being more liberal for lower structures and much more conservative for higher structures.

This analysis also accounts most reasonably for the failures of very high structures to protect nearby structures within the

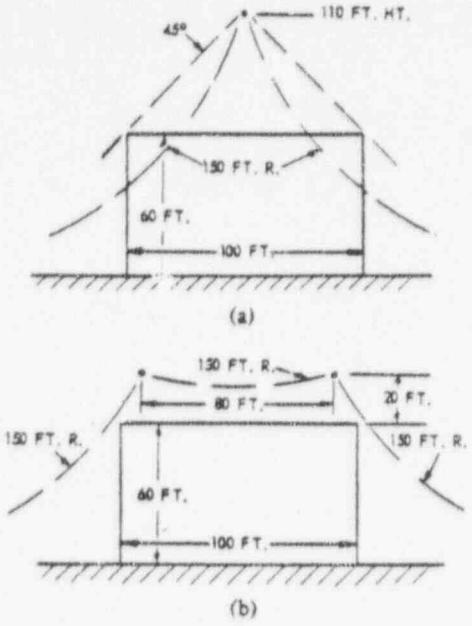

Fig. 6. Protection of tank. (a) Single wire 45° angle. Ineffective shielding. (b) Two wires, 150 ft radius zone. Effective shielding.

linear cone space, and for the instances when such structures are struck below their tops.

The extent of both theoretical and practical test work included in the EEI project and the satisfactory performance of electric transmission lines utilizing it appears reason enough to extend its application to lightning protection for structures of all types.

The hypothesis of W. H. Preece of 1881, shows that he was 100 years ahead of his time in concept. Recognition of his work would have been highly advantageous to the utility industry. Since these utilities have now proven this approach to be the correct one for their use, there is little reason to delay its adoption for other structures.

APPENDIX

Whitehead and others developed the analytical system referred to as the electrogeometrical model for determination of the effectiveness of lightning protection. By this means, the part to be protected is made less attractive to lightning than either the protecting structure or the ground itself. This is done by determining the length of the "striking distance," a term noted even in Franklin's writings, though the modern stepped leader phenomenon was not known then. Currently, this is the length of the last step of the leader under the influence of an attracting terminal on or attached to the earth. This distance determines the position of the shielding structure with respect to the structure to be protected, taking into consideration the height of each above ground.

Practically, a graphical analysis involves scribing arcs of circles of radius equal to the striking distance about both the protecting structure and that to be protected. If the intersection of these arcs occurs at a height above ground less than the length of the striking distance, the protecting system is effective. If the intersection is higher than the striking distance, the shielding is not effective. By this means, it is readily seen that the higher above ground, the smaller the angle of protection,

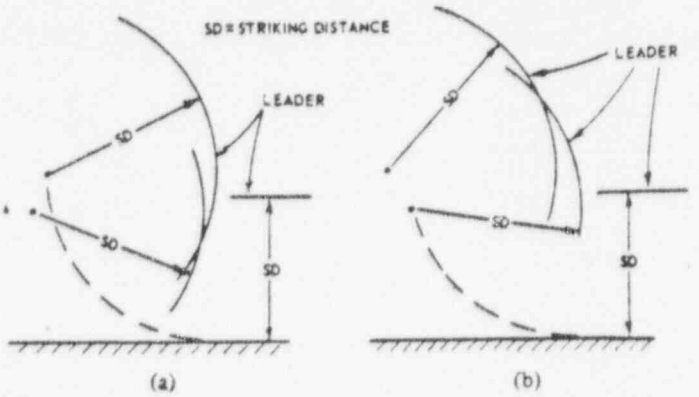

Fig. 7. Intersection below SD above ground. (a) Effective shielding. (b) Ineffective shielding.

to the end that at heights close to or greater than the striking distance, the protecting structure must be outboard of that to be protected. Fig. 7 illustrates the electrogeometric model.

The striking distance is dependent on the flashover voltage (over porcelain and through air) of the line, and on its surge impedance [9], [10]. For diverter structures to protect buildings and similar structures, the surge impedance and flashover voltages would apply in this determination. Ordinarily, the spacings and design would make the 1400 kV BIL data of Figs. 1 and 2 applicable.

REFERENCES

[1] B. F. Schonland, "The work of B. Franklin on thunderstorms and the development of the lightning rod," *J. Franklin Inst.*, vol. 253, p. 375, 1952.
[2] B. Wilson, "Report on lightning incident at purfleet," *Phil. Trans. Royal Soc.*, vol. 68, p. 239, 1778.
[3] O. J. Lodge, *Lightning Conductors and Lightning Guards.* London: Whitaker, 1892.
[4] W. H. Preece, "On the space protected by a lightning conductor," *Phil Mag.*, vol. 10, p. 427, 1880.
[5] F. W. Peek, *Dielectric Phenomena in High-Voltage Engineering.* New York, McGraw-Hill, 1929.
[6] R. Anderson, *Lightning Conductors.* London, New York: E. & F. N. Spon., 1879.
[7] R. H. Golde, "The lightning conductor," *J. of the Franklin Inst.*, vol. 283, no. 6, June 1967.
[8] C. F. Wagner, "Lightning and transmission lines," *J. Franklin Inst.*, vol. 283, no. 6, June 1967.
[9] E. R. Whitehead, "Mechanism of lightning flashover," *EEI Res. Proj. RP 50, Pub. 72-900.* Chicago, IL: Ill. Inst. Tech. Feb. 16, 1971.
[10] A. M Mousa, "Shielding HV and EHV Substations," IEEE Trans. *Power App. Syst.*, F-76-097-6, July/Aug. 1976, p. 1303.

Discussion

D. F. Shankle, (Westinghouse Electric Corporation, Pittsburgh, PA): In Fig. 6(b) and associated text, it is not clear if shield wires *B* and *C* are two parallel wires or a cross section of a ring of 80-ft diameter around the top. A ring of 80-ft diameter might be a better illustration of the principle.

Allan Greenwood (Rehsselaer Polytechnic Institute, Troy, NY): In Fig. 2, it is suggested that lines be drawn from the 0-ft line and heights and angles derived from Fig. 1 to obtain the locus of the protection surface. For example, the 10° slope

line would start at 125-ft height, 0-ft distance, and the 20° slope line would start at 100 ft, 0 ft, the 33° slope line would start at 75 ft, 0 ft, etc. The outer envelope of these lines would then form the protection surface delineation and would be to the left of the author's Fig. 2 line.

On the "rolling sphere" model, it appears that the diameter of the sphere is a variable, as indicated in Golde's paper [7]. The diameter would depend on the strength of the leader. We request clarification on how the leader strength would affect the sphere radius, as possibly differing from 150 ft.

Ralph H Lee: We appreciate the interest engendered by this treatment of the subject. This must stem from the historic failures of the previously held linear cone protection principle and the premise that this system would provide correction.

Mr. Shankle is correct in that the theoretical position of the shield wires in Fig. 6(b) is a ring of 80-ft diameter. Our concept of the practical protection was, however, simply two parallel overhead wires separated 80 ft, to provide protection for the maximum "width" dimension of the tank, partly because of difficulties in supporting a ring separate from the tank itself. For complete protection, the diverter elements and grounding conductors need to be separated by not less than about 5 ft from the component to be protected. Thus separately supported diverters are desirable and can be most economically provided here by the two parallel wires at 80-ft separation. The "ends" of the tank, then, are well below the 150-ft radius virtual arc between the two wires, as long as they are continued out to no less than 10 ft short of the "length" of the tank.

Dr. Greenwood proposes an ultra-conservative approach which can be illustrated as not conforming with the analysis illustrated in Figs. 7(a) and 7(b) of the Appendix. While these these figures are not specific to the discussion, they illustrate that the critical protection position occurs when the distances from the leader end to the diverter, the item to be protected, and the distance to ground are all equal, and equal to the "striking distance", which is here taken as 150 ft. With this concept, the positions of the diverter, protected item, and ground tangent all fall along an arc of 150-ft radius, which then agrees with Fig. 2–4.

Looking at Fig. 2, it is logical to start each new slope at the lower end of the height interval (±12.5 ft) of the next higher zone, since all locations closer to the "0 distance" line are protected by higher zone slopes. Also, our illustrations may be confusing since, for protecting diverters less than 150-ft high, the "zero distance" point moves out to a point where the diverter height touches the 150-ft radius arc. So the "distance-feet" abscissa markings are simply a footage scale, not to be used as an absolute distance except for protecting elements equal to or higher than 150 ft.

Dr. Greenwood's second point brings up a quite valid argument. The radius *does* vary with the amperage of the stroke, lower amperages requiring shorter radii, for which the 150-ft radius is not sufficiently conservative and vice versa. This aspect has resulted in substantially more study, to develop a correlation between critical radius and stroke current, and incidentally BIL. This work is being presented in a paper at the IAS Conference in Toronto, ON, Canada, October 1978. Briefly, the 150-ft radius corresponds with a stroke current of 10 000 A and a BIL of 1400 kV. This is found to be about the lowest level of stroke capable of damaging buildings. Data are developed for a current range 4.4–16.1 kA, BIL range of 600–2200 kV, and yielding critical radii from 72–204 ft.

Some of the illustrations of the sequel paper are useful in clarifying points brought up by Dr. Greenwood, also.

We would be remiss in not noting that NFPA #78, Lightning Protection Code, 1977 Edition, also adopts the circular-sided cone protection surface for buildings 50–100-ft high. The radius prescribed there is 100 ft, which, from calculations for the second paper, corresponds to a peak current of 7 kA and BIL of 950 kV.

Again, we thank our discussors for their analyses, all of which contribute to a better understanding of this very elusive subject.

Ralph H. Lee (SM'48–F'71) received the B.Sc. degree in electrical engineering from the University of Alberta, Edmonton, AB, Canada, in 1934.

From 1934 to 1937, he worked at a gas utility company, and from 1937 to 1942, he was with the National Geophysical Company, where he was involved with seismic oil exploration. From 1942 to 1976, he was with the E. I. duPont de Nemours and Company as Principal Electrical Consultant to the Engineering and Manufacturing Departments. He is presently with Lee Electrical Engineering, Inc., Wilmington, DE, doing electrical consulting and testing, particularly for industrial systems. His activities have included design and test experience in nuclear and industrial distribution and utilization systems, THWN building wire, TC and SNM tray cable, cable tray systems, motor control centers, concrete reinforcing bar grounding electrodes, reliability and testing of medium voltage cable systems, and human electrical safety.

Mr. Lee is a member of the National Electrical Code Panels 4 and 13, the NEC Subcommittee on O/C Protection, and the NFPA 70-E Committee on Safety Electrical Code for OSHA. He was Local Chairman of the Delaware Bay IEEE Section from 1962 to 1963 and an organizer of the joint IAS-PES Chapter in 1966. He is a Registered Professional Engineer in the State of Delaware. He was the 1976 recipient of the IEEE-IAS Outstanding Achievement Award, the 1976 recipient of the IEEE-IAS Prize Paper Award, the 1975 recipient of the IEEE-IAS-ICPS Achievement Award, and the 1970 recipient of the IEEE-IAS-ICPS Prize Paper Award.